GEOLOGICAL SURVEY OF CANADA
COMMISSION GÉOLOGIQUE DU CANADA

PAPER
ÉTUDE 82-1C



# CURRENT RESEARCH PART C

# RECHERCHES EN COURS PARTIE C

Canada

1982

## Notice to Librarians and Indexers

The Geological Survey's thrice-yearly *Current Research* series contains many reports comparable in scope and subject matter to those appearing in scientific journals and other serials. All contributions to the Scientific and Technical Report section of *Current Research* include an abstract and bibliographic citation. It is hoped that these will assist you in cataloguing and indexing these reports and that this will result in a still wider dissemination of the results of the Geological Survey's research activities.

## *Avis aux bibliothécaires et préparateurs d'index*

*La série* Recherches en cours *de la Commission géologique paraît trois fois par année; elle contient plusieurs rapports dont la portée et la nature sont comparable à ceux qui paraissent dans les revues scientifiques et autres périodiques. Tous les articles publiés dans la section des rapports scientifiques et techniques de la publication* Recherches en cours *sont accompagnés d'un résumé et d'une bibliographie, ce qui vous permettra, nous l'espérons, de cataloguer et d'indexer ces rapports, d'où une meilleure diffusion des résultats de recherche de la Commission géologique.*


**Technical editing and compilation**
***Rédaction et compilation techniques***
W.C. Morgan
H. Dumych
P.J. Griffin
L. Machan
W.C. Morgan

**Production editing and layout**
***Préparation et mise en page***
M.J. Kiel
D. Busby

**Typed and checked by**
***Dactylographie et vérification***
Jacinthe Caron
Janet Legere
Janet Gilliland
Shirley Kostiew
Sharon Parnham

GEOLOGICAL SURVEY
PAPER 82-1C

COMMISSION GÉOLOGIQUE
ÉTUDE 82-1C

# CURRENT RESEARCH
# PART C

# RECHERCHES EN COURS
# PARTIE C

1982

Available in Canada through

authorized bookstore agents
and other bookstores

or by mail from

Canadian Government Publishing Centre
Supply and Services Canada
Hull, Québec, Canada K1A 0S9

and from

Geological Survey of Canada
601 Booth Street
Ottawa, Canada K1A 0E8

A deposit copy of this publication is also available
for reference in public libraries across Canada

Cat. No. M44-82/1CE Canada: $8.00
ISBN 0-660-11225-6 Other countries: $9.60

Price subject to change without notice

**Separates**

A limited number of separates of the papers that appear in this volume are available by direct request to the individual authors. The addresses of the Geological Survey of Canada offices follow:

601 Booth Street,
OTTAWA, Ontario
K1A 0E8

Institute of Sedimentary and Petroleum Geology,
3303-33rd Street N.W.,
CALGARY, Alberta
T2L 2A7

Cordilleran Geology Division
100 West Pender Street,
VANCOUVER, B.C.
V6B 1R8

Atlantic Geoscience Centre,
Bedford Institute of Oceanography,
P.O. Box 1006,
DARTMOUTH, N.S.
B2Y 4A2

When no location accompanies an author's name in the title of a paper, the Ottawa address should be used.

***Tirés à part***

*On peut obtenir un nombre limité de "tirés à part" des articles qui paraissent dans cette publication en s'adressant directement à chaque auteur. Les adresses des différents bureaux de la Commission géologique du Canada sont les suivantes:*

*601, rue Booth*
*OTTAWA, Ontario*
*K1A 0E8*

*Institut de géologie sédimentaire et pétrolière*
*3303-33rd, St. N.W.,*
*CALGARY, Alberta*
*T2L 2A7*

*Division de la géologie de la Cordillère*
*100 West Pender Street*
*VANCOUVER, Colombie-Britannique*
*V6B 1R8*

*Centre géoscientifique de l'Atlantique*
*Institut océanographique de Bedford*
*B.P. 1006*
*DARTMOUTH, Nouvelle-Ecosse*
*B2Y 4A2*

*Lorsque l'adresse de l'auteur ne figure pas sous le titre d'un document, on doit alors utiliser l'adresse d'Ottawa.*

## SCIENTIFIC AND TECHNICAL REPORTS

## RAPPORTS SCIENTIFIQUES ET TECHNIQUES



## SCIENTIFIC AND TECHNICAL NOTES

## NOTES SCIENTIFIQUES ET TECHNIQUES

## RUBIDIUM-STRONTIUM AND URANIUM-LEAD ISOTOPIC AGE STUDIES

## ÉTUDES DES DATATIONS ISOTOPIQUES PAR LES MÉTHODES RUBIDIUM-STRONTIUM ET URANIUM-PLOMB

## SCIENTIFIC AND TECHNICAL REPORTS
## RAPPORTS SCIENTIFIQUE ET TECHNIQUES

1. **THE C.H. KINDLE COLLECTION: MIDDLE CAMBRIAN TO LOWER ORDOVICIAN TRILOBITES FROM THE COW HEAD GROUP, WESTERN NEWFOUNDLAND**

Project 500029

C.H. Kindle[1]
Institute of Sedimentary and Petroleum Geology, Ottawa

*Kindle, C.H., The C.H. Kindle Collection: Middle Cambrian to Lower Ordovician Trilobites from the Cow Head Group, western Newfoundland; in Current Research, Part C, Geological Survey of Canada, Paper 82-1C, p. 1-17, 1982.*

***Abstract***

*My trilobite collection of approximately 20 000 specimens was transferred to the Geological Survey of Canada, Ottawa, in 1978. The material is Middle Cambrian through early Lower Ordovician in age, and is mainly from boulders in the Cow Head Group, western Newfoundland. The boulders are from slump deposits comprising strata of several depositional facies. Boulders from shallow water carbonates contain standard trilobites known from the North American Faunal Province. Boulders from carbonate mounds and buildups of shallow to intermediate depths contain Lévis-type trilobites. Boulders originating from relatively deep water deposits and adjacent interbedded strata contain trilobites known from the Acado-Baltic Faunal Province. This mixing of faunas representing different faunal environments has produced a unique opportunity for correlating across facies barriers.*

*The trilobites reported here have been separated into four Middle Cambrian and four Upper Cambrian informal zones. They have been identified to generic level, and some to specific level, but systematic studies have not been attempted.*

### Introduction

In 1978 my trilobite collection was transferred to the Geological Survey of Canada[2] in Ottawa for permanent storage and greater scientific access. The material is housed separate from other collections, under my name and cataloguing system. The collection comprises approximately 20 000 specimens, 90 per cent of which are from 460 Cow Head Group boulders. The remaining material is from elsewhere in Newfoundland and from Québec, New York, Vermont and Pennsylvania. Most of the trilobites are Middle Cambrian through early Lower Ordovician in age, reflecting their source, which is rare fossiliferous boulders within thick beds of Cow Head conglomerate (Fig. 1.1, 1.2). Each fossiliferous boulder was assigned a number and each trilobite extracted from a given boulder received that number. Prior to 1978 the cleaning, tentative identification, and storage of the material took place in my home in Upper Nyack or at City College of New York.

Acknowledgments

Over the years my colleagues have offered assistance with the identification of the fossils, and for this I am pleased to acknowledge help by B.F. Howell, A.A. Opik, A.R. Palmer, H.B. Whittington, W.H. Fritz and others. Members of my family and H.B. and D. Whittington shared in the field work. Others, such as G. Henningsmoen (who located boulders 74 and 166), made brief but fruitful field visits. M.J. Copeland shouldered the burden of arranging and supervising the transfer of the fossils to the Geological Survey of Canada. W.H. Fritz and M.J. Copeland generously assisted with the completion of the present paper. Finally, I would like to thank L.M. Cumming for suggestions to improve the manuscript and R. Ludvigsen for the identifications of trilobites shown in figures 1, 10-12, and 16 on Plate 1.5.

[1] 332 N. Midland Ave., Upper Nyack, New York, 10960 U.S.A.
[2] This acquisition has been made possible by a contribution from the Government of Canada under the terms of the Cultural Property Export and Import Act.

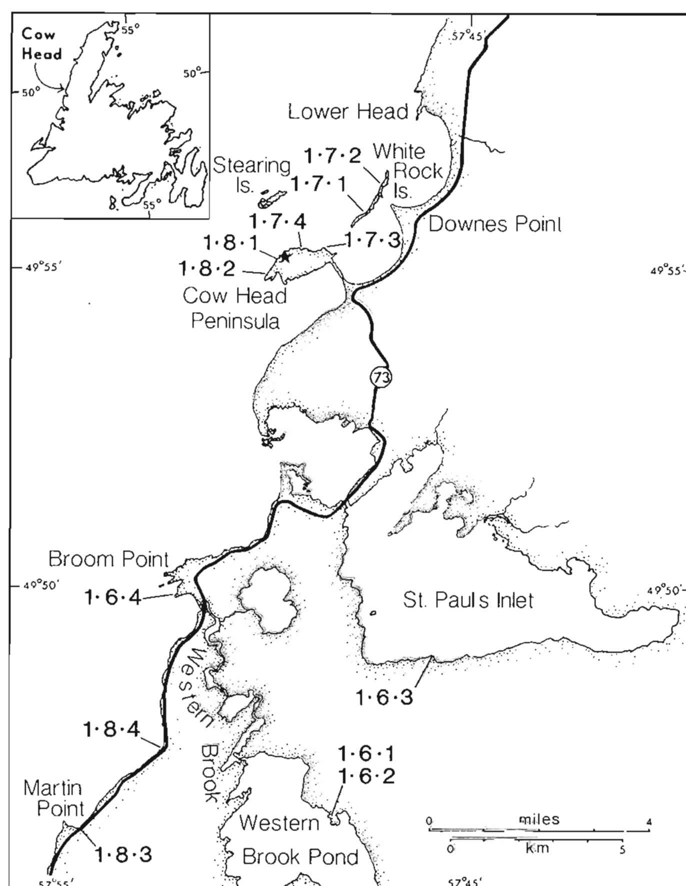


*Figure 1.1. General location for fossil localities mentioned in the text. Numbers (1.6.1, 1.6.2, etc.) locate views of outcrops (figures) shown in Plates 1.6, 1.7, and 1.8. Star on Cow Head Peninsula gives position of lighthouse. Figure is modified from Kindle and Whittington (1959, Fig. 1).*

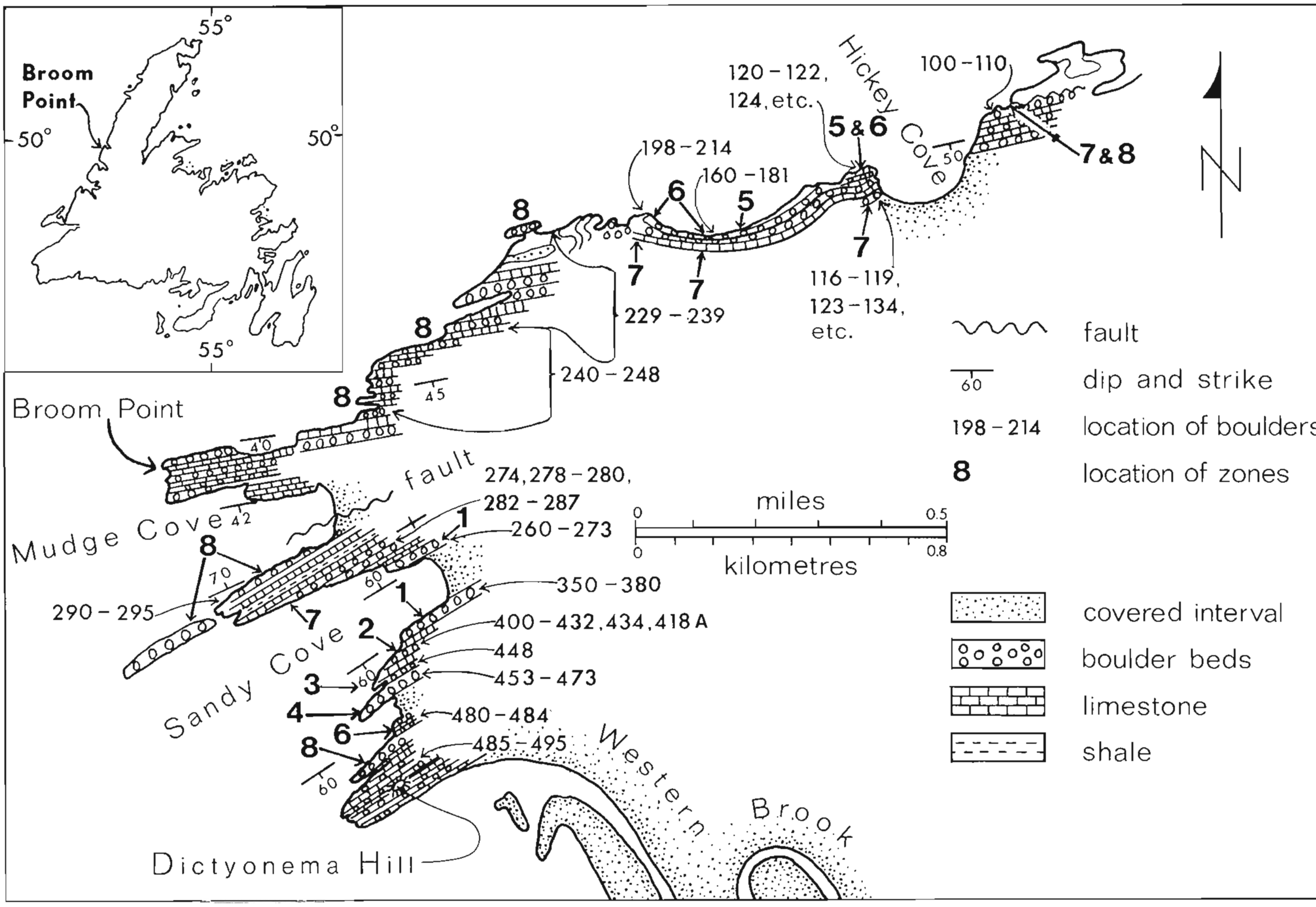


***Figure 1.2.*** *Enlargement of area around Broom Point (located on Figure 1.1). Numbers in light type locate boulder fossil localities. Numbers in heavy type locate fossil zones. Figure is modified from Kindle and Whittington (1959, Fig. 2).*

**PLATE 1.1** (opposite)

Zones 1 and 2

**Zacanthoides**? sp.
Figure 1. Incomplete cranidium, X3, boulder 376, GSC 69492.

**Zacanthoides** sp. 1
Figure 2. Cranidium, X3, boulder 358, GSC 69493.
Figure 6. Pygidium with four pairs of spines, X3, boulder 358, GSC 69494.

aff. **Parkaspis** sp.
Figure 3. Cranidium with long occipital spine, X3, boulder 358, GSC 69495.
Figure 7. Pygidium with slender upturned spines, X3, boulder 379, GSC 69496.
Figure 11. Pygidium with the upturned spines broken off and with smaller, blunt spines, X5, boulder 358, GSC 69497.

**Chancia** sp.
Figure 4. Cranidium, coarsely pustulose, X3, boulder 380, GSC 69498.

**Bathyuriscus adaeus** Walcott.
Figure 5. Pygidium, X4, boulder 363. GSC 69499.

**Tonkinella** sp. 1.
Figure 8. Cranidium, X5, boulder 380, GSC 69500.
Figure 12. Pygidium, X13, boulder 380, GSC 69502.

**Peronopsis** sp.
Figure 9. Pygidium with deep transverse furrow on posterior portion of axial lobe, X9, boulder 380, GSC 69501.

**Elrathina** sp.
Figure 10. Cranidium, X6, boulder 376, GSC 69503.

**Ptychagnostus** cf. **P. gibbus** (Linnarsson).
Figure 13. Cephalon, X10, boulder 362, GSC 69504.
Figure 18. Pygidium, X8, boulder 419, GSC 69505.

**Zacanthoides** sp. 2
Figure 14. Cranidium with larger preglabella field than on Z. sp. 1., X1.5, boulder 413, GSC 69506.
Figure 19. Pygidium with five pairs of spines, X6, boulder 413, GSC 69507.

**Kootenia** sp.
Figure 15. Pygidium, X3, boulder 378, GSC 69508.

**Pagetia** sp.
Figure 16. Cranidium, X12, boulder 372, GSC 69509.
Figure 17. Pygidium, X8, boulder 372, GSC 69510. This species has a smooth surface. Another species in the same boulder (not illustrated) has tubercules.

**Alokistocare** sp.
Figure 20. Incomplete cranidium, X6, boulder 372, GSC 69511.

**Bathyuriscus** sp.
Figure 21. Pygidium, X4, boulder 378, GSC 69512.

PLATE 1.1

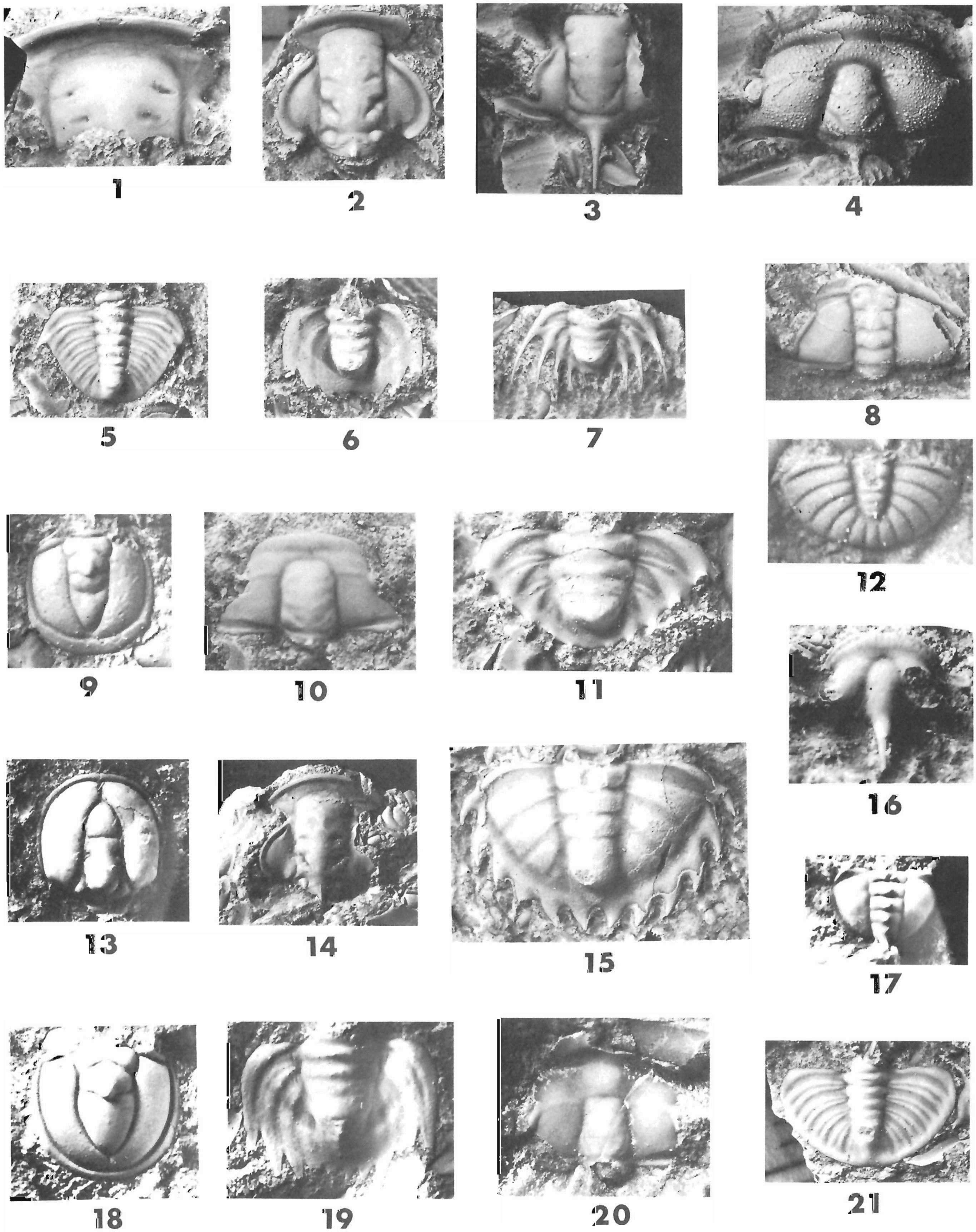

### Purpose of Paper

Just as with an art collection, a large fossil collection contributes little to society unless it is known to those having a potential interest in it. Once alerted, questions as to the materials' source, quality, and uniqueness usually must be answered before an effort is made to view the collection. This paper is intended to announce the collection to the scientific community and is an attempt to answer these questions. Many of these answers come from the published history of the Cow Head Group, as wide interest in both the host rock and the fossils have been intermingled. As will be seen, the discovery of the fossils in increasing numbers led to more than the usual refining of the age of a map unit, for the fossils were instrumental in overturning a classical interpretation of the stratigraphy and structure of western Newfoundland.

Less public attention has been given to the fossils' high quality of preservation, and therefore numerous photos are presented in Plates 1.1-1.5. This rare preservation has been noted in fossils from sparse boulders and beds in the Quebec Lowlands, New York, and Vermont. However, these fossils and those in the present collection are the product of extensive searches in Taconic terrains where trilobites are known to be rare, and it can be expected that additional material will only arrive in small collections and in limited numbers.

The usual diversity of the material is yet another aspect of the collection. An adequate description of this diversity must await systematic studies and more knowledge on the interrelationship between faunal environments and faunal provinces. For the present, the material is identified to the generic level and the fossils grouped into numbered faunas. A limited attempt is made to correlate these faunas with zones in the North American and Acado-Baltic faunal provinces.

### Early Work on the Cow Head Group

James Richardson (in Logan, 1863, p. 291, 292) first studied the strata that now are relegated to the Cow Head Group, and noted the unusually large and abundant boulder beds. He found fossils in both the conglomerate and interbedded strata in the upper part of the group, and Logan (1863, p. 865) placed the map unit above strata now assigned to the Middle Ordovician Table Head Formation. In 1934 Schuchert and Dunbar published their conclusions on the Cow Head boulders in a classical paper that strongly influenced the stratigraphic thinking on western Newfoundland. They (Schuchert and Dunbar, 1934, p. 84) believed that the conglomerates "formed at the nose of thrust sheets that were in movement during the Middle Ordovician". Fossils that they had previously collected from the Cow Head boulders were dated by Raymond (1925) as being equivalent to the Table Head faunas, and the Cow Head strata with its "derived boulder fossils" were placed by Schuchert and Dunbar (1934, p. 16) above the "Long Point series". The selected position was in the Middle Ordovician and at a level still higher than that chosen by Logan. Lochman's 1938 description of early Upper Cambrian trilobites from Cow Head did not include a change in age of the Cow Head strata, thus giving implied agreement to Schuchert and Dunbar's thrust concept.

### Contemporary Work

The Geological Survey of Newfoundland commissioned H. Johnson to do further work on the stratigraphy of western Newfoundland, and Johnson in turn invited me to be his assistant in 1938 and 1939. This offer was gratefully accepted as with it came permission for me to keep any fossils that I might find. Johnson (1941, p. 143) noted that the Cow Head breccias did not fit with the laterally adjacent

**PLATE 1.2** (opposite)

Zone 2 – Figure 1
Zone 3 – Figures 2-13
Zone 4 – Figures 14-23

**Centropleura** sp. 1.
Figure 1. Incomplete cranidium, X1.5, boulder 425, GSC 69513.

**Ptychagnostus atavus** (Tullberg).
Figure 2. Cephalon, X9, boulder 619, GSC 69514.

**Olenoides** cf. **O. schucherti** Kindle.
Figure 3. Pygidium, X2.5, boulder 619, GSC 69515.
Figure 4. Cranidium, X2, boulder 619, GSC 69516.

**Eodiscus** cf. **E. punctatus scanicus** (Linnarsson).
Figure 5. Cephalon, X9, boulder 633, GSC 69517.
Figure 9. Pygidium, X9, boulder 633, GSC 69518.

**Tomagnostus fissus** (Lundgren ms, Linnarsson).
Figure 6. Cephalon, X7.5, boulder 448, GSC 69519.
Figure 10. Pygidium, X7, boulder 448, GSC 69520.

**Meneviella venulosa** (Salter).
Figure 7. Cranidium, X4, boulder 450, GSC 53574.

**Orria** sp.
Figure 8. Pygidium, X1, boulder 606, GSC 69521.

**Kingstonioides** sp. 1.
Figure 11. Cranidium, view of left side showing brim extending horizontally, X2.5, boulder 603, GSC 69522.

**Kingstonioides** sp. 2.
Figure 12. Cranidium, view of left side showing less convexity and a different brim from that of **K.** sp. 1, X3, boulder 603, GSC 69523.

**Centropleura** sp. 2.
Figure 13. Pygidium, X3, boulder 632, GSC 69524.

**Bolaspidella**? sp.
Figure 14. Cranidium with upturned projection on anterior border, X5, boulder 468, GSC 69525.

**Brassicicephalus** sp.
Figure 15. Cranidium, X6, boulder 468, GSC 69526.

**Ptychagnostus aculeatus** (Angelin).
Figure 16. Copy of Plate 12, fig. 8 of Westergard, 1946, X5.
Figure 19. Anterior portion of cephalon, X8, boulder 458, GSC 69527.
Figure 23. Posterior portion of right side of cephalon, X7, boulder 458, GSC 69528.

Unnamed genus and species.
Figure 17. Cranidium showing flat occipital ring merging with fixed cheek, X5.5, boulder 467, GSC 69529.

**Hemirhodon** sp.
Figure 18. Cranidium, X1, boulder 466, GSC 69530.

Unnamed genus and species, aff. **Drumaspis.**
Figure 20. Cranidium, X3.5, boulder 472, GSC 69531.

**Corynexochus** sp.
Figure 21. Cranidium, X7, boulder 471, GSC 69532.

**Modocia** sp.
Figure 22. Cranidium with punctate surface, X2, boulder 468, GSC 69533.

PLATE 1.2

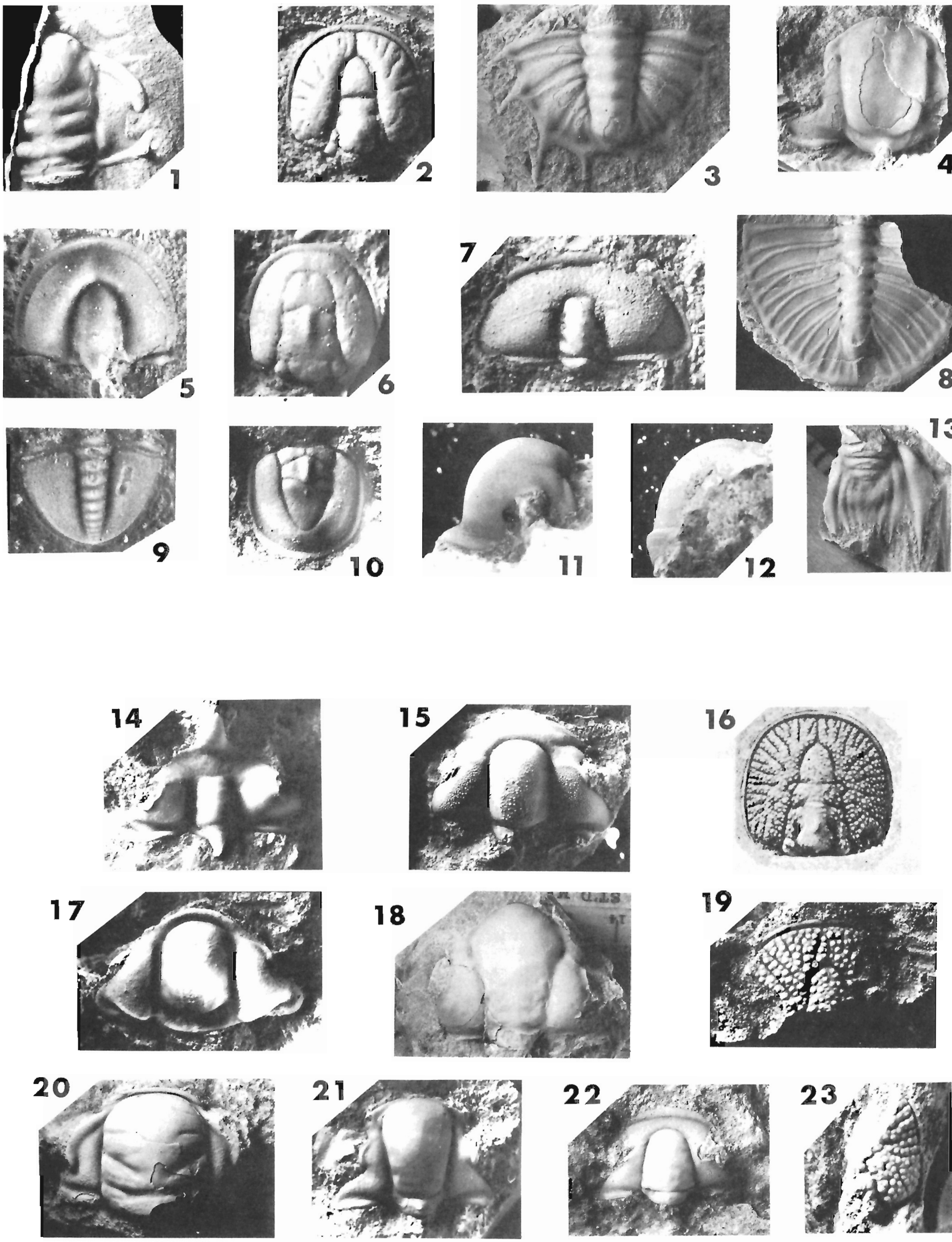

stratigraphic sequence, and that some breccias were interbedded wih graptolite-bearing shales. While with Johnson, I discovered an abundance of trilobites in rare Cow Head boulders, and made collections from Lower Head, Cow Head Peninsula, the entrance of St. Pauls Inlet and Martin Point (Kindle, 1942, 1943). A boulder (no. 555) from the latter locality produced a new species described by F. Rasetti (1948).

In 1952 more trilobite collections from western Newfoundland were added while working for John Fox oil enterprises. At that time P. Oxley, then mapping for the Geological Survey of Newfounland, kindly pointed out trilobites in regularly stratified Cow Head beds exposed at low tide at the mouth of Western Brook (Fig. 1.1). He also mentioned agnostids in a dislodged block at Sandy Cove (Fig. 1.2). This block (no. 448) was traced by me to Middle Cambrian regularly stratified beds, and it was immediately clear that deposition of the group began at least by Middle Cambrian time. Oxley (1953), however, retained Schuchert and Dunbar's Middle Ordovician age for the group in his report.

In 1955, 1957, 1958, 1961, and 1965 I carried out paleontological investigations in western Newfoundland with H.B. Whittington. During this time the Cambrian fossils were retained by me and the Ordovician fossils went to Whittington. Our collections demonstrated that Cow Head deposition started at least (base covered) by Middle Cambrian time and continued into the early Middle Ordovician (Kindle and Whittington, 1958). In addition, we demonstrated with few exceptions, that the fauna within any one layer of conglomerates is the same age or younger than the fauna in the underlying layer (Kindle and Whittington, 1959). Ordovician trilobites from the Cow Head Group exposed at Lower Head were described by Whittington in 1963, and laterally equivalent trilobites from the Table Head Formation exposed along the coast farther north were described by him in 1965.

In 1963 Rodgers and Neale used the fossil dates from the relatively deep water Cow Head and Humber Arm groups to prove that they are contemporaneous with the surrounding shallow water facies consisting of the Labrador Group through Table Head Formation. They proposed that the deep water strata had been thrust westward as part of the same Middle Ordovician Taconic Orogeny that had effected the eastern part of the United States. In this hypothesis Cow Head deposition took place just east of the continental platform in relatively deep water where slow mud deposition was sporadically interrupted by turbidity currents (Rodgers and Neale, 1963, p. 719).

Whittington and Kindle (1969) agreed with the slope concept for the Cow Head, and attributed the wide variety in the fauna to different life positions on and above the slope before slumping and turbidity currents brought the animal remains together. Furthermore, they noted that intermixed with the expected fossils are genera that were previously thought to represent different faunal provinces. From this they postulated that Pacific Faunal Province genera, such as **Elrathia, Kootenia,** and **Zacanthoides,** originated in shallow water above the slope. Lévis-type faunas (Québec Lowlands), such as **Onchonotopsis** and **Kingstonioides,** inhabited carbonate mounds and buildups of shallow and intermediate depths. Atlantic Faunal Province genera, such as **Meneviella** and **Tomagnostus,** lived in deep water. The Cow Head association of faunas therefore should present a warning to those using fossils to define sutures between major tectonic plates (faunal provinces) without regard to facies relationships.

Petrographic studies by James (1981) confirm the interpretation that large boulders in the Cow Head Group are redeposited fragments of carbonate mounds and buildups

**PLATE 1.3** (opposite)

Zone 5 – Figures 1-12
Zone 6 – Figures 13-22

**Tricrepicephalus** sp. 1.
Figure 1. Cranidium, X2, boulder 11, GSC 69534.
Figure 5. Pygidium, X2, boulder 21, GSC 69535.

**Cedaria** sp.
Figure 2. Pygidium, X2, boulder 15, GSC 69536.

**Clavagnostus** cf. **C. sulcatus** Westergard
Figure 3. Cephalon, X12, boulder 3, GSC 69537.
Figure 4. Cephalon (a) and pygidium (b) from Westergard, 1946, Pl. 4, fig. 25, 26, X7.
Figure 7. Cephalon, X9, Murphy Creek Formation, Gaspé Co., Québec, GSC 69538.
Figure 8. Pygidium, X14, Murphy Creek Formation, Gaspé Co., Québec, GSC 69539.

**Crepicephalus** sp.
Figure 6. Pygidium, X2, boulder 11, GSC 69540.

**Terranovella** sp.
Figure 9. Cranidium, X6, boulder 15, GSC 69541.

**Coosella** sp.
Figure 10. Pygidium, X1.7, boulder 12, GSC 69542.

**Deiracephalus unicornis** Palmer.
Figure 11. Cranidium showing spine rising from posterior part of glabella, X6, boulder 39, GSC 69543.

**Deiracephalus** sp.
Figure 12. Cranidium of common species, X8, boulder 11, GSC 69544.

**Agnostus inexpectans** Kobayashi.
Figure 13. Cephalon, X15, boulder 49, GSC 69545.
Figure 17. Pygidium, X12, boulder 49, GSC 69546.

**Aphelaspis** sp. 1
Figure 14. Cranidium, X4.5, boulder 56, GSC 69547.

**Dunderbergia** sp.
Figure 15. Cranidium, X2, boulder 49, GSC 69548.

**Pterocephalops** sp.
Figure 16. Cranidium, X5.5, boulder 166, GSC 69549.

**Glyptagnostus reticulatus** (Angelin).
Figure 18. Pygidium, X7, boulder 56, GSC 53531.

**Cheilocephalus** sp.
Figure 19. Cranidium, X5.5, boulder 180, GSC 68550.

**Aphelaspis** sp. 2
Figure 20. Cranidium, X2, boulder 49, GSC 69551.

**Onchopeltis** cf. **O. spectabilis** Rasetti.
Figure 21. Cranidium, X1.3, boulder 166, GSC 69552.
Figure 22. Side view of same cranidium, X1.3.

PLATE 1.3

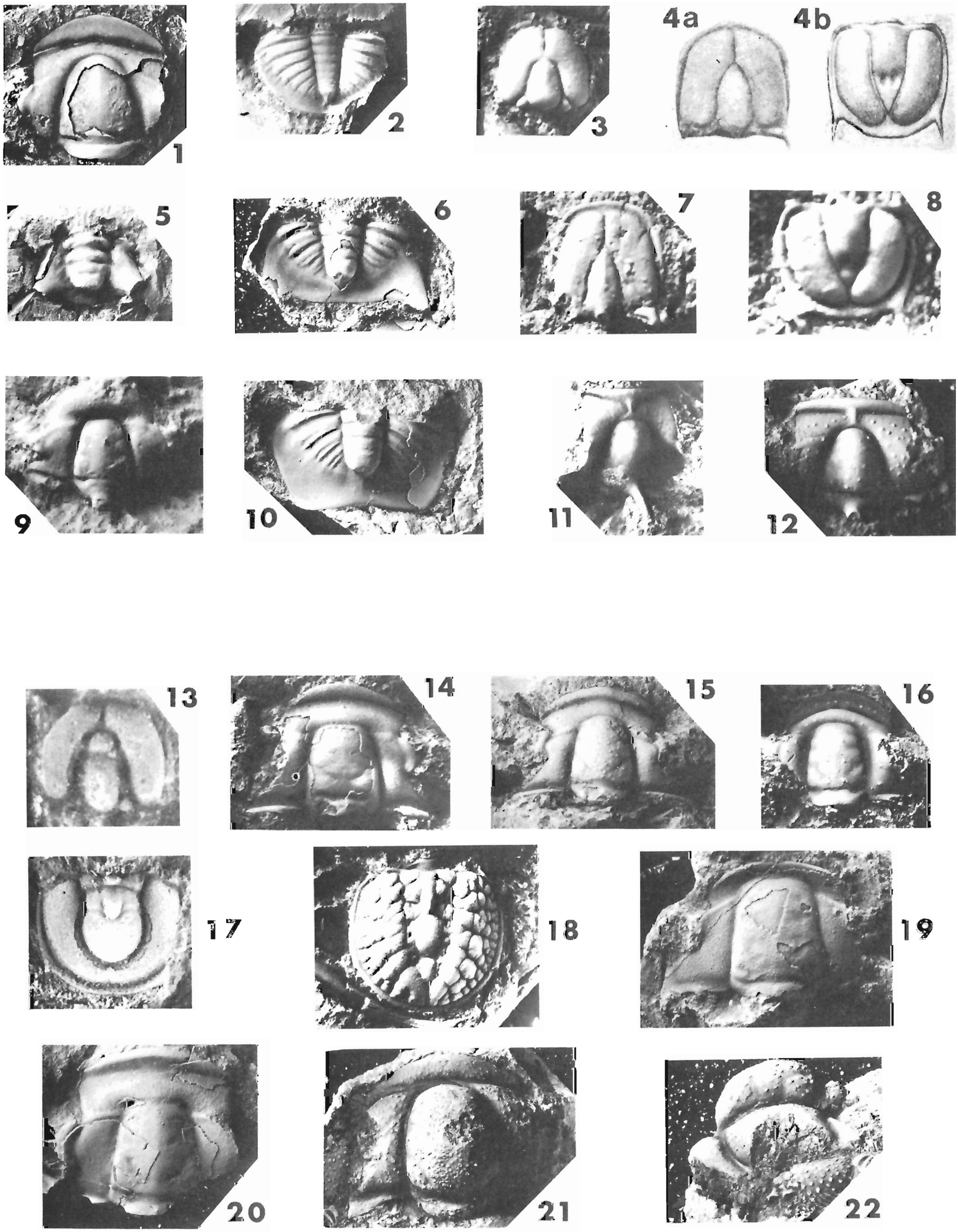

originating in shallow and intermediate depths at the outer margin of a carbonate shelf. James (1981, p. 805) also observed that the boulders are almost identical to the Lévis boulders of Québec. As earlier noted (Kindle, 1948, p. 442) the faunas from the boulders in the two areas are nearly identical. Conodonts (Fahraeus and Nowlan, 1978) have also been extracted from the Cow Head carbonates, and have produced close correlations with the Lower Ordovician of the Atlantic Province.

The value of using the Cow Head fossils of mixed environments for international correlation has been emphasized by Fortey and Skevington (1980). By moving laterally along the conglomerate beds, they located a favourable proportion of breccias (shallow water) to regular beds (deep water) in a section that crosses the Cambro-Ordovician boundary. From this section they collected a closely dated succession of graptolites and trilobites that is of great importance for wide correlation.

### Illustrations in Present Paper

Colour slides of the trilobites shown in Plates 1.1-1.5 were made for a presentation before the Eastern Canada Paleontology and Biostratigraphy Seminar in 1978 (abstracts not published). In a similar talk before the Second International Symposium on the Cambrian System (Kindle, 1981) the trilobites were arranged in numbered zones. Negatives from the original coloured slides were later made by the Geological Survey of Canada to produce the trilobite photos shown in Plates 1.1-1.5, and other coloured slides were likewise processed to show views of strata in Plates 1.6-1.8.

The general locations of Cow Head Group collecting localities are shown in Figure 1.1. Numbers keyed to outcrop views in Plates 1.6-1.8 have also been placed on Figure 1.1 to provide rapid access to greater detail. In Figure 1.2 Cow Head boulder localities in the Broom Point area are shown in standard type and the fossil zones in heavy type. Other Cow Head localities can be located by referring to an earlier publication by Kindle and Whittington (1958). The latter publication locates fossiliferous conglomerate beds for which fossil lists are given. No attempt is made there to list the boulder numbers with the fauna.

### Trilobite Zones in the Cow Head Group

The trilobites in the present collection have been placed in eight zones that range from the medial Middle Cambrian to the latest Upper Cambrian. The faunal assemblage comprising each zone can be demonstrated in the field to stratigraphically over- or underlie the next older or younger zone in at least one outcrop area. No attempt has been made to subdivide the zone within a single conglomerate bed, as, within one bed, boulder position cannot be equated with stratigraphic position. However, it is assumed that the trilobites within a single boulder are of equal age, and therefore the contents of various representative boulders are listed to give the contemporaneous elements within a single zone.

The trilobites mentioned indicate that some genera extend beyond their expected range, and it is anticipated that when other workers complete systematic studies of the material the present zones and correlations will be altered and/or refined.

#### Zone 1

Zone 1 trilobites are known from the oldest exposed conglomerate in the Cow Head Group. The conglomerate outcrops near the axis of an anticline passing through the middle of Sandy Cove (Fig. 1.2), and is exposed at the water's

**PLATE 1.4** (opposite)

Zone 7 – Figures 1-11
Zone 8 – Figures 12-19

**Peratagnostus** sp.
Figure 1. Cephalon, X7, boulder 211, GSC 69553.
Figure 5. Pygidium, X8, boulder 211, GSC 69554.

**Levisella brevifrons** Rasetti.
Figure 2. Cranidium, X2.5, boulder 146, GSC 69555.

**Hungaia** sp.
Figure 3. Pygidium, X2.5, boulder 555, GSC 69556.

**Loganopeltoides kindlei** Rasetti
Figure 4. Cranidium, X2.3, boulder 172, GSC 53569.

**Paraphoreotropis** sp.
Figure 6. Cranidium, X10, boulder 554, GSC 69557.

**Oligometopus** sp.
Figure 7. Cranidium, X7, boulder 554, GSC 69558.

**Irvingella** sp.
Figure 8. Cranidium, X3.4, boulder 119, GSC 53570.

aff. **Xenocheilus** sp.
Figure 9. Cranidium with depressed eyeline, X10, boulder 279, GSC 69559.

**Protopeltura** sp.
Figure 10. Cranidium, X5, boulder 176, GSC 69560.

**Parabolina** cf. **P. lobata lobata** (Brogger).
Figure 11. Cranidium, X3.5, boulder 176, GSC 69561.

**Pseudosaukia brevifrons** (Clark).
Figure 12. Cranidium, X5, boulder 71, GSC 69562.

**Keithiella** sp.
Figure 13. Cranidium, X4.5, boulder 74, GSC 53566.

**Rasettia capax** (Billings).
Figure 14. Cranidium, X3, boulder 71, GSC 69563.

**Onchonotus** sp.
Figure 15. Cranidium, X4.2, boulder 74, GSC 69564.

**Loganellus similis** Rasetti.
Figure 16. Cranidium, X2.5, boulder 73, SC 69565.

**Hungaia quadrispinosa** Rasetti
Figure 17. Pygidium, X2, boulder 74, GSC 69566.

**Richardsonella** sp.
Figure 18. Cranidium, X2.5, boulder 73B, GSC 69567.

**Peltura** sp.
Figure 19. Cranidium, X7, boulder 73, GSC 69568.

PLATE 1.4

edge on either side. The zone is so far definitely recorded from conglomerate boulders 358, 362, and 380 containing **Bathyuriscus adaeus** Walcott, **Chancia** with strong pustules, **Peronopsis** sp. with a deep transverse furrow on the posterior lobe of the pygidium, **Tonkinella** sp. and aff. **Parkaspis** sp. with slender upturned pygidial spines. Other Zone 1 trilobites that range into Zone 2 are **Elrathia** sp., **Kootenia** sp., **Onchocephalites** sp., **Pagetia** sp., **Peronopsis** sp. and **Ptychagnostus** cf. **P. gibbus** (Linnarsson). These trilobites are present in the oldest conglomerate and in the succeeding 4-foot conglomerate (separated by regular limestone beds), which is exposed on the southeast limb of the anticline (Plate 1.6, fig. 4).

Zone 2

Trilobites used in the recognition of Zone 2 are **Baltagnostus** sp., **Zacanthoides** sp. 2 (6 pairs of spines), and the first occurrence of **Centropleura** sp. (cranidium) in deep water limestone. These trilobites as well as those mentioned above as being common to Zones 1 and 2 are known from the 4-foot conglomerate. Zones 1 and 2 are correlated with the **Bathyuriscus-Elrathina** Zone of the North American Faunal Province. **Ptychagnostus** cf. **P. gibbus** is used to correlate Zones 1 and 2 with Westergard's (1946) Zone B1 of the Middle Cambrian of Sweden (Acado-Baltic Faunal Province).

Zone 3

Zone 3 trilobites were collected in the white limestone beds overlying the 4-foot conglomerate on the southeast limb of the anticline (Plate 1.6, fig. 4), from some white limestone boulders in a 50-foot conglomerate stratigraphically higher (above dark shale which is so far barren), and on White Rock Islets (Plate 1.7, fig. 1,2). The locations and trilobites are listed below:

Boulder 448 (white limestone beds) – **Tomagnostus fissus** (Lundgren in Linnarsson), **Hypagnostus** sp., **Cotalagnostus**? sp., **Meneviella venulosa** (Salter), and **Alokistocare**? sp.

Boulder 450 (50-foot conglomerate) – **Peronopsis** sp., **Tomagnostus** sp., **Meneviella venulosa** and **Bailiaspis** sp.

Boulder 452 (50-foot conglomerate) – **Eodiscus** sp., **Hypagnostus**? sp. 1, **Tomagnostus** sp., **Ptychagnostus atavus** (Tullberg), **Alokistocare** sp., and **Spencella** sp.

Boulder 632 (White Rock Islets) – **Tomagnostus fissus**, **Hypagnostus** sp. **Peronopsis** sp., **Bailiaspis** sp., **Solenopleura**? sp., **Elrathia**? sp., and **Centropleura** sp. (pygidium).

Boulder 603 (White Rock Islets) – **Kingstonioides** spp. (2 species), **Bolaspidella** sp., **Catillicephalites** sp., **Alokistocare** sp., **Orria** sp., **Olenoides** sp. (large strong spines), **Modocia** sp., **Elrathia** sp., **Spencella** sp., **Bathyuriscidella**? sp., and **Corynexochides**? sp.

Boulder 619 (White Rock Islets) – **Ptychagnostus atavus**, **Hypagnostus parvifrons** (Linnarsson), **Peronopsis** sp., **Bathyuriscus** sp., and **Olenoides** sp.

Some of these trilobites are seen in the outer reefs of Stearing Island (**Ptychagnostus atavus**), at White Point in St. Pauls Inlet (**Orria** sp., **Kingstonioides** sp.), and at Eastern Point in Western Brook Pond (**Bolaspidella**? sp., **Pagetia** sp.), though the last mentioned locality is best regarded as Zone 2 (see localities on Fig. 1.1; Plate 1.6, fig. 1-3.

Zone 3 is correlated with the **Bolaspidella** Zone in the North American Faunal Province. The presence of **Tomagnostus fissus, Ptychagnostus atavus** and **Hypagnostus parifrons** is used to correlate Zone 3 with Westergard's (1946) Zones B2 and B3 in the Middle Cambrian of Sweden.

**PLATE 1.5** (opposite)

Zone 8 – Figures 1-19
Lower Tremadocian (Ordovician) – Figures 20-22

aff. **Raymondina** sp.
Figure 1. Cranidium, X10, boulder 73A, GSC 69569.

**Apatokephaloides** sp.
Figure 2. Cranidium, X2.7, boulder 80, GSC 69570.

**Hungaia magnifica** (Billings).
Figure 3. Anterior portion of cranidium, X2, boulder 82, GSC 69571.
Figure 4. Pygidium, X2, boulder 81, GSC 69572.

**Punctularia** sp.
Figure 5. Cranidium, X7, boulder 80, GSC 69573.

**Yukonaspis** sp.
Figure 6. Cranidium, X8, boulder 86, GSC 69574.

**Bienvillia corax** (Billings).
Figure 7. Cranidium, X15, boulder 81, GSC 69575.

**Paranorwoodia** sp.
Figure 8. Cranidium, X7, boulder 81, GSC 69576.

**Keithia** sp.
Figure 9. Cranidium, X10, boulder 81, GSC 69577.

**Kathleenella** sp.
Figure 10. Cranidium, X12, boulder 246, GSC 69578.

Unnamed genus and species
Figure 11. Cranidium with break crossing anterior lobe of glabella, X12, boulder 80, GSC 69579.

**Zacompsus** sp.
Figure 12. Cranidium with longitudinal ridge on posterior half of glabella, X10, boulder 240, GSC 69580.

Undescribed agnostid.
Figure 13. Cephalon, X9, boulder 493, GSC 69581.
Figure 17. Pygidium, X10, boulder 493, GSC 69582.

**Saukiella**? sp.
Figure 14. Cranidium, X3, boulder 492, GSC 69583.

**Lotagnostus** sp.
Figure 15. Cephalon, X3.5, boulder 290, GSC 69584.

**Heterocaryon** sp.
Figure 16. Cranidium, X5.5, boulder 492, GSC 69585.

**Lecanopyge** sp.
Figure 18. Cranidium, X2, boulder 86, GSC 69586.

**Loganopeltoides** sp.
Figure 19. Pygidium, X4, boulder 240, GSC 69587.

**Symphysurina** sp.
Figure 20. Cranidium, X2, boulder 496, GSC 69588.

**Boeckaspis** cf. **B. hirsuta** (Brogger).
Figure 21. Cranidium, X7, boulder 496, GSC 69589.

**Hystricurus** sp.
Figure 22. Cranidium, X2.7, boulder 496, GSC 69590.

PLATE 1.5

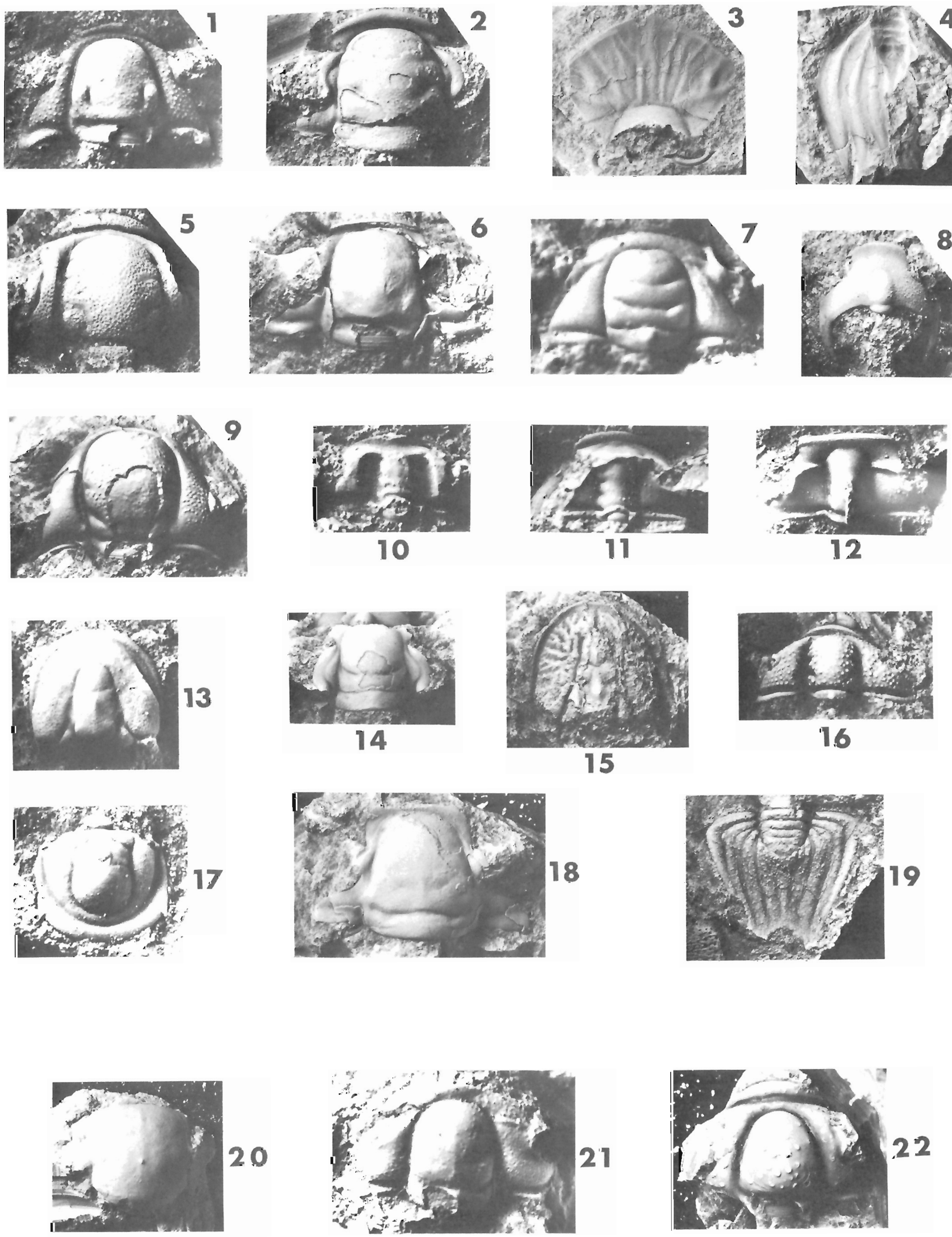

# PLATE 1.6


**Figure 1.** Outcrop of Zone 2 (background between levels of shoulder and top of C.H. Kindle Jr.'s head), Eastern Point, Western Brook Pond. Photo taken during exceptionally low water level. Precambrian rocks form cliffs rising 600 m above Pond. GSC photo 203852.


**Figure 2.** Zone 2 conglomerate that contained boulders WBP 1-7, westernmost outcrop on Eastern Point, Western Brook Pond. Same (or similar) Zone 2 conglomerate outcrops across syncline (?) near the eastern side of Eastern Point. However, at latter locality adjacent massive white limestone is present that is not seen on west side. M.A. Kindle provides scale. GSC photo 203852-B.


**Figure 3.** Zone 3 conglomerate that contained boulders 90-98, White Point, south shore of St. Pauls Inlet. Vertically dipping autochthonous Lower Cambrian sandstone outcrops a short distance inland from this locality. The sandstone is exposed at the base of a high, intermittent waterfall issuing from a small cirque. East of the Zone 3 outcrop and along the shoreline is an exposure of autochthonous St. George Formation (Ordovician) overlying Precambrian rock. GSC photo 203852-G.

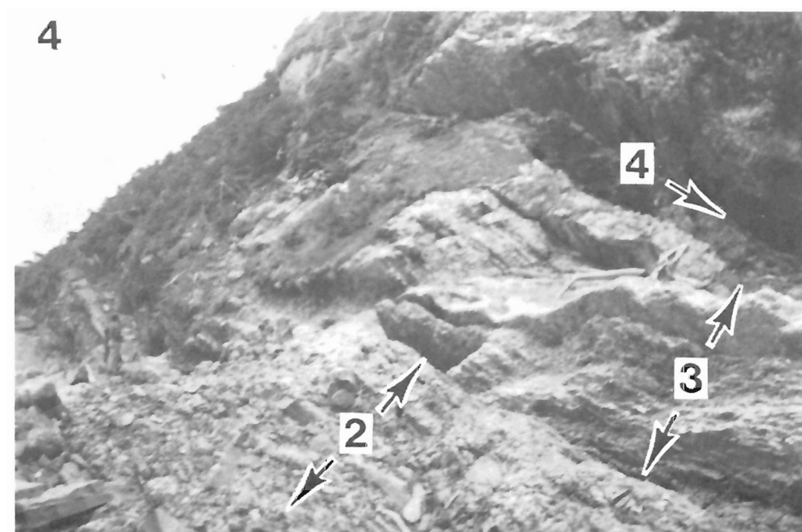


**Figure 4.** Strata on the south side of Sandy Cove, Broom Point area. Four-foot conglomerate containing Zone 2 fossils is in interval 2. The overlying white limestone that produced Zone 3 fossils is in interval 3. The base of the 50-foot conglomerate containing Zone 4 boulders and some white boulders of Zone 3 is located immediately above horizon 4. Between the top of interval 3 and horizon 4 is a recessive, so far barren, black shale. GSC photo 203852-D.

1

**Figure 1.** Zone 3 conglomerate exposed on low, curving White Rock Islets surrounded by water in middleground. Boulders 600-609, 611-628, and 630-634 are from this locality. View is to northeast from Cow Head Peninsula. GSC photo 203775-Y.

2

**Figure 2.** East dipping Zone 3 conglomerates on White Rock Islets. Parson Pond Hill, an asymmetric anticline, is on far skyline. GSC photo 203852-C.

3

**Figure 3.** Zone 5 conglomerates, northeast shore of Cow Head Peninsula. These beds provided boulders 8A, 10-16. GSC photo 203775-W.

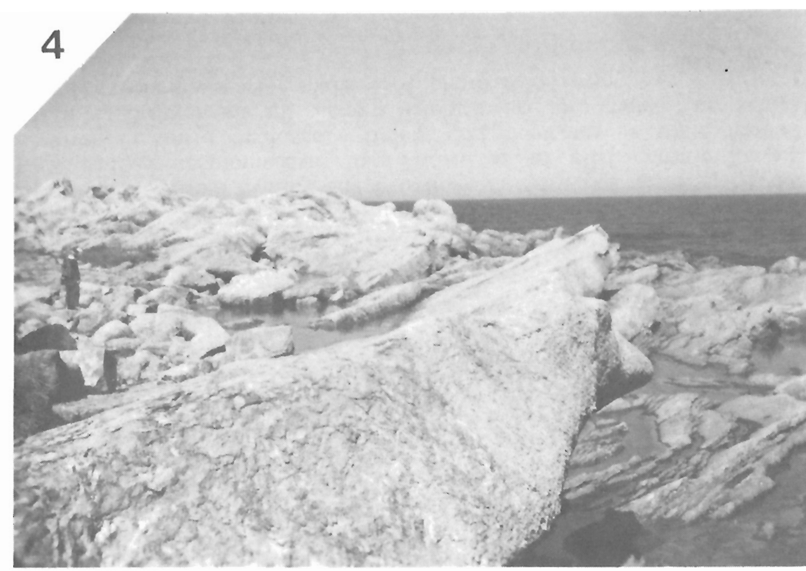

4

**Figure 4.** View to northwest of conglomerate bed between lighthouse and Beachy Cove on Cow Head Peninsula (Kindle and Whittington, 1958, Fig. 2). Diagnostic fossils were not found in bed in foreground, but Zone 5 fossils were located along the shore on either side of bed. Zone 8 trilobites were also collected in boulders 73, 73A, 73B, etc., at top of cliffs to the left of view. GSC photo 203775-X.

**PLATE 1.7**

1

**Figure 1.** View looking south at Cow Head Peninsula from Stearing Island. Cow Head Group conglomerate in foreground belongs to the Ordovician. GSC photo 203852-E.

2

**Figure 2.** View to southeast from boat of beds 6 and 7 at Crow's Nest, Cow Head Peninsula (Kindle and Whittington, 1958, Fig. 2; Pl. 2, fig. 1). Thick bedded conglomerates (bed 7) at top of cliff contain Zone 8 trilobites in white boulders. Below conglomerates is shale (bed 6) containing **Dictyonema** sp. Zone 8 trilobites are also known from strata below **Dictyonema**-bearing shale. GSC photo 203852-A.

3

**Figure 3.** View to west of Martin Point from highway. Visible are conglomerate beds belonging to Zone 7 (boulders 527, 529-555). At base of cliff (not visible) below grass in foreground is a conglomerate bed in which H.B. Whittington located Zone 6 boulder 528. GSC photo 203852-F.

4

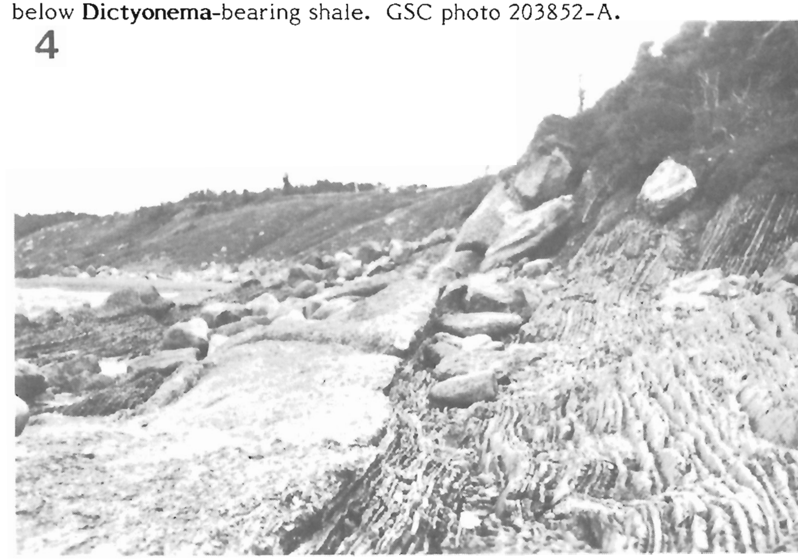

**Figure 4.** View to northeast between Martin Point and Broom Point of interbedded platy limestone and shale. Thick conglomerate bed contains only small pebbles. Experience has shown that conglomerates of this type rarely produce trilobites. A simialr conglomerate bed to left of view contained a large boulder (525) with fossils belonging to Zone 6. GSC photo 203775-Z.

**PLATE 1.8**

Zone 4

Boulders and trilobites belonging to Zone 4 in the 50-foot conglomerate in the Broom Point area are as follows:

Boulder 458 – **Ptychagnostus aculeatus** (Angelin), **Phalacroma glandiforme** (Angelin), **Lecanopleura** sp., **Bynumia**? sp., and **Onochonotopsis** sp. (with occipital spine).

Boulder 466 – **Blountia** sp. and **Hemirhodon** sp.

Boulder 468 – **Phalacroma glandiforme, Bynumia**? sp., **Modocia** sp., **Bolaspidella**? sp. (with projection on anterior border), **Lonchocephalus**? sp., new genus (flat occipital ring merging with fixed cheeks), and **Liostracinoides**? sp. (pitted surface).

Boulder 469 – **Bolaspidella** sp., **Bolaspidella**? sp. (with projection on anterior border), and **Liostracinoides** sp. (pitted with some pustules).

Boulder 470 – **Kormagnostus** sp., **Homagnostus**? sp., **Hemirhodon** sp., **Bolaspis**? sp. (swollen brim and flat occipital spine), **Arapahoia** sp., and **Aposolenopleura**? sp.

Boulder 472 – undescibed genus aff. **Dartonaspis** sp. and **Liostracinoides**? (pitted surface).

Zone 4 is correlated with the uppermost part of the **Bolaspidella** Zone in the North American Fauna Province. **Ptychagnostus aculeatus** and **Phalacroma glandiforme** are used to correlate Zone 4 with Westergard's (1946) Zone C2 in the Middle Cambrian of Sweden.

Zone 4 fossils were found only in the 50-foot conglomerate on the southeast limb of the Sandy Cove anticline. There the next highest collection belongs to Zone 6. On the northwest limb no fossils were found between Zone 1 and Zone 7.

Zone 5

Zone 5 fossils are from conglomerate beds 1, 3 and 4 on the north shore of Cow Head Peninsula (Kindle and Whittington, 1958, Fig. 2, 3). **Pseudagnostus** sp. is common in this and younger zones, and is therefore omitted from the following lists.

Boulder 11 – **Clavagnostus** sp., **Baltagnostus**? sp., **Cedaria** sp., **Crepicephalus** sp., **Tricrepicephalus** sp., **Meteoraspis**? sp., **Kingstonia** sp., **Holcacephalus** sp., **Blountia** sp., **Onchonotopsis** sp., **Bolaspidella**? sp., and **Liostracinoides**? sp.

Boulder 15 – **Cedaria** sp., **Crepicephalus** sp., **Kingstonia** sp., **Deiracephalus** sp., **Holcacephalus** sp., and **Terranovella obscura** Lochman.

Boulder 34 – **Clavagnostus** sp., undescribed agnostid, **Cedaria** sp., **Meteroaspis** sp., **Deiracephalus unicornis** Palmer, **Coosella**? sp., and **Coosia**? sp.

Boulder 39 – **Acmarhachis** sp., **Kormagnostus** sp., **Pseudagnostina** sp., **Hypagnostus** sp., **Aspidagnostus** sp., **Cedaria** sp., **Meteoraspis** sp., **Crepicephalus**? sp., **Blountia** sp., **Holcacephalus** sp., **Deiracephalus unicornis, Kingstonia** sp., and **Lecanopleura** sp.

At Hickey Cove, 1.6 km east of Broom Point (Fig. 1.2), Zone 5 boulders are mixed with those of Zone 6. Stratigraphically higher are Zone 7 trilobites in boulders surrounded by a matrix that is more recessive than that surrounding Zone 6 and 7 boulders below.

In addition to the Cow Head Group material, I have collected Zone 5 trilobites from Murphy Creek on the Gaspé Peninsula, Québec (Kindle, 1948). The Murphy Creek material includes **Clavagnostus** cf. **C. sulcatus** Westergard.

Zone 5 is correlated with the **Cedaria** and **Crepicephalus** zones in the North American Faunal Province. The presence of **Clavagnostus** cf. **C. sulcatus** on the Gaspé Peninsula suggests that at least part of Zone 5 correlates with the uppermost Middle Cambrian (Westergard, 1946, Zone C3) in Sweden.

Zone 6

The following Zone 6 fossils were found in bed 5 located (Kindle and Whittington, 1958, Fig. 2) northwest of the lighthouse on Cow Head Peninsula:

Boulder 48 – **Aphelaspis** sp., and **Blountia** sp.

Boulder 49 – **Pseudagnostus communis** (Hall and Whitfield), **Agnostus inexpectans** Kobayashi, **Homagnostus** cf. **H. obesus** (Belt), **Aphelaspis** sp., **Dunderbergia** sp., and **Onchopeltis**? sp.

Boulder 51 – **Aphelaspis** sp., **Dytremacephalus** sp., and **Tholifrons** sp.

Boulder 56 – **Aphelaspis** sp. and **Glyptagnostus reticulatus** (Angelin).

Boulder 57 – **Acmarhachis** sp., **Homagnostus** cf. **H. obesus, Bathyholcus** sp., **Cheilocephalus** sp., **Pterocephalops** sp., **Tholifrons** sp., **Bellaspis**? sp., and **Quebecaspis** spp. (2 species).

Zone 6 boulders from elsewhere in the Cow Head Group are listed as follows:

Boulder 166 – (1.16 km east of Broom Point) **Onchopeltis** sp., **Dunderbergia** sp., **Dytremacephalus** sp. and **Pterocephalops** sp.

Boulder 528 – (lowest conglomerate at Martin Point) **Aphelaspis** sp., **Dunderbergia** sp., **Dytremacephalus** sp., **Pterocephalops** sp.

Other Zone 6 fossils were collected at the bend of the shore line midway between Western Brook and Martin Point.

Zone 6 fossils are correlated with the upper part of the Dresbachian Stage in the North American Faunal Province. **Glyptagnostus reticulatus** is used to correlate Zone 6 with Westergard's (1947) Swedish Zones 2a and 2b.

Zone 7

The best boulders containing Zone 7 faunas are from 1.6 km east of Broom Point, north of Sandy Cove, and Martin Point. Locations east of Broom Point for the first five boulders mentioned below are shown in Figure 1.2.

Boulder 168 – **Homagnostus** sp., **Irvingella** sp., **Bathyholcus** sp., **Oligometopus** sp., **Xenocheilus** sp., and **Richardsonella** sp.

Boulder 172 – **Loganopeltoides** sp., **Taenicephalina** sp., and **Phoreotropis** sp.

Boulder 176 – **Parabolina** cf. **P. lobata lobata** (Brögger), **Protopeltura** sp., and cf. **Ctenopyge** sp. (glabella too wide).

Boulder 177 – **Protopeltura** sp., **Levisella brevifons** Rasetti, **Resseraspis** sp., and **Liostracinoides** sp.

Boulder 211 – **Peratagnostus** sp. and **Elvinia** sp.

Boulder 555 – (Martin Point) **Levisella brevifrons** Rasetti, **Simulolenus** sp., **Hungaia** sp. 1, **Liostracinoides** sp. and **Loganopeltoides kindlei** Rasetti.

Boulder 554 – (highest conglomerate at Martin Point) **Bathyholcus** sp., **Quebecaspis** cf. **Q. conifrons** Rasetti, **Richardsonella** sp. **Paraphoreotropis** sp., **Oligometopus** sp., **Xenocheilos** sp., and cf. **Xenocheilos** sp.

Zone 7 is correlated with the Franconian Stage in the North American Faunal Province. **Parabolina lobata lobata** (Brögger) and **Protopeltura** sp. occur (Henningsmoen, 1957, p. 300) in Norwegian strata equivalent to Westergard's (1947) Zone 5 in Sweden. The genus **Peratagnostus** is described by Opik (1967, p. 86) from the Idamean Stage of Australia.

Zone 8

Boulder 71 from thick sandstone in front of the lighthouse on Cow Head Peninsula probably represents the oldest part of Zone 8. It contains **Pseudosaukia brevifrons** (Clark), **Rasettia capax** (Billings), **Rasettia marcoui** (Clark), **Keithiella** sp., **Onchonotus globosus** (Billings), **Glyptometopus laflammei** (Clark), **Heterocaryon**? sp., and ?**Levisella brevifrons** Rasetti.

A probably somewhat younger conglomerate is present at the top of the cliff northeast of the lighthouse and near the bend in the shoreline. Blocks of conglomerate separating from the cliff produced boulders (74, 73, 73A, 73B, etc.) containing **Hungaia quadrispinosa** Rasetti, **Bienvillia** sp., **Peltura** sp., **Keithia** sp., **Richardsonella** sp., **Loganellus** sp., **Loganopeltoides** sp., aff. **Raymondina** sp., **Onchonotus** sp., **Keithiella** sp., **Stenopilus** sp., and **Apatokephaloides** sp.

Blocks (80-82, 86) fallen from the cliff southwest of the lighthouse have provided ?**Hungaia magnifica** (Billings), **Punctularia** sp., **Yukonaspis** sp. and an undescribed genus. Other trilobites from this area, from northeast of the lighthouse, and from east of Broom Point are: **Keithia** sp., **Keithiella** sp., **Bienvillia** sp., **Loganopeltoides** sp., and **Apatokephaloides** sp.

Boulder 245 (5th conglomerate bed below **Dictyonema** sp., east of Broom Point) – **Pseudagnostus gyps** (Clark), **Pseudagnostus canadensis** (Billings), **Litagnostus** sp., **Corbinia** sp., **Yukonaspis** sp., **Bienvillia** sp., **Onchonotus** sp., **Loganopeltoides** sp., **Keithia** sp., **Keithiella** sp., **Aposolenopleura** sp., **Westonaspis** sp., **Leiocoryphe** sp., **Idiomesus** (2 sp.), **Phoreotropis** sp., **Talbotina**? sp., **Apatokephalus**? sp., **Apatokephaloides** sp., **Ambonolium** sp., **Euptychaspis** sp., **Plethometopus** sp., **Glyptometopus** sp., **Stenopilus** sp., unidentified genus.

Boulder 493 (north of **Dictyonema** Hill near mouth of Western Brook) – **Prosaukia** sp. or **Saukiella** sp., **Yukonaspis** sp., **Euptychaspis**? sp., **Stenopilus** sp., **Leicoryphe** sp., **Idiomesus** sp., **Theodenisia gibba** (Rasetti), unidentified agnostid.

**Corbinia** sp. and **Yukonaspis** sp. also occur east of Broom Point in conglomerates below **Dictyonema** sp. and near the mouth of Western Brook. Boulder 290 from the south side of Mudge Cove provided a cephalon of **Lotagnostus** sp.

Trilobites in Zone 8 are correlated with the Trempealeauan Stage in the North American Faunal Province. **Peltura** sp. and **Lotagnostus** sp. in the present collections are also known from Westergard's (1947) Upper Cambrian Zone 5.

### Locality Data for Boulders

| | |
|---|---|
| Zone 1 | 260-273: lowest conglomerate, north side of Sandy Cove (Fig. 1,2).<br>350-380, 433: lowest conglomerate, south side of Sandy Cove (Fig. 1.2). |
| Zone 2 | 400-432, 434, 418A: 4-foot conglomerate, south side of Sandy Cove (Plate 1.6, fig. 4).<br>WBP 1, WBP 3, WBP 5-9: conglomerate at west end of Eastern Point, Western Brook Pond (Plate 1.6, fig. 2).<br>WBP 2, WBP 4: conglomerate 12 m east of synclinal cove, Eastern Point, Western Brook Pond. |
| Zone 3 | 90-98: White Point, St. Pauls Inlet (Plate 1.6, fig. 3).<br>140: 10 m from sea, northwest of lighthouse, Cow Head Peninsula.<br>448: white, bedded limestone above 4-foot conglomerate, south side of Sandy Cove (Plate 1.6, fig. 4).<br>450-452: 50-foot conglomerate, south side of Sandy Cove (Plate 1.6, fig. 4).<br>600-635, 600A, 601A, 602A, 606A, 607A, 615A, 615B, 615C: White Rock Islets (Plate 1.7, fig. 1, 2).<br>640-644: outer reef, Stearing Island. |
| Zone 4 | 453-473: 50-foot conglomerate, south side of Sandy Cove (Plate 1.6, fig. 4). |
| Zone 5 | 1-9, 17-20, 21-25: Beachy Cove, Cow Head Peninsula.<br>8A, 10-16: east end of Cow Head Peninsula (Plate 1.7, fig. 3).<br>26-39: northwest of lighthouse, Cow Head Peninsula.<br>127, 138, 198, 199, 213: 1.1 to 1.6 km east of Broom Point (Fig. 1.2).<br>MC: Murphy Creek, Gaspé County, Québec (Kindle, 1942). |
| Zone 6 | 48-69, 69B, 72: bed 5, northwest of lighthouse, Cow Head Peninsula (Kindle and Whittington, 1958, Fig. 2).<br>120-122, 124, 125, 129, 166, 173A, 179, 180, 194-197, 200-210, 212-214, 214A, 214B, 214C, 214D: 1.1 to 1.16 km east of Broom Point (Fig. 1.2).<br>480-484: above 50-foot conglomerate, south Sandy Cove (Plate 1.6, fig. 4).<br>523-525: bend in shoreline midway between Western Brook and Martin Point (Fig. 1.1; Plate 1.8, fig. 3).<br>528: lowest conglomerate at Martin Point (Fig. 1.1; Plate 1.8, fig. 3).<br>BC1, BC2: White Rocks (Islands), Bear Cove, lat. 49° 01' 20"N, long. 58° 28' 30"W. (Kindle and Whittington, 1965, Fig. 1). |
| Zone 6 or 7 | 160-165: 1 km east of Broom Point (Fig. 1.2). |
| Zone 7 | 70, 75: northwest of lighthouse, Cow Head Peninsula.<br>100-106, 108-110: 2.0 km east of Broom Point.<br>116-119, 123, 126, 128, 130-134, 136, 137, 139, 141-147, 167-178, 181, 182, 211, 124A, 132A: 1.6 km east of Broom Point.<br>274, 278-280, 282-287: north side of Sandy Cove.<br>526, 527, 529-555, 541A, 550A, 550B: Martin Point (Plate 1.8, fig. 3). |
| Zone 8 | 71, 73, 73A-N, 73U-Y, 74, 75a, 76, 78-86: near lighthouse, Cow Head Peninsula.<br>88: Green Island, entrance to St. Pauls Inlet.<br>107: 2.0 km east of Broom Point.<br>135, 148: 1.5 km east of Broom Point.<br>229-239: 0.46 to 0.85 km east of Broom Point (below sixth conglomerate to promitory).<br>240-248: first to sixth conglomerate below **Dictyonema**, 0.15 to 0.46 km east of Broom Point.<br>290-295, 290A, 290B, 291A, 291B: upper conglomerate, south side of Mudge Cove.<br>485-495: north of **Dictyonema** hill, mouth of Western Brook (Fig. 1.2).<br>SR: bedded strata along shoreline and 0.4 km south of mouth of Serpentine River, lat. 48° 56' 18"N, long. 58° 30' 35"W. (Kindle and Whittington, 1965, Fig. 1).<br>HF: Highate Falls, Vermont. |

**References**


Fåhraeus, L.E. and Nowlan, G.S.
1978: Franconian (Late Cambrian) to early Champlainian (Middle Ordovician) conodonts from the Cow Head Group, western Newfoundland; Journal of Paleontology, v. 52, no. 2, p. 444-471.

Fortey, R.A. and Skevington, D.
1980: Correlation of Cambrian-Ordovician boundary between Europe and North America: new data from western Newfoundland; Canadian Journal of Earth Sciences, v. 17, p. 382-388.

Henningsmoen, G.
1957: The trilobite family Olenidae; Skrifter utgitt av Det Norske Videnskaps-Akademi I Oslo, Matematisk-Naturvidenskapelig. Klasse, no. 1, 303 p.

James, N.P.
1981: Megablocks of calcified algae in the Cow Head Breccia, western Newfoundland: vestiges of Cambro-Ordovician platform margin; Geological Society of America, Bulletin, Pt. 1, v. 92, p. 799-811.

Johnson, H.
1941: Paleozoic lowlands of northwestern Newfoundland: New York Academy of Science, Transactions, ser. 2, v. 3, no. 6, p. 141-145.

Kindle, C.H.
1942: **Alsataspis** in Newfoundland; The Canadian Field-Naturalist, v. 56, no. 3, p. 33.

1943: A preliminary list of Late Cambrian trilobites found on the west coast of Newfoundland; The Canadian Field-Naturalist, v. 57, p. 7-8.

1948: Crepicephalid trilobites from Murphy Creek, Québec, and Cow Head, Newfoundland; American Journal of Science, v. 246, no. 7, p. 441-451.

1981: Cambrian faunas in the limestone conglomerates of western Newfoundland; in Short Papers for the Second International Symposium on the Cambrian System, 1981; United States Geological Survey, Open-file Report 81-743, p. 106-110.

Kindle, C.H. and Whittington, H.B.
1958: Stratigraphy of the Cow Head region, western Newfoundland; Geological Society of America, Bulletin, v. 69, p. 315-342.

1959: Some stratigraphic problems of the Cow Head area in western Newfoundland; Transactions of the New York Academy of Sciences, ser. II, v. 22, no. 1, p. 7-18.

1965: New Cambrian and Ordovician fossil localities in western Newfoundland; Geological Society of America, Bulletin, v. 76, p. 683-688.

Lochman, C.
1938: Middle and Upper Cambrian faunas from western Newfoundland; Journal of Paleontology, v. 12, p. 461-477.

Logan, W.E.
1863: Report of progress from its commencement to 1863; Geological Survey of Canada, 983 p.

Opik, A.A.
1967: The Mindyallan fauna of north-western Queensland; Australian Bureau of Mineral Resources, Geology and Geophysics, Bulletin no. 74, 404 p.

Oxley, P.
1953: Geology of Parsons Pond-St. Pauls area, West Coast; Newfoundland Geological Survey Report 5, 53 p.

Rasetti, F.
1948: Cephalic sutures in **Loganopeltoides** and the origin of the "hypoparian" trilobites; Journal of Paleontology, v. 22, p. 25-29.

Raymond, P.E.
1925: Some trilobites of the lower Middle Ordovician of eastern North America; Museum of Comparative Zoology of Harvard College, Bulletin v. 67, no. 1, 180 p.

Rodgers, J. and Neale, E.R.W.
1963: Possible "Taconic" klippen in western Newfoundland; American Journal of Science, v. 261, p. 713-730.

Schuchert, C. and Dunbar, C.O.
1934: Stratigraphy of western Newfoundland; Geological Society of America, Memoir 1, 123 p.

Westergard, A.H.
1946: Agnostidea of the Middle Cambrian of Sweden; Sveriges Geologiska Undersokning, Ser. C, no. 477, Arsbok 40 (1946), no. 1, 140 p.

1947: Supplementary notes on the Upper Cambrian trilobites of Sweden; Sveriges Geologiska Undersokning, Ser. C, no. 489, Arsbok 41 (1947), no. 8, 34 p.

Whittington, H.B.
1963: Middle Ordovician trilobites from Lower Head, Western Newfoundland; Bulletin of the Museum of Comparative Zoology, at Harvard College, v. 129, no. 1, 118 p.

1965: Trilobites of the Ordovician Table Head Formation, Western Newfoundland; Bulletin of the Museum of Comparative Zoology, Harvard University, v. 132, no. 4, 441 p.

Whittington, H.B. and Kindle, C.H.
1969: Cambrian and Ordovician stratigraphy of Western Newfoundland; in North Atlantic-geology and continental drift; American Association of Petroleum Geologists, Memoir 12, p. 655-664.

2.

# GEOCHEMICAL INVESTIGATIONS OF URANIUM ANOMALIES IN THE ARCHEAN HOPEDALE BLOCK AND PROTEROZOIC ISLAND HARBOUR INTRUSIVE COMPLEX, LABRADOR

Project 760043

D.R. Boyle
Resource Geophysics and Geochemistry Division

*Boyle, D.R., Geochemical investigations of uranium anomalies in the Archean Hopedale Block and Proterozoic Island Harbour Intrusive Complex, Labrador; in Current Research, Part C, Geological Survey of Canada, Paper 82-1C, p. 19-29, 1982.*

***Abstract***

*Regional lake water and lake sediment uranium anomalies in the Archean Hopedale Block and Island Harbour Intrusive Complex appear to be related to accelerated weathering of well exposed bedrock having an open structural fabric. Structurally-controlled groundwater leaching may be a major control on hydromorphic dispersion in some areas whereas the coarse grained nature of intrusive rocks in areas such as the Island Harbour Intrusive Complex may be a major factor contributing to accelerated weathering and release of labile uranium. Rock units underlying anomalous areas in this region are not enriched in U; some are depleted compared to their counterparts in other Shield areas. Ground and airborne radiometric surveys failed to delineate areas of mineralization within these anomalies.*

## Introduction

Geochemical lake sediment and lake water reconnaissance surveys carried out in Labrador under the auspices of the joint Federal-Provincal Uranium Reconnaissance Program have outlined a number of anomalous areas for uranium (Fig. 2.1). As part of the follow-up studies, three of these anomalies in the northeastern portion of Labrador were investigated by the author. These three anomalies, which occur in both waters and sediments, are outlined in Figure 2.1 as the Hunt River Belt (area A), Hunt Lake area (area B) and the Island Harbour Intrusive Complex (area D). Two other anomalies, one near Shapio Lake (area C) and the other at Ugjoktok Bay (Florence Lake Group, area G) were visited only briefly in the time available; these two areas were found to be very similar in geological settings to the Hunt Lake and Hunt River Belt areas respectively. Previous to the investigations carried out by the author, detailed lake sediment, lake water and airborne radiometric surveys of the Hunt River Belt, Hunt Lake and Island Harbour Intrusive Complex anomalies were carried out by McConnell (1980) in order to obtain a better definition of anomalous patterns. The geochemical component of these surveys confirmed the presence of the anomalies although indicating that they were somewhat more diffuse than outlined by the regional interpretation. The Hunt River Belt and Hunt Lake anomalies occur within the Archean Hopedale Block (Ermanovics and Raudsepp, 1979; Ermanovics, 1980, 1981; and Ermanovics and Korstgard, 1981) and the Island Harbour anomaly occupies the northern portion of the Island Harbour Intrusive Complex. Since the Uranium Reconnaissance Program extends only as far south as 55°N in this region, no information is available on the distribution of U in the southern portions of either the Hopedale Block or the Island Harbour Intrusive Complex.

Five possible causes of the U anomalies considered during the investigations are:

a. regional mineralizing event(s),
b. underlying lithologies with a high uranium donor capacity,
c. leaching of glacial material,
d. accelerated weathering due to a high degree of exposure and/or an open, well-developed structure, and
e. environmental influences such as pH and sediment composition.

Since adequate data on lake sediment geochemistry was already available (McConnell, 1980), the greatest emphasis was placed on lithogeochemical studies, ground traverses to delineate mineralized zones, the influence of glacial material and the relationship between anomalies and basement structure.

Access to these areas is by fixed wing aircraft from Goose Bay to inland waters or by boat along the Atlantic coast to Hopedale. Work within the areas was supported by helicopter. The climate for this region is typically maritime with prolonged periods of rain and fog.

## Lake Sediment Geochemistry

To date approximately 134 000 $km^2$ of Labrador have been covered by regional lake sediment and water geochemistry under the Uranium Reconnaissance Program. Data from these surveys have been released as separate open files (Geological Survey of Canada Open Files 509, 510, 511, 512, 513, 557, 558, 559, 560) and as two collated files represented by 1:2 000 000 Applicon coloured compilations (Geological Survey of Canada Open Files 748 and 749). Approximately 9055 lake sites were sampled for a sample density of approximately one sample per 15 $km^2$.

The possibility that the anomalies in the Hopedale Block and Island Harbour Complex are the result of environmental factors related to such parameters as pH, sediment composition or Fe and Mn scavenging was investigated by comparing the chemical characteristics of lakes in the anomalous areas with the regional data from the Uranium Reconnaissance Program. Table 2.1 represents a comparison of correlation coefficients for data obtained from the anomalous areas (McConnell, 1980) and the regional coverage. As can be seen in this table there is a strong correlation between most of the coefficients generated from the two data sets. Data from the anomalous areas would appear to be a good subset of the regional data and the fact that correlation coefficients between U and pH, Fe, Mn and loss on ignition are not uniquely different from those of the regional data indicates that these anomalies are not the result of environmental factors of either a hydrochemical or compositional (sediment) nature. Climatic conditions are relatively homogeneous over most of the coastal region of Labrador and therefore cannot be considered as a local influence in forming anomalies.

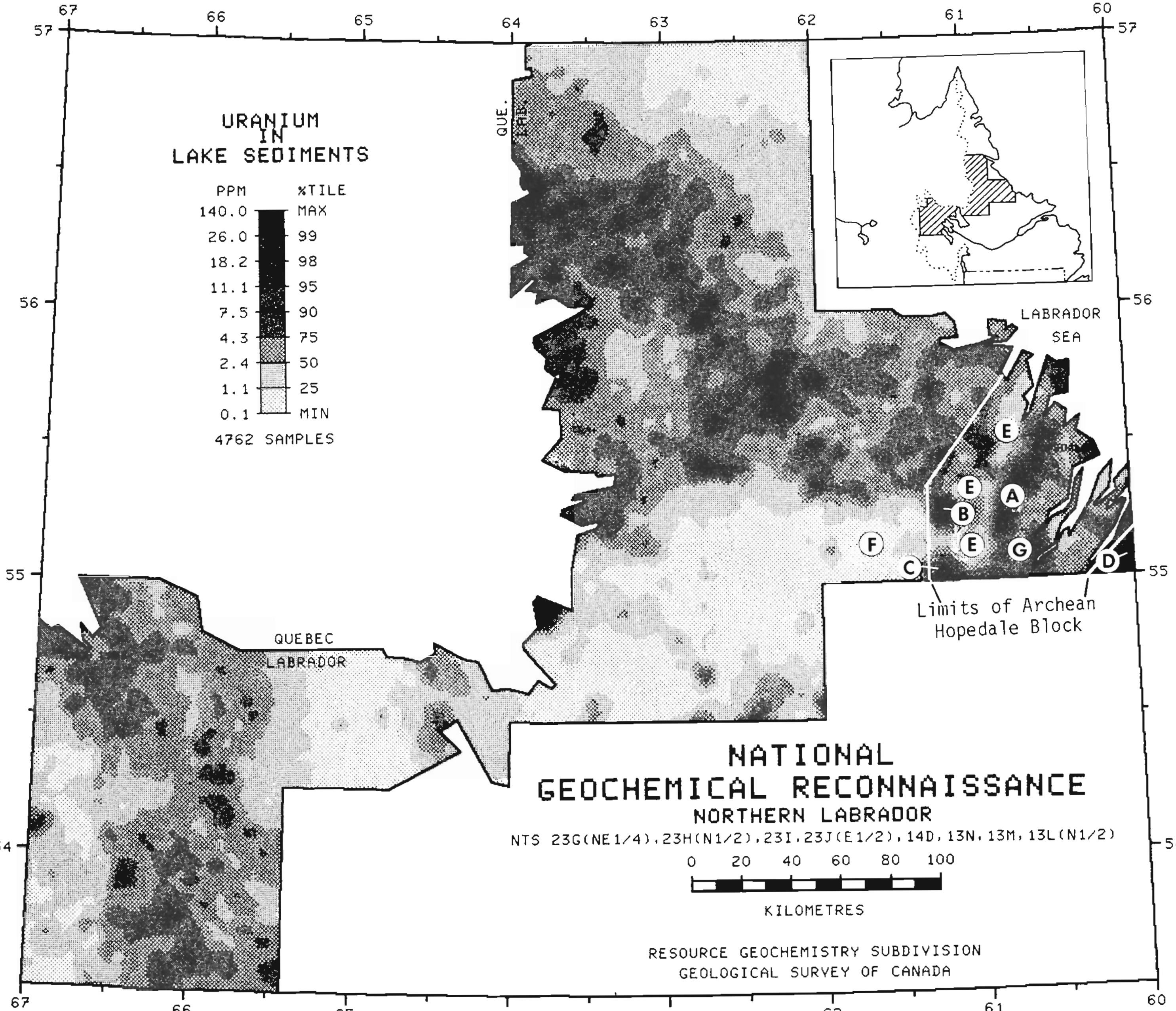


- A. *Hunt River Belt anomaly*
- B. *Hunt Lake anomaly*
- C. *Shapio Lake anomaly*
- D. *Island Harbour Intrusive Complex anomaly*
- E. *Ugjoktok-Big Bay glacial sand plain*
- F. *Harp Lake Anorthosite Complex*
- G. *Florence Lake anomaly*

***Figure 2.1.*** *Applicon contour plot of uranium in lake sediments, northern Labrador.*

Table 2.1

Correlation coefficients for follow-up lake sediment and water geochemistry on uranium anomalies in northeast Labrador; 369 sample sites, $\log_{10}$ transformed data (from McConnell, 1980)

| | U in Lake Sediments | | U in Lake Waters | |
|---|---|---|---|---|
| | Anomalous Areas (n = 369) | Regional Data (n = 9055) | Anomalous Areas (n = 369) | Regional Data (n = 9055) |
| U (sediment) | 1.00 | 1.00 | .59 | .56 |
| U (water) | .59 | .56 | 1.00 | 1.00 |
| pH | -.01 | .15 | .22 | .25 |
| Loss on Ignition | .06 | -.17 | -.15 | -.12 |
| F (water) | .08 | .31 | .26 | .28 |
| F (sediment) | .21 | .50 | .15 | .26 |
| Zn (water) | .05 | - | .22 | - |
| Zn (sediment) | .34 | .31 | -.01 | .12 |
| Cu (sediment) | .41 | .43 | -.01 | .13 |
| Pb (sediment) | .21 | .37 | .23 | .29 |
| Co (sediment) | .26 | .25 | .05 | .08 |
| Ni (sediment) | -.02 | .13 | .11 | .08 |
| Ag (sediment) | .21 | .18 | -.13 | .09 |
| Mn (sediment) | .26 | .25 | -.02 | .06 |
| Fe (sediment) | .29 | .29 | -.06 | .05 |
| Mo (sediment) | .36 | .58 | -.05 | .34 |
| Area | .12 | - | -.07 | - |
| Depth | .40 | - | -.05 | - |

The main direction of ice movement during glacial times was northwestward off the Harp Lake anorthosite complex. The possibility that these anomalies were created by leaching of glacially deposited material is extremely unlikely for the following reasons:

a. The Harp Lake Anorthosite complex (area F, Fig. 2.1), which contributed a considerable amount of the glacial till material, has a very low U content as exemplified by the regional survey. Very little U, therefore, would be available for leaching.

b. Much of the lowland area of the Hopedale Block is occupied by the Ugjoktok-Big Bay sand plain which represents outwash from glacial retreat. This area (area E, Fig. 2.1) is outlined quite well by the regional survey as a uranium low.

c. Within the anomalies, lakes displaying high U contents tend to be located in areas where there is very little glacial cover. In fact for some anomalous areas bedrock exposure is greater than 80 per cent.

It is evident, therefore, that glaciation, if anything, has had a negative effect on uranium concentration in lake sediments and waters.

For the regional data, the threshold values for U in lake sediments and waters, calculated as mean plus two standard deviation levels of log 10 transformed data, are 12 ppm and 0.20 ppb respectively. These levels have been used to show the distribution of U within the three anomalous areas investigated (Fig. 2.2-2.4). As a measure of correlation between U in waters and sediments, different symbols have been used to represent anomalies in waters only, sediments only or both. There is a strong significant correlation between U in sediments and U in waters for data from both the follow-up and regional surveys ($r = 0.59$ and $0.56$ respectively, Table 2.1).

Ground radiometric surveys were carried out in areas with a high cluster of anomalous lakes to delineate mineralized zones. Surface rock samples were collected to give an adequate sample density for the various units in each of the anomalous areas; samples were analyzed for U (delayed neutron activation) and selectively for Th (X-ray fluorescence). Recent glaciation insured that relatively fresh samples could be taken. The samples analyzed represent those taken by the author during traverses and helicopter checks as well as those taken by I. Ermanovics (Geological Survey of Canada) during 1:100 000 scale mapping of the Hunt River Belt and parts of the Island Harbour Intrusive Complex. Data for these rocks are listed in Tables 2.2, 2.3, and 2.4. A description of the results of investigations in each of the three anomalous areas follows.

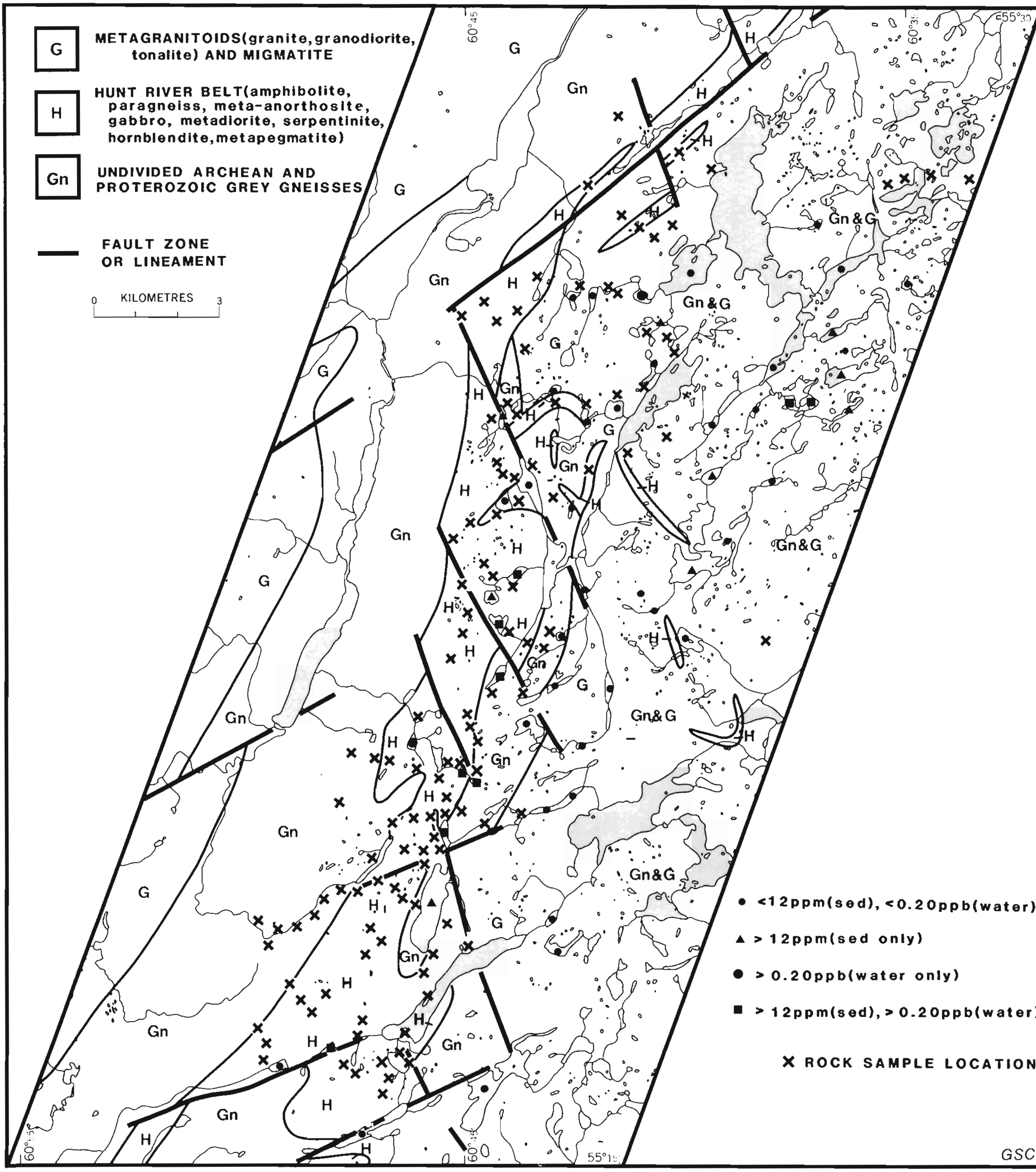


*Figure 2.2.* Generalized geology of Hunt River Belt (after Ermanovics, 1981), rock sample locations and distribution of uranium in lake waters and sediments. Regional threshold values for U in waters and sediments are 0.20 ppb and 12 ppm respectively.

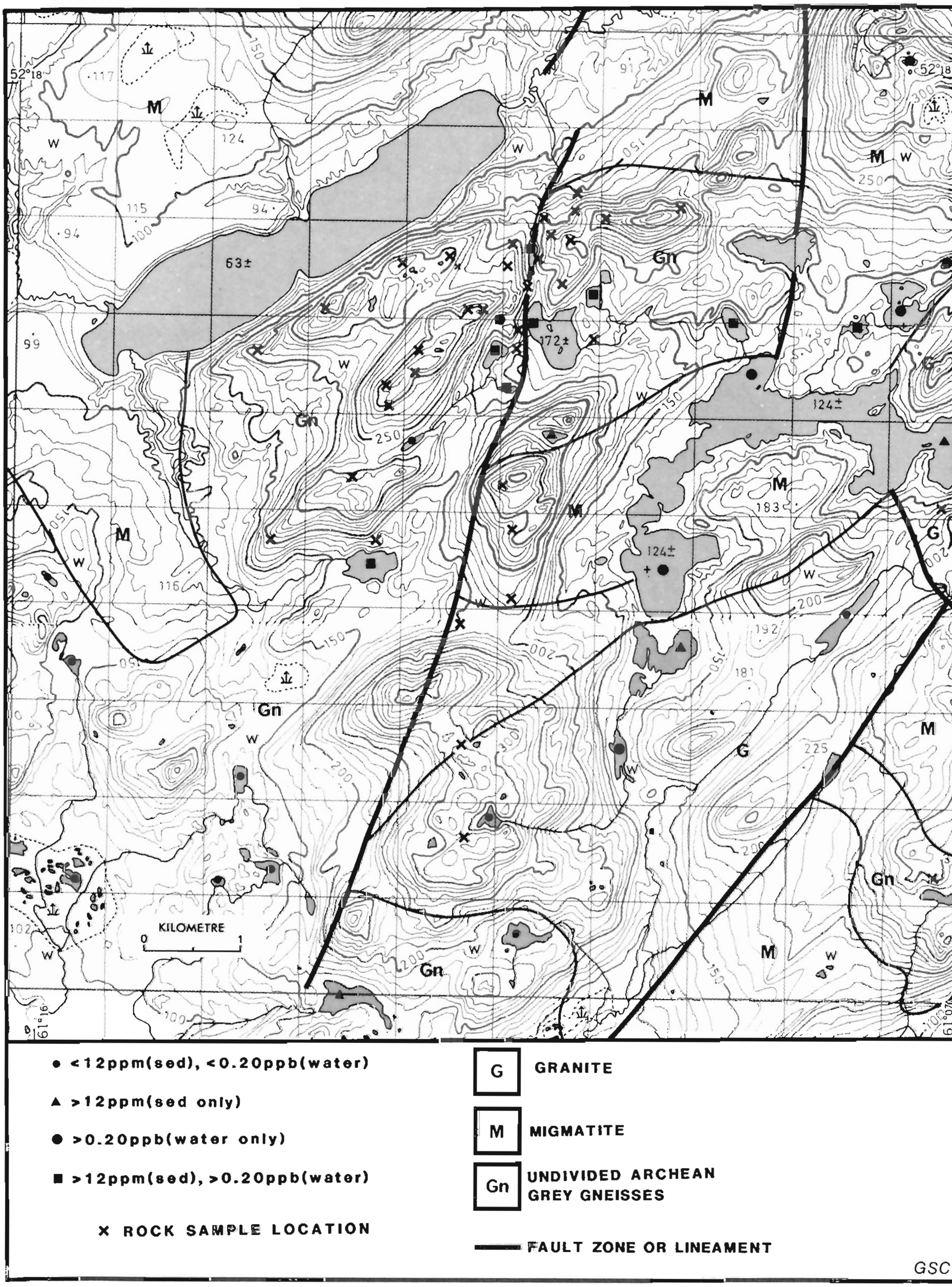


*Figure 2.3.* *Generalized geology of Hunt Lake area (I. Ermanovics, personal communication), rock sample locations and distribution of uranium in lake waters and sediments. Regional threshold values for U in waters and sediments are 0.20 ppb and 12 ppm respectively.*

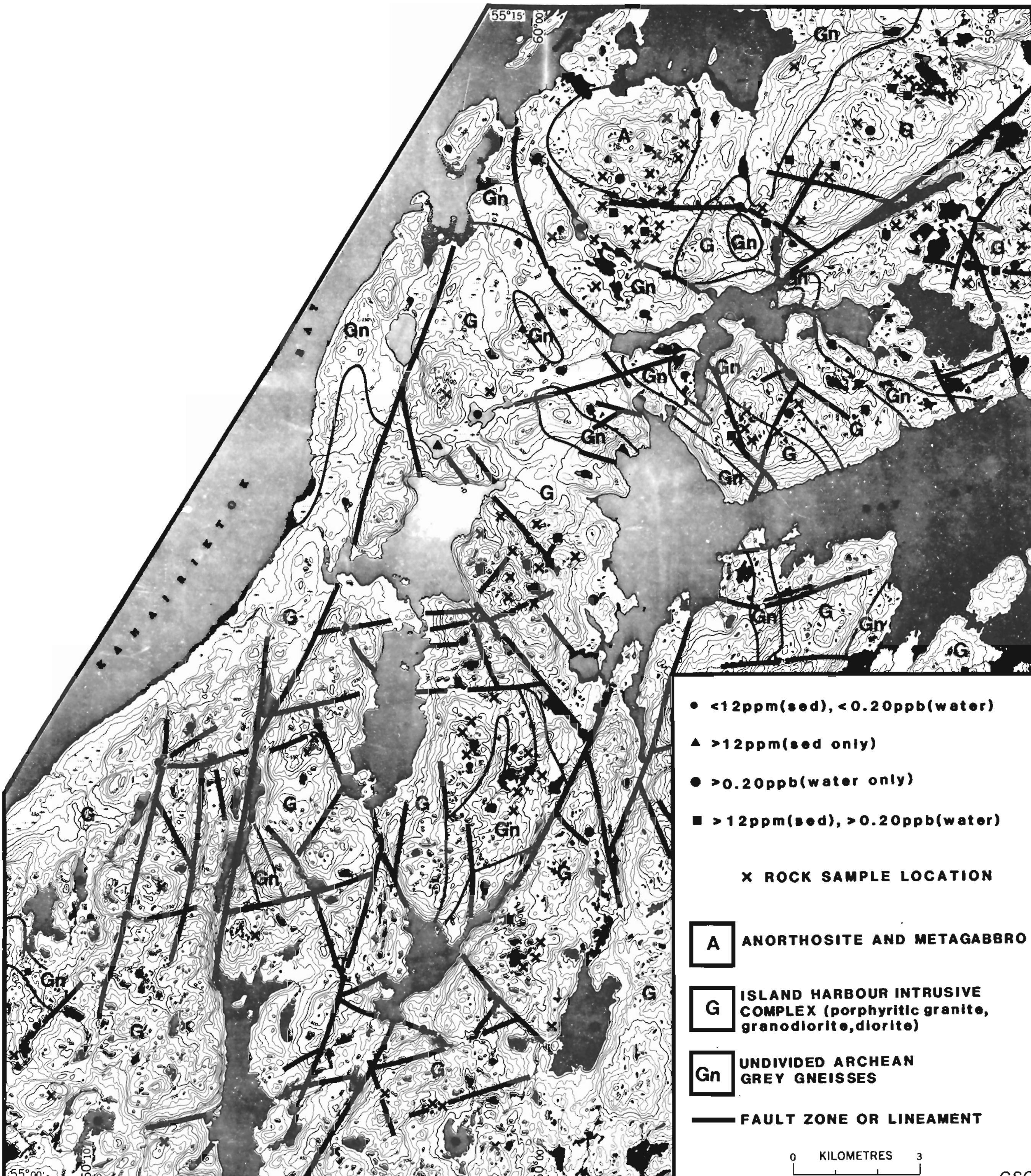


*__Figure 2.4.__ Generalized geology of Island Harbour Intrusive Complex (I. Ermanovics, personal communication), rock sample locations and distribution of uranium in lake waters and sediments. Regional threshold values for U in waters and sediments are 0.20 ppb and 12 ppm respectively.*

**Archean Hopedale Block**

The rocks of the Archean Hopedale Block comprise ortho- and paragneiss as well as metavolcanic supracrustal rocks and late granitoids (Ermanovics and Raudsepp, 1979; Ermanovics 1980, 1981; Ermanovics and Korstgard, 1981). To the north and west this block is intruded by Elsonian igneous rocks composed largely of anorthosite (e.g. Harp Lake Complex, area F, Fig. 2.1). To the south the Archean rocks are unconformably overlain by the Proterozoic Seal Lake and Moran Lake groups and are also intruded in the southeast by the Island Harbour Intrusive Complex.

The oldest rocks of the Hopedale Block comprise the Weekes amphibolite and Maggo gneiss. The Weekes amphibolite has been correlated to the Hunt River volcanics (Ermanovics and Korstgard, 1981). The Maggo gneiss is included in the Archean grey gneisses of Figures 2.2, 2.3, and 2.4. These rocks consist of medium grained, granoblastic quartzofeldspathic grey gneiss containing less than 20 per cent garnet, biotite, pyroxene and hornblende (Ermanovics, 1981). Apart from the supracrustal rocks other units of the Hopedale Block include migmatitic gneiss, included with metagranitoids in the Hunt River Belt (Fig. 2.2) and recognized as a separate unit in the Hunt Lake area (Fig. 2.3), and the Kanairiktok intrusions consisting of tonalitic, granodioritic and minor granitic late granitoids intrusive into all other units of the Hopedale Block.

Two Archean supracrustal metavolcanic belts (Hunt River Belt and Florence Lake Group) occur within the Hopedale Block. Both these belts have associated regional anomalies (areas A and G, Fig. 2.1). However, only the northern tip of the Florence Lake Group has been covered by the Uranium Reconnaissance Survey and interpretation of geochemical anomalies over this group will have to await completion of regional surveys. Rocks of the Hunt River Belt consist of intercalated amphibolite, metabasalt, variegated schist and lesser amounts of felsic gneiss and ultramafic rocks. The Florence Lake Group is made up of mafic flows and intermediate to felsic pyroclastic rocks.

With the exception of the late granitoids, which have been subject to lower amphibolite facies metamorphism, all of the Archean rock units in the Hopedale Block have undergone upper amphibolite grade metamorphism and some have been overprinted by middle greenschist facies metamorphism (Ermanovics and Raudsepp, 1979).

The only Proterozoic rocks recognized in the area are crosscutting diabase dykes and small bodies of metagabbro.

Ermanovics and Korstgard (1981) have recognized four main structural trends in the Hopedale Block based mainly on directional homogeneity of planar and/or linear structures:

a. the Hopedale Trend characterized by a NW-SE striking, steeply dipping NE planar trend and a SE plunging linear trend

b. the Fiord Trend typified by a NE-SW subvertical planar trend and a NE plunging linear trend

c. the Makkovik Trend confined to the southern part of the Hopedale Block and having a similar planar trend to the Fiord Trend but with linear structures plunging steeply WSW, and

d. the Kanairiktok Shear Zone which is a NNE-SSW subvertical zone along the southern boundary of the Hopedale Block.

Table 2.2

Uranium and thorium contents of major rock units in the Hunt River Belt, Labrador

| Rock Unit | U (ppm)* | | Th (ppm)* | | Th/U | |
|---|---|---|---|---|---|---|
| | Range | Average | Range | Average | Range | Average |
| SUPRACRUSTALS: | | | | | | |
| amphibolite | <0.2- 6.1 | 0.5(42) | <1.0- 6.0 | 1.9(14) | <1.0- 6.0 | 3.8 (3) |
| paragneiss | <0.2- 3.7 | 0.6(28) | <1.0- 5.0 | 1.6 (9) | <1.0- 5.0 | 4.0 (4) |
| schist | 0.2- 1.0 | 0.5 (4) | <1.0 | <1.0 (3) | - - | - (-) |
| metadiorite | <0.2- 2.7 | 0.9(10) | <1.0- 7.0 | 2.4 (9) | 1.3- 5.0 | 2.6 (7) |
| ultramafic | <0.2- 0.4 | 0.1 (6) | <1.0, 4.0 | 2.2 (2) | - - | - (-) |
| ORTHOGNEISSES: | | | | | | |
| leucocratic gneiss | <0.2- 3.1 | 1.0(22) | 1.0- 5.0 | 1.9(13) | 0.5- 5.0 | 2.9 (7) |
| mafic gneiss | 0.4- 1.1 | 0.8 (5) | <1.0- 3.0 | 1.1 (4) | 3.3 | 3.3 (1) |
| LATE GRANITOIDS: | | | | | | |
| pegmatite | 2.0- 5.4 | 3.4 (6) | <1.0-47.0 | 13.0 (6) | 2.2- 8.7 | 3.9 (5) |
| felsic gneiss | 0.3- 3.3 | 1.7 (4) | <1.0- 7.0 | 4.3 (3) | 2.2, 4.2 | 3.2 (2) |
| aplite | 0.3- 2.4 | 1.2 (3) | <1.0- 9.0 | 3.3 (3) | 1.3, 3.3 | 2.3 (2) |
| granodiorite | <0.2- 2.3 | 0.7 (9) | <1.0 | <1.0 (4) | - | - (-) |
| diabase | 0.3- 0.9 | 0.6 (7) | 1.0- 7.0 | 5.0 (7) | 5.6-12.5 | 7.0 (7) |
| CATACLASTIC ROCKS: | | | | | | |
| sheared orthogneiss | 1.0- 4.0 | 2.3 (6) | <1.0- 3.0 | 1.4 (5) | 0.6- 1.4 | 0.9 (3) |
| sheared metadiorite | 0.5 | 0.5 (1) | 2.0 | 2.0 (1) | 4.0 | 4.0 (1) |
| fault breccia | 0.3 | 0.3 (1) | <1.0 | <1.0 (1) | - - | - (-) |

*number of analyses in brackets

Table 2.3

Uranium and thorium content of rocks in the Hunt Lake anomaly

| Rock Unit | U (ppm)* | | Th (ppm)* | | Th/U | |
|---|---|---|---|---|---|---|
| | Range | Average | Range | Average | Range | Average |
| pegmatite | 1.1-15.4 | 7.1 (4) | 3.0,51.0 | 27.0 (2) | 0.2, 4.8 | 2.5 (2) |
| granite | 0.3- 2.0 | 0.9 (6) | 4.0,14.0 | 9.0 (2) | 2.0, 9.3 | 5.6 (2) |
| monzonite | 0.4- 6.9 | 3.3 (4) | <1.0- 4.0 | 21.7 (3) | 1.3, 3.8 | 2.1 (2) |
| granodiorite | 0.6- 1.7 | 1.3 (3) | <1.0-12.0 | 4.7 (3) | 2.9, 7.1 | 5.0 (2) |
| tonalite | <0.2- 5.3 | 1.2 (9) | <1.0 | <1.0 (5) | - - | - (-) |
| orthogneiss | <0.2- 1.1 | 0.7(10) | <1.0 | <1.0 (4) | - - | - (-) |
| paragneiss | 0.5, 0.5 | 0.5 (2) | <1.0 | <1.0 (2) | - - | - (-) |
| migmatite | 0.4 | 0.4 (1) | - - | - (-) | - - | - (-) |
| mylonite | 6.6 | 6.6 (1) | 4.0 | 4.0 (1) | 0.6 | 0.6 (1) |

*number of analyses in brackets

Many of these trends, especially the Hopedale and Fiord Trends, also parallel major fault and lineament structures as shown in Figures 2.2 and 2.3.

## Hunt River Belt Anomaly

The Hunt River Belt has been mapped in detail by Jesseau (1976) and Ermanovics (1981). The geology, rock sample locations, and results of follow-up lake sediment geochemistry carried out by McConnell (1980) are presented in Figure 2.2. Uranium and thorium analyses for rocks are presented in Table 2.2. The regional anomaly shown in Figure 2.1 covers an area of approximately 15 km by 50 km. There is considerable outcrop in this area and the supracrustal rocks which form the backbone of this anomaly represent only a portion of the underlying lithology. Moreover the size of this anomaly, the diverse rock types over which it occurs, and the association of many anomalous lakes with fault zones or major lineaments suggest that it overlies a major tectonic element of the Hopedale Block, the majority of which is characterized by the presence of a supracrustal belt of metavolcanic and metasedimentary rocks. The strongest lake anomalies often occur at the junction of major fault zones or lineaments. Many of the lakes in this belt appear to be fed, at least in part, by subterranean waters which are probably structurally controlled. Molybdenum, which has similar hydrochemical dispersion characteristics to U, is the only element which displays a similar pattern to U over this belt.

Airborne gamma ray spectrometry (McConnell, 1980) failed to delineate significant areas of high radioactivity over this anomaly, the count rate for U remaining fairly steady. Ground traverses in some of the more clustered anomalies failed to outline any enrichments in uranium.

Results of U and Th analyses of the various rock units associated with this anomaly are given in Table 2.2. The supracrustal rocks in the Hunt River Belt and the orthogneisses surrounding these are not enriched in U compared to other Shield areas which have undergone amphibolite facies metamorphism. The range in values for the supracrustals and orthogneisses varies from less than 0.2 to 6.1 ppm with the vast majority of samples (83%) having U concentrations of less than 1.0 ppm. For amphibolite facies rocks in the northern Quebec Shield area, Fahrig et al. (1967) reported a range of 0.6 to 2.3 ppm with an average of 2.3 ppm. Elsewhere higher values for U in amphibolite facies rocks have been reported (Heier and Adams, 1965; see Rogers and Adams, 1969).

Rocks representing the late granitoids are not enriched in U compared to their counterparts in other Shield areas. This may be a primary feature or may be due to mobilization of U during metamorphism. Since these rocks have undergone only lower amphibolite facies metamorphism the former is most likely the case. No evidence of mineralizing events associated with these granitoids could be found. During higher grades of metamorphism, especially granulite facies, significant U losses have been noted for Shield areas (Heier and Adams, 1965; Fahrig et al., 1967; Dostal and Capedri, 1978). The low Th/U ratios for rocks in the Hunt River Belt would appear to indicate a significant loss of primary U during metamorphism, and thus possible concentration in structural traps. The U concentrations in cataclastic rocks sampled in this belt display normal values (Table 2.2). Overall, the average U content of the crustal segment making up this belt is well below the crustal average of 2.7 ppm calculated by Taylor (1964) and the Canadian Shield average of 2.5 ppm calculated by Shaw et al. (1967).

Without more intensive research, the only reasonable explanation that can be given for the presence of such a large regional anomaly in the absence of mineralization or lithological enrichment seems to lie in the greater involvement and leaching ability of subterranean waters resulting in increased hydromorphic dispersion. The tectonic history and complexity of the structure in this area (see Jesseau, 1976 and Ermanovics, 1981) and the localization of most of the highly anomalous lakes over structural zones indicate that this is a reasonable premise to guide more advanced research.

A similar argument can be put forward for the Florence Lake anomaly (area G, Fig. 2.1) although further regional geochemical coverage to the south will be required to confirm this.

## Hunt Lake Anomaly

The general geology of the Hunt Lake anomaly has been taken from preliminary mapping by I. Ermanovics (personal communication, 1981). The anomaly (area B, Fig. 2.1) is located just south of Hunt Lake and is underlain mainly by Archean grey gneisses and migmatites similar to those in the Hunt River Belt. Foliated granitic, granodioritic and tonalitic intrusive rocks occur in the southeastern part of the area. Rock exposure is approximately 60 per cent and glacial deposits are very thin. There are a number of escarpments which appear to be related to major structural zones.

Ground traversing failed to outline any area of U enrichment. A few pegmatite bodies were encountered but these were found to be mica-poor bodies which often exhibited lower radioactivity than the surrounding rocks. An airborne gamma ray survey of this anomaly (McConnell, 1980) showed a relatively homogeneous distribution of uranium.

The U and Th content of rocks taken from this area are given in Table 2.3. U concentrations for the various rock types are remarkably low and the average crustal abundance for this area is well below the 2.7 ppm level calculated by Taylor (1964). The low Th/U ratios indicate that there has been little loss of U during metamorphism.

There is a reasonably good correlation between anomalous uranium concentrations in lake waters and lake sediments in this area. Lakes located on the foliated intrusive rocks are not particularly anomalous compared to those associated with major structural zones in the gneiss-migmatite basement. The strongest anomalies occur in lakes located on or adjacent to a major ENE structural zone (see Fig. 2.3) which, from the presence of various fault escarpments in the area, appears to have a NE-SW conjugate set of associated fault zones. A linear lake located over this structural zone contains one of the highest levels of U encountered in the Uranium Reconnaissance Program of Labrador (129 ppm in sediment; 1.58 ppb in water). Other lakes on either side of this structure contain U in their sediments and waters in excess of 25 ppm and 0.5 ppb respectively. Detailed ground traverses over this structural zone failed to indicate the presence of any mineralization. Most of the lakes in this area were found to be spring fed by structurally controlled groundwaters and it is most likely therefore, that this anomaly is related to deep seated weathering of a major structural zone within the Archean basement.

The geological setting and nature of the geochemical anomalies in the Shapio Lake area (area C, Fig. 2.1) are very similar to the Hunt Lake anomaly.

**Island Harbour Intrusive Complex**

Only the northern half of the Island Harbour Intrusive Complex was covered by the Uranium Reconnaissance Program (area D, Fig. 2.1). The anomaly investigated covers an area of approximately 15 km by 30 km. The batholith has been smoothed by glaciation and is characterized by abundant outcrops and tundra vegetation. Ermanovics (1980) has given the following description of the batholith:

> "Porphyroblastic granodiorite and minor coarse grained granite dominate the Bay of Islands complex within the map area. The granitoids form an oval-shaped southwest-northeast trending batholith whose dimensions in plan are 20 by 100 km. The rocks are massive to weakly foliated, except near the margins where screens of layered gneisses are accompanied by pronounced gneissosity in granodiorite. Lit-par-lit migmatite is extensively developed around the southern portion of the pluton where it is dominantly granodioritic. In the northeast the pluton becomes granitic and intrusive contacts which gneiss are generally sharp and discordant with extensive development of granitic pegmatite. This change in plutonic composition and the nature of intrusive relationships suggests that the southwestern portion of the pluton is a synkinematic ($D_4$) deeper level intrusion compared to the granitic phase of the pluton in the northeast. Although granite and granodiorite appear to be cogenetic, the granite phase may have crystallized later than granodiorite.
>
> The granodiorite is a medium grained, grey biotite + epidote (8 per cent), zoned oligoclase-andesine bearing rock commonly containing porphyroblastic microcline. Microcline is poikilitic, enclosing epidotized plagioclase, chloritized biotite, and quartz, and hence appears to be a late crystal phase in these rocks. Granitic phases are richer in allanite, zircon, fluorite and sphene than granodioritic members."

Table 2.4

Uranium and thorium contents of the Island Harbour granitoids and related rocks

| Rock Unit | U (ppm)* | | Th (ppm)* | | Th/U | |
|---|---|---|---|---|---|---|
| | Range | Average | Range | Average | Range | Average |
| INTRUSIVE ROCKS: | | | | | | |
| pegmatite | 1.2- 6.0 | 3.1 (4) | 3.0-15.0 | 7.0 (4) | 0.8- 4.8 | 2.8 (4) |
| aplite | 0.7-14.1 | 4.6 (5) | 13 ,16 | 14.5 (2) | 0.9, 4.6 | 2.7 (2) |
| porphyritic granite | 0.6- 2.4 | 1.3(17) | <1.0-15.0 | 6.5 (1) | 0.7-13.0 | 5.0 (9) |
| biotite granite | 0.8- 3.3 | 1.8(17) | <1.0-17.0 | 6.0(15) | 1.9- 6.7 | 4.2(10) |
| biot-qtz monzonite | 0.7- 5.1 | 2.0 (6) | 1.0-11.0 | 4.4 (5) | 0.8- 5.8 | 3.5 (4) |
| porphyritic granodiorite | 1.2- 3.4 | 1.8 (7) | <1.0- 6.0 | 3.3 (7) | 1.2- 3.3 | 2.3 (6) |
| granodiorite | 0.7- 5.7 | 1.7(11) | <1.0- 9.0 | 2.1 (9) | 1.4- 4.5 | 2.3 (5) |
| diorite | <0.2- 0.8 | 0.3 (6) | - - | - (-) | - - | - (-) |
| diabase | 1.5 | 1.5 (1) | 6.0 | 6.0 (1) | 4.0 | 4.0 (1) |
| METAMORPHIC ROCKS: | | | | | | |
| amphibolite | <0.2- 1.4 | 0.8 (6) | 2.0 | 2.0 (1) | 1.4 | 1.4 (1) |
| orthogneiss | <0.2- 0.7 | 0.3 (6) | <1.0- 2.0 | 1.0 (4) | 5.0, 5.0 | 5.0 (2) |
| migmatite | <0.2- 0.3 | 0.2 (3) | - - | - (-) | - - | - (-) |

*number of analyses in brackets

Table 2.5

Chemistry of lake waters situated on well exposed bedrock of the Island Harbour Intrusive Complex

| Sample No. | Principle Rock Type | U (ppb) | Spec. Cond. (umhos/cm) | pH |
|---|---|---|---|---|
| WK-1 | musc-granite | 4.00 | 51 | 6.81 |
| -2 | porphyritic granite | 0.52 | 13 | 7.05 |
| -3 | porphyritic granite | 0.24 | 12 | 6.60 |
| -4 | porphyritic granite | 0.48 | 16 | 6.68 |
| -5 | porphyritic granite | 0.28 | 13 | 6.62 |
| -6 | orthogneiss | 0.10 | 11 | 5.76 |
| -7 | granite and aplite | 1.28 | 13 | 6.81 |
| -8 | biot-qtz-monzonite | 0.80 | 20 | 6.70 |
| -9 | porphyritic gabbro | 0.10 | 9 | 6.36 |
| -10 | granodiorite | 0.10 | 10 | 6.38 |
| -11 | granodiorite | 0.10 | 9 | 5.92 |
| -12 | granodiorite | 0.10 | 20 | 7.05 |

Airphotos show the complex to be dominated by a checkerboard pattern of lineaments many of which are fault zones or are occupied by later dyke phases (Fig. 2.4).

An airborne gamma ray survey of this anomaly failed to delineate any zones of high radioactivity. Ground radiometric and geological traverses in some of the more anomalous areas of the batholith also failed to demonstrate mineral potential.

The U and Th contents of the various intrusive phases of the Island Harbour Complex as well as the metamorphic rocks bordering it or forming roof pendants on it are presented in Table 2.4. The U contents of the intrusive rocks vary from less than 0.2 ppm for the mafic and intermediate varieties to highs of between 3.5 and 14 ppm for late phase granitoids such as pegmatite and aplite. The granitic phases of this batholith have an average U content of about 1.7 ppm which is well below crustal abundance (2.7 ppm, Taylor, 1964) and world averages for granitic (4.8 ppm, Rogers and Adams, 1969) and silicic plutonic rocks (4.7 ppm, Peterman in McNeal et al., 1981). The Th/U ratios vary with rock type but the coarser grained varieties such as the porphyritic granite, biotite-granite and biotite-quartz-monzonite phases which dominate the batholith show higher than normal ratios suggesting a depletion of U which is probably due to weathering. Because of their coarse grained nature, most of the rocks in this complex exhibit a much greater degree of weathering than intrusive rocks observed in the Hopedale Block.

Rock exposure varies from about 40 per cent to greater than 80 per cent and the complex is covered by a large number of bowl shaped lakes and ponds on well exposed outcrop which act as 'collector basins' for precipitation runoff. The waters from some of these 'collector basins' were analyzed for U, conductivity and pH (Table 2.5). The conductivity and pH levels are very similar to those of rainwater sampled in the area (10 umhos/cm and 6.2 respectively) and since evaporation in this region is almost nil lake water chemistry largely reflects the introduction of weathering products. The U content of some of these lake waters greatly exceeds the 95% percentile (0.20 ppb) for the regional data. In particular, lakes located on the porphyritic and muscovitic granite phases show a large introduction of labile U from surficial weathering. Highly anomalous areas shown in Figure 2.4 were found to be underlain mainly by the porphyritic granite phase. In addition, a number of lakes investigated were found to be spring fed and located along prominent structural features such as contacts, faults and dykes.

Despite the low U content of the rocks comprising this batholith, it would appear that lake water and lake sediment anomalies associated with it are the result of accelerated weathering of a well exposed, moderately fractured and dominantly coarse grained intrusive body.

**Conclusions**

None of the anomalies investigated were found to be underlain by significant concentrations of uranium neither in the form of mineralization nor as lithogeochemical enrichments. Because of the very large size of these anomalies any mineralizing event(s) would have been regional in extent. This, however, has not been borne out by either ground or airborne radiometric surveys.

Parameters such as pH and sediment composition and processes such as Fe and Mn scavenging have not been involved in the formation of these U anomalies. Glaciation would appear to have had a negative effect on anomaly formation by supplying large quantities of material with a low U content (mainly anorthositic).

All of the main rock types in the Hunt River Belt, Hunt Lake area and Island Harbour Intrusive Complex display U concentrations which are significantly below those of their counterparts in other Shield areas. Average crustal abundances for each of these three areas are well below 2.0 ppm as compared to 2.5 ppm calculated for the Canadian Shield as a whole (Shaw et al., 1967).

All of the anomalous areas have a well developed structural fabric of major lineaments and fault zones. Supracrustal rocks in the Hunt River Belt may signify the presence of a major deep seated structural zone in this area.

The following factors suggest that these three regional U anomalies are the result of accelerated weathering of bedrock having a relatively open structural fabric:

a. the high degree of exposure of bedrock in all three areas as compared to other parts of the Hopedale Block and surrounding regions,

b. the strong association between individual anomalous lakes and clusters of anomalous lakes with minor and major structural zones respectively. In some cases (e.g. Hunt Lake anomaly) anomalous lakes are strung out along a major structural zone suggesting leaching of uranium by structurally controlled groundwaters,

c. the occurrence of many lakes on well exposed outcrop in the Island Harbour Intrusive Complex having conductivities only slightly higher than rainwater but containing high concentrations of U, indicating rapid leaching of the intrusive rocks, and

d. the clustering of anomalous lakes on the coarse grained and easily weathered porphyritic granite phase of the Island Harbour Intrusive Complex.


### Acknowledgments

The author would like to thank I. Ermanovics of the Geological Survey of Canada for many stimulating discussions on the geology of this region and for supplying the author with preliminary geological information and representative rock samples from the various study areas. The logistical support of Brinco Ltd. and permission to use their helicopter is also greatly appreciated. I would like to thank Y.T. Maurice and K.A. Richardson for critically reviewing the manuscript.


### References


Dostal, J. and Capedri, S.
1978: Uranium in metamorphic rocks; Contributions to Mineralogy and Petrology, v. 66, p. 409-414.

Ermanovics, I.
1980: Geology of the Hopedale Block of Nain Province, Labrador: Report 2, Nain-Makkovik boundary zone; in Current Research, Part B, Geological Survey of Canada, Paper 80-1B, p. 11-15.

1981: Hunt River Belt map area, Labrador (parts of 13 N/7, 9, 10, 15, 16); Geological Survey of Canada, Open File 778.

Ermanovics, I. and Korstgard, J.A.
1981: Geology of Hopedale Block and adjacent areas, Labrador: Report 3; in Current Research, Part A, Geological Survey of Canada, Paper 81-1A, p. 69-76.

Ermanovics, I. and Raudsepp, M.
1979: Geology of the Hopedale Block of Nain Province, Labrador: Report 1; in Current Research, Part B, Geological Survey of Canada, Paper 79-1B, p. 341-348.

Fahrig, W.F., Eade, K.B., and Adams, J.A.S.
1967: Abundances of radioactive elements in crystalline shield rocks; Nature, v. 214, p. 1002-1003.

Heier, K.S. and Adams, J.S.A.
1965: Concentrations of radioactive elements in deep crustal material; Geochimica et Cosmochimica Acta, v. 29, p. 53-61.

Jesseau, C.W.
1976: A structural-metamorphic and geochemical study of the Hunt River supracrustal belt, Nain Province, Labrador; unpublished M.Sc. thesis, Memorial University of Newfoundland, 211 p.

McConnell, J.W.
1980: Detailed lake sediment, water and radiometric survey of 14 base metal and uranium anomalies in Labrador; Newfoundland Department of Mines and Energy, Labrador Open File 224.

McNeal, J.M., Lea, D.E., and Millard, H.T., Jr.
1981: The distribution of uranium and thorium in granitic rocks of the Basin and Range Province, Western United States; Journal of Geochemical Exploration, v. 14, p. 25-40.

Rogers, J.J.W. and Adams, J.A.S.
1969: Uranium; in K.H. Wedepohl, ed., Handbook of Geochemistry, V 0/1. Springer-Verlag, Berlin, p. 90-1 to 90-0-1.

Shaw, D.M., Reilly, G.A., Muysson, J.R., Pattenden, G.E., and Campbell, F.E.
1967: An estimate of the chemical composition of the Canadian Precambrian Shield; Canadian Journal of Earth Sciences, v. 4, p. 829-853.

Taylor, S.R.
1964: Chondritic Earth model; Nature, London, v. 202, p. 281-282.

# 3. REGIONAL METALLOGENY OF THE NORTHERN CORDILLERA: BIOSTRATIGRAPHY, CORRELATION AND METALLOGENIC SIGNIFICANCE OF BEDDED BARITE OCCURRENCES IN EASTERN YUKON AND WESTERN DISTRICT OF MACKENZIE

Project 740098

Kenneth M. Dawson and Michael J. Orchard[1]
Economic Geology Division, Vancouver

*Dawson, K. M. and Orchard, M. J., Regional metallogeny of the northern Cordillera: biostratigraphy, correlation and metallogenic significance of bedded barite occurrences in eastern Yukon and western District of Mackenzie; in Current Research, Part C, Geological Survey of Canada, Paper 82-1C, p. 31-38, 1982.*

***Abstract***

*Limestone beds in and adjacent to nine bedded barite occurrences in the Macmillan Pass-Howards Pass region yield conodont faunas that define two principal intervals of barite deposition in the lower Earn Group and one in the upper Earn Group. The oldest is of late Middle Devonian age, the next is early Upper Devonian, and the youngest is of upper Early Mississippian age. The early Upper Devonian (Frasnian) barite interval is of regional extent and corresponds to one of the stratiform Pb-Zn-Ag-Ba horizons at Macmillan Pass.*

## Introduction

Field work in the Macmillan Pass-Howards Pass area since 1974 has included the study of numerous bedded barite occurrences within Devono-Mississippian clastic strata. Numerous horizons of barite and base metal-barite have been recognized, and difficulties encountered in lithological correlation of clastic units over the extensive area of barite occurrence have made evident the need for biostratigraphic control.

Rare limestone beds, where present in and adjacent to bedded barite, were sampled and the specimens processed for conodont recovery. Stratigraphic sections in which barite occurred were measured. Faunal data and ages of ten bedded barite occurrences are presented here, including the Cathy, Bar, Oro, Pete, GHMS, Gargantua North, Jeff and Tea, plus unnamed occurrences near Howards Pass (Fig. 3.1) and Porcupine Creek (105 F/15). Detailed sections of two upper Devonian (Pete, GHMS) and two middle Devonian (Cathy, Oro) occurrences are given.

## Barite in the Earn Group

Stratiform barite is hosted by a thick and extensive blanket of cherty clastic rocks that overlies middle Paleozoic and older strata in the northern Canadian Cordillera. Shelf and basinal rocks of miogeoclinal character and cratonal provenance are overlain, often unconformably, by a thick succession of chert, shale, siltstone, sandstone and conglomerate of dominantly turbiditic origin and westerly source. Rocks previously informally designated 'black clastic group' and variously correlated with the Besa River, Canol and Imperial formations by Blusson (1976) and Dawson (1977) have been assigned, in the Macmillan Pass-Nahanni areas, to the Earn Group by Gordey et al. (1982, p. 98).

The lower Earn Group, host to most of the barite occurrences in this study, was defined at its base by Gordey et al. (1982) as the first cherty and fine clastic strata to overlie the dolomitic siltstone and/or silty limestone of late Silurian to middle Devonian age, at the top of the 'Road River group'. Basal black chert, cherty shale and siltstone grade upward to coarser grained rhythmically laminated siltstone/shale with minor limestone and bedded barite, and locally, as at Macmillan Pass, chert pebble conglomerate. An overlying, ubiquitous silver to gun-blue weathering black siliceous shale unit marks the resumption of quiescent depositional conditions and contains a regional Upper Devonian bedded barite horizon.

The onset of deposition of brown-weathering clastic sediments, viz grit, siltstone, sand, shale and conglomerate, heralds the upper Earn Group in late Frasnian to Famennian time. Upper Earn Group lithologies are generally coarser grained and more resistant than underlying strata, and include reddish brown weathering, in part turbiditic, sandstone, siltstone, shale and conglomerate with only minor chert and black shale.

Bedded barite occurrences in both lower and upper Earn Group strata are restricted to relatively fine grained clastic successions (shale and siltstone), often bounded above and below by coarser grained clastic sediments of turbiditic affinity, and accompanied by chert and limestone. In a few locations stratiform assemblages of zinc, lead and iron sulphides accompany the bedded barite.

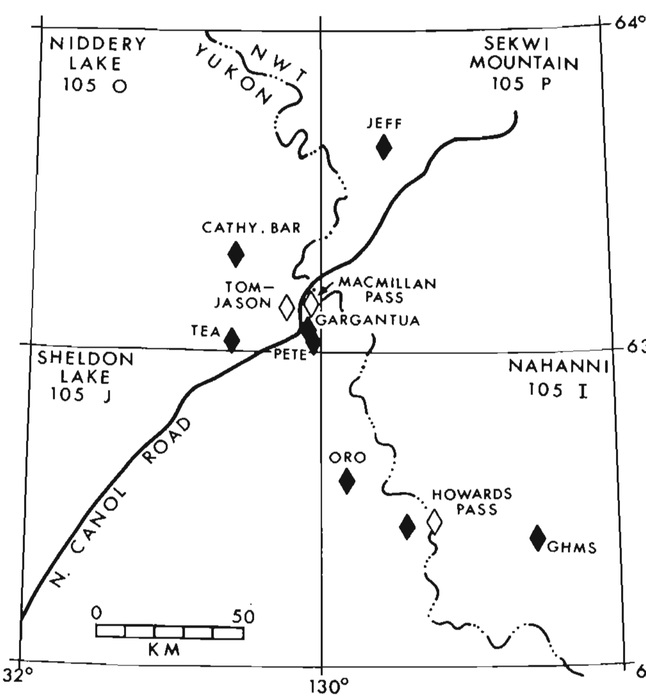


*Figure 3.1. Bedded barite occurrences (solid symbols) studied in the Macmillan Pass-Howards Pass area.*

[1] Cordilleran Geology Division, Vancouver

## Upper Devonian Barite Horizon

Limestone beds associated with the Pete, GHMS, Jeff and Gargantua North barite occurrences have yielded conodont faunas whose ages group tightly in or about the middle Frasnian (Fig. 3.2), defining an upper Devonian barite horizon that appears to be of regional extent. These four deposits plus several others in the Macmillan Pass-Howards Pass area occur in the upper part of the lower Earn Group. They are usually underlain and hosted by turbiditic siltstone/sandstone and overlain by a black siliceous shale unit that is overlain, in turn, by brown weathering, commonly coarse grained clastic rocks of the upper Earn Group. The deposits represent three important variants of bedded barite within this regional Upper Devonian barite interval: 1) the distal part of Macmillan Pass mineralized strata according to Smith (1978) (Pete, Gargantua North); 2) the nodular barite deposits in a shelf depositional environment (Jeff); and 3) the interbedded barite/siltstone of the Frasnian regional barite-bearing interval in general (GHMS).

### Pete and Gargantua North Occurrences

The Pete (105 O/1; 63°02'N, 130°06'W) and Gargantua North, sometimes called North Gary, (105 O/1; 63°06'N, 130°11'W) occurrences, which are 15 and 7 km respectively south of the TOM deposit at Macmillan Pass, were staked in 1974 and 1975 by Clyde Smith for Ogilvie Joint Venture (Brinco Ltd., Mitsubishi Metals Corp., Ventures West Capital). At Gargantua North, folded chert-celsian-witherite beds are devoid of galena and sphalerite. I.R. Jonasson and J.W. Lydon (personal communication, 1980) attributed the development of celsian ($BaAl_2Si_2O_8$), the barium analogue of anorthite, and the barium carbonate witherite to thermal metamorphism of barite-chert beds by an adjacent Cretaceous granitoid stock. A 0.5 m-thick limestone bed 25 m above the celsian-rich strata yielded middle Frasnian conodonts (Fig. 3.2). An early upper Devonian or older age of baritic beds is indicated.

The baritic interval at Pete is hosted by a 30 m-thick unit of siliceous and pyritic argillite and siltstone (Fig. 3.3). A 2 m-thick bed of white barite is both overlain and underlain by lamellar barite in argillite/siltstone. Traces of sphalerite and galena occur near the upper contact of the barite. Underlying siltstone/shale beds grade through spotted slate to hornfels as a plutonic contact 500 m to the east is approached. A dark grey limestone bed 1 m thick that immediately underlies the Pete barite bed yielded middle Frasnian conodonts (Fig. 3.2).

### Jeff Occurrence

The Jeff bedded barite occurrence 105 P/12; 63°36.6'N, 129°39.5'W) that is 25 to 30 km northeast of other barite occurrences studied in calcareous to cherty shale of the lower Earn Group, is underlain by a middle Devonian (Eifelian) limestone-shale unit (Gordey et al., 1982, Section K). A mid-Frasnian age, also based on conodonts, is

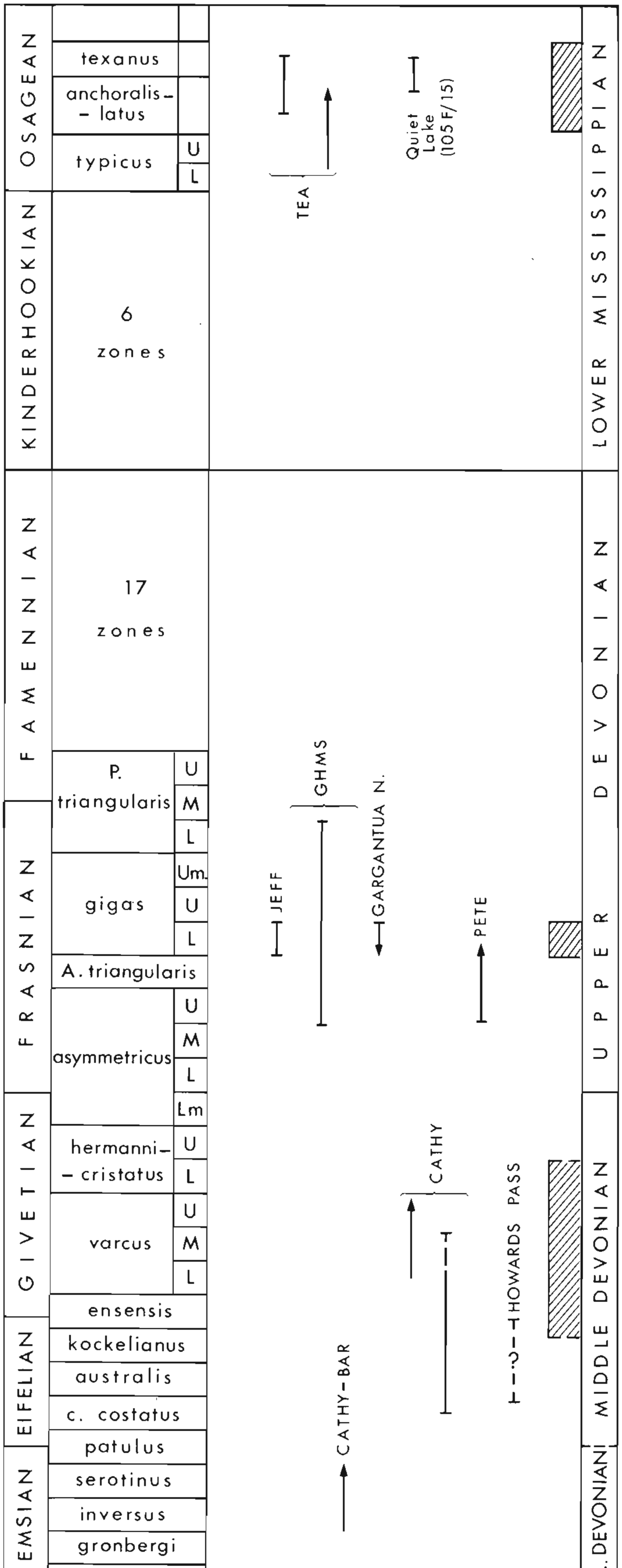


***Figure 3.2***

*Ages of conodont faunas associated with bedded barite. The solid bars represent the time interval from within which the conodont faunas date at the named locations (see Appendix for details). The age of the faunas may lie anywhere within the range of the bar. A closed bar indicates the fauna was collected within barite, arrows indicate the fauna originated beneath or above a barite horizon; dashed bars represent uncertainty. Boxes on the right show approximate positions of proven barite development. Conodont zonal schemes after Klapper and Ziegler, 1979 (Devonian), Sandberg et al., 1978 (Kinderhook), and Lane et al., 1980 (post-Kinderhook).*

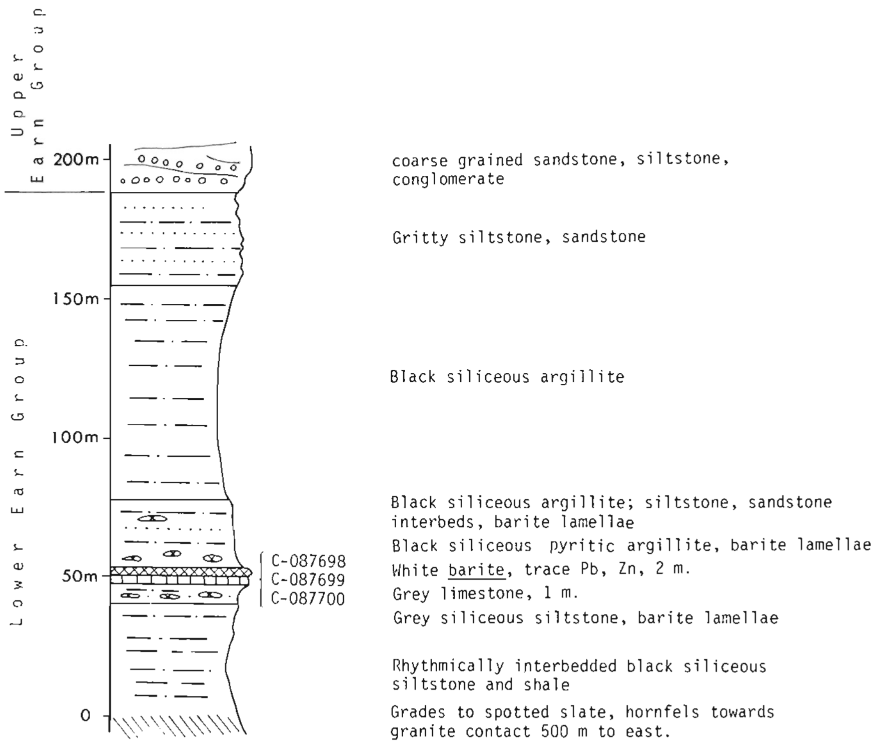


***Figure 3.3.*** *Pete barite section (105 O/1; 63°02'N 130°06'W).*

## Middle Devonian Barite Interval

Conodont fauna from barite occurrences at the Cathy and Bar define a middle Devonian interval of barite deposition of late Eifelian through Givetian age (Fig. 3.2). Further showings at Oro and an unnamed occurrence 13 km west of the large stratiform base metal deposit in Silurian mudstone at Howards Pass are tentatively correlated. Rocks of this interval, near the base of the lower Earn Group, are well exposed and have been dated at the Cathy and Bar claims 16 km east of Macmillan Pass. Conodonts extracted from the Oro deposit and an occurrence near Howards Pass are less diagnostic. Tentative correlations of these middle Devonian beds with Macmillan Pass barite occurrences are here proposed (see Discussion Section).

### Cathy Deposit and Bar Occurrence

The Cathy (or Walt) property (105 O/7; 63°16.5'N, 130°33'W) of Baroid of Canada was diamond drilled in 1980, delimiting a main zone up to 30 m thick and at least 150 m long with reserves in excess of 450 000 tonnes of barite with a specific gravity greater than 4.25 (Abbott in Yukon Geology and Exploration, 1981, p. 217). The presence of minerals other than barite in the ore horizon was confirmed by XRD analysis by R.N. Delabio[1] of 4 Cathy specimens that showed, in addition to barite, gypsum, barytocalcite and traces of witherite in one, calcite in another, and gypsum in a third.

reported by Gordey et al. (1982, locality no. 11) for limy beds within the upper part of a nodular barite-shaly barite sequence over 50 m thick. The baritic beds are composed of distinctive barite nodules consisting of grey radiating barite crystals. Such nodules characterize several similar barite occurrences in the northwestern Sekwi Mountain (105 P) map area, and have been described for an occurrence 13 km northwest of Jeff by Laznicka (1976).

### GHMS Occurrence

The barite-bearing section on the GHMS property (105 I/7, 8; 62°24, 128°30) of Placer Development Ltd. is typical of the regional mid-Frasnian barite interval. One main 'bed' of thin bedded grey barite 8 to 12 m thick plus barite lamellae in underlying and overlying siltstone outcrops over a strike length of 2.5 km. The barite/siltstone interval in the lower Earn Group contains several grey baritic limestone interbeds and is overlain, successively, by black siliceous shale of the lower Earn Group and brown weathering, locally coarse grained clastic rocks of the upper Earn Group (Fig. 3.4). A generalized stratigraphic column of the GHMS area is given by Lord et al. (1981). Two limestone beds 6 and 15 m below the main barite bed yielded conodont faunas of early to mid Frasnian age. A third limestone bed that immediately underlies the main barite bed (Fig. 3.4) yielded conodonts of mid-Frasnian, the age of bedded barite at GHMS.

Numerous similar, although commonly thinner and less extensive bedded barite occurrences have been observed in lower Earn Group strata in the Nahanni (105 I) map area, an example of which is described by Gordey et al. (1982) from section M, locality no. 12; a mid-Frasnian limestone bed, 5 m above a thin barite bed, is unconformably overlain by upper Earn Group cross-laminated siltstone and shale. The problems of correlating lithologies associated with the Frasnian barite interval are exemplified by this occurrence where uppermost lower Earn Group lithologies apparently were cut out beneath an unconformity.

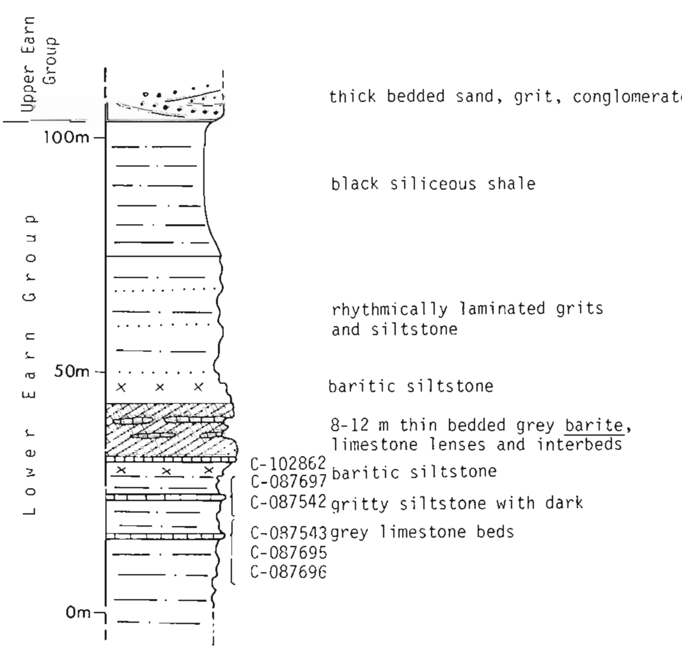


***Figure 3.4.*** *GHMS barite section (105 I/7, 8; 62°24'N, 128°30'W).*

[1] Central Laboratories and Technical Services Division, Geological Survey of Canada

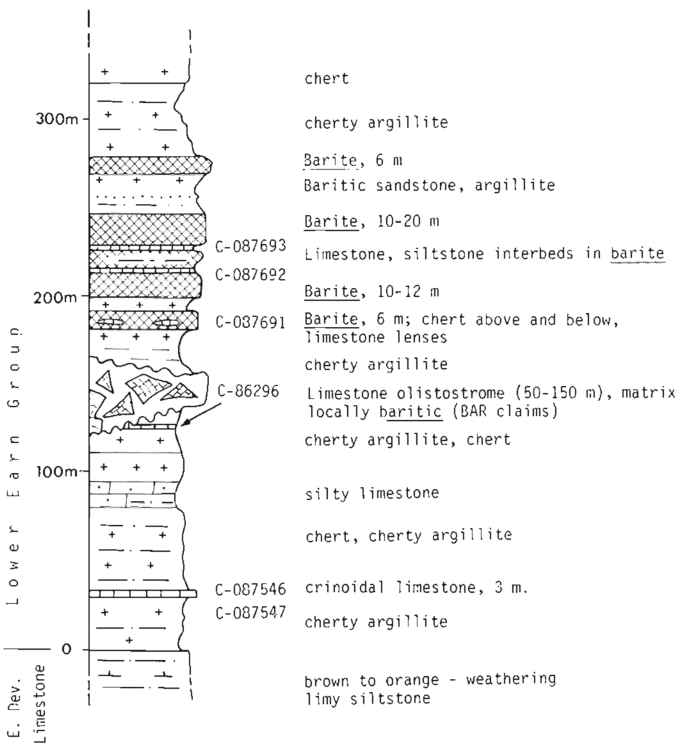


***Figure 3.5.*** *Cathy barite section (105 O/7; 63°16.5'N, 130°33'W).*

At least 5 principal barite beds occur within a 100 m thick sequence of cherty argillite, chert, siltstone and sandstone (in part baritic), minor limestone and conglomerate (Fig. 3.5). Large olistostromal lenses of limestone breccia up to 150 m thick that underlie the upper 4 barite horizons contain barite both within the predominantly calcareous matrix and as discontinuously overlying beds, as on the Bar claims (105 O/7; 63°17.5'N, 130°34'W) of D. Woodcock. Limestone breccia is underlain by up to 200 m of cherty argillite, chert and silty limestone. This sequence, typical of basal Earn Group strata, overlies a lower Devonian calcareous siltstone unit that marks the top of the 'Road River group' (Gordey et al., 1982). Barite beds and enclosing strata are imbricated with Road River and older rocks in a series of thrust faults.

Three thin limestone beds within the main barite zone on Cathy yield faunas no younger than late Givetian (mid Devonian). A limestone bed below a barite bed on Bar is late Emsian. A crinoidal limestone bed about 25 m above the base of the lower Earn Group yields Pragian (mid lower Devonian) fauna. Thus, much of the Lower and Middle Devonian appears to be represented within the lower Earn Group at and stratigraphically below the Cathy and Bar barite beds.

### Oro Deposit and an Occurrence West of Howards Pass

The Oro deposit (105 I/12; 63°27'N, 129°46'W) of Noranda Mines Ltd. lies 35 km northwest of the XY Pb-Zn deposit of Placer Development Ltd. at Howards Pass and 63 km southeast of the Tom Pb-Zn-Ba deposit at Macmillan Pass. Diamond drilling in 1973 outlined a lenticular body of grey, thinly bedded barite 1100 m long, 15 to 50 m wide and up to 50 m thick. Barite beds grade upward to siliceous siltstone that is overlain by a pebbly mudstone-chert pebble conglomerate-siltstone-sandstone unit typical of the upper part of lower Earn Group locally (Gordey et al., 1982, section O).

The barite horizon, averaging 15 to 30 m thick, is underlain by a stockwork of quartz-ankerite-pyrite-barite veins within silicified, locally pyritic grey siltstone and argillite (Fig. 3.6). The fractures, now filled by the above vein minerals, appear to have served as hydrothermal conduits in the altered footwall of the barite orebody. Footwall siltstone is underlain by 100 m of chert and cherty argillite typical of basal Earn Group strata that overlies, in turn, a regional orange-weathering dolomitic siltstone unit at the top of the 'Road River group'.

A dark grey silty limestone bed 0.7 m thick that lies 34 m below interbedded barite and siltstone in Oro drillhole no. 73-6 yielded a small **Polygnathus** conodont fauna of possible Middle Devonian age.

In 1980, R.G. Anderson (GSC) sampled a baritic limestone bed in lower Earn Group strata 13 km west (105 I/6; 62°27'7"N, 129°26'W) of the XY deposit of Placer Development Ltd. at Howards Pass. A single conodont fragment extracted from the sample indicates an Eifelian (early Middle Devonian) age. The large stratiform XY Pb-Zn deposit in lower Silurian mudstone of the 'Road River group' contains no barite and is unrelated to Devono-Mississippian stratiform barite and Pb-Zn-Ba deposits in the region.

### Mississippian Barite Occurrences

The Tea barite deposit (105 O/2; 63°01.5'N, 130°36.5'W) of Yukon Barite Co. Ltd. is 28 km southwest of the Tom deposit at Macmillan Pass and 130 km northeast of Ross River. James S. Dodge, President of Yukon Barite, reported the following deposit data in a written communication (1982):

> "The Tea property was diamond drilled by Yukon Barite Company in 1980, delimiting a zone up to 30 m thick, over 100 m wide, and at least 150 m long, only to the extent tested by the initial drill program and by cliff outcrop exposures; the ultimate strike length is 'open' geologically. The measured ore reserves are in excess of 225,000 tonnes of barite with specific gravity averaging 4.24".

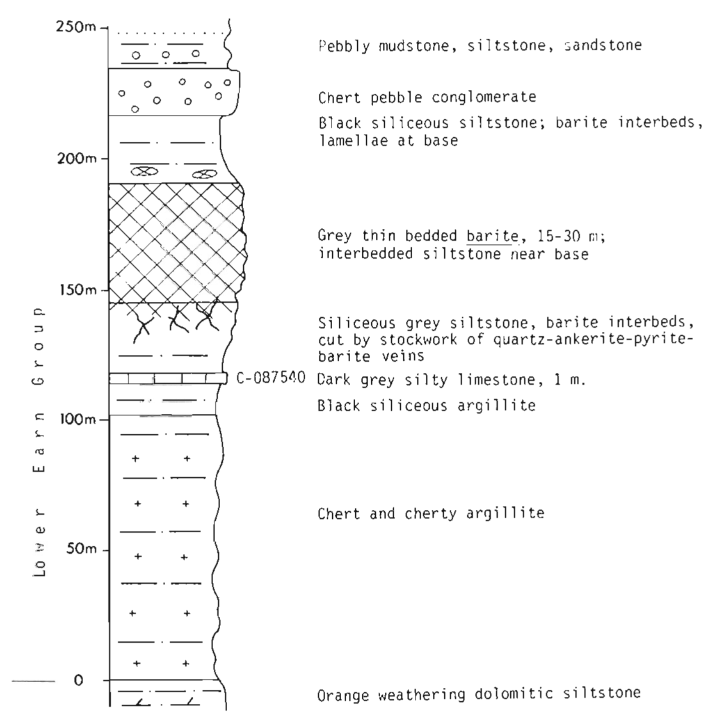


***Figure 3.6.*** *Oro barite section (105 I/12; 63°27'N, 129°46'W).*

Carne (1976) mapped a barite zone with interbedded baritic shale and limestone, chert and witherite, up to 90 m thick. Subsequent mineralogical studies by Lydon et al. (1979) confirmed the presence of barite, calcite and quartz, but not witherite. Barytocalcite in Tea specimens was identified by I.R. Jonasson (personal communication, 1982).

The thick Tea barite section is underlain by 100 m of black pyritic siliceous shale, siltstone, chert and minor limestone. The black shale unit is underlain by a coarse clastic assemblage of sandstone, conglomerate and siltstone. Barite beds are overlain by several hundred metres of black siltstone and chert that grade upward to greenish siltstone, sandstone and conglomerate.

A grey limestone interbed several metres thick 17 m above the exposed base of the main barite unit at Tea was sampled in 1976. A poorly preserved brachiopod and conodont fauna was tentatively assigned to a broad 'Devono-Mississippian' range by B.E.B. Cameron in Dawson (1977). A re-examination of the sample by the junior author yielded a definitive conodont fauna of Osagean (late Lower Mississippian) age: GSC Loc. No. C-087721, Appendix.

Limestone clasts from a conglomeratic limestone bed in black siltstone approximately 50 m below the barite also produced fauna of Osagean age. A sample from a nearby outcrop of fossiliferous limestone rich in brachiopods, collected by I.R. Jonasson (personal communication, 1980) yielded a comparable fauna. A 0.5 m thick limestone interbed near the base of the main barite unit yielded a single conodont of probable Mississippian age.

The Tea deposit represents a significant and relatively young interval of barite deposition in lower Mississippian, upper Earn Group strata. A further Mississippian barite horizon was recognized by Tempelman-Kluit (1976) in early-mid Osagean black slate at a locality 15 km east-southeast of Porcupine Creek in the Quiet Lake (105 F/15) map area (see Appendix).

## Discussion: Correlation and Metallogenic Significance of Barite Beds

Widespread barite deposition during a relatively short period in the Late Devonian is indicated by the similarity in ages of the Macmillan Pass area occurrences with the distant Jeff and GHMS. At Macmillan Pass, the Frasnian occurrences Pete and Gargantua North are correlated by Smith (1978) with the youngest of three Macmillan Pass barite horizons, represented by the barite-rich stratiform Pb-Zn-Ag deposits Tom West and Jason Main. Although definitive fossil data are lacking, an early Upper Devonian age for this horizon is supported by the identification by Nassichuk in 1977 (unpublished paleontological report 1-WNN-1977) of a Frasnian ammonite resembling **Ponticeras tchernyschewi** from beds probably immediately overlying Tom West. The traces of galena and sphalerite within stratiform barite at Pete (Fig. 3.3), about 15 km from the Tom-Jason deposits, may represent the southern limit of sulphide deposition related to terminal barium-rich exhalations centred at or near the Macmillan Pass deposits. However, barite deposition devoid of base metals, but probably related to exhalative centres like Macmillan Pass, may extend far beyond the local area of base metal-barite deposition.

The Jeff and GHMS occurrences, as well as numerous others hosted by the lower Earn Group, but not yet documented nor dated, apparently are products of an exhalative event or events of similar late Devonian age and regional influence. Barite beds deposited at a distance from an exhalative source, as proposed for GHMS, would be characteristically thinner and more abundantly interbedded with fine clastic sediments than the massive, relatively pure deposits accumulated close to the source, consistent with Sato's (1972) model of submarine metalliferous brines. Distinctive nodular bedded barite also may represent deposition distant from an exhalative vent, but possibly in a relatively shallow, oxygenated environment as indicated by the shelf-type carbonate beds underlying Jeff, rather than within the same seafloor depression as the vent. No chemical or physical explanation is known for the primary nodular texture. The Jeff occurrence, in its location shelfward of probably time equivalent base metal-barite deposits at Macmillan Pass, appears similar in texture, setting and age to the nodular barite of the Kwadacha deposit (94 F/10) 18 km northeast of the large Cirque base metal-barite deposit (94 F/6, 11) in northern British Columbia, as described by MacIntyre and Diakow (1982).

The Middle Devonian age indicated for Oro and the occurrence west of Howards Pass is insufficiently defined to allow correlation with either middle Devonian barite beds at Cathy or possibly equivalent mineralized horizons at Macmillan Pass. The adjacent Macmillan Pass barite occurrences, Moose and South Gary, although not dated with fossils, are correlated and assigned by Smith (1978), to beds immediately overlying the top of 'Road River group' strata, corresponding to the base of the lower Earn Group. The recently discovered Jason End Zone is assigned by Abbott (Tempelman-Kluit et al., 1981, p. 216) to a lower stratigraphic horizon than Jason Main Zone or Tom West Zone, near the base of the 'Canol Formation', i.e. lower Earn Group, that may correlate with Moose and South Gary. Although no firm correlation can be drawn between these undated Macmillan Pass beds and barite beds at Cathy, the preliminary fossil data indicate that widespread barite deposition in the Middle Devonian may correspond to the earliest stage of Macmillan Pass Pb-Zn-Ag-Ba deposition. A post-early Middle Devonian (post-mid Eifelian) age for lowermost Macmillan Pass mineralized strata was indicated by Gordey et al. (1982).

The lower Mississippian Tea deposit is significant because of its large size and relatively young age. No other Mississippian barite deposits have been documented in the Macmillan Pass-Howards Pass region. The thick sequence of fine to coarse clastic sediments, chert, limestone and barite at Tea is not obviously correlative with upper Earn Group lithologies in the area described by Gordey et al. (1982). The Tea deposit and its host rocks may represent a local depositional environment similar to that at nearby Macmillan Pass, but developed in early Mississippian time.

Mississippian barite and base metal-barite stratiform deposits have been recognized in the Pelly Mountains by Tempelman-Kluit (1976) and Morin (1977, 1981), and in the Tay River area (105 K) by Cyprus Anvil geologists (G. Jilson, personal communication, 1982). A relationship may exist between these deposits and the Tea in upper Earn Group strata. Further studies of these Carboniferous rocks and barite deposits are in progress.

## Acknowledgments

The writers gratefully acknowledge the co-operation and access to exploration data offered by J.S. Brock of Welcome North Mines Ltd., R.B. Dickerson formerly of N.L. Baroid, G.E. Dirom of Noranda Exploration Co. Ltd., J.S. Dodge of Yukon Barite Co. Ltd., J.M. Morganti of Placer Development Ltd. and J.R. Woodcock, consultant.

The paper benefitted from the critical reading and suggestions offered by I.R. Jonasson, R.I. Thorpe, S.P. Gordey, J.W. Lydon, H. Gabrielse, D.F. Sangster and R.S. Hewton.

## References


Blusson, S.L.
1976: Selwyn Basin, Yukon and District of Mackenzie; in Report of Activities, Part A, Geological Survey of Canada, Paper 76-1A, p. 131-132.

Carne, R.C.
1976: The Tea barite deposit; Canada Department Indian and Northern Affairs, Open File Report EGS 1976-16, p. 20-31.

Dawson, K.M.
1977: Regional metallogeny of the Northern Cordillera; in Report of Activities, Part A, Geological Survey of Canada, Paper 77-1A, p. 1-4.

Gordey, S.P., Abbott, J.G., and Orchard, M.J.
1982: Devono-Mississippian (Earn Group) and younger strata in east-central Yukon; in Current Research, Part B, Geological Survey of Canada, Paper 82-1B, p. 93-100.

Klapper, G. and Ziegler, W.
1979: Devonian conodont biostratigraphy; The Palaeontological Society, London. Special papers in Palaeontology, v. 23, p. 199-224.

Lane, H.R., Sandberg, C.A., and Ziegler, W.
1980: Taxonomy and phylogeny of some Lower Carboniferous conodonts and preliminary standard post-Siphonodella zonation; Geologica et Palaeontologica, v. 14, p. 117-164.

Laznicka, P.
1976: Barite nodules of possibly late diagenetic origin from Twitya River area, Mackenzie Mountains, Northwest Territories; Canadian Journal of Earth Sciences, v. 13, p. 1446-1455.

Lord, C., Laporte, P.J., Gibbins, W.A., Seaton, J.B., Goodwin, J.A., and Padgham, W.A.
1981: GHMS claims; in Mineral Industry Report, 1977, Northwest Territories, Indian and Northern Affairs, Canada, p. 124-125.

Lydon, J.W., Lancaster, R.D., and Karkkainen, P.
1979: Genetic controls of Selwyn Basin stratiform barite/sphalerite/galena deposits: an investigation of the dominant barium mineralogy of the Tea deposit, Yukon; in Current Research, Part B, Geological Survey of Canada, Paper 79-1B, p. 223-229.

MacIntyre, D.G. and Diakow, L.
1982: Kwadacha barite deposit; in Geological Fieldwork 1981, B.C. Ministry of Energy, Mines and Petroleum Resources, Paper 1982-1, p. 149-155.

Morin, J.A.
1977: AgPbZn mineralization in the MM deposit and associated Mississippian felsic volcanic rocks in the St. Cyr Range, Pelly Mountains; in Canada Department of Indian and Northern Affairs, Mineral Industry Report, 1976, Yukon Territory, EGS 1977-1, p. 83-97.

Morin, J.A.
1981: A note on the rock geochemistry of the Clear Lake massive sulphide; in Indian and Northern Affairs Canada, Yukon Geology and Exploration 1979-1970, p. 85-87.

Sandberg, C.A., Ziegler, W., Leuteritz, K., and Brill, S.M.
1978: Phylogeny, speciation, and zonation of Siphonodella (Conodonta, Upper Devonian and Lower Carboniferous); Newsletter in Stratigraphy, v. 7, p. 102-120.

Sato, T.
1972: Behaviours of ore-forming solutions in seawater; Mining Geology, v. 22, p. 31-42.

Smith, C.L.
1978: Geological setting of Jason and Tom deposits, Macmillan Pass area, Eastern Yukon; Summary of Presentation, Whitehorse Geoscience Forum 1978, 6 p.

Tempelman-Kluit, D.J.
1976: Stratigraphic and structural studies in the Pelly Mountains, Yukon Territory; in Report of Activities, Part A, Geological Survey of Canada, Paper 76-1A, p. 97-106.

Tempelman-Kluit, D.J., Morin, J.A., Abbott, J.G., and Debicki, R.
1981: Yukon Geology and Exploration 1979-1980, Indian and Northern Affairs, Canada, 364 p.

## APPENDIX

CATHY. Niddery Lake map area (105 O/7), 63°16.5'N, 130°33'W.

GSC Loc. No. C-087547. 2 m limestone bed in Lower Earn Group. Fauna: **Eognathodus sulcatus kindlei** Lane & Ormiston, **Icriodus steinachensis** Al Rawi β morphotype Klapper & Johnson, ?**Ozarkodina selfi** Lane & Ormiston, **Pandorinellina steinhornensis** (Ziegler), **Pelekysgnathus** sp., **Belodella** sp., **Panderodus** sp.

GSC Loc. No. C-087546. As C-087547. Fauna: **Eognathodus sulcatus kindlei** Lane & Ormiston, **Icriodus** sp. indet., **Pedavis** sp. indet., **Pandorinellina** sp., **Panderodus** sp.

GSC Loc. No. C-087691. 0.4 m limestone bed in grey lower barite. Fauna: **Polygnathus** cf. **linguiformis** Hinde, **Polygnathus** sp. indet. (posterior platform fragment resembling **P. pseudofoliatus** Wittekindt or similar species).

GSC Loc. No. C-087692. 1.5 m of lenticular limestone in cherty siltstone 14 m below upper barite. Fauna: **Polygnathus linguiformis linguiformis** Hinde, **P. timorensis** Klapper, Philip & Jackson, P. cf. **P. varcus** Stauffer, ?P.? **geniculatus** Uyeno, **Belodella** sp.

GSC Loc. No. C-087693. Small limestone bed directly below upper barite. Fauna: **Polygnathus linguiformis linguiformis** Hinde, **P. linguiformis.** ?epsilon morphotype Ziegler, Klapper & Johnson, **P. timorensis** Klapper, Philip & Jackson, **Icriodus** sp. indet.

CATHY-BAR. Niddery Lake map area (105 O/7), 63°17.5'N, 130°34'W.

GSC Loc. No. C-086296. 1 m blue-grey weathering limestone within Lower Earn Group. Fauna: **Polygnathus inversus** Klapper & Johnson, **Pandorinellina** cf. **P. exigua** (Philip), **P. steinhornensis** (Ziegler).

HOWARDS PASS. Nahanni map area (105 I/6), 62°27'N, 129°26'W.

GSC Loc. No. C-087552. Baritic limestone in Lower Earn Group 13 km west of XY deposit. Fauna: ?**Tortuodus kockelianus** (Bischoff & Ziegler) (a single fragment).

ORO. Nahanni map area (105 I/12), 62°37'N, 129°46'N

GSC Loc. No. C-087540. Diamond-drillhole 73-6' Base of barite beds at 22 m (73 ft.). Limestone underlying barite, at 56 m (185-187 ft.). Fauna: **Polygnathus** sp.

PETE. Niddery Lake map area (105 O/1), 62°02'N, 130°06'W.

GSC Loc. No. C-087698. Base of black limestone that lies beneath barite with minor amounts of bedded zinc-lead-silver mineralization. Fauna: **Icriodus symmetricus** Branson & Mehl, **Palmatolepis punctata** (Hinde), **Ancyrodella** cf. **A. curvata** (Branson & Mehl), **Polygnathus** sp. indet.

GSC Loc. No. C-087699. Centre of black limestone as above. Fauna: **Ancyrodella** cf. **A. gigas** Youngquist, **Palmatolepis** cf. **P. subrecta** Miller & Youngquist, **Polygnathus** sp., **Icriodus** sp.

GSC Loc. No. C-087700. Top of black limestone as above. Fauna: **Palmatolepis punctata** (Hinde), **P.** cf. **P. subrecta** Miller & Youngquist, **Icriodus** sp.

GHMS. Nahanni map area (105 I/7, 8), 62°24'N, 128°30"W.

GSC Loc. No. C-087543. Grey limestone with calcite veins, ?15 m below barite. Fauna: **Mesotaxis asymmetricus** (Bischoff & Ziegler).

GSC Loc. No. C-087542. Grey limestone bed 6 m below barite. Fauna: **Polygnathus** cf. **P. dubius** Hinde, **P.** cf. **P. dengleri** Bischoff & Ziegler, ?**P. varcus** Stauffer group, **Icriodus** sp. indet., **'Spathognathodus'** sp.

GSC Loc. No. C-087696. Grey limestone bed ?15 m below barite. Fauna: **Mesotaxis asymmetricus** (Bischoff & Ziegler), **Polygnathus** sp.

GSC Loc. No. C-087697. Grey limestone bed ?6 m below barite. Fauna: **Polygnathus dubius** Hinde.

GSC Loc. No. C-087695. Grey limestone bed ?15 m below barite. Fauna: **Mesotaxis asymmetricus** (Bischoff & Ziegler), **Polygnathus** sp.

GSC Loc. No. C-101979. Limestone bed immediately beneath barite. Fauna: **Ancyrodella** cf. **A. curvata** (Branson & Mehl).

GARGANTUA NORTH. Niddery Lake map area (105 O/1); 63°06'N, 130°11'W.

GSC Loc. No. C-086425. 0.5 m limestone bed in middle of chert beds, 25 m below hornfelsed shale, 25 m above uppermost barite strata (chert). Fauna: **Palmatolepis** cf. **P. subrecta** Miller & Youngquist, **P.** cf. **P. proversa** Ziegler, **P.** cf. **P. subrecta** Miller & Youngquist, Collected by I.R. Jonasson and J.W. Lydon.

JEFF. Sekwi Mountain map area (105 P/12), 63°36.6'N, 129°39.4'W.

GSC Loc. No. C-087558. From limey interval of bedded barite. Fauna: **Palmatolepis gigas** Miller & Youngquist, **P. subrecta** Miller & Youngquist, **P. hassi** Müller & Müller, **Ancyrodella nodosa** Ulrich & Bassler, **Polygnathus**? **ancyrognathoidea** Ziegler.

UN-NAMED. Quiet Lake map area (105 F/15), 61°47'30"N, 132°43'30"W, 9.5 miles ESE of Porcupine Creek.

GSC Loc. No. C-93428a. Carbonate associated with bedded barite of unit 5 of map 7-1960. Fauna: **Gnathodus pseudosemiglaber** Thompson & Fellows, **'Spathognathodus'** sp. indet.

GSC Loc. No. C-93428b. As C-93428a. Fauna: **Doliognathus**? sp. indet., **Gnathodus** sp. indet., **'Hindeodella' segaformis** Bischoff.

GSC Loc. No. C-93428c. As C-93428a. Fauna: **'Hindeodella' segaformis** Bischoff.

TEA. Niddery Lake map area (105 O/2), 63°01-5'N, 130°36.5'W.

GSC Loc. No. C-086426. Fossiliferous limestone in trenches at bottom of Tea Hill; at least 50 m below lowermost exposed barite beds, talus intervening. Fauna: **Protognathodus praedelicatus** Lane, Sandberg & Ziegler, including specimens transitional to **Gnathodus cuneiformis** Mehl & Thomas, **Pseudopolygnathus multistriatus** Mehl & Thomas, **Ploygnathus communis communis** Branson & Mehl, **'Spathognathodus'** sp. Collected by I.R. Jonasson and J.W. Lydon.

GSC Loc. No. C-087721. From within barite beds, 17 m above exposed base. Fauna: **'Hindeodella' segaformis** Bischoff.

# THE PRE-LATE WISCONSINAN FORAMINIFERAL ASSEMBLAGE OF ST. LAWRENCE BAY, CAPE BRETON ISLAND, NOVA SCOTIA

Project 750038

J.-P. Guilbault[1]
Atlantic Geoscience Centre, Dartmouth

*Guilbault, J.-P., The pre-Late Wisconsinan foraminiferal assemblage of St. Lawrence Bay, Cape Breton Island, Nova Scotia; in Current Research, Part C, Geological Survey of Canada, Paper 82-1C, p. 39-43, 1982.*

***Abstract***

*In the classical cliff section at St. Lawrence Bay, the fossiliferous stony silt previously considered as in situ marine is probably a till or an ice-rafted sediment. It contains a composite foraminiferal assemblage representing various bathymetries; the deepest elements (the* ***Bulimina*** *assemblage) are found living today in the Gulf of St. Lawrence only in Atlantic water, at depths greater than 100 m. Combined conditions of relative sea level and climate have probably never been adequate for this deposit to have formed in situ. A glacier advancing from the N or NE seems the most likely transport agent.*

## Introduction

Nineteen samples from a Quaternary deposit in a coastal cliff at St. Lawrence Bay, northern Cape Breton Island, Nova Scotia, have been studied for their foraminiferal content. The sampling was carried out by Serge Occhietti of University of Quebec in Montreal. The section has been visited and described by different authors; a summary of the literature as well as the exact location can be found in Wagner (1977). The lithostratigraphy of the section reported here is, from top to bottom (Occhietti and Rutter, 1982):

| | Thickness (m) |
|---|---|
| - coarse material | up to 30 |
| - lenticular bed (≈300 m long) of roughly stratified and fossiliferous stony silt with pockets and lenses of sand and pebbles; elevation between 14 and 21 m a.s.l. | 0.1 to 3.5 |
| - gravelly and coarse material, with some silt beds | 4 to 6 |
| - lenticular organic bed (≈400 m long) with silt beds, wood dated by $^{14}C$ at >38 000 years B.P., GSC-283 | 0.01 to 0.45 |
| - gravelly material | 4 to 5.5 |
| - lens (≈400 m long): shore deposits | 0.1 to 1.5 |

This section rests upon a bedrock platform 2.6 to 7 m a.s.l. and higher laterally.

The faunas reported here come from the upper fossiliferous stony silt layer. The samples have been collected at 10-cm intervals on the average, but only 19 samples out of 32 have been studied. The sequence of facies described above is agreed upon all authors having studied this locality. For more details about the lithostratigraphy, the reader is referred to Occhietti and Rutter (1982). Earlier micropaleontological work on the upper silt layer includes a foraminiferal analysis of one sample by Vilks (in Wagner, 1977) and a pollen diagram by Mott and Prest (1967) covering the whole bed (12 samples).

## Methods

The foraminifera were extracted by dispersing the sediment in a detergent solution, washing it through a 63 µm sieve and floating the dried sieve residue in a 10:4 mixture of bromoform and acetone. Only the fraction larger than 125 µm has been studied.

## Results

Fifty-three taxa (including forms of **Elphidium excavatum**) have been identified (Table 4.1). They have been listed following the classification of Feyling-Hanssen et al. (1971). The species of **Lagena**, **Oolina**, and **Fissurina** have been grouped under their respective generic names. Some authors might prefer to synonymize some of the forms listed here (e.g., the species of **Bulimina** and **Buccella**) but at this early stage it seems preferable to split the material into a maximum number of taxonomic units to avoid losing potentially useful information. The number of specimens of each species has not yet been determined. The diagram shows instead a visual estimation of the relative abundance of each species. Three arbitrary classes are used: rare, frequent, and abundant. In two of the samples, the total numbers are so small that absolute figures are given. Some biases may arise from the 'method' of visual estimation. Nevertheless, if used in a consistent way, it can give an idea of the dominant forms and identify any obvious stratigraphic variations.

As can be seen from Table 4.1, there is no significant variation in faunal composition between the base and the top of the bed, as if it was representing a single homogeneous environment. Most of the population recorded at St. Lawrence Bay can be found living today in the Gulf of St. Lawrence at depths of less than 100 m. This includes the frequent-to-abundant forms **Cassidulina reniforme, Islandiella helenae, I. norcrossi, Nonion labradoricum**, and **E. excavatum** forma **clavata**. **I. islandica** may also be important in the present day gulf, but because of confusion with **C. reniforme** in the literature, its distribution is poorly known. Except for **I. islandica**, the species just mentioned and many others listed in Table 4.1 have been found in the Champlain Sea (Guilbault, 1980), and are among the most frequent inhabitants of glacial-isostatic seas. On the other hand, none of the very widespread arenaceous species found today in the area are present in the section, but this may be due to selective destruction of their tests by postdepositional diagenetic processes.

[1] Gulf of Canada, Research Exploration Department, P.O. Box 130, Calgary, Alberta T2P 2H7

Table 4.1

Distribution of foraminifer species in the St. Lawrence Bay section

| Species | Sampled Interval (cm) | | | | | | | | | | | | | | | | | | |
|---|---|---|---|---|---|---|---|---|---|---|---|---|---|---|---|---|---|---|---|
| | bottom | | | | | | | | | | | | | | | | | | top |
| | 395-400 | 365-470 | 345-350 | 335-340 | 285-290 | 265-270 | 245-250 | 225-230 | 205-210 | 185-190 | 165-170 | 145-150 | 125-130 | 105-110 | 85-90 | 65-70 | 45-50 | 25-30 | 0-8 |
| **Silicosigmoilina groenlandica** Cushman | | | | | | | | - | | | | | | | | | | | |
| **Dentalina** spp. | - | | | | | | | | | - | | | | | | | | | |
| **Astacolus hyalacrulus** Loeb. and Tap. | | | | - | | | | | | | | | | | | | | | |
| **Lagena** spp. | | | - | - | - | | | | | | - | | | | | | - | | |
| Undifferentiated Polymorphinidae | | | | | | | | | | | - | | | | - | | | - | |
| **Oolina** spp. | | | | - | - | | - | | - | | | | | | | | | - | |
| **Fissurina** spp. | | | | - | | - | | | - | | | | | | | | | - | |
| **Bulimina exilis** Brady | - | | - | | | | | | | | | | | | | | | | |
| **B. aculeata** d'Orbigny | f | f | | - | - | - | f | | - | - | f | | - | | - | | f | - | f |
| **B. marginata** d'Orbigny | - | f | f | f | - | f | f | f | f | - | f | | - | | - | - | - | f | - |
| **Globobulimina auriculata** (Bailey) | - | - | - | f | - | - | - | - | - | | | | | | - | | f | f | - |
| **Virgulina concava** Hoglund | - | - | - | - | - | - | - | - | | | | | | | - | | | - | - |
| **V. schreibersiana** Czjzek | | | | - | | | | - | | | | | | | - | | | - | - |
| **Trifarina angulosa** (Williamson) | | | | - | - | | | | | | | | | | | | | | |
| **T. fluens** (Todd) | - | | - | - | | | - | - | - | | | | | | - | | | - | |
| **Bolivina subaenariensis** Cushman | A | f | f | f | - | f | f | A | f | f | f | 2 | f | 1 | f | - | f | f | f |
| **Cassidulina reniforme** Norvang | A | A | A | - | A | A | f | A | A | A | A | 1 | f | 1 | A | f | A | A | A |
| **C. laevigata** d'Orbigny cf. **teretis** Tappan | | - | - | - | | - | - | - | - | | - | | | | | | | - | |
| **Islandiella helenae** F.-H. and Buzas | f | A | - | f | f | f | - | f | f | f | A | 1 | f | 1 | - | f | | f | - |
| **I. islandica** Noervang | f | f | f | f | f | - | f | f | f | f | f | 1 | - | | - | - | - | f | |
| **I. norcrossi** (Cushman) | A | A | A | A | A | A | A | A | A | A | A | 5 | A | 2 | A | A | A | A | A |
| **Bucella frigida** (Cushman) | - | - | | - | | - | | | - | - | | | | | - | | | - | |
| **B. hannai** (Phleger and Parker) | - | - | - | - | | - | - | f | - | | - | | - | | - | | - | - | f |
| **B. tenerrima** (Brady) | - | - | | - | | | - | | | | | | - | | | - | - | - | |
| **Epistominella vitrea** Parker | | | | | | - | | - | | | | | | | | | | - | |
| **Gyroidina quinqueloba** Uchio | | | - | - | | | - | | | | | | | | - | | | - | - |
| **Eoeponidella pulchella** (Parker) | | | | | | | | | | | - | | | | | | | | |
| **Cibicides lobatulus** (Walker and Jacob) | - | - | - | - | - | - | - | - | - | - | - | 1 | - | | - | | - | - | - |
| **Cibicides** indeterminate | | | | | | - | | - | | | - | | | | - | | | - | |
| cf. **Nonion grateloupi** d'Orbigny | | | | | | - | | | | | | 1 | - | | | | | - | |
| **Nonionella** aff. **auricula** | - | | - | | | - | - | | | | | | | | | - | - | - | - |
| **N. auricula** H.-A. and Earland | | | | | | | | | | | | | | | | | - | | |
| **N. turgida** (Williamson) | | | | | | - | | | | | | | | | - | | - | - | |
| **Astrononion gallowayi** Loeb. and Tap. | - | - | - | - | - | - | - | - | | | - | | | | - | | - | - | |
| **Melonis barleanum** (Williamson) | - | - | - | - | - | | | - | - | - | - | | - | 1 | - | - | - | - | - |
| **Pullenia bulloides** d'Orbigny | - | | | - | - | | - | - | | | - | | - | | - | - | | - | |
| **P. quinqueloba** (Reuss) | - | | | | - | | - | - | | | | | | | - | | | | |
| **Haynesina orbiculare** (Brady) | | | | | | - | | - | - | | | | | | | | - | | - |
| **Elphidium albiumbilicatum** (Weiss) | - | - | | | - | | - | | | - | | | | | | | - | | |
| **E. bartletti** Cushman | | | | | | | | | | | | | | | | | | | - |
| **E. hallandense** Brotzen | | | | - | | | - | - | - | | - | | | | - | | - | - | |
| **E. incertum** (Williamson) | - | | | f | | | | | | | | | | | - | | | - | |
| **E. excavatum** forma **clavata** Cushman | A | A | A | A | A | f | A | A | A | A | A | 2 | f | 3 | A | f | A | A | A |
| **E. e.** forma **excavata** Terquem | f | - | f | f | | - | - | f | f | | f | | | | f | f | - | - | f |
| **E. e.** forma **selseyense** H.-A. and Earland | - | | | - | | | - | | | | | | | | | | | | |
| **E. groenlandicum** Cushman | f | - | - | f | - | - | - | f | - | - | - | | | | - | - | - | f | - |
| Undifferentiated planktonics | A | f | f | f | f | f | A | f | f | f | f | 1 | - | | f | - | f | f | f |

A = abundant
f = frequent
\- = rare

Species suggestive of very shallow water such as **Haynesina orbiculare, Elphidium albiumbilicatum, E. hallandense** and **E. incertum** are either rare or absent. They are usually small and underdeveloped. Under nearshore conditions (a few metres depth) they would be numerous, large and well developed.

The most frequent form of **E. excavatum** is **E. excavatum** forma **clavata,** which is probably the most common near-ice shelf species. **E. excavatum** f. **excavata** is rather frequent but never as abundant as forma **clavata.** A few specimens of forma **selseyense** also occur. Because the formae grade one into the other, their identification is frequently difficult. In many cases, only a SEM study could allow a definite separation of the formae. Poor preservation is another factor making identification difficult. Therefore, the proportions suggested by Table 4.1 are approximate. However, the presence of a noticeable amount of **excavata** and of a few **selseyense** seems to suggest warmer water (sub-Arctic to cool temperate) than a pure **clavata** assemblage (Miller et al., 1982).

The most remarkable feature of the St. Lawrence Bay assemblage is the presence of species that are found today only below the 100 m isobath and reach their maximum development below 200 m along the outer margin of the Scotian Shelf, in basins of the Scotian Shelf and in the Laurentian Channel. They are: **Bulimina aculeata, B. marginata, B. exilis, Gyroidina quinqueloba, Bolivina subaenariensis, Nonionella turgida, Melonis barleeanum, Pullenia bulloides, Pullenia quinqueloba,** and **Cassidulina laevigata.** Other St. Lawrence Bay species such as **Nonion labradoricum** and **Globobulimina auriculata** are found both above and below the 100 m level in the modern gulf, but reach their greatest abundance in deeper waters.

Planktonic foraminifera occur as 'frequent' throughout the section. Nearly all can be assigned to the species **Neogloboquadrina pachyderma.** Usually, planktonics are rare or absent at such nearshore locations (because of the local setting – a north-facing half-circle of hills with altitudes of up to 400 m – it is unlikely that this site has ever been far from shore, even at the highest sea level stand).

Another interesting point is the presence of two forms not found alive today off eastern Canada: **Elphidium groenlandicum** and a variant of **Cassidulina laevigata** here designated **Cassidulina** cf. **teretis.** Cole (personal communication) has not observed any living **E. groenlandicum** off eastern Canada but frequently recorded dead tests. The species can also be found in boreholes drilled in redeposited sediments, but the time of its disappearance from the area is unknown. The **Cassidulina** cf. **teretis** reported here differs from **C. laevigata** in having on the average one additional chamber in the last whorl and a well defined umbilical boss. It differs from the typical **C. teretis** from Baffin Island illustrated by Feyling-Hanssen (1976, 1980) in being smaller and having on the average one fewer chamber per whorl. It is thus intermediate between **laevigata** and **teretis** and it grades into **laevigata.** Therefore, it has been grouped together with this last species in Table 4.1. Comparable **'C.** cf. **teretis'** forms are not observed in eastern Canada in late- and postglacial deposits. On the other hand, they can be found in redeposited sediments along with **E. groendlandicum** in borings from the Sable Island Bank, and in association with near-ice shelf species in turbidite beds from the Sohm Abyssal Plain. The material in these turbidites is thought to originate on the Scotian Shelf and the Grand Banks (Vilks, personal communication). Forms intermediate between **C. teretis** and **C. laevigata** can be found living today in the deep sea, but as a shelf species they disappeared from eastern Canada before the late Wisconsinan. Nobody knows when, but investigations by Feyling-Hanssen (1980) suggested that **C. teretis** reaches its peak abundance in late Pliocene early Pleistocene time and that on the shelf it is replaced subsequently by an **Islandiella** assemblage. Therefore, its final disappearance may be quite ancient.

## Discussion

The St. Lawrence Bay assemblage is a rather unusual mixture of species. Most of the fauna belongs to species that can be found either in near-ice marine sediments or in the calcareous part of the fauna observed in modern sediments in the present day gulf, at intermediate depths (20 to 100 m) and in association with cold (0°C) and marginal marine (30 to 33‰ salinity) gulf water. There are some species suggestive of very shallow water (less than 20 m) but they constitute a minor factor of the assemblage. Being few and underdeveloped, their occurrence does not have a great paleoecologic significance. The most common form of **E. excavatum** is the cold-water forma **clavata,** but the warmer and shallower formae **excavata** and **selseyense** are also present.

The other species present – possibly up to 20 per cent of the total – are found living in association with the deeper 'Atlantic' water (4°C, 34‰) which occupies the Laurentian Channel. These species – the **Bulimina marginata** assemblage – appear below 100 m (Cole, personal communication) to 125 m (Rodrigues, 1980), but reach their maximum development below 200 m. They are absent or extremely scattered above 100 m. The same assemblage occurs on the edge of the Scotian Shelf and in deep basins (200 m or more) in the middle of it (Williamson, personal communication). The main constituents of the **Bulimina marginata** assemblage occur also along the edge of the shelf south of the Gulf of Maine (Culver and Buzas, 1980). It is thus an assemblage of southern origin along with the water in which it lives. Its representatives are rare in modern cold shelf seas such as the Labrador Sea and Hudson Bay. They are totally absent from Pleistocene glacial-isostatic seas (Champlain Sea, Goldthwait Sea, Tyrrell Sea) whatever their depth.

As a consequence of the preceding, we must suppose that either the intermediate depth assemblage – 80 to 90 per cent of the St. Lawrence Bay fauna – has been carried downslope below the 100 m paleo-isobath or that the whole assemblage has lived in situ in the transitional zone just below the 100 m paleo-isobath. In both cases, we need a paleobathymetry of more than 100 m. If we suppose that the hydrology of the gulf area has been the same as today during other Quaternary interglacials, it is impossible to explain the St. Lawrence Bay deposit without raising the relative sea level by at least 100 + 15 = 115 m (minimum depth of the **Bulimina** assemblage, plus present altitude of the deposit a.s.l.). This is much higher than for the highest sea level stand proposed for any interglacial. During interstadials and during full glacials, either the region would have been ice-covered or the eustatic sea level would have been too low. The only time when such a high relative sea level could have taken place would be at the time of the retreat of a major ice sheet. The paleogeographic reconstructions of the late Wisconsinan usually accepted today do not call for the kind of large and thick ice sheet that could produce such an isostatic downwarping. On the other hand, during earlier Wisconsinan stadials, huge amounts of ice appear to have covered the Maritimes (Grant, 1977) and might have produced the necessary downwarping. Quinlan and Beaumont (1981) made theoretical estimations of the relative sea level changes at the time of the last deglaciation. They used both a minimum and a maximum ice model. The maximum ice model does not fit the late Wisconsinan field data, but might apply to the end of an early Wisconsinan stadial, when glaciation was extensive. The maximum relative sea level predicted by the maximum ice model for northern Cape Breton is approximately 50 m a.s.l., 6000 years after the peak of glaciation (Quinlan, personal communication). A more protracted melting period would have produced a still lower RSL. Although this model has been conceived for application to the last deglaciation, extrapolation suggests a very high stand of sea level is most unlikely. Furthermore, even if a glacial-isostatic sea with a 115 m RSL had been present at St. Lawrence Bay, its fauna would probably have been entirely of the near-ice type, as in the Champlain Sea. The **Bulimina** assemblage could not live, and has never been observed to live, under such conditions. By the time the ice had receded enough to allow the 'Atlantic' water and the **Bulimina** fauna to move in, isostatic rebound processes would have already reached so far as to make impossible the deposition of the St. Lawrence Bay assemblage at its present location.

The only alternative left for supporting an in situ origin would be to suppose different hydrologic conditions, viz., an interstadial where the Atlantic waters reached close to the surface. Bartlett and Molinsky (1972) reported the subtropical planktonic form **Globigerinoides ruber** in postglacial cores in the Gulf of St. Lawrence. However, the presence of the **Bulimina** fauna in intermediate to shallow water deposits of the same age has never been observed. Thus, the presence of subtropical planktonics seems to be an unusual accident. If so, the existence of a relatively shallow **Bulimina** fauna in the gulf area is unlikely at any time since the Pliocene or the early Pleistocene. For St. Lawrence Bay, such an age is improbable on faunal grounds (see faunal sequence of Feyling-Hanssen, 1980, for eastern Baffin Island). Therefore, it seems impossible to explain the St. Lawrence Bay deposit as being in situ. This agres well with the fact that no raised marine deposit has ever been found in neighbouring areas to suggest the existence of a high marine stand – even no more than 15 m a.s.l. – at any time in the Quaternary and especially during the Wisconsinan. An in situ marine deposit at this location would be an anomaly that would put a strong strain on any reconstruction for the area.

If the fauna is not in situ, it has to be partially or totally reworked. Arguments favouring redeposition (apart from lithologic characters) include the uniformity in faunal composition from the very base to the very top of the section. There are variations in the total number of individuals, but there is little variation in the proportion of each species. Another argument in favour of redeposition is the preservation, which is not good, specimens having frequently lost many chambers. The simultaneous presence of species inhabiting different bathymetries and the consistent presence of frequent planktonics at this nearshore location also suggest some form of redepositon. An argument against this interpretation is the lack of granulometric sorting of the tests. One way to solve the problem would be to invoke a form of glacial transport allowing material to be picked up from the bottom of the gulf (including the Laurentian Channel) by an advancing glacier and redeposited at St. Lawrence Bay. It would explain at the same time the poor sorting of the sediment and formaminifera and the fact that they have been carried up from the Laurentian Channel to their present location. It would not contradict the palynologic results of Mott and Prest (1967) who reported an environment cooler than today's, with an admixture of hystrichosopheres, possibly Paleozoic. This idea also agrees with the results of Wagner (1977) who found that the molluscs reported by Newman (1971), except for one species, presently live at depths greater than 25 m. The glacial transport hypothesis implies the existence of grounded ice in the Laurentian Channel. MacLean and King (1971) reported the presence of a till ("Laurentian Drift") on the bottom of the Laurentian Channel. Its age is not known but it shows that at some time in the past there has been grounded ice in the Laurentian Channel.

The deposition of the assemblage could have taken place by ice-rafting, but it could also be a flow-till or an ablation till. The first two hypotheses imply the presence of water, which could be either a glacial-isostatic sea or a proglacial lake. Evidence against a marine environment is the lack of other raised marine deposits in the area. Deposition in a marine environment might allow the additional hypothesis that only the deep-water **Bulimina** assemblage was redeposited, the other species having lived in situ. However, the preservation of all the different forms being comparable, it is more likely that all have been subjected to the same transport process. The hypothesis of a lacustrine environment is favoured by the local topography, a north-facing half-circle of hills that could easily have been blocked by a glacier lobe.

The third hypothesis (an ablation till) is certainly not impossible as foraminifera from tills may be very well preserved. As a comparison, samples from the interstadial locality at Salmon River, western Nova Scotia (see Wagner, 1977, locality 4), were studied. The red fossiliferous till (a basal till) underlying the stratified silty sand was found to contain an assemblage of **Cibicides lobatulus** and **E. excavatum** whose degree of preservation (mechanical breakage, abrasion) was similar to, though not as good, as that of St. Lawrence Bay. The deeper water species were lacking, but that may be only because the glacier at the origin of the Salmon River red till, coming from the northwest, did not overrun deeper water marine deposits. One must keep in mind that the distance between the St. Lawrence Bay section and the 200 m isobath in the Laurentian Channel is only 30 km while the distance to the 100 m isobath is only 5 km. Thus, the material in the St. Lawrence Bay section could well have been picked in the depression around St. Paul Island and on the bottom of St. Lawrence Bay itself. There is no evidence however that the St. Lawrence Bay deposit is an allochthonous thrust mass of sediment.

Age

Given that the intertidal bedrock platform underlying the section is of Sangamon age, the bed studied has to be Wisconsinan (Prest, 1977). As it cannot be late Wisconsinan (see earlier), it has to date from either of the two other Wisconsinan stadials or from their retreating phase, that is, if we accept the glacial redeposition hypothesis. For the deposit to be entirely in situ, it would be necessary to suppose a rather old age – probably Sangamon or older – in order to accommodate the 'old' species **E. groenlandicum** and mostly **C. teretis**. This would contradict the Sangamon age hypothesis for the bedrock surface and, therefore, it is supporting indirectly the redeposition hypothesis.

## References

Bartlett, G.A. and Molinsky, L.
1972: Foraminifera and the Holocene history of the Gulf of St. Lawrence; Canadian Journal of Earth Sciences, v. 9, no. 9, p. 1204-1215.

Culver, S.J. and Buzas, M.A.
1980: Distribution of recent benthic foraminifera off the North American Atlantic coast; Smithsonian Contributions to Marine Sciences no. 6, 512 p.

Feyling-Hanssen, R.W.
1976: The Clyde Foreland Formation: a micro-paleontological study of Quaternary stratigraphy; Maritime Sediments, Special Publication no. 1, p. 315-377.

1980: Microbiostratigraphy of young Cenozoic marine deposits of the Qivituq Peninsula, Baffin Island; Marine Micropalentology, v. 5, p. 153-184.

Feyling-Hanssen, R.W., Joergensen, J.A., Knudsen, K.L., and Lykke Andersen, A.-L.
1971: Late Quaternary foraminifera from Vendsyssel, Denmark and Sandnes, Norway. Bulletin, Geological Society of Denmark, v. 21, p. 67-317.

Grant, D.R.
1977: Glacial style and ice limits, the Quaternary stratigraphic record, and changes of land and ocean level in the Atlantic Provinces, Canada; Géographie physique et Quaternaire, v. 31, no. 3-4, p. 247-260.

Guilbault, J.-P.
1980: A stratigraphic approach to the study of the Late-Glacial Champlain Sea deposits with the use of foraminifera; Unpublished Licentiat thesis, Aarhus University, Aarhus, Denmark, 294 p.

MacLean, B. and King, L.H.
1971: Surficial geology of the Banquereau and Misaine Bank map area, Geological Survey of Canada, Paper 71-52, 19 p.

Miller, A.A.L., Scott, D.B., and Medioli, F.S.
1982: **Elphidium excavatum** (Terquem): Part I. Ecophenotypic versus subspecific variation; Journal of Foraminiferal Research, v. 12, no. 2, p. 116-144.

Mott, R.J. and Prest, V.K.
1967: Stratigraphy and palynology of buried organic deposits from Cape Breton Island, Nova Scotia; Canadian Journal of Earth Sciences, v. 4, p. 709-724.

Newman, W.A.
1971: Wisconsin glaciation of northern Cape Breton Island, Nova Scotia, Canada; Unpublished Ph.D. thesis, Syracuse University, Syracuse, N.Y. University Microfilms, Ann Arbor, Michigan.

Occhietti, S. and Rutter, N.
1982: Acides aminés et interstades du Wisconsinien de la Vallée du Saint-Laurent et de l'Île du Cap Breton, Current Research, Part B, Geological Survey of Canada, Paper 82-1B, p. 301-305.

Prest, V.K.
1977: General stratigraphic framework of the Quaternary in Eastern Canada; Géographie physique et Quaternaire, v. 31, no. 1-2, p. 7-14.

Quinlan, G. and Beaumont, C.
1981: A comparison of observed and theoretical postglacial relative sea level in Atlantic Canada; Canadian Journal of Earth Sciences, v. 18, p. 1146-1163.

Rodrigues, C.G.
1980: Holocene microfauna and paleoceanography of the Gulf of St. Lawrence; Ph.D. thesis, Carleton University, 352 p.

Wagner, F.J.E.
1977: Paleoecology of marine Pleistocene mollusca, Nova Scotia; Canadian Journal of Earth Sciences, v. 14, p. 1305-1323.

5.

# OXYGEN ISOTOPE GEOCHEMISTRY OF THE SHALES HOSTING Pb-Zn-Ba MINERALIZATION AT THE JASON PROSPECT, SELWYN BASIN, YUKON

E.M.R. Research Agreements 40/6/81 and 22/4/82

F.J. Longstaffe[1], B.E. Nesbitt[1], and K. Muehlenbachs[1]
Economic Geology Division

*Longstaffe, F.J., Nesbitt, B.E., and Muehlenbachs, K., Oxygen isotope geochemistry of the shales hosting Pb-Zn-Ba mineralization at the Jason Prospect, Selwyn Basin, Yukon; in Current Research, Part C, Geological Survey of Canada, Paper 82-1C, p. 45-49, 1982.*

### Abstract

*Oxygen isotope analyses have been obtained for whole rock and clay mineral samples of shales hosting Pb-Zn-Ba mineralization at the Jason prospect, Selwyn Basin, Yukon. Drill cores from two zones of mineralization were sampled: 1) the Main Zone, which is a stratiform body of interlaminated barite and sulphides; and 2) the South Zone, which appears to be stratigraphically lower than the Main Zone, and consists both of massive and laminated sulphide ± barite mineralization and is in part stratigraphically underlain by a mineralized stockwork zone. Within 1-2 m above and below the Main Zone, whole rock samples are depleted in $^{18}O$ by about 1 to 2 ‰. The <2 μm clay fractions from the same samples show much larger shifts in $^{18}O/^{16}O$ ratios from about +16 to +19 to as low as +5.6 for samples in contact with the sulphides. This dramatic shift in $\delta^{18}O$ as the mineralized body is approached is accompanied by a change in clay mineralogy from illite to kaolinite. Shales about the South Zone are also depleted in $^{18}O$ by 2 to 4 ‰. The isotopic alteration begins within 1 to 2 m of the upper contact with the sulphides and extends well into a zone of alteration located below the mineralization. The <2 μm clay fraction is depleted in $^{18}O$ by up to 6 ‰ but remains dominated by illite, rather than kaolinite, within the low-$^{18}O$ halo in the footwall.*

*The oxygen isotope data for the silicate host rocks are compatible with an exhalative origin for the mineralization. The results are consistent with the interpretation that the ore fluids migrated vertically below the South Zone and laterally in the Main Zone. The kaolinite oxygen isotope values can be modelled from fluids similar in isotopic composition to ocean water or formation fluids. The ocean water model suggests maximum temperatures of 270°C for kaolinite precipitation, whereas lower temperature estimates can be obtained for a model employing formation fluids with a significant component of meteoric water.*

## Introduction

Preliminary results of oxygen isotope analyses of shales/argillites hosting the Jason Pb-Zn-Ba deposit, Yukon Territory are described in this paper. The Jason deposit is one of many stratiform sulphide/barite deposits within the Selwyn Basin. Details of these deposits can be found in reports by Carne and Cathro (1982), Large (1981), Lydon et al. (1979), Dawson (1977), and Blusson (1976), among others. The Jason and the adjacent Tom deposit are located in the Macmillan Pass area, within the upper Devonian "Black Clastic group" (Dawson, 1977). Winn et al. (1981) reported that the stratiform mineralization at Jason is hosted by a sequence of sedimentary breccias, pebbly mudstones and argillites, and some coarser units of turbidite affinity. The bedded mineralization is underlain by a stockwork zone of silicified and sideritized host rock that contains galena, sphalerite, chalcopyrite and pyrite.

Carne and Cathro (1982), following earlier studies of Carne (1979) on the Tom deposit, proposed that the Pb-Zn mineralization is related to rifting and that the transport of ore fluids were along basin margin fault zones onto the seafloor. Winn et al. (1981) postulated that the sulphides at Jason were precipitated on the seafloor within a small graben, from hydrothermal fluids that travelled upwards along fault zones.

The purpose of this study is to elucidate the nature of the ore-fluid/wall rock exchange during the mineralization events at Jason by studying changes in the oxygen isotope composition of the shale/argillite and its constituent clay minerals. The oxygen isotope values of clay minerals formed or modified during hydrothermal processes are dependent primarily on the temperature(s) of the mineral-rock interaction and the isotopic compositions of fluid(s) involved before, during, and after sulphide deposition.

## Analytical Techniques

The silicate samples were analyzed by the $BrF_5$ method of Clayton and Mayeda (1963). The data are reported in the usual δ notation with respect to Standard Mean Ocean Water (SMOW: Craig, 1961) using a $CO_2$-$H_2O$ fractionation factor of 1.0407. The standard deviation calculated from the pooled residual variance of replicate analyses performed during the course of this study is ±0.11‰. Clay minerals were separated from whole rock samples by standard sedimentation procedures and identified by X-ray diffraction analysis. Kaolin group polytypes were determined by Debye-Scherrer X-ray powder camera techniques.

## Results

More than 70 whole rock (shale/argillite) and clay mineral samples have been analyzed from seven drill cores that intersect two major zones of mineralization within the Jason property. In the Main Zone, the mineralization consists of a stratiform body of interlaminated barite and sulphides. In the South Zone, the mineralization consists of both massive and laminated textural types and is underlain in places by a mineralized stockwork in a zone of silicified host rock (B. Smee, personal communication).

The whole rock $\delta^{18}O$ values for samples from the Main Zone range from +16.0 to +22.5, which is within the range typical for clastic sedimentary rocks (e.g., Magaritz and Taylor, 1976; Eslinger and Savin, 1973; Longstaffe et al., 1980). Only a small depletion in $^{18}O$ (about 1‰) occurs at the upper and lower contacts with the mineralization (Fig. 5.1). The <2 μm clay fraction ranges in $\delta^{18}O$ from +17.1 to +21.6, again normal for clay minerals of detrital origin (Savin and Epstein, 1970; Longstaffe, 1981), to as low as +5.6 at the contact with mineralized zones. The largest

[1]Department of Geology, University of Alberta, Edmonton, Alberta. T6G 2E3

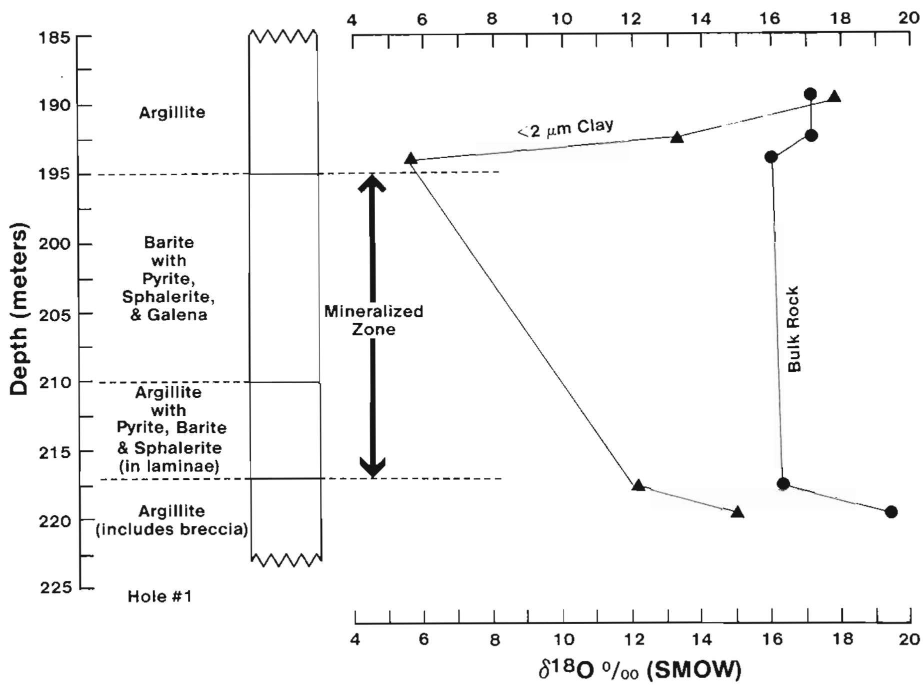


***Figure 5.1.*** *Oxygen-isotope results for whole rock and <2 μm clay samples from the Main Zone. Data shown are for drillhole 78-27 (hole no. 1); see Table 5.1.*

Table 5.1

Oxygen-isotope results for shale/argillite and constituent clay minerals hosting mineralization at Jason prospect

| Sample | $\delta^{18}O$ Whole Rock | $\delta^{18}O$ <2 μm |
|---|---|---|
| Main Zone | | |
| 78-27-12362 (189.5 m) | +17.1 | +17.8 |
| 78-27-12359 (192.5 m) | +17.1 | +13.3 |
| 78-27-12276 (194.0 m) | +16.0 | + 5.6 |
| 78-27-12292 (217.5 m) | +16.3 | +12.1 |
| 78-27-12365 (219.5 m) | +19.4 | +15.0 |
| South Zone | | |
| SI-19 (512.9 m) | +18.6 | +16.4 |
| SI-18 (524.0 m) | +18.5 | +16.1 |
| SI-9 (533.3 m) | +19.8 | +17.2 |
| SI-8 (542.7 m) | +19.4 | |
| SI-7 (543.7 m) | +20.3 | |
| SI-6 (548.0 m) | +20.5 | +17.1 |
| SI-5 (553.2 m) | +19.3 | +14.8 |
| SI-4 (554.9 m) | +20.8 | +18.0 |
| SI-3 (557.2 m) | +19.8 | +15.7 |
| SI-2 (558.8 m) | +19.2 | +16.6 |
| SI-1 (560.9 m) | +16.8 | +11.4 |
| SI-10 (589.6 m) | +16.9 | +12.3 |
| SI-11 (608.2 m) | +16.1 | +11.9 |
| SI-17 (616.8 m) 'chert' | +18.9 | |
| SI-16 (673.0 m) 'chert' | +19.8 | |
| SI-12 (674.7 m) | +19.2 | +15.4 |

shift in clay $\delta^{18}O$ values is obtained for samples transecting the Main Zone (Fig. 5.1, Table 5.1). The 12 ‰ depletion in $^{18}O$ as the sulphides are approached is accompanied by a change in clay mineralogy from illite in the unaltered country rocks to kaolinite at the contact with the bedded mineralization (Fig. 5.2, Table 5.1). Scanning electron photomicrographs show the kaolinite to have euhedral morphology and a mode of aggregation typical of an authigenic phase. The changes in mineralogy and oxygen isotope composition start only 2 or 3 m from the contact with the mineralization. Data from other drillholes that transect the Main Zone suggest that the magnitude of the $^{18}O$ shift, and the kaolinite/illite ratio, are smaller adjacent to the more weakly mineralized portions of the Main Zone.

Whole rock $\delta^{18}O$ values for shale/argillite and chert samples from the South Zone range from +16.1 to +20.8 (Table 5.1). The lower values occur only within a few metres of the massive mineralization, and decrease by as much as 4 ‰ close to the host rock-sulphide contact (Fig. 5.3). This shift is about twice that obtained for whole rock samples about the Main Zone. Figure 5.3 also indicates that, unlike the Main Zone, the depletion in $^{18}O$ within the zone of footwall alteration below the South Zone continues for at least 20 m below the massive sulphide contact.

The <2 μm mineral fraction ranges in $\delta^{18}O$ from +11.4 to +18.0 (Table 5.1). Depletion in $^{18}O$ from 'normal' values (+16 to +18) occurs only within 1 to 2 m of the upper contact with the mineralization; as for whole rock samples, the $^{18}O$-depletion halo continues below the zone of mineralization. Unlike the Main Zone, the dominant low-$^{18}O$ clay mineral in both the hanging wall and the footwall to the South Zone is illite and not kaolinite. Kaolinite is present in significant quantities in only one sample, which is located at the lower contact with the massive sulphides. The true size of the $^{18}O$ depletion of the illite cannot be determined from the existing data as attempts to obtain pure illite samples for analysis have not yet been successful.

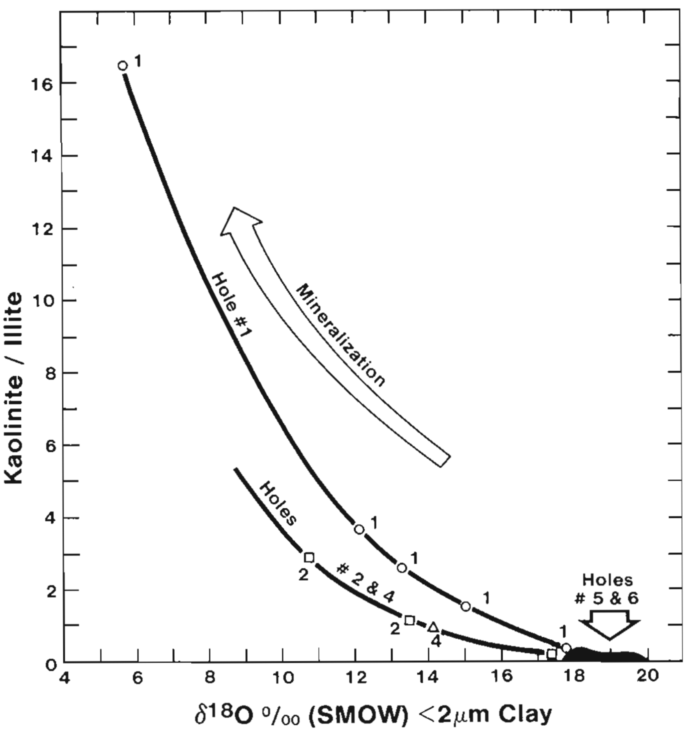


*Figure 5.2.* *Kaolinite/illite ratio versus $\delta^{18}O$ for the clay minerals. Hole no. 1 represents samples from drillhole 78-27. Holes 2 and 4 intersect more weakly mineralized portions of the Main Zone. Holes 5 and 6 intersect a small zone of sulphides in the South Zone, located above the major zone of mineralization illustrated by Figure 5.3.*

## Discussion

The most widely accepted hypothesis for the origin of sediment-hosted Pb-Zn deposits like Jason is the submarine exhalative model (e.g., Hodgson and Lydon, 1977; Large, 1980; Russell et al., 1981; Carne and Cathro, 1982). Large (1980) suggested that such deposits formed at locations of unusually high heat flow, for example, in regions of extensional fracturing of the continental crust. The oxygen-isotope and mineralogical data obtained for Jason are consistent with the exhalative model. The $^{18}O$-depletion halos about the mineralized zones are almost certainly caused by interaction of the sediment with hot fluids (see Taylor, 1979). That the $^{18}O$ depletion extends for some distance into the footwall rocks of the South Zone compared to the hanging wall $^{18}O$ depletion, implies a vertical component to the fluid flow in that locality and may suggest that these footwall rocks represent a vent or near-vent facies to the mineralization. In contrast, the spatially constrained zone of $^{18}O$ depletion at the upper and lower contacts of the bedded mineralization associated with the Main Zone is compatible with horizontal fluid transport along the seafloor or through the sedimentary rocks (or sediments) themselves. If the sulphides were precipitated onto the seafloor, the occurrence of low-$^{18}O$ kaolinite in the hanging wall of the Main Zone suggests that the hydrothermal flow regime continued for some time following mineralization.

Unambiguous estimates of the fluid temperatures or compositions cannot yet be made from the isotope data. However, the following speculations may be pertinent. Firstly, the dominance of $^{18}O$-depleted illite in the South Zone and its footwall rocks versus authigenic low-$^{18}O$ kaolinite about the Main Zone suggests that the fluids passing through the former were hotter and/or had higher $K^+/H^+$ ratios than the fluids forming the latter (Montoya and Hemley, 1975).

Secondly, we can use the relationship proposed by Land and Dutton (1978) between temperature, $\delta^{18}O$ for kaolinite, and $\delta^{18}O$ for $H_2O$:

$$\delta^{18}O_{Kaolinite} - \delta^{18}O_{H_2O} \simeq 10^3 \ln\alpha_{Kaolinite-H_2O} = (2.5)(10^6)T^{-2} - 2.87 \qquad (1)$$

where T = °K, to place some constraints upon the types of fluids and the temperatures involved in formation of the low-$^{18}O$, kaolinite-enriched halo about the Main Zone. Our calculations using equation 1 have assumed $\delta^{18}O$ value for kaolinite of +5.6, which is the value of kaolinite located at the upper contact between the Main Zone mineralization and the shale host rocks (sample no. 27-12276, Table 5.1).

Ore fluids of different origins have been suggested for shale-hosted, Pb-Zn deposits; these include ocean water, formation water and magmatic water (Badham, 1981). Unmodified magmatic waters have $\delta^{18}O$ values of about +5.5 to +10.0 (Taylor, 1974). Fluids of such composition were clearly not involved in the formation of the most $^{18}O$-depleted kaolinite; all values for the oxygen-isotope composition of magmatic water give meaningless solutions to equation 1.

Ocean water is a logical candidate for involvement in the formation of shale-hosted, Pb-Zn mineralization. The present oxygen-isotope composition of ocean water is 0.

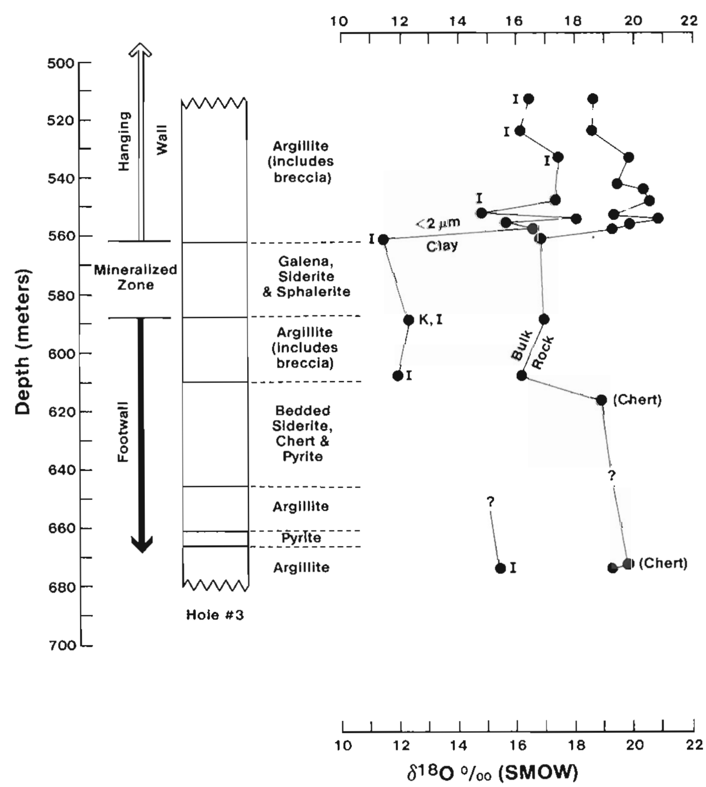


*Figure 5.3.* *Oxygen-isotope results for whole rock and <2 μm mineral samples from the South Zone (hole no. 3). The sulphide mineralization is underlain by a zone of extensive alteration. The <2 μm samples are composed mostly of illite (I); the presence of a kaolin group mineral is indicated by 'K'. All samples contain quartz in the <2 μm size fraction.*

Only in localities of extreme evaporation can values rise as high as +2. Only if all ice caps were to melt could values as low as -1 be obtained (Taylor, 1974). Most investigators agree that the oxygen-isotope composition of ocean water has remained between these limits throughout Phanerozoic time (Muehlenbachs and Clayton, 1976). A solution of equation 1 using water $\delta^{18}O$ of 0 yields a temperature of +270°C for kaolinite formation. Such a temperature lies near the upper end of the range expected for such exhalative solutions (Large, 1977; Finlow-Bates and Large, 1978). Rye and Williams (1981) reported oxygen- and sulphur-isotope data for similar mineralization at McArthur River, Australia. They deduced a temperature range of 100 to 260°C for concordant mineralization at this locality. Oxygen-isotope data for dolomites altered by the ore-bearing solutions yield maximum temperatures of +170 to +240°C.

Badham (1981) has suggested that shale-hosted, Pb-Zn deposits may have been formed by formation fluids derived by dewatering of thick sedimentary prisms. Badham implied that temperatures in excess of 150°C are uncommon for this type of mineralization. His model is more difficult to test because the $\delta^{18}O$ values of formation waters from modern basins are known to vary considerably (-20 to +10; e.g. see summary in Taylor, 1979). No data for putative paleoformation waters are available for the Selwyn Basin, and such information will be difficult to obtain. Most formation waters, however, contain a significant component of meteoric water and have $\delta^{18}O$ values less than 0. Examination of equation 1 shows that as the oxygen-isotope composition of the putative fluid is lowered, the temperature necessary to form low-$^{18}O$ kaolinite decreases. For example, if a maximum temperature for mineralization in the Main Zone of +150°C is postulated, then a fluid composition of $\delta^{18}O = -5.5$ is required. Such compositions are typical of many modern formation waters.

We cannot yet make similar calculations for the South Zone, simply because all <2 µm samples analyzed contain quartz. Resolution of this difficulty is in progress.

Our future studies will be directed towards eliminating some of the permissive aspects of the isotope models. Oxygen-isotope analyses of coexisting clay-carbonate pairs may permit temperature estimates that are independent of assumed fluid isotopic compositions. Fluid inclusion studies that are in progress (D. Gardiner, personal communication), if successful, will provide temperature estimates that can be employed when calculating the $\delta^{18}O$ of putative ore-forming fluids. Isotopic study of purified clay mineral samples from the South Zone may reveal differences in the temperature and fluid composition of the ore fluids involved between the South Zone and the Main Zone. More detailed sampling throughout the Jason property will allow the vertical and horizontal extent of the isotopic variations to be determined and provide information about the flow regimes during mineralization. Finally, some estimates concerning the total water/rock ratio involved in the passage of hydrothermal fluids during and following mineralization will be required to evaluate whether the oxygen-isotope compositions of the fluids should be modelled as a constant or as a variable, changing in $\delta^{18}O$ because of interaction with the host sediments or during fluid mixing.

## Acknowledgments

We would like to thank G. Dickie for first introducing us to this problem; B. Smee and Aberford Resources Ltd. (formerly Pan Ocean Oil Limited) for providing samples, information and advice; E. Toth and D. Caird for assistance in the laboratory; J.W. Lydon and R.I. Thorpe for reviewing the manuscript; and the Department of Energy, Mines and Resources for financial support (EMR Research Agreements 40/4/81 and 22/4/82 to F.J.L.).

## References

Badham, J.P.N.
1981: Shale-hosted Pb-Zn deposits: products of exhalation of formation waters?; Transactions, Institution of Mining and Metallurgy, Section B, v. 90, p. B70-B76.

Blusson, S.L.
1976: Selwyn Basin, Yukon and District of Mackenzie; in Report of Activities, Part A, Geological Survey of Canada, Paper 76-1A, p. 131-132.

Carne, R.C.
1979: Geological setting and stratiform mineralization, Tom claims, Yukon Territory; Department of Indian Affairs and Northern Development, Report EGS 1979-4.

Carne, R.C. and Cathro, R.J.
1982: Sedimentary exhalative (sedex) zinc-lead-silver deposits, northern Canadian Cordillera; Canadian Mining and Metallurgical Bulletin, v. 75, no. 840, p. 66-78.

Clayton, R.N. and Mayeda, T.K.
1963: The use of bromine pentafluoride in the extraction of oxygen from oxides and silicates for isotopic analysis; Geochimica et Cosmochimica Acta, v. 27, p. 43-52.

Craig, H.
1961: Standard for reporting concentrations of deuterium and oxygen-18 in natural waters; Science, v. 133, p. 1833-1834.

Dawson, K.M.
1977: Regional metallogeny of the northern Cordillera; in Report of Activities, Part A, Geological Survey of Canada, Paper 77-1A, p. 1-4.

Eslinger, E.V. and Savin, S.M.
1973: Oxygen isotope geothermometry of the burial metamorphic rocks of the Precambrian Belt Supergroup, Glacier National Park, Montana; Bulletin of Geological Society of America, v. 84, p. 2549-2560.

Finlow-Bates, T. and Large, D.E.
1978: Water depth as a major control on the formation of submarine exhalative ore deposits; Geologisches Jahrbuch, Reihe D, Band D30, p. 27-39, Hannover.

Hodgson, C.J. and Lydon, J.W.
1977: Geological setting of some volcanogenic massive sulphide deposits and active hydrothermal systems: some implications for exploration; Canadian Mining and Metallurgical Bulletin, v. 70, no. 786, p. 95-106.

Land, L.S. and Dutton, S.P.
1978: Cementation of a Pennsylvanian deltaic sandstone: isotopic data; Journal of Sedimentary Petrology, v. 48, p. 1167-1176.

Large, D.E.
1980: Geological parameters associated with sediment-hosted, submarine exhalative Pb-Zn deposits: an empirical model for mineral exploration; Geologisches Jahrbuch, Reihe D, v. 40, p. 59-129.

Large, D.E.
1981: The geochemistry of the sedimentary rocks in the vicinity of the Tom Pb-Zn-Ba deposit, Yukon Territory, Canada; in Geochemical Exploration 1980, ed. A.W. Rose and H. Gundlach; Journal of Geochemical Exploration, v. 15, p. 203-217.

Large, R.R.
1977: Chemical evolution and zonation of massive sulfide deposits in volcanic terrains; Economic Geology, v. 72, p. 549-572.

Longstaffe, F.J.
1981: Oxygen-isotope geochemistry of clay minerals from the Upper Cretaceous Milk River Formation, Alberta; Geological Association of Canada, Program with Abstracts, v. 6, p. 36.

Longstaffe, F.J., Smith, T., and Muehlenbachs, K.
1980: Oxygen-isotope evidence for the genesis of Upper Paleozoic granitoids from southwestern Nova Scotia; Canadian Journal of Earth Sciences, v. 17, p. 132-141.

Lydon, J.W., Lancaster, R.D., and Karkkainen, P.
1979: Genetic controls of Selwyn Basin stratiform barite/sphalerite/galena deposits: an investigation of the dominant barium mineralogy of the Tea deposit, Yukon; in Current Research, Part B, Geological Survey of Canada, Paper 79-1B, p. 223-229.

Magaritz, M. and Taylor, H.P., Jr.
1976: Oxygen, hydrogen and carbon isotope studies of the Franciscan Formation, Coast Ranges, California; Geochimica et Cosmochimica Acta, v. 40, p. 215-234.

Montoya, J.W. and Hemley, J.J.
1975: Activity relations and stabilities in alkali feldspar and mica alteration reactions; Economic Geology, v. 70, p. 577-583.

Muehlenbachs, K. and Clayton, R.N.
1976: Oxygen isotope composition of the oceanic crust and its bearing on seawater; Journal of Geophysical Research, v. 81, p. 4365-4369.

Russell, M.J., Solomon, H., and Walsh, J.L.
1981: The genesis of sediment-hosted zinc plus lead deposits; Mineral. Deposita, v. 16, p. 113-127.

Rye, D.M. and Williams, N.
1981: Studies of the base metal sulfide deposits at McArthur River, Northern Territory, Australia: III. The stable isotope geochemistry of the H.Y.C., Ridge, and Cooley deposits; Economic Geology, v. 76, p. 1-26.

Savin, S. and Epstein, S.
1970: The oxygen and hydrogen isotope geochemistry of clay minerals; Geochimica et Cosmochimica Acta, v. 34, p. 25-42.

Taylor, H.P., Jr.
1974: The application of oxygen and hydrogen isotope studies to problems of hydrothermal alteration and ore deposition; Economic Geology, v. 69, p. 843-883.

1979: Oxygen and hydrogen isotope relationships in hydrothermal mineral deposits; in Geochemistry of Hydrothermal Ore Deposits, 2nd edition, ed. H.L. Barnes, p. 236-277.

Winn, R.D., Jr., Bailes, R.J., and Lu, K.I.
1981: Mudclast breccias, turbidites, lead-zinc sulfides: sedimentation along a Devonian fault scarp, Jason prospect, Yukon Territory; Geological Society of America, Abstracts with Programs, v. 13, p. 583.

# WHOLE ROCK, OXYGEN ISOTOPE RESULTS FOR COUNTRY ROCKS AND ALTERATION ZONES OF THE SULLIVAN MASSIVE SULPHIDE DEPOSIT, BRITISH COLUMBIA

EMR Research Agreement 64-4-82

Bruce E. Nesbitt[1] and Fred J. Longstaffe[1]
Economic Geology Division

*Nesbitt, B.E. and Longstaffe, F.J., Whole rock, oxygen isotope results for country rocks and alteration zones of the Sullivan massive sulphide deposit, British Columbia; in Current Research, Part C, Geological Survey of Canada, Paper 82-1C, p. 51-54, 1982.*

**Abstract**

*The geochemistry of oxygen isotopes in the country rocks and alteration zones of the Sullivan mine has been examined to determine the extent and nature of water-rock interactions during the formation of the deposit and to evaluate the potential of the use of $\delta^{18}O$ analyses as an exploration tool for Sullivan-type deposits. The results to date indicate that (1) there are no significant differences in whole rock $\delta^{18}O$ values between country rocks and the units immediately adjacent to the ore; (2) the tourmalinite alteration zone has essentially the same $\delta^{18}O$ values as the background level in the Aldridge Formation; and (3) the albite-chlorite alteration zone has significantly lower values for $\delta^{18}O$ than the country rocks or the tourmalinite zone. The lack of any significant gradient in $^{18}O/^{16}O$ values towards the ore indicates that oxygen isotope analyses are not an effective tool in exploration or Sullivan-type deposits. The $\delta^{18}O$ results for the alteration zones and country rocks suggest that only in the albite-chlorite zone has significant $\delta^{18}O$ depletion occurred.*

## Introduction

The Sullivan Fe-Pb-Zn-Ag sulphide deposit is located in southeastern British Columbia in Proterozoic metasedimentary rocks of the Aldridge Formation, Purcell Supergroup. As one of the largest ore deposits in Canada and one of the earliest recognized examples of sediment-hosted ore deposits, it has been the subject of a significant amount of research over the past years. However, several questions about the origin of the Sullivan deposit remain unanswered. In particular, little is known of the source and chemistry of the solutions involved in the pre- and post-ore alteration as well as the nature of the metal-bearing fluids themselves. In addition, the scope and chemistry of water-rock interactions associated with the formation of the ore is only now receiving significant attention (Shaw and Hodgson, 1980). The objectives of this project on $^{18}O/^{16}O$ geochemistry of the Sullivan host rocks and alteration zones are to provide information on the origins of fluids involved in the formation of the deposit and to evaluate the potential of $\delta^{18}O$ analyses as an exploration tool for Sullivan-type deposits. In this preliminary report, we discuss the progress to date from whole rock $^{18}O/^{16}O$ analyses, especially as they pertain to exploration for syngenetic lead-zinc deposits. Work on analyses of mineral separates is in progress. This additional work will aid in the development of genetic models for the deposit.

### Regional Geology

The local and regional geology of the Sullivan deposit has been thoroughly summarized in a variety of articles (Hamilton et al., in press; Hamilton et al., 1981) and

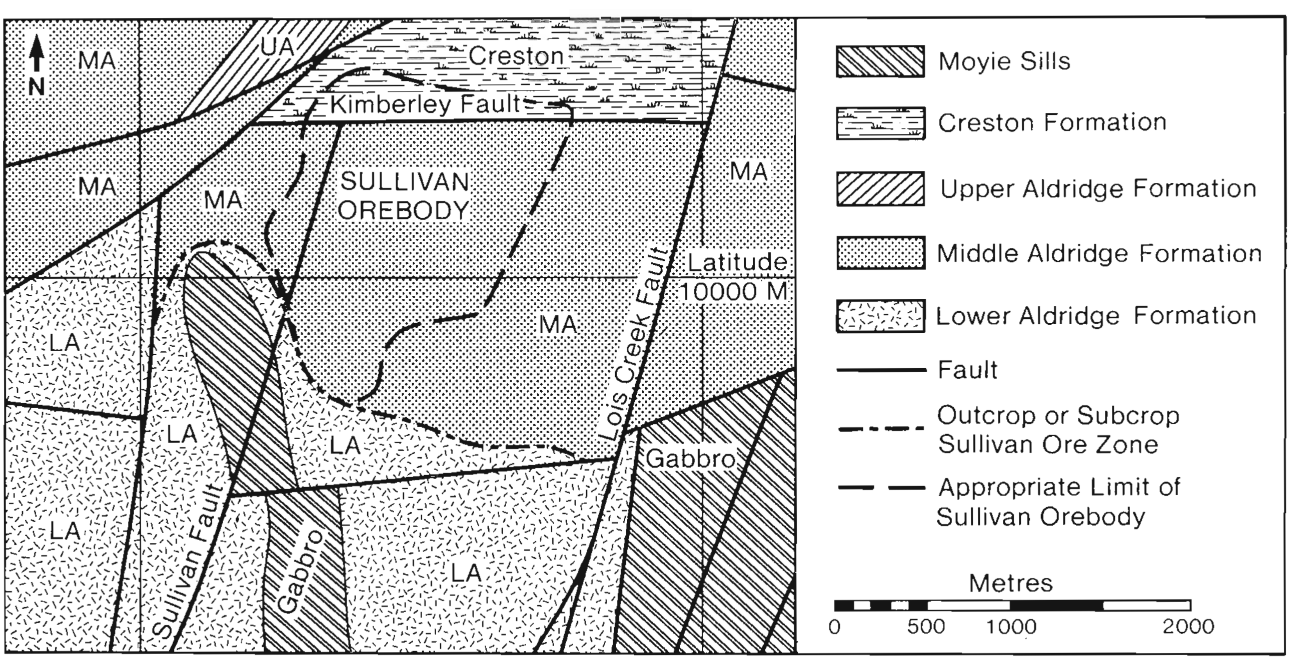


***Figure 6.1.*** *Simplified geological map of the Sullivan ore deposit and adjacent units. After Hamilton et al. (in press).*

[1]Department of Geology, The University of Alberta, Edmonton, Alberta, T6G 2E3

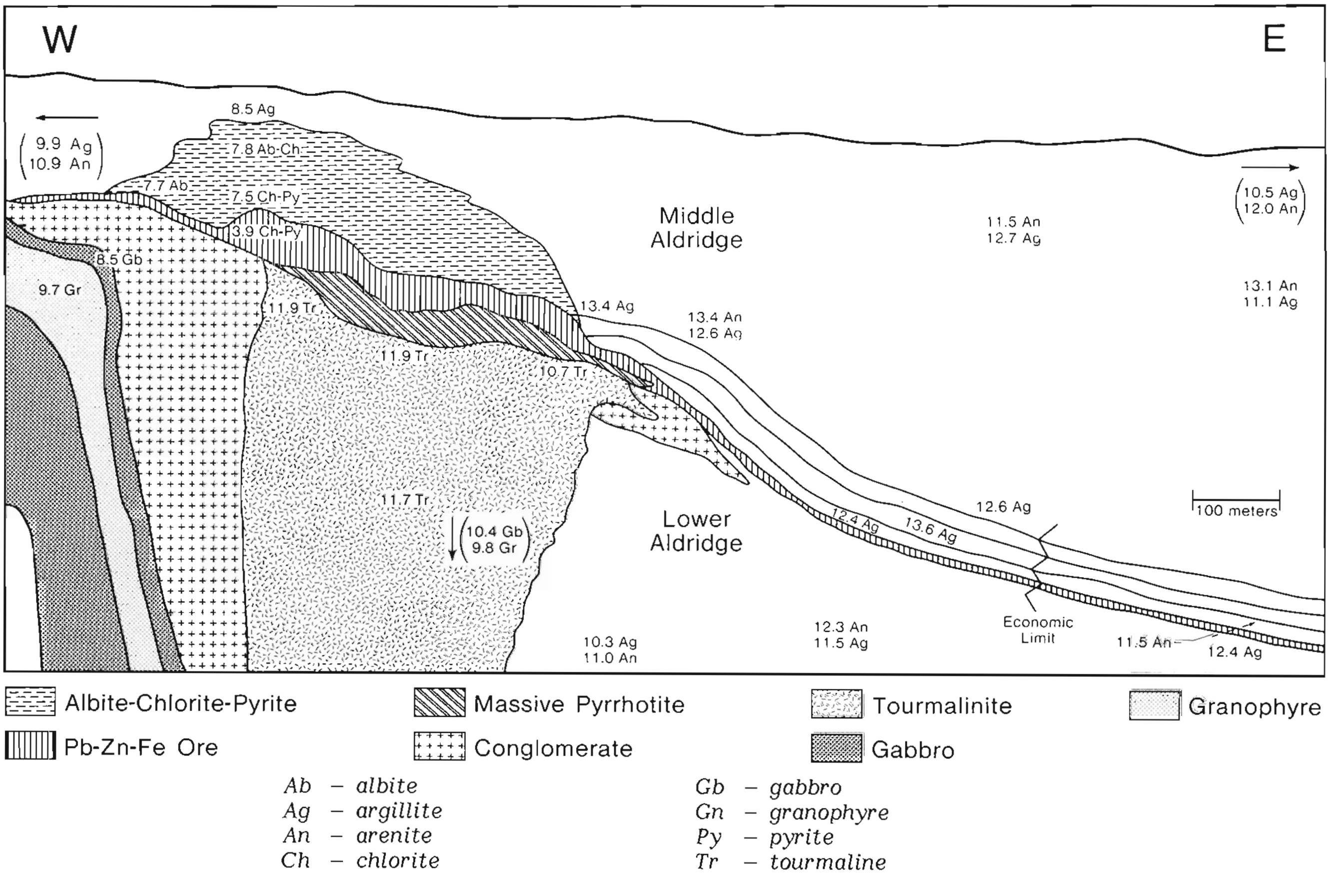


***Figure 6.2.*** *Idealized cross-section through the deposit showing the distribution of the $\delta^{18}O$ values listed in Table 6.1. Heavy lines paralleling the ore in the eastern portion of the section represent the hanging wall, ore sequences (I, H, HU in mine terminology).*

consequently will be only briefly reviewed here. The ores are situated near the top of the lower Aldridge Formation in a series of flyschoid sedimentary rocks containing alternating units of fine grained quartzite and mudstone (Fig. 6.1). The orebody has the shape of an inverted and tilted saucer with a maximum dimension of 2000 m, north to south (Hamilton et al., in press). The western portion of the ore is massive and varies from pyrrhotite-rich at the base to banded sphalerite and galena ore at the top. Underlying the western portion of the ore is a zone in which the rock is composed of very fine grained tourmaline in interstices between quartz grains. This tourmaline-rich part of the footwall is referred to as the "tourmalinite zone" (Hamilton et al., in press). The hanging wall of this portion of the deposit contains albite and albite-chlorite alteration zones which were produced by hydrothermal alteration of the Aldridge sedimentary rocks overlying the deposit (Shaw and Hodgson, 1980). The eastern portion of the ore consists of sulphides interbedded with clastic sedimentary rocks. The various sulphide units in this portion are remarkably continuous and conformable throughout the region. The ores are believed to have been deposited around 1450 Ma (LeCouteur, 1979; Zartman et al., in press). Approximately 20 Ma after formation of the deposit, the underlying gabbro-granophyre sill was emplaced and still later the entire region was metamorphosed to greenschist facies.

**Sample Selection and Analytical Procedure**

In order to evaluate variations in $^{18}O/^{16}O$ whole rock values in and around the ore, samples were collected from drill core from a variety of locations in the Aldridge Formation and alteration zones. To examine changes in $\delta^{18}O$ values of the sedimentary host rocks as a function of distance from the ore, samples were taken from the Aldridge Formation several kilometres from known mineralization and from several sites in the hanging wall and footwall sedimentary rocks at specific distances from the ore. The samples were divided into two different groups; argillite composed of fine grained, white mica (illite with minor kaolinite), chlorite and biotite, with subordinate amounts of quartz and plagioclase; and arenite composed of quartz, plagioclase, white mica, chlorite, biotite, and occasionally garnet. Samples also were collected from several locations within the tourmalinite and albite-chlorite zones to examine the average values of these zones and any internal variations within them. The silicate samples were analyzed by the $BrF_5$ method of Clayton and Mayeda (1963). The data are reported in the usual $\delta$ notation with respect to standard mean ocean water (SMOW: Craig, 1961) using a $CO_2$-$H_2O$ fractionation factor of 1.0407. The standard deviation calculated from the pooled residual variance of replicate analyses performed during the course of this study is $\pm 0.09‰$.

Table 1

Summary of $\delta^{18}O$ whole rock analyses for samples from the Sullivan Mine and surrounding area

| ALDRIDGE FORMATION | | | | | |
|---|---|---|---|---|---|
| Sample | Regional Samples Rock Type | $\delta^{18}O$ Results | Sample | Samples Adjoining Ore Rock Type | $\delta^{18}O$ Results |
| 5481-344 | Argillite | +10.5 | 6799-14 | Argillite | +13.4 |
| 5481-984 | Arenite | +12.0 | 478-1691 | Arenite | +11.5 |
| 6448-3482 | Argillite | + 9.9 | 478-1696 | Arenite | +12.8 |
| 6448-3511 | Arenite | +10.9 | 478-1705 | Argillite | +12.4 |
| 3660-327 | Arenite | +13.1 | 468-1598 | Argillite | +12.6 |
| 3660-332 | Argillite | +11.1 | 468-1636 | Argillite | +13.6 |
| 468-285 | Arenite | +11.5 | 3979-5 | Arenite | +13.4 |
| 468-297 | Argillite | +12.7 | 3979-145 | Argillite | +12.6 |
| 6799-3893 | Argillite | +10.3 | | | |
| 6799-3995 | Arenite | +11.0 | | | |
| 3300-982 | Argillite | +11.5 | | | |
| 3300-988 | Arenite | +12.3 | | | |

| ALTERATION ZONES | | | | | |
|---|---|---|---|---|---|
| Sample | Tourmalinite Zone Rock Type | $\delta^{18}O$ Results | Sample | Albite-Chlorite Zone Rock Type | $\delta^{18}O$ Results |
| 61-610 | Tourmalinite | +11.9 | 61-156 | Argillite | + 8.5 |
| 6799-895 | Tourmalinite | +11.7 | 61-219 | Albite-Chlorite | + 6.8 |
| 6799-67 | Tourmalinite | +10.7 | 61-396 | Albite-Chlorite | + 7.8 |
| 4477-63 | Tourmalinite | +11.9 | 61-472 | Chlorite-Pyrite | + 7.5 |
| | | | 61-520 | Chlorite-Pyrite | + 3.9 |
| | | | 4477-318 | Albite | + 7.7 |

| GABBRO-GRANOPHYRE | | | |
|---|---|---|---|
| Gabbro | | Granophyre | |
| Sample | $\delta^{18}O$ Results | Sample | $\delta^{18}O$ Results |
| 6799-1447 | +10.4 | 6799-1648 | + 9.8 |
| 5451-829 | + 8.5 | 5451-765 | + 9.7 |

**Results of $^{18}O/^{16}O$ Analyses**

Results of $\delta^{18}O$ whole rock analyses of samples from the Aldridge Formation indicate a range of values of +10.9 to +13.1 for the meta-arenites and +9.9 to +12.7 for the meta-argillites (Table 6.1, Fig. 6.2). In the eastern portion of the mine, very little variation is noted in the $\delta^{18}O$ values in and around the ore with respect to the regional values since values for meta-arenites adjacent to the ore range from +11.5 to +13.4 and for meta-argillites from +12.4 to +13.6

In the tourmalinitized alteration zone, values for $\delta^{18}O$ range from +10.7 to +11.9. The results do not show any spatial variation between the various portions of the zone (Fig. 6.2). Minor tourmalinites present in the hanging wall yield values similar to the massive tourmalinite of the footwall. Whole rock $\delta^{18}O$ values for samples from the albite and albite-chlorite zones are distinctly lower than those for the Aldridge Formation or tourmalinite, ranging from +3.9 to +8.5. These values do show a spatial variation within the alteration zone with the lowest values located near the centre of the zone directly over the ore and decreasing outward (Fig. 6.2). Average whole rock $\delta^{18}O$ values for rocks of the gabbro-granophyre complex are +9.8 for the granophyre and +9.5 for the gabbro. This $\delta^{18}O$ value for gabbro is higher than typical values for gabbros and indicates some contamination or alteration of the unit.

**Discussion**

The lack of any significant differences between the regional whole rock $\delta^{18}O$ values of the Aldridge Formation and the values for rocks immediately adjoining the ore indicates that whole rock $^{18}O/^{16}O$ analysis is not an effective tool in exploration for deposits similar to Sullivan. There is a slight increase in average $\delta^{18}O$ values in the rocks around the ore, +12.8 (adjoining ore) as compared to +11.4 (regional samples). However, the ranges in values of the two sets overlap considerably (+11.5 to +13.6 as compared to +9.9 to +13.1) and we do not believe that the difference in averages is significant. Assuming that the distal sulphides were deposited from hydrothermal brines moving along the ocean floor, the lack of variation in $\delta^{18}O$ values is most likely the result of a continuing and substantial influx of clastic sediments during deposition of the sulphides. The effects of any water-sediment interaction occurring during the deposition of ore which may have created $\delta^{18}O$ depletion was overwhelmed by the high sedimentation rate.

The $\delta^{18}O$ results for the tourmalinite zone, interestingly, are very similar to those for the Aldridge Formation. There are two possible explanations for this result. The hydrothermal fluids responsible for the formation of the tourmalinite may have been relatively low temperature and simply supplied B to the pre-existing sediments in conjunction with leaching of K, Na and Ca. Alternatively, the introduction of B may have occurred at a higher temperature with fluids of the correct $\delta^{18}O$ to produce the same $\delta^{18}O$ whole rock values as the units of the Aldridge Formation. The analysis, currently in progress, of mineral separates from this zone should aid in the determination of which of these two models is correct.

The hydrothermal alteration of the overlying Aldridge sedimentary rocks resulting in the albite and albite-chlorite rocks has produced a distinct shift in $\delta^{18}O$ values (Table 6.1). Assuming the hydrothermal fluid involved in the alteration process had a $\delta^{18}O$ value of 0.0, SMOW, and the $\delta^{18}O$ value of the albite is about +7.0, then at isotopic equilibrium the temperature of alteration would have been in the range of 250°C to 280°C. This temperature range is most likely a minimum because for the temperature of equilibration to be less than the specified range, the $^{18}O/^{16}O$ value would have to be less than 0.0. The addition of meteoric water could cause the fluid to be less than 0.0; however, this possibility is unlikely at Sullivan, given its marine setting.

## Further Work

To better understand the details of variations in $\delta^{18}O$ values in these rocks various phases are being separated from the tourmalinites, albite-chlorite rocks and country rocks. It is hoped that the results of $^{18}O/^{16}O$ analyses of the mineral separates will yield more precise information as to the temperature and origin of the metal-bearing and alteration fluids as well as the extent of water-rock interactions during the various stages of formation of the deposit.

## Acknowledgments

We would like to thank the geology staff at Cominco's Sullivan operations and in particular John Hamilton and Gary Delaney for their assistance in the sampling for the study. Discussions with David Shaw were beneficial in improving our understanding of the various stages of alteration associated with the deposit. We would also like to thank Karlis Muehlenbachs for the use of his isotope laboratory facilities; Elizabeth Toth for assistance in the laboratory; John Lydon for his careful review of the manuscript; and Energy, Mines and Resources for financial support (EMR Research Agreement 64/4/82).

## References

Craig, H.
1961: Standard for reporting concentrations of deuterium and oxygen-18 in natural waters; Science, v. 133, p. 1833-1834.

Clayton, R.N. and Mayeda, T.K.
1963: The use of bromine pentafluoride in the extraction of oxygen from oxides and silicates for isotopic analysis; Geochimica et Cosmochimica Acta, v. 27, p. 43-52.

Hamilton, J.M., Bishop, D.T., Morris, H.C., and Owens, O.E.
Geology of the Sullivan orebody, Kimberley, B.C., Canada: in Major Sulphide Deposits of Canada and Environs, the H.S. Robinson memorial volume, ed. R.W. Hutchinson; Geological Association of Canada, Special Paper 25. (in press)

Hamilton, J.M., Hauser, R.L., and Ransom, P.W.
1981: The Sullivan Orebody: in Field Guides to Geology and Mineral Deposits, ed. R.I. Thompson and D.G. Cook, Geological Association of Canada, fieldtrip guidebook, p. 44-49.

LeCouteur, P.C.
1979: Age of the Sullivan lead-zinc deposit (Abs.): Geological Association of Canada, Programme and Abstracts, Cordilleran Section.

Shaw, D.R. and Hodgson, C.J.
1980: Wall-rock alteration at the Sullivan mine, Kimberley, British Columbia (abstract); Canadian Institute of Mining and Metallurgy Bulletin, v. 73, no. 821, p. 75.

Zartman, R.E., Peterman, Z.E., Obradovich, J.D., Gallego, M.D., and Bishop, D.T.
K-Ar, Rb-Sr, and U-Th-Pb ages of the Crossport C still near Crossport, Idaho; Idaho Bureau of Mines and Geology. (in press)

7. **DEPOSITIONAL HISTORY OF THE DEVONIAN SUCCESSION IN THE ROCKY MOUNTAINS SOUTHWEST OF THE PEACE RIVER ARCH**

Project 790038

H.H.J. Geldsetzer
Institute of Sedimentary and Petroleum Geology, Calgary

*Geldsetzer, H.H.J., Depositional history of the Devonian succession in the Rocky Mountains southwest of the Peace River Arch; in Current Research, Part C, Geological Survey of Canada, Paper 82-1C, p. 55-64, 1982.*

***Abstract***

*The Devonian succession southwest of the Peace River Arch is represented by four depositional episodes (sequences) – all dominated by carbonates. They are separated by unconformities and, except for the uppermost (Famennian) sequence, are characterized by basal quartzose sandstones.*

*The lowest sequence – thick, sandy dolomites of Zlichovian(?) age (Stone Formation) – rests unconformably on lower Paleozoic rocks and was largely eroded during the Eifelian. Transgression during the Givetian left another carbonate horizon (Dunedin Formation) which in turn was eroded to the south and east(?) prior to the Frasnian. The Frasnian sequence starts with a widespread biostrome (Flume Formation). The carbonate environment was temporarily eliminated by the influx of fine terrigenous clastics (Perdrix Formation), but became dominant again in the late Frasnian (Mt. Hawk Formation, Simla Formation). The Frasnian sequence is separated from the youngest Devonian sequence, of Famennian age, by a minor unconformity, although faunal changes across this break are quite profound. The Famennian sequence is again carbonate-dominated (Palliser Formation) and appears to be confined to the lower and middle Famennian. This depositional episode was terminated by uplift, erosion, and the later influx of fine terrigenous clastics of the Exshaw and Besa River formations, both yielding miospore assemblages of Tournaisian age (Tn2 or younger).*

*The sedimentary facies of the Devonian sequences and the bounding unconformities suggest that the sediments were deposited on the inner shelf and/or cratonic margin.*

## Introduction

This report presents data on the stratigraphic framework and depositional development of the Devonian succession in the Rocky Mountains of east-central British Columbia and west-central Alberta, between 53°N and 55°N latitude (Fig. 7.1). The field area lies southwest of the Peace River Arch and crosses, from northwest to southeast, the Monkman Pass map area (NTS 93I), the northeastern part of the McBride map area (NTS 93H), and the northwestern part of the Robson map area (NTS 83E).

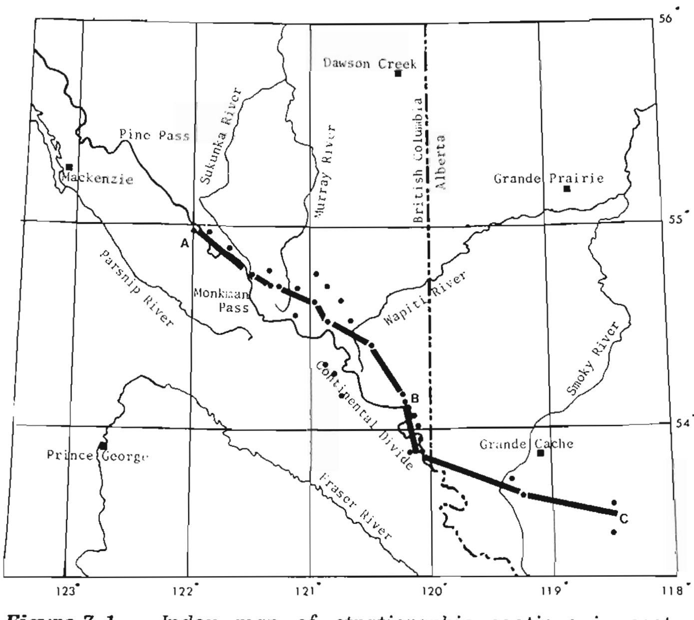


***Figure 7.1.*** *Index map of stratigraphic sections in east-central British Columbia and west-central Alberta.*

The results of this report are based on 30 measured sections.

Previous geological reports on the area include Taylor and Stott (1979) for the Monkman Pass map area; Campbell et al. (1973) for the McBride map area; and Mountjoy (1980) for the Robson map area.

The stratigraphic nomenclature in this report is essentially the same as that used by Taylor and Mackenzie (1970) in northeastern British Columbia, and by Mountjoy and Mackenzie (1973) in the Ancient Wall carbonate complex in the central part of the Robson map area. The only departure is the resurrection of the name Simla Formation, applied earlier in the Ancient Wall area by McLaren and Mountjoy (1962).

## Acknowledgments

The writer is grateful to many geologists for discussions on Devonian stratigraphic problems, particularly to N.C. Meijer Drees, E.W. Mountjoy, G.C. Taylor, R.I. Thompson and R. Workum. The manuscript was critically read and improved by A.W. Norris.

The writer thanks M. Ferguson, B. Fischer, D. Keller and his son Torsten for able assistance (voluntary in the case of his son) at various stages of the field work.

## Structural Setting

Devonian strata are exposed along the central part of the Rocky Mountain thrust belt, in a zone defined on the northeast and southwest by major, southwest-dipping thrusts. The one to the southwest is the Snake Indian Thrust, which is present throughout the Monkman Pass area (Tipper et al., 1979) and can be traced into the Robson area to the southeast (Mountjoy, 1980). The northeastern boundary thrust is continuous for 75 km in Monkman Pass area, but difficult to trace through the wide, forested valleys of Murray River in

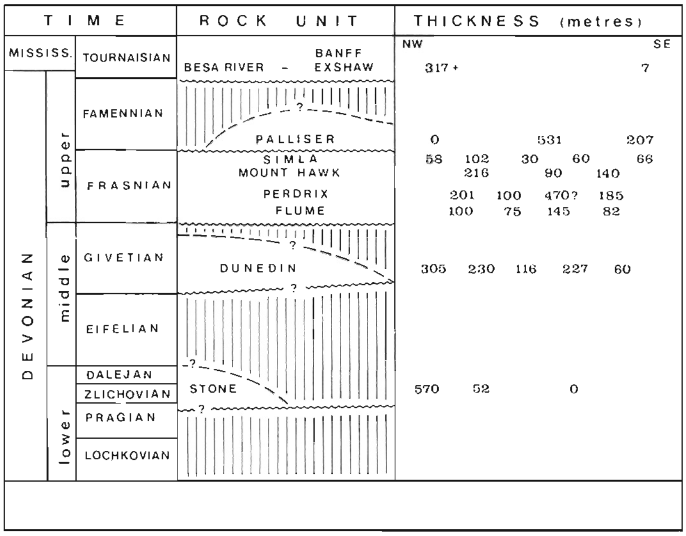


***Figure 7.2.*** *Diagrammatic representation of depositional and hiatal episodes. Variations in thickness of individual units are shown on right.*

the north and Narraway River and Sheep Creek in the south. It appears to continue to the southeast into Robson map area as the Rocky Pass Thrust (Mountjoy, 1980).

The structure of the strata between these two boundary thrusts consists, in general terms, of a western anticlinal and an eastern synclinal development. Secondary thrusts and folds characterize both parts. Strata along the transition from the anticlinal to the synclinal belt are typically overturned and the site of intense shearing and thrusting.

Preservation of Devonian rocks is much better in the eastern synclinal belt than in the western anticlinal belt.

### Stratigraphic Relationships

The Devonian succession in the field area includes four distinct depositional episodes, which are designated: the Stone Formation of probable Zlichovian age; the Dunedin Formation of Givetian age; the Fairholme Group of Frasnian age; and the Palliser Formation of Famennian age (Fig. 7.2).

The lower and middle Devonian rocks occur only in the western anticlinal belt of the central thrust zone, where they rest unconformably on Ordovician carbonates. They wedge out to the northeast and southeast, but continue into the Pine Pass area to the northwest (Taylor and Bamber, 1970) and thicken considerably in the Halfway River area beyond (Thompson, 1978).

Upper Devonian rocks are found typically in the eastern synclinal belt, unconformably overlying Ordovician carbonates. However, upper Devonian remnants are locally preserved in the western anticlinal belt where they rest unconformably on the middle Devonian Dunedin Formation.

The Frasnian Fairholme Group does not seem to vary in thickness across the area, but the overlying Famennian Palliser Formation thins to the southeast and wedges out completely northwest of Murray River. Lithostratigraphic and preliminary biostratigraphic data suggest a post-Palliser hiatus, during which the Palliser Formation was eroded, partly in some areas, entirely in others.

The Palliser is overlain by a black shale sequence, the Besa River Formation, which thins rapidly to the southeast and appears to grade into the Exshaw Formation. Miospore assemblages, identified by D.C. McGregor and J. Utting, of the Geological Survey of Canada, suggest a Tournaisian age (Tn2 or younger).

Sedimentary facies of the Devonian sequences vary from nonmarine to shallow marine, and sedimentation was frequently interrupted by periods of uplift and erosion. A time-rock projection (Fig. 7.2) illustrates a rather incomplete record for the Devonian. A comprehensive compilation of data relating to Devonian rocks along the Cordilleran belt of the United States, by Poole et al. (1977), shows a very similar fragmented record along the cratonic margin and the inner shelf. This zone, if projected into Canada, apparently passed through the area covered in this report.

#### Lower and Middle Devonian

Rocks of lower and middle Devonian age are restricted to the western anticlinal belt of the central thrust zone just east of the Snake Indian Thrust. Despite their common outcrop area and shared trend to wedge out toward the southeast, they display differing diagenetic histories. The lower Devonian Stone Formation is completely dolomitized, whereas the overlying middle Devonian Dunedin Formation is mainly a limestone. Evidence presented below suggests that both the Stone and Dunedin formations are bounded by regional unconformities.

Stone Formation (Zlichovian?). The Stone Formation thins rapidly toward the south and east along a northwest-southeast trending outcrop belt, thinning from 570 m, in the extreme northwest corner of the Monkman Pass area, to 52 m over the first 25 km southeast and to zero over the next 55 km (Fig. 7.3).

The lower 337 m of the Stone Formation are dominated by light grey dolomite, locally displaying fine laminae and small mound-like structures of probable algal origin. Discontinuous quartzose sandstone bands and disseminated quartz grains are typical features throughout most of the dolomite. The sandstone bands occur at fairly regular intervals and increase in frequency near the bottom and top of the lower Stone Formation. The basal unit of the formation is a 34 m thick quartzite, characterized by wide, shallow channels. Near the top of the quartzite, parallel-bedded sandstone predominates. This sandstone has abundant ripple cross-laminations and a dolomite cement – features that also occur in sandstone beds higher in the section.

Deposition of Stone Formation sediments was preceded by a long hiatal period of uplift and erosion. The basal quartzite is a mature lag deposit, which accumulated following the hiatus and was probably repeatedly reworked by wind and wave action during the initial stage of renewed slow subsidence.

Sediments of the lower Stone Formation were probably deposited in a very shallow, nearshore environment. Laminae and mounds suggest the existence of widespread algal mats, trapping quartz grains blown, or washed in, from emerging parts of the eroded Ordovician surface. The algal mats were frequently buried by thin beds of quartz grains – the result of occasional sheet floods. Subsidence was very gradual, thus permitting the algal-mat facies to continue.

The upper Stone Formation is 235 m thick and is marked by the first appearance of dark grey to black, laminated dolomite. The laminae are laterally discontinuous and commonly grade into flaser bedding or nodular bedding. Skeletal debris is frequently visible. These dark dolomites commonly grade upward into light grey dolomites, some of which display even laminae and quartzose bands, identical to

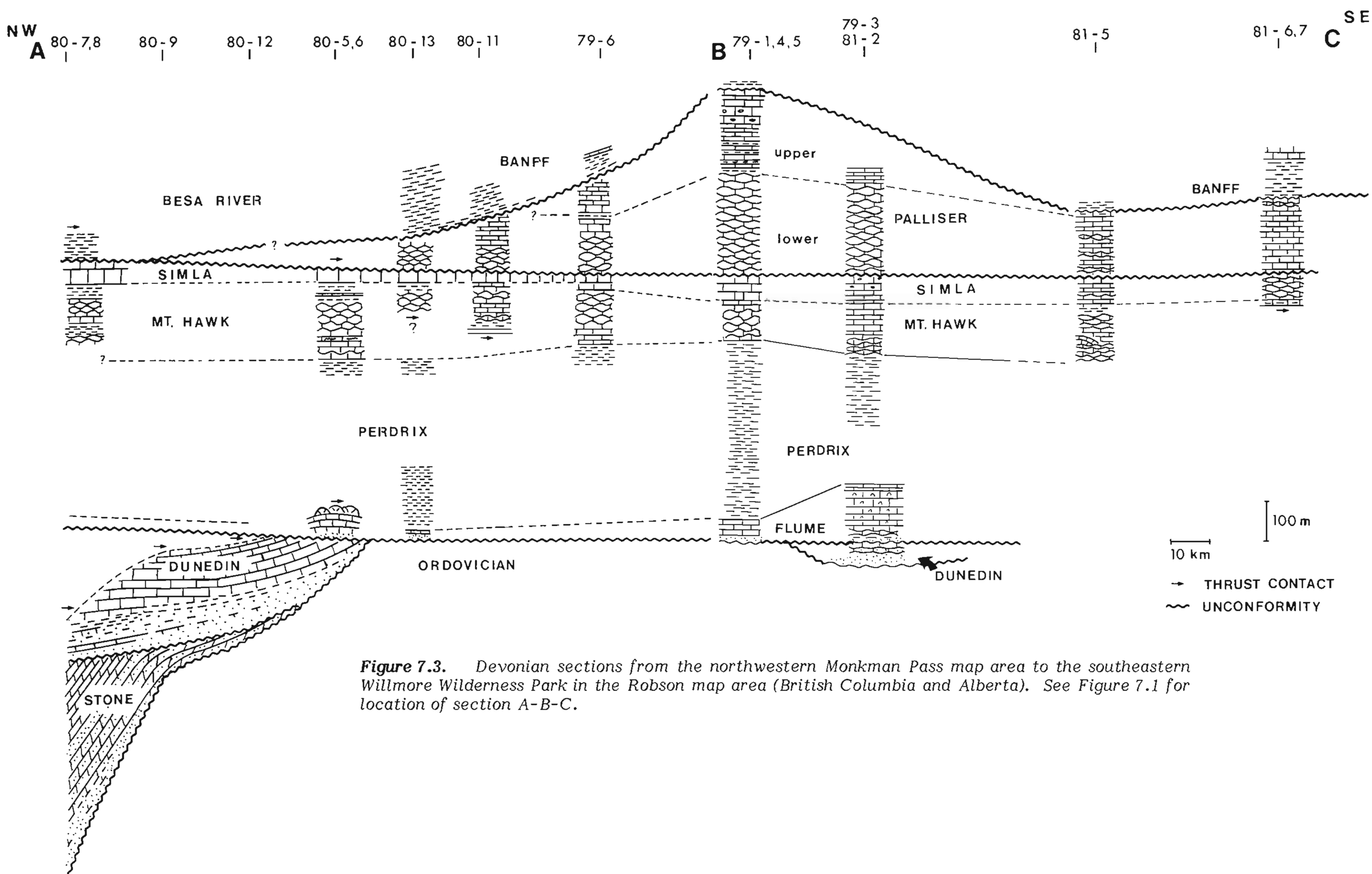


***Figure 7.3.*** *Devonian sections from the northwestern Monkman Pass map area to the southeastern Willmore Wilderness Park in the Robson map area (British Columbia and Alberta). See Figure 7.1 for location of section A-B-C.*

the lithologies of the lower Stone Formation. The cycles persist throughout the upper Stone Formation and, in some places, terminate in breccias.

Sedimentary features and the cyclic character of the upper Stone Formation suggest repeated fluctuations from shallow subtidal (discontinuous laminae) to algal-mat facies (continuous laminae). The algal-mat facies is reminiscent of the lower Stone Formation, and probably represents periods of lesser subsidence, whereas shallow, subtidal conditions were established during times of increased subsidence. Periodically, the algal-mat facies was exposed over prolonged periods of time and, consequently, reworked into breccia beds.

Age. Corals from a narrow, fossiliferous band in the upper Stone Formation, 410 m above the base, have been tentatively assigned by A.E.H. Pedder to the Zlichovian or Dalejan Stage. Conodonts collected by G.C. Taylor from the Stone Formation in the Caribou Range of northeastern British Columbia (NTS 94N) have been assigned by T.T. Uyeno to the Pragian/Zlichovian boundary and to the Zlichovian Stage. The Zlichovian and Dalejan stages are approximately equivalent to the Emsian Stage, i.e. the late Early Devonian.

Dunedin Formation. The Dunedin Formation thins southeastward from more than 250 m in the northwest corner of the Monkman Pass area to 60 m in the northeastern corner of the McBride area, a distance of approximately 175 km (Fig. 7.3). The Dunedin thins more gradually than the Stone Formation and its southeasterly termination is caused by a thrust fault.

The Dunedin is subdivided into a lower clastic part and an upper carbonate (Fig. 7.4). The clastics vary from siltstones to coarse grained sandstones, are commonly crossbedded and interbedded with thin dolomitic or calcareous carbonates which, near the base, are of algal origin. This lower, clastic-dominated succession thins rapidly from 116 m in the northwest to about 50 m over a distance of 50 km, maintaining that thickness until it is terminated in the southeast. Locally, the basal sedimentary rocks deviate considerably from the general lithologic sequence. At one locality, near Mount Myhan, 17 m of sandy limestone underlie the terrigenous clastics and overlie dolomite across a karsted surface. Near Herricks Pass, a boulder conglomerate, several metres thick, overlies Ordovician dolomites. Both the sandy limestone and the conglomerate preceded the normal depositional episode of the Dunedin Formation.


*Figure 7.4. Overturned section at Ekusquin Mountain (Section 81-3). Dunedin Formation with thick basal sandstone and massive upper limestone. Dun.= Dunedin Formation, Flu.= Flume Formation, Per.= Perdrix Formation.*

*Figure 7.5. Band of stringocephalid brachiopods in upper Dunedin carbonates.*

The upper Dunedin Formation is characterized by cliff-forming, yellowish grey, medium- to thick-bedded limestone. The contact with the lower clastic sequence is sharp. The lithology is dominated by biomudstones and wackestones, interrupted by a few bands of tightly packed stringocephalid brachiopods (Fig. 7.5) or amphiporid stromatoporoids. The thickness of the upper carbonate sequence varies considerably depending upon the depth of erosion prior to the deposition of the Frasnian sediments. Maximum and minimum measurements are 189 m and 15 m respectively.

Deposition of the Dunedin Formation was preceded by dolomitization, uplift, and erosion of the underlying Stone Formation. Boulder conglomerates accumulated in local depressions during this hiatal period. Karst surfaces, which had developed on exposed carbonates, were infilled by sandy limestone. The unbedded, unfossiliferous nature of this limestone, and the random distribution of clastic grains, resembles that of recent calcretes. This interpretation is strengthened by the appearance of concretionary limestone horizons at the top of individual, crossbedded sandstone units above this basal limestone. These concretionary layers are less well developed calcretes, which formed between periods of sandstone deposition. The calcrete horizons, as well as several thin algal beds, indicate rather arid conditions fluctuating between subaerial and intertidal.

Current measurements from the basal, crossbedded sandstones suggest a transport direction toward the east. This direction deviates from the "normal" southwesterly transport direction for the sandstones at the base of the underlying Stone Formation and for the basal clastics of the overlying Flume Formation. The anomalous easterly transport direction at the base of the Dunedin Formation could indicate an area of gentle uplift to the west, during the Eifelian, which subsided again during the Givetian.

The terrigenous clastics of the lower Dunedin Formation become increasingly interbedded upwards with fossiliferous, shaly and sandy limestone. Marine conditions apparently expanded, whereas the influx of terrigenous debris diminished and ceased altogether with the deposition of the cliff-forming carbonates. Subtidal deposition of lime muds below wave base dominated, interrupted occasionally by the formation of shoals, which became the site for amphiporid stromatoporoids. The beds of tightly packed brachiopods (mostly stringocephalid) are interpreted as lag deposits, left behind when wave base was temporarily lowered during storms.

The Dunedin Formation illustrates a gradual deepening from subaerial to shallow subtidal conditions during its early stages. A fairly constant subtidal environment lasted throughout the later stages of Dunedin deposition.

Age. The occurrence of stringocephalid brachiopods suggests that the Dunedin Formation lies within the upper Middle Devonian (Givetian).

Upper Devonian

Upper Devonian sediments accumulated during two depositional episodes which coincide with parts of the Frasnian and Famennian stages. The Frasnian Fairholme Group shows a similar development as the off-reef facies to the south - a basal carbonate platform (Flume Formation), a thick shaly interval (Perdrix Formation) grading upsection into a carbonate (Mount Hawk Formation) and, finally, a carbonate bank (Simla Formation) which, in contrast to the more restricted distribution of a typical off-reef section, persists throughout the field area. The Famennian Palliser Formation is a thick carbonate blanket with minor facies changes in the upper part.

Flume Formation. Sediments of the Flume Formation overlie an erosion surface which truncates part of the Dunedin Formation and older Ordovician units. The surface had an extremely low relief, because the thickness of the overlying Flume remains rather constant between 55 and 75 m over a distance of 150 km.

Where the entire Flume is exposed it displays a distinct vertical facies change (Fig. 7.6). A thin, basal, crossbedded, quartzose sandstone is followed by an interval of interbedded,

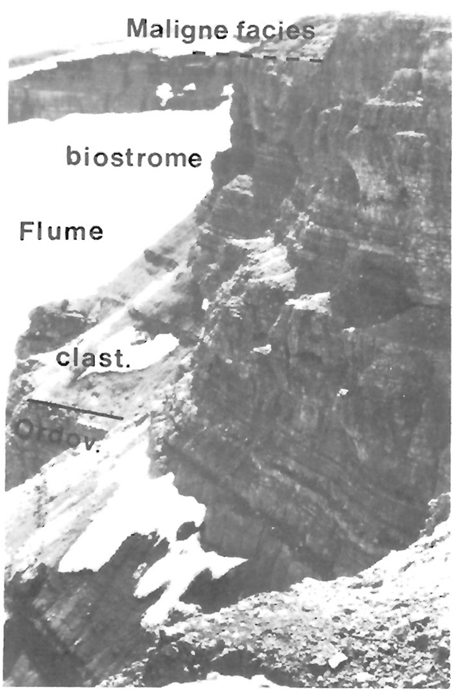


*Figure 7.6.* *Flume section above Kakwa Lake (Section 79-1). Recessive parts are basal clastics and brachiopod-bearing Maligne facies at top. Cliff consists of stromatoporoid biostrome.*

calcareous shales and discontinuous limestone beds, which contain abundant brachiopods. A stromatoporoid biostrome follows above. This biostrome is normally less than 50 m thick, but reaches 111 m near Mount Buchanan (Section 81-2). It is sharply overlain by well-bedded, commonly shaly limestones containing abundant brachiopods and crinoids. Upsection, these limestones are increasingly interbedded with black shales, which become the dominant lithology, and are then referred to as the Perdrix Formation.

Deposition of the Flume Formation was preceded by a period of regional uplift during which underlying units were bevelled to a very low relief surface. Renewed subsidence led to the spreading of thin basal sands. Crossbeds indicate a southwesterly transport direction. This early phase of sedimentation was probably nonmarine, judging by the common occurrence of fish fragments in the basal sandstones and by the position of these sandstones on a subaerial erosion surface.

Shallow marine conditions developed with the deposition of brachiopod-bearing, muddy carbonates and shales. Fine terrigenous clastics soon disappeared, probably because the source had been exhausted, and clear water conditions encouraged the growth of biostrome banks, the main builders being stromatoporoids.

Biostrome development ceased with the return of turbid conditions caused by the influx of fine terrigenous clastics. Some areas were not affected by the environmental change, probably because the sediment-carrying currents were diverted around prominent shoals. In such areas the stromatoporoid biostromes continued to prosper and ultimately formed reef-like buildups, such as in the Alberta Basin to the south. The prominent stromatoporoid bank near Mount Buchanan apparently was an area where clear water conditions persisted for some time, before it was also blanketed by fine grained terrigenous clastics.

The sharp contact between the biostrome and the overlying shaly carbonate suggests that the environmental change was very rapid. Less turbidity-sensitive organisms, such as brachiopods and crinoids, prospered temporarily, and are represented by a succession of dark grey, shaly carbonates, referred to as the Maligne Formation to the south (Taylor, 1957). In this report, the brachiopod- and crinoid-bearing limestones, above the stomatoporoid biostrome, are treated as the Maligne facies of the Flume Formation.

Age. The lower Flume from the northeastern McBride area has yielded brachiopod assemblages that were identified by A.W. Norris as latest Givetian/earliest Frasnian, whereas assemblages collected from the same stratigraphic interval farther to the northwest, in the central part of the Monkman Pass area, are Early Frasnian in age, and equivalent to similar assemblages from the Calumet Member of the Waterways Formation.

Perdrix Formation. The Perdrix Formation is a succession of greyish green to black shales and siltstones, normally laminated and displaying cross-lamination, scouring and deformation on a micro-scale. In the lower part a few yellow weathering, black dolomicrites occur and, within a few metres of the contact with the overlying Mount Hawk Formation, thin pelmicrites appear and quickly increase in abundance toward the contact. More significant, however, are thin (15 cm thick, or less) yellow- or brown-weathering oolite beds, which first appear about 30 to 40 m below the Mount Hawk contact (Fig. 7.7). In some of these oolite beds the top few centimetres consist of imbricated pebbles also made up of oolites.

***Figure 7.7.*** *Oolite horizon in upper Perdrix fine clastics. Note imbrication at top of oolite band.*

Macrofossils are restricted to thin, calcareous bands, and consist mainly of gastropods. The fine clastics normally yield excellent miospore assemblages.

Due to the recessive, nonresistant character of the shales, the Perdrix Formation is rarely exposed in its entirety. Nonexposure, dip changes, and zones of deformation, make it nearly impossible to accurately measure the thickness of the formation. Values range from 100 to 470 m, but their accuracy must be questioned for the reasons mentioned.

The first influx of fine terrigenous particles occurred at the Flume - Maligne contact. Water depth was probably very shallow, as the stromatoporoid biostrome can be assumed to have grown within the photic zone, keeping up with the rate of subsidence. It is likely that the accumulation rate of the biostrome was not matched by the shaly limestone of the Maligne facies and fell even further behind during the deposition of the Perdrix shales.

The occurrence of oolite bands near the top of the Perdrix Formation suggests very shallow marine conditions, if the oolites are autochthonous. The presence of imbricated oolitic fragments at the top of oolite bands, and the general lack of oolites in the Mount Hawk Formation above, argue for an in situ origin of the oolites. Oolite banks formed as soon as the influx of fine grained terrigenous clastics had waned sufficiently, so that local shoals were temporarily beyond the dispersal range of terrigenous debris. Such conditions could, of course, only arise if such shoals were sufficiently shallow to allow the formation of ooids. This in turn suggests that the influx of terrigenous material had increased steadily since its first appearance near the top of the Flume Formation and slowly aggraded the regions around areas of continued stomatoporoid growth. It is enigmatic why the formation of oolite banks did not increase with the ever decreasing influx of terrigenous particles. Instead, pelmicrites, biomudstones and wackestones become more and more common and lead gradually into the Mount Hawk Formation. Some unknown dynamic factor, such as salinity or temperature, was probably instrumental in the regional and temporal confinement of oolite production.

In summary, the fine grained terrigenous clastics of the Perdrix Formation terminated carbonate deposition in all areas except on regional or prominent shoals protected from currents, where biostrome growth of the Flume Formation continued. These organic buildups form the well-known reef complexes of the Cairn, Southesk, and Leduc formations.

Clastic influx increased gradually and aggraded the depositional environment. At a later stage, terrigenous supply decreased, allowing carbonate environments to become established again, first in the form of oolite banks and later as normal shallow subtidal shelf carbonates. Therefore, the vertical facies change from shales into carbonates of the Mount Hawk Formation is not a response to shallowing conditions but due to a decreasing availability of terrigenous clastics.

Age. Miospore assemblages assign the Perdrix Formation to the middle and late Frasnian.

Mount Hawk Formation. The name Mount Hawk Formation has been applied to a cliff-forming limestone above the shales of the Perdrix Formation and below the very conspicuous, light grey exposures of the Simla Formation. Even though the lower boundary of the Mount Hawk Formation is gradational over several metres (Fig. 7.8), it can be better defined than the contact with the overlying Simla Formation, because the characteristic lithology of the Simla Formation does not come in along a distinct horizon. For this reason, the thickness of the Mount Hawk Formation varies considerably between 90 and 216 m. However, the combined thickness of the Mount Hawk and Simla formations varies only moderately between 170 and 278 m.

The Mount Hawk Formation is characterized by thin bedded, nodular limestone. There are intervals of shaly limestone or calcareous shale, which increase in number to the northwest. Occasionally the monotony of the nodular lithology is interrupted by thick bedded ledges of limestone. The carbonates are invariably very fossiliferous, with gastropods and corals the dominant organisms. Thin sections reveal an abundance of stomatoporoid fragments. The nodular limestones are mostly biomudstones and wackestones, whereas the ledges are biowackestones and grainstones. Coral colonies are common.

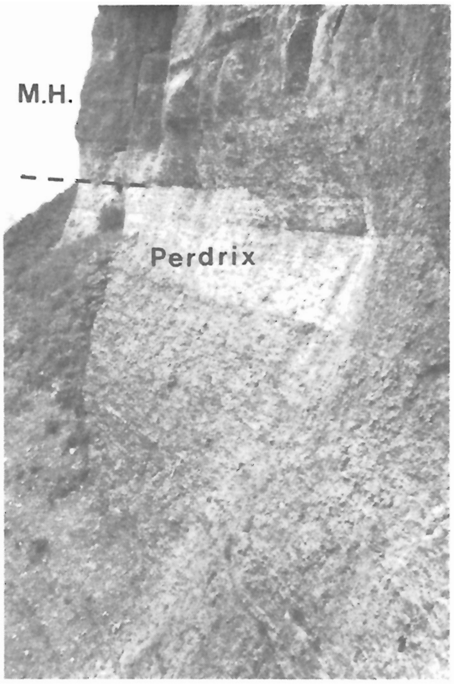


***Figure 7.8.*** *Transition zone from Perdrix clastics into fossiliferous carbonates of Mount Hawk Formation. Section is about 10 m thick. M.H.= Mount Hawk Formation.*

In the Winnifred Pass area (Section 81-5), several moderately sized bioherms (about 20 m high and 20-30 m wide) occur in the lower part of the Mount Hawk Formation. Their internal framework is considerably recrystallized. Bioherms of similar size have been described from the Ancient Wall area to the south (Mountjoy and Riding, 1981), where they are dominated by a stromatoporoid/renalcid assemblage.

Another abnormal facies within the Mount Hawk Formation consists of finely laminated algal beds (Fig. 7.9), some of which are more than a metre thick, occurring locally in groups of two or three. Their distribution within the formation appears to be fairly random, although they are perhaps slightly more abundant in the lower part.

Deposition of Mount Hawk strata was initiated by the re-establishment of a carbonate environment. In the discussion of the Perdrix sediments it was argued that this environmental change was not caused by shallowing, but was triggered by a sharp decrease in terrigenous influx. Water depth had been shallow, at least during later Perdrix time, as documented by the presence of oolitic beds within the shales. Shallow marine conditions persisted into Mount Hawk time, occasionally reaching the intertidal range, particularly during the early stages of Mount Hawk deposition. This intertidal environment is represented by beds of algal laminites. The fact that their stratigraphic position varies considerably from section to section suggests that regional shoals, within the intertidal range, existed somewhere at all times during early Mount Hawk deposition. The paleogeography is probably best envisaged as one of anastomosing shoals separated by very shallow bodies of water.

This paleogeographic setting also explains the origin of the most abundant lithology of the Mount Hawk Formation, the nodular biomudstones and wackestones. These lithologies are normally regarded as deeper, subtidal sediments, deposited below wave base. Their association, in the Mount Hawk Formation, with algal laminites, argues against such an interpretation. Instead, the mudstones and wackestones apparently accumulated between shoals that were separated by relatively short distances (fetch), too short to generate waves with an effective wave base of more than a few metres. Thus, the fines were not winnowed out and the only structure was probably ripple bedding which was modified by biogenic activity and compaction to the present nodular pattern. A few bands of amphiporid stromatoporoids are further evidence for shallow, near-lagoonal conditions.

***Figure 7.9.*** *Algal laminites in lower Mount Hawk Formation at Windy Peak (Section 80-6).*

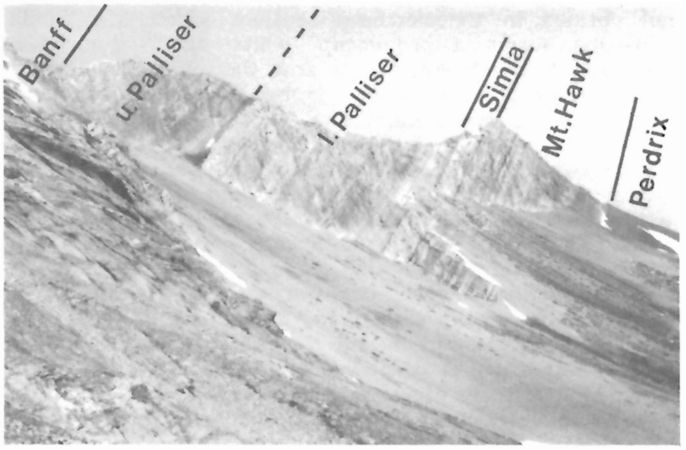


***Figure 7.10.*** *Excellent Upper Devonian section near Belcourt Mountain. From right to left - Perdrix, Mount Hawk, Simla, lower Palliser, upper Palliser with black band at base, and Banff formations.*

The thick bedded, ledge-forming beds of grainstone within the nodular biomudstones and wackestones obviously record periods of winnowing. Their thickness and internal make-up argues against storm deposits as a possible origin. The winnowing may have been caused by currents, which shifted from time to time in response to a change in the distribution of the shoals. The grainstone ledges may also simply be the product of the temporary lowering of wave base, when the location of shoals changed in such a way that a wide body of open water was created, allowing the generation of larger waves due to the increased fetch.

The bioherms in the Winnifred Pass section (Section 81-5) may indicate slightly deeper subtidal conditions to the southeast. This is corroborated by the absence of algal laminites in the same section and by the disappearance of oolites in the upper Perdrix Formation southeast of the Monkman Pass map area.

Age. Miospore, brachiopod and coral assemblages point to late Frasnian age for the Mount Hawk Formation.

Simla Formation. The name Simla Formation has been applied to a sequence of light grey, resistant limestone overlying the Mount Hawk Formation and underlying the Palliser Formation. The limestone is thick bedded to massive; bedding planes, if visible, are normally wavy. The weathered surface is normally coated with a crust of porous, light grey lime, effectively disguising all textures and structures. There are invariably, however, horizons within the formation where stromatoporoids or corals have been selectively silicified, revealing such an abundance of these organisms that these sections, at least, can be referred to as biostromes. Their lateral and vertical extent is hard to assess, because the rock is featureless where silicification is not present. The silicification continues occasionally as bands or nodules of black chert. In thin section the lithology is best described as a grainstone, composed of skeletal and nonskeletal (?) components.

The thickness of the formation varies between 30 and 103 m with a strong mode at 70 m. The upper contact is always sharp and, on a regional basis, may be interpreted as an unconformity, but within the field area there is no evidence for erosion along this break.

The lower contact with the Mount Hawk Formation is well defined in the northern sections where the Simla Formation forms a prominent "white band" (Fig. 7.10). Southeast of the Monkman Pass area the lower boundary of this "white band" extends down section into the Mount Hawk Formation but, at the same time, nodular bands of darker grey appear in the lower Simla Formation. In other words, Mount Hawk and Simla lithologies alternate and become less distinguishable to the southeast. This trend is first noticed at Bastille Mountain (Section 79-3), increases at Winnifred Pass (Section 81-5) until, at the southeasternmost sections (81-6 and 81-7), the Simla Formation strongly resembles the Mount Hawk Formation below. However, a terrigenous unit of reddish siltstones separates both formations at Winnifred Pass. This clastic unit is still present at the southeastern section and identifies the overlying section as the Simla Formation. A shaly sequence also separates the formations in the northwesternmost sections. This shaly interval belongs depositionally to the Mount Hawk Formation, because shaly horizons do occur lower in the same formation, but are characteristically lacking in the Simla Formation.

The name Simla had previously been applied to the highest member of the Southesk Formation in the Ancient Wall reef complex, which forms part of the northern boundary of Jasper National Park (McLaren and Mountjoy, 1962). The Ancient Wall area is the northernmost point to which the surface terminology of the upper Devonian Fairholme Group has been applied and is, therefore, the obvious connecting point between the Devonian of the northern Robson and Monkman Pass areas.

The Simla Member is 77 m thick at the type section in the Ancient Wall reef complex, and consists of 58 m of cliff-forming, thick bedded, very light grey limestone, underlain by 6 m of dolomitic, fossiliferous limestone and a largely covered, recessive section of siltstone 12.5 m thick.

The correlation with the Winnifred Pass section is evident, the upper cliff-forming, light grey limestones are the prominent "white band", whereas the underlying siltstones at Winnifred Pass have been included in the Mount Hawk Formation, because of their depositional affinity with that formation.

The Simla Member was later replaced by the Arcs and Grotto members, the Arcs comprising the upper 58 m of cliff-forming, very light grey limestone, and the Grotto including the dolomitic limestones and siltstones below (Mountjoy and MacKenzie, 1972). This new assignment was primarily based on the non-recognition of the Ronde Member (the uppermost member of the Southesk Formation in the Miette reef complex), rather than on a positive identification of the Grotto and Arcs members. The stratigraphic correlation has been questioned recently (Mountjoy, 1980; Workum, personal communication, 1982). It seems best, therefore, not to use the names Arcs, Grotto or Ronde, but to resurrect the term Simla. In its original usage the Simla was considered a member of the Southesk Formation, which makes up the upper part of the Frasnian reef complexes in the mountains. Except for the Berland buildup, there are no reef complexes to the northwest, whereas the Simla lithology continues in that direction. Therefore, since the Southesk Formation cannot be identified northwest of the Ancient Wall reef complex, the Simla lithologic unit has been raised from member to formation status.

The shallow marine conditions during Mount Hawk time continued during deposition of the Simla sediments. Algal laminites, at or near the lower and upper contacts of the Simla Formation, indicate temporary intertidal conditions. The fact that the formation consists mainly of grainstones, and the presence of crossbedding and shallow channels at Mount Hannington (Section 79-4), is further documentation of shallow marine conditions, above wave base.

A significant deviation from Mount Hawk sediments is the lack of terrigenous clastics. The dispersal range of terrigenous material had apparently retreated beyond the region. Clear seawater conditions allowed stromatoporoids to flourish and to become once again the most abundant organic component, as was the case during Flume time. The selective silicification of stromatoporoids and corals suggests that a large part of the Simla Formation may in fact be boundstones, rocks consisting of an organically bound framework.

In summary, the anastomosing shoals of Mount Hawk time had changed to a shallow, submerged carbonate bank. Sediments accumulated generally above wave base and were frequently covered by biostromes of stromatoporoids and corals. Intertidal shoals formed again towards the end of Simla time, perhaps a first indication of the brief period of non-deposition and emergence (?) prior to Palliser time.

Age. Coral assemblages were collected from various stratigraphic positions in the Simla Formation. All assemblages were assigned by A.E.H. Pedder (personal communication) to the latest Frasnian, and compared with similar assemblages collected from the Simla Member at the Ancient Wall reef complex, and from the Kakisa Formation of the southwestern District of Mackenzie.

Palliser Formation. The Palliser Formation is a thick succession of limestones, reaching 530 m at Mount Hannington (Section 79-4), decreasing to about 200 m to the southeast, and wedging out to the northwest (Fig. 7.3). In the thicker sections the formation can be conveniently sudivided into lower and upper parts, separated by a distinct "black band", a finely laminated lime mudstone (Fig. 7.10).

Directly above the contact with the underlying Simla Formation, the Palliser Formation starts locally with a few centimetres of brown, fossil hash, overlain by up to several

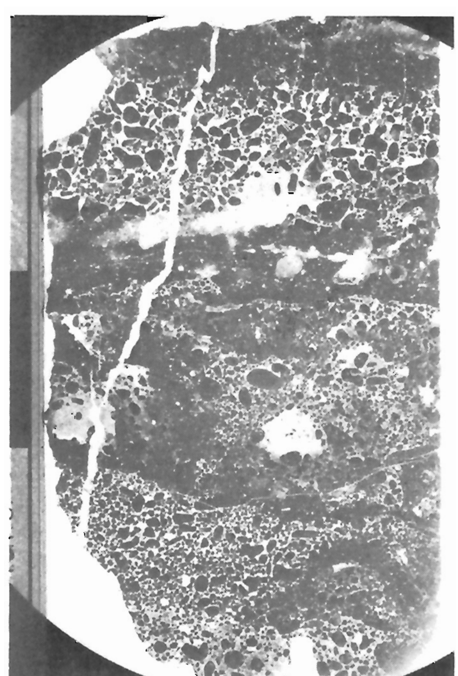

***Figure 7.11.*** *Thin section of typical lower Palliser sediments. Bioturbated mudstone with pellet-intraclasts filling intersecting burrows. Black bar is 1 cm long.*

metres of thin bedded grainstone to rudstone. Flat-pebble beds are very common in the lower 30 m, so is silt-sized quartz, which gradually disappears upsection.

The bulk of the lower Palliser Formation is a monotonous succession of ledges and recesses, the ledges invariably consisting of grainstones, which grade upsection into recessive mudstones, with pockets and fractures filled with grainstone. The components of the grainstones cover a wide range of sizes (Fig. 7.11), varying from pellets to intraclasts (0.2 mm is the conventional lower size boundary of intraclasts). Fossils, particularly brachiopods, are present near the base, but become very scarce upsection.

The limestones of the lower Palliser Formation have typically wavy, almost nodular, bedding planes, and are mottled in tones of grey. There are a few thin flat-pebble beds with a reddish, iron-oxide coating, and some distinctly yellow-brown mottled horizons. These beds cannot be traced to other sections, but are very useful for locating repetitions of strata across otherwise unrecognizable bedding-plane thrusts. To the southeast, into the Robson area, the nodular or wavy bedding of the lower Palliser Formation grades into an evenly bedded succession and the mottling disappears. Thin sections of the nodular, mottled facies reveal intense bioturbation and burrowing, with the entire rock having been reworked. To the southeast, the burrows are separated from each other and, for that reason, become much more visible, even though the intensity of bioturbation decreases.

The upper Palliser Formation is preserved only in the central part of the study area (Fig. 7.3), where it reaches a thickness of 241 m. The base is defined by a black, laminated, unfossiliferous lime mudstone, which rests along a sharp contact on typical lower Palliser lithology. The black lime mudstone is about 10 m thick and, above the basal 2.5 m, is interbedded with thin, brown, shaly limestone beds, which commonly display shallow updoming of probable algal origin. Grey, calcareous shales and thin (5 cm), evenly bedded lime mudstones, with trace fossil marks on bedding planes, make up the next few tens of metres. The shaly component slowly disappears upsection and the thin, evenly bedded limestones become increasingly brown-grey mottled, a lithology which, in some sections, continues to the Banff contact. Elsewhere, the highest Palliser beds are yellow, platy, slightly shaly limestones, or grey, well-bedded calcisiltites. Black chert nodules may occur at various stratigraphic levels. Macrofossils are crinoid ossicles and rare brachiopods. The dominant lithology seen in thin section is a pellet grainstone.

The contact with the fine grained, black, terrigenous clastics of the overlying Besa River or Exshaw formations is sharp and is an unconformity (Fig. 7.12). This interpretation is documented by the occurrence, along the contact, of a thin layer of "fossil hash", or by a quartzose sandstone, or by calcareous concretions. It is further supported, on the basis of preliminary data, by the age discrepancy of fossil assemblages across the contact. Due to erosional truncation, only 4 m of the upper Palliser Formation are preserved at Winnifred Pass (Section 81-5) to the southeast, whereas, to the northwest, the entire Palliser is missing beyond Hook Lake (Section 80-10).

A period of non-deposition and emergence preceded the deposition of the Palliser Formation. South of the area under investigation, topographic depressions in underlying sediments were filled, after this hiatus, by the Sassenach Formation – a succession dominated by terrigenous detrital sediments. The Simla Formation to the north was apparently a resistant carbonate platform of negligible relief, probably remaining above base level during the pre-Palliser hiatal period. The only evidence of a hiatus there are silt-sized quartz grains, which occur sporadically in the lower 30 m of the Palliser Formation. The grain size and the good sorting suggest an aeolian origin, documenting that emergent conditions persisted near by into early Palliser time.

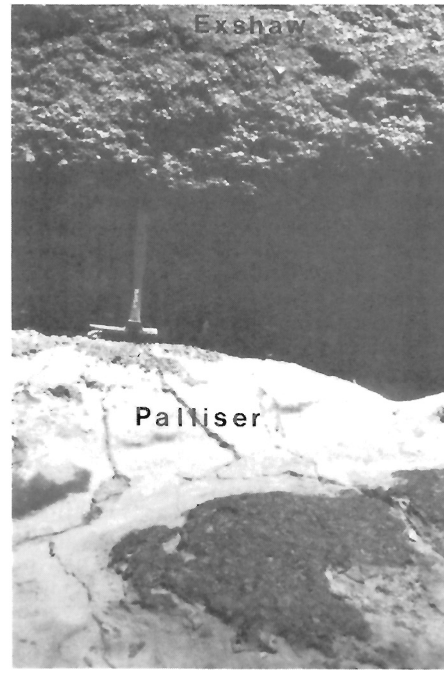


***Figure 7.12.*** *Palliser-Exshaw unconformity at Winnifred Pass (Section 81-5). Black chert patches on the carbonate surface mark unconformity.*

The basal sediments of the Palliser Formation were deposited within wave base; a few centimetres of calcite-cemented "fossil hash" occurs locally as discontinuous patches, directly above the contact with the underlying Simla Formation. The dominant fossil forms are crinoids, gastropods and brachiopods. The presence of flat-pebble beds above, suggests frequent reworking of semiconsolidated lime muds. With increasing water depth, deposition took place below wave base, and lime muds were strongly bioturbated. The cyclic pattern of grainstone to mudstone indicates that water depth was repeatedly moving above and below wave base. This cyclicity may be due to eustatic sea level changes, or changes in the rate of subsidence. Another possibility is the periodic formation of shoals without the area ever reaching the intertidal range.

The paucity of skeletal material, the high degree of bioturbation, and the presence of abundant pellet-intraclast grains in the lower Palliser seem interrelated. Sediment feeders were probably the dominant organisms and responsible for the disaggregation of lime mud. Some ecologic change (temperature, salinity) must have rendered the environment hostile for shelly organisms, even though the lower Palliser sediments superficially resemble the wavy, nodular limestones of the Mount Hawk Formation, suggesting that the overall depositional environment was still shallow marine.

The abrupt facies change into a black, laminated lime mudstone at the base of the upper Palliser Formation, indicates a radical change of the circulation pattern, from open marine to restricted marine. The association of the black laminated mudstone with algal structures and the lack of other fossils, suggest lagoonal, perhaps hypersaline, conditions. The minor influx of fine grained terrigenous material may in fact be another response to the same cause that brought about the temporary, restrictive conditions. A drastic decrease in the rate of subsidence, and a simultaneous shift of the dispersal range of terrigenous material into the study area, as a result of a distant uplift, may well explain the lithologic changes.

With the disappearance of the fine terrigenous clastics, open, shallow, marine conditions returned. Skeletal fragments, particularly crinoidal, are normally present. At the same time, the strong intraclast component of the lower Palliser sediments decreases. However, pelletization of lime mud is still intense, even though the size of the pellets is considerably smaller than in the lower Palliser sediments. This could be explained by a number of ecological changes, such as a return to normal salinities and, particularly, to different sediment feeders.

Shallow marine, subtidal conditions persisted in some areas right up to the contact with the overlying Exshaw or Besa River sediments; elsewhere (Onion Lake, Section 80-1; Bone Mountain, Section 80-2) the highest Palliser sediments suggest very shallow, even intertidal or supratidal, conditions (imbricated mud chips, crossbedding, channelling). This formation of shoals is probably the first sign of the post-Palliser hiatus, during which regional uplift occurred and part of the Palliser and older sediments were removed by erosion.

Age. The Palliser Formation has been extensively collected for brachiopods by Sartenaer (1969), who assigned the formation to the early and middle Famennian. A more recent study of ostracods was undertaken by Lethiers (1981). His work was concentrated more on subsurface equivalents of the Palliser Formation. Lethiers (1981) concluded that the subsurface sediments may be as young as late Famennian, whereas the Palliser Formation in the mountain sections is restricted to the early and middle Famennian. Conodonts from Palliser sections in the Monkman Pass area are early and middle Famennian in age (Chatterton, personal communication). A miospore assemblage, from the base of the upper Palliser at Winnifred Pass (Section 81-5), may be as old as early Famennian, according to D.C. McGregor (personal communication).

**References**


Campbell, R.B., Mountjoy, E.W., and Young, F.G.
1973: Geology of McBride map-area, British Columbia; Geological Survey of Canada, Paper 72-35, 104 p.

Lethiers, F.
1981: Ostracodes du Dévonien terminal de l'ouest du Canada: Systématique, biostratigraphie et paléoécologie; Géobios, Mémoire spécial no. 5, Lyon, 236 p.

McLaren, D.J. and Mountjoy, E.W.
1962: Alexo equivalents in the Jasper region, Alberta; Geological Survey of Canada, Paper 62-23, 36 p.

Mountjoy, E.W.
1980: Geology, Mount Robson, west of sixth meridian, Alberta - British Columbia; Geological Survey of Canada, Map 1499A.

Mountjoy, E.W. and MacKenzie, W.S.
1973: Stratigraphy of the southern part of the Devonian Ancient Wall carbonate complex, Jasper National Park, Alberta; Geological Survey of Canada, Paper 72-20, 121 p.

Mountjoy, E.W. and Riding, R.
1981: Foreslope stromatoporoid - renalcid bioherm with evidence of early cementation, Devonian Ancient Wall reef complex, Rocky Mountains; Sedimentology, v. 28, p. 299-319.

Poole, F.G., Sandberg, C.A., and Boucot, A.J.
1977: Silurian and Devonian paleogeography of the western United States; in Paleozoic Paleogeography of the Western United States, J.H. Stewart, C.H. Stevens and A.E. Fritsche, ed.; Society of Economic Paleontologists and Mineralogists, Pacific Section, Pacific Coast Paleogeography Symposium 1, p. 39-65.

Sartenaer, P.
1969: Late Upper Devonian (Famennian) Rhynchonellid brachiopods from western Canada; Geological Survey of Canada, Bulletin 169, 269 p.

Taylor, G.C. and Bamber, E.W.
1970: Paleozoic stratigraphy of Pine Pass, northeastern British Columbia; in Peace River, Pine Pass, Yellowhead 1970, Field Conference Guidebook; G.L. Bush and Dooge, J., ed.; Edmonton Geological Society, Guidebook, p. 46-57.

Taylor, G.C. and MacKenzie, W.S.
1970: Devonian stratigraphy of northeastern British Columbia; Geological Survey of Canada, Bulletin 186, 62 p.

Taylor, G.C. and Stott, D.F.
1979: Monkman Pass (93 I) map area, northeastern British Columbia; Geological Survey of Canada, Open File 630.

Taylor, P.W.
1957: Revision of Devonian nomenclature in the Rocky Mountains; Journal of the Alberta Society of Petroleum Geologists, v. 5, p. 183-195.

Thompson, R.I.
1978: Geologic maps and section of Halfway River map-area, British Columbia (94 B); Geological Survey of Canada, Open File 536.

Tipper, H.W., Campbell, R.B., Taylor, G.C., and Stott, D.F.
1979: Parsnip River, British Columbia, sheet 93; Geological Survey of Canada, Geological Atlas, Map 1424A.

8.

# PRELIMINARY RESULTS ON RANK AND COMPOSITION OF COALS FROM THE GETHING FORMATION NORTH OF PEACE RIVER, NORTHEASTERN BRITISH COLUMBIA

Project 810019

W. Kalkreuth
Institute of Sedimentary and Petroleum Geology, Calgary

*Kalkreuth, W., Preliminary results on rank and composition of coals from the Gething Formation north of Peace River, northeastern British Columbia; in Current Research, Part C, Geological Survey of Canada, Paper 82-1C, p. 65-69, 1982.*

**Abstract**

*Coals from three outcrop sections of the Gething Formation north of Peace River were collected and analyzed micropetrologically. Rank was determined by measuring mean maximum vitrinite reflectances. At Fiddes Creek the reflectance values indicate high-volatile A bituminous coals, whereas at Halfway River and Pink Mountain the rank ranges from high-volatile A bituminous to medium-volatile bituminous. Composition was determined by maceral analysis. The content of vitrinite, liptinite and inerts shows great variation throughout the coal-bearing succession. At Pink Mountain high amounts of semifusinite and inerts, in coals collected from the upper part of the Gething Formation, indicate a shift to drier conditions in the peat swamp.*

*Results of rank and maceral analyses indicate that some coals fall into the range of coals considered to have good coking properties. However, seams observed so far in this area have maximum thicknesses of 0.75 m and are of no economic value.*

## Introduction

The Gething Formation of the Bullhead Group, in the Rocky Mountain Foothills of northeastern British Columbia, consists of a sequence of sandstones, siltstones, carbonaceous shales, mudstones and coals. In the vicinity of Peace River, at Carbon Creek (Fig. 8.1), the formation is 1100 m thick, containing in excess of 100 seams of coal, which range in thickness from a few centimetres to 4.30 m (Gibson, in press). At the type section near W.A.C. Bennett Dam on Peace River (Fig. 8.1) the Gething is approximately 550 m thick and contains a total of more than 40 coal seams up to 1.20 m thick (Stott, 1969). The rank of the Gething coals in these areas varies widely, ranging from high-volatile bituminous to low-volatile bituminous.

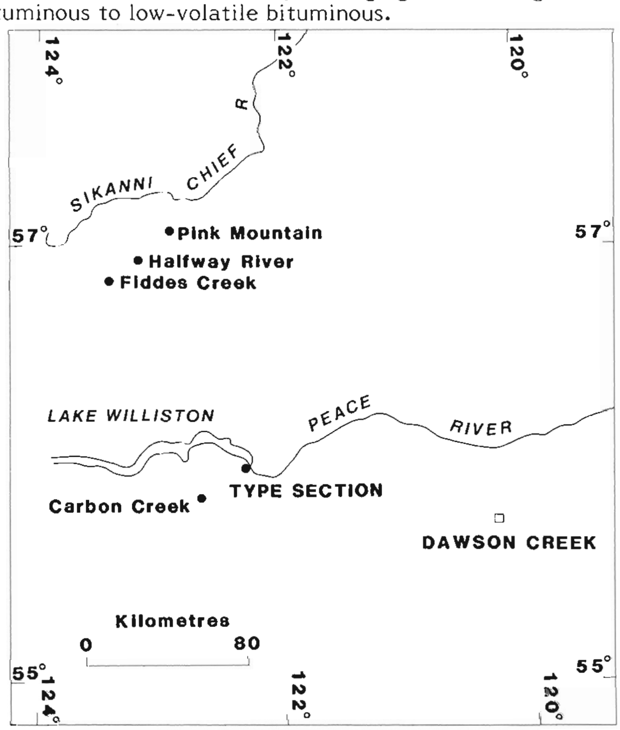


*Figure 8.1.* *Map showing sample locations.*

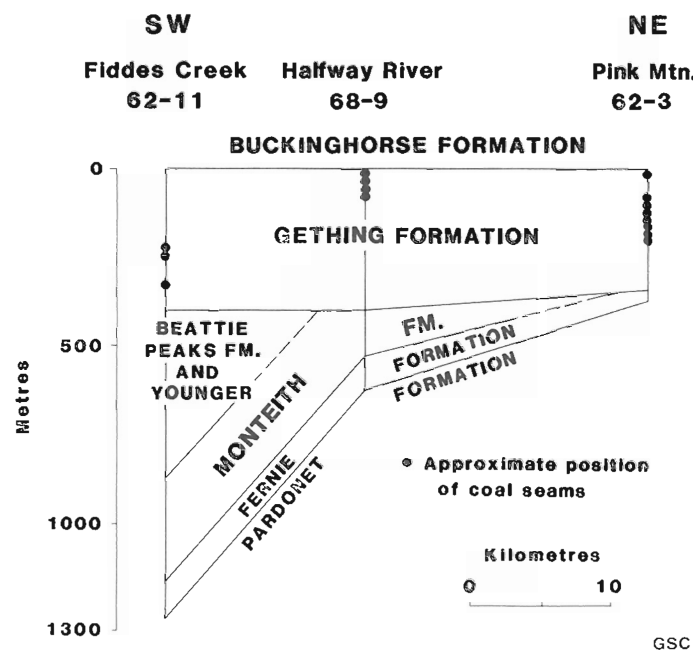


*Figure 8.2.* *Schematic diagram illustrating thickness of Gething Formation and older strata at Fiddes Creek, Halfway River and Pink Mountain, after Stott (1969, 1973).*

North of Peace River, coal occurs less abundantly in the Gething Formation. The northern limit of coal development appears to be at Sikannni Chief River, where thin seams have been reported by Stott (1973). Little is known about rank and composition of coals in this northern area. In the present report, results of petrographic analyses are given for coals collected at three localities between Peace and Sikanni Chief Rivers: Fiddes Creek, Halfway River, and Pink Mountain (Fig. 8.1). A detailed lithologic description for these sections has been published by Stott (1969, 1973). A schematic diagram illustrating the thickness of the Gething Formation at these locations, and the approximate positions of coal seams, is given in Figure 8.2. Due to an eastward truncation of older beds in this area

(Pre-Bullhead unconformity), from southwest to northeast, the Gething Formation lies on successively older strata. At Fiddes Creek and Halfway River it overlies the Beattie Peaks and Monteith formations of the Minnes Group and at Pink Mountain the Gething overlies Jurassic shales of the Fernie Formation (Fig. 8.2, 8.3).

### Sample Preparation and Analytical Methods

The coals were crushed to a maximum particle size of 850 microns (20 mesh), mounted in epoxy resin, and then ground and polished.

Rank was determined by measuring maximum vitrinite reflectances using a Leitz MPV II microscope under standardized conditions (465 nm, oil immersion, etc.), following the procedure outlined in the International Handbook of Coal Petrography (I.C.C.P., 1971). The mean maximum vitrinite reflectance was derived from these measurements. ASTM rank classes were obtained by using the maximum reflectance limits for ASTM rank classes as published by Davis (1978).

Maceral analyses were carried out using a Swift automatic point counter and mechanical stage. Each composition is based on 300 points. Vitrinite was counted either as vitrinite A (homogeneous vitrinite particles) or as vitrinite B (vitrinite intimately associated with other macerals). Within the liptinite group, five macerals were distinguished, four by their characteristic morphology (alginite, sporinite, cutinite and resinite) and reflectance, while the fifth (liptodetrinite) is composed of liptinite fragments too small or too badly disintegrated to be reliably assigned to the other liptinite macerals. Semifusinite was counted separately, whereas other macerals of the inertinite group (fusinite, macrinite, micrinite and sclerotinite) were grouped together under inerts.

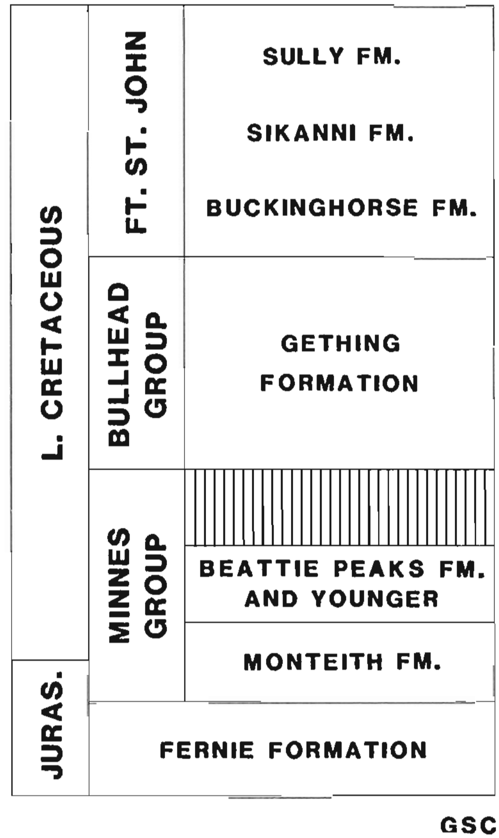


***Figure 8.3.*** *Chart illustrating Jurassic – Lower Cretaceous stratigraphy south of Sikanni Chief River, after Stott (1974).*

Table 8.1

Rank determinations from Pink Mountain, Halfway River and Fiddes Creek areas

| Section | Sample | Formation | Depth (m) | Thickness (m) | Maximum Reflectance [%] Mean | S | N | A.S.T.M. Rank Classes |
|---|---|---|---|---|---|---|---|---|
| Pink Mountain | 610/81 | Gething | 87.84 | 0.20 | 1.05 | 0.04 | 50 | High-vol. bituminous A |
| Pink Mountain | 609/81 | Gething | 98.82 | 0.05 | 1.08 | 0.04 | 50 | High-vol. bituminous A |
| Pink Mountain | 608/81 | Gething | 112.24 | 0.20 | 1.09 | 0.05 | 50 | High-vol. bituminous A |
| Pink Mountain | 607/81 | Gething | 141.21 | 0.45 | 1.19 | 0.05 | 50 | Med.-vol. bituminous |
| Pink Mountain | 606/81 | Gething | 141.98 | 0.50 | 1.21 | 0.05 | 50 | Med.-vol. bituminous |
| Pink Mountain | 605/81 | Gething | 145.48 | 0.41 | 1.17 | 0.05 | 50 | Med.-vol. bituminous |
| Pink Mountain | 604/81 | Gething | 148.84 | 0.15 | 1.20 | 0.05 | 50 | Med.-vol. bituminous |
| Pink Mountain | 603/81 | Gething | 148.99 | 0.20 | 1.21 | 0.06 | 50 | Med.-vol. bituminous |
| Pink Mountain | 601/81 | Gething | 177.05 | 0.10 | 1.16 | 0.04 | 50 | Med.-vol. bituminous |
| Pink Mountain | 600/81 | Gething | 197.64 | 0.10 | 1.21 | 0.05 | 50 | Med.-vol. bituminous |
| Halfway River | 615/81 | Gething | - | 0.20 | 1.12 | 0.06 | 50 | Med.-vol. bituminous |
| Halfway River | 616/81 | Gething | - | 0.20 | 1.03 | 0.07 | 50 | High-vol. bituminous A |
| Halfway River | 617/81 | Gething | - | 0.05 | 1.05 | 0.06 | 50 | High-vol. bituminous A |
| Halfway River | 618/81 | Gething | - | 0.30 | 1.14 | 0.07 | 50 | Med.-vol. bituminous |
| Fiddes Creek | 612/81 | Gething | - | 0.50 | 0.87 | 0.05 | 50 | High-vol. bituminous A |
| Fiddes Creek | 613/81 | Gething | - | 0.75 | 1.02 | 0.06 | 50 | High-vol. bituminous A |
| Fiddes Creek | 614/81 | Gething | - | 0.30 | 0.95 | 0.06 | 50 | High-vol. bituminous A |

S = standard deviation
N = number of measurements

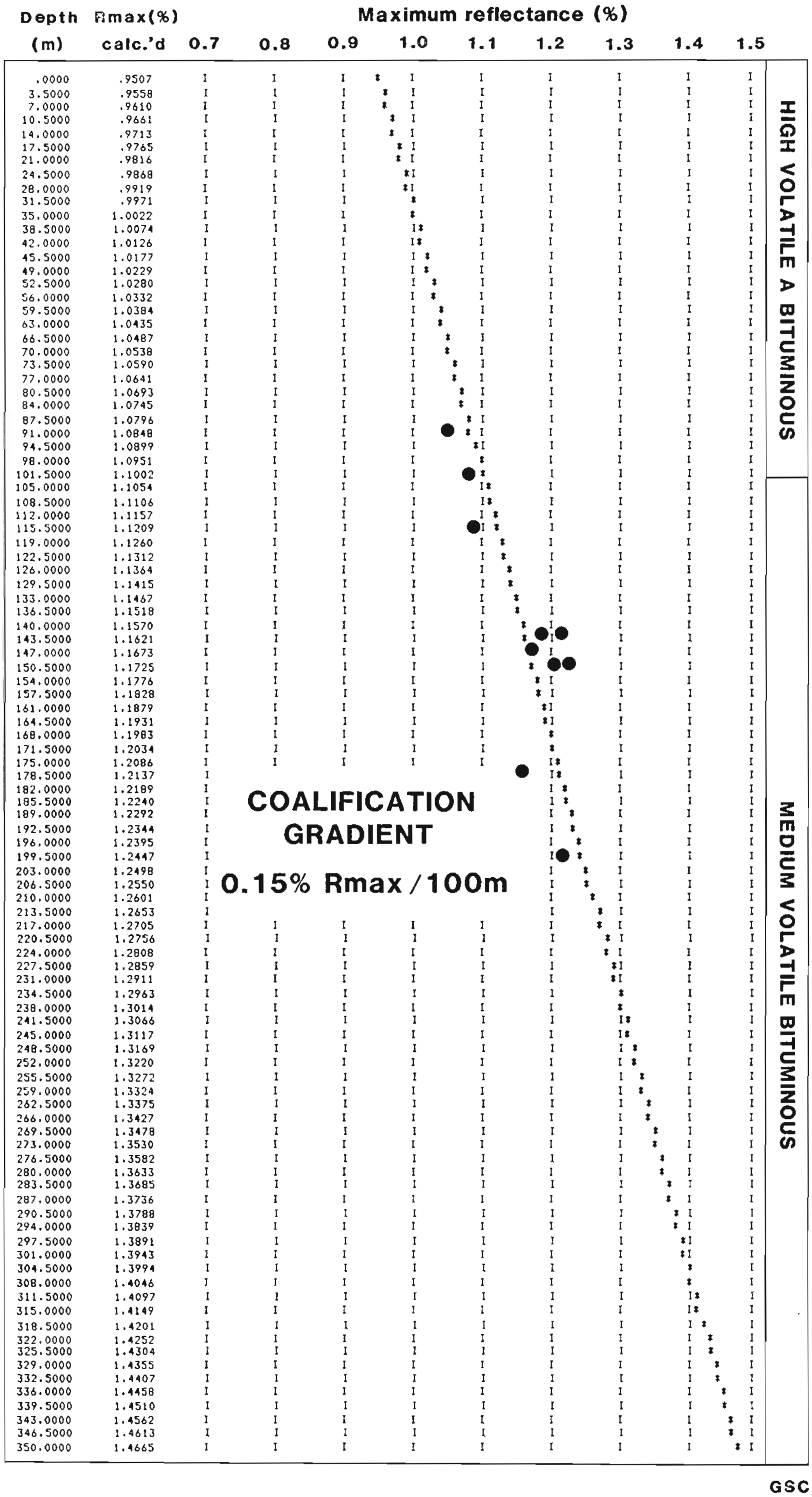


***Figure 8.4.*** *Rank-to-depth relationship of Gething strata at Pink Mountain based on vitrinite-reflectances.*

## Results and Discussion

### Rank variations

The results of the rank determinations are listed in Table 8.1.

Pink Mountain. At Pink Mountain 10 coal seams were sampled, ranging in thickness from 0.05 m to 0.50 m. The rank ranges from high-volatile bituminous A to medium-volatile bituminous. A coalification profile from the Gething Formation at Pink Mountain, based on a first order regression line, is given in Figure 8.4. In the left outer column the depth (from top of the formation) is shown in steps of 3.50 m. For each of these steps the corresponding calculated or theoretical reflectance value is shown in the left inner column. Figure 8.4 shows that the rank increases from high-volatile A bituminous at the top of the formation to medium-volatile at the base of the formation. The coalification gradient is 0.15% Rmax/100 m.

Halfway River. Four coal samples were collected at this location. The coal seams occur in the upper part of the Gething Formation, ranging in thickness from 0.05 m to 0.30 m. Two coals are high-volatile A bituminous, the other two are medium-volatile bituminous.

Fiddes Creek. Three coals were obtained from the lower part of the Gething Formation at Fiddes Creek. The thickness of the coal seams varies between 0.30 m and 0.75 m. All three coals are high-volatile bituminous A, although the reflectance data indicate a somewhat lower coalification here as compared to the high-volatile coals from the Pink Mountain and Halfway River sections.

### Maceral Analyses

Results of maceral analyses are listed in Table 8.2 and also plotted in Figure 8.5.

Pink Mountain. The content in vitrinite, liptinite and inerts shows a great variation throughout the coal-bearing succession. Total vitrinite content ranges from 35-98 per cent, whereas inerts, including semifusinite, range between 2 and 62 per cent. Liptinite, mainly in the form of sporinite, cutinite and liptodetrinite constitutes up to 5 per cent.

Halfway River and Fiddes Creek. The coals obtained from these sections are similar in composition to those analyzed from Pink Mountain. Vitrinite, semifusinite and inerts are the main components, occurring in varying amounts. The liptinite content constitutes up to 7 per cent at Fiddes Creek and 9 per cent at Halfway River.

Table 8.2

Maceral-analysis vol % (m.m.f.)

| | | | Vitrinite | | | | Liptinite | | | | | Inertinite | | | |
|---|---|---|---|---|---|---|---|---|---|---|---|---|---|---|---|
| Location | Sample | Formation | A | B | Total | Alginite | Sporinite | Resinite | Cutinite | Lipto-detrinite | Total | Semi-fusinite | Inerts | Total | Mineral Matter |
| Pink Mountain | 610/81 | Gething | 14 | 21 | 35 | - | 2 | - | <1 | <1 | 3 | 42 | 20 | 62 | 9 |
| Pink Mountain | 609/81 | Gething | 68 | 25 | 93 | - | 2 | - | 1 | 2 | 5 | 1 | <1 | 2 | <1 |
| Pink Mountain | 608/81 | Gething | 22 | 25 | 45 | - | 1 | - | 1 | 1 | 3 | 34 | 18 | 52 | 3 |
| Pink Mountain | 607/81 | Gething | 80 | 12 | 92 | - | 2 | - | <1 | 2 | 5 | 2 | 1 | 3 | 3 |
| Pink Mountain | 606/81 | Gething | 46 | 15 | 61 | - | 1 | - | <1 | - | 2 | 25 | 12 | 37 | <1 |
| Pink Mountain | 605/81 | Gething | 46 | 8 | 54 | - | - | - | <1 | - | <1 | 25 | 21 | 46 | 8 |
| Pink Mountain | 604/81 | Gething | 87 | 6 | 93 | - | 3 | - | - | 2 | 5 | - | 2 | 2 | 3 |
| Pink Mountain | 603/81 | Gething | 97 | 1 | 98 | - | <1 | - | - | - | <1 | <1 | 1 | 1 | 8 |
| Pink Mountain | 601/81 | Gething | 86 | 6 | 92 | - | - | - | - | - | - | 3 | 5 | 8 | 10 |
| Pink Mountain | 600/81 | Gething | 97 | 1 | 98 | - | - | - | - | - | - | <1 | 2 | 2 | 2 |
| Halfway River | 615/81 | Gething | 60 | 27 | 87 | - | 1 | - | 6 | 3 | 9 | 2 | 2 | 4 | 71 |
| Halfway River | 616/81 | Gething | 47 | 14 | 61 | - | 1 | - | <1 | <1 | 2 | 17 | 20 | 37 | 18 |
| Halfway River | 617/81 | Gething | 89 | 2 | 91 | - | <1 | - | <1 | 1 | 2 | - | 7 | 7 | 14 |
| Halfway River | 618/81 | Gething | 20 | 19 | 39 | - | 3 | - | <1 | 1 | 5 | 30 | 26 | 56 | <1 |
| Fiddes Creek | 612/81 | Gething | 18 | 50 | 68 | - | 3 | - | 1 | - | 4 | 14 | 14 | 28 | 1 |
| Fiddes Creek | 613/81 | Gething | 62 | 21 | 83 | <1 | 2 | - | 3 | 2 | 7 | 6 | 4 | 10 | - |
| Fiddes Creek | 614/81 | Gething | 27 | 30 | 57 | - | 2 | - | - | 1 | 3 | 22 | 18 | 40 | 4 |

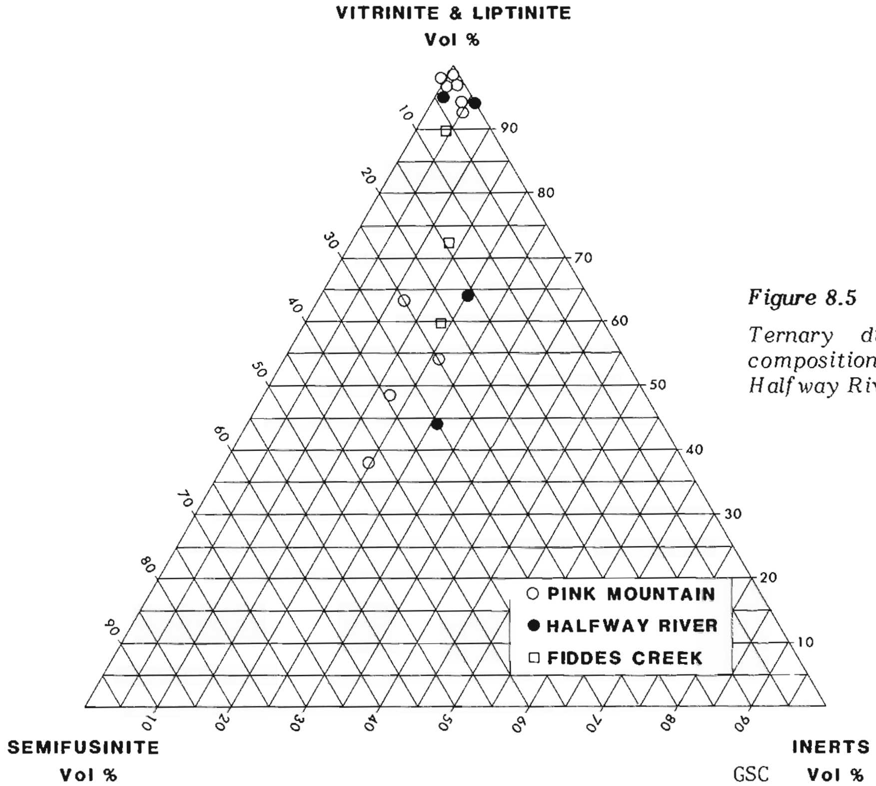


*Figure 8.5*

*Ternary diagram illustrating maceral composition of coals from Fiddes Creek, Halfway River and Pink Mountain.*

## Conclusions

Preliminary results on the coals from Fiddes Creek, Halfway River and Pink Mountain indicate that there are no major changes in rank in these areas as compared to the rank of the Gething coals farther south. Hacquebard and Donaldson (1974) reported high-volatile to medium-volatile bituminous rank from the type section of the Gething Formation at Peace River Canyon (1.05-1.36% Rmax). To the southwest, in the Carbon Creek Basin (Fig. 8.1), similar reflectances of 0.93-1.36% Rmax have been determined. Although, at the moment, there is no control for the coalification pattern of the Gething Formation between Peace River/Carbon Creek and the sections at Fiddes Creek, Halfway River and Pink Mountain, it appears that in this northern area of the Peace River Coalfield the rank ranges between high-volatile A and medium-volatile bituminous coals.

In terms of maceral composition the coals of the three sections analyzed show drastic changes within each section. At Pink Mountain there appears to be a trend from vitrinite-rich, liptinite- and inertinite-poor coals at the bottom of the coal-bearing succession, to coals characterized by alternating high amounts of vitrinite and semifusinite/inerts at the top of the coal-bearing strata. The high amounts of semifusinites and inerts in these coals are an indication of a shift to drier conditions in the peat swamp. Under these conditions, accelerated oxidation, mouldering and/or fungal attack on the organic material, would have led to an enrichment of semifusinite and inertinitic macerals.

## Technological Properties

Rank and maceral results indicate that some of the medium-volatile coals from Pink Mountain and Halfway River fall into a compositional range considered to have good coking properties. However, seams so far observed in this area have maximum thicknesses of 0.50 m and are apparently of no economic value.

## References


Davis, A.
1978: The measurement of reflectance of coal macerals – its automation and significance; The Pennsylvania State University, Technical Report 10, 88 p.

Gibson, D.W.
Stratigraphy and sedimentology of the Lower Cretaceous Gething Formation, Carbon Creek Coal Basin, northeastern British Columbia; Geological Survey of Canada. (in press)

Hacquebard, P.A. and Donaldson, J.R.
1974: Rank studies of coals in the Rocky Mountains and Inner Foothills Belt, Canada; Geological Society of America, Special Paper 153, p. 75-94.

I.C.C.P.
1971: International Committee for Coal Petrology, International Handbook of Coal Petrography, 2nd Edition 1963. Supplement to 2nd Edition 1971, Centre National de la Recherche Scientifique, Paris.

Stott, D.F.
1969: The Gething Formation at Peace River Canyon, British Columbia; Geological Survey of Canada, Paper 68-28, 30 p.

1973: Lower Cretaceous Bullhead Group between Bullmoose Mountain and Tetsa River, Rocky Mountains Foothills, northeastern British Columbia; Geological Survey of Canada, Bulletin 219, 228 p.

9. **NEW ZLICHOVIAN (EARLY DEVONIAN) RUGOSE CORALS FROM THE BLUE FIORD FORMATION OF ELLESMERE ISLAND**

Project 680093

A.E.H. Pedder
Institute of Sedimentary and Petroleum Geology, Calgary

*Pedder, A.E.H., New Zlichovian (Early Devonian) rugose corals from the Blue Fiord Formation of Ellesmere Island; in Current Research, Part C, Geological Survey of Canada, Paper 82-1C, p. 71-82, 1982.*

### *Abstract*

*The genera **Taimyrophyllum**, **Cavanophyllum** and **Radiastraea** are reviewed. A lectotype is chosen for **Phillipsastraea scheii** Loewe, 1913, to make it a junior objective synonym of **Iowaphyllum alpenense** (Rominger, 1877). This allows **Taimyrophyllum nolani** Merriam, 1974, which would otherwise be a junior subjective synonym of **Phillipsastrea scheii**, to stand. **T. nolani beaumannense** subsp. n., **Cavanophyllum uyenoi** sp. n. and **Radiastraea pulchra** sp. n. are described from the early Zlichovian part of the **dehiscens** Zone, at localities close to the outcrop known as the Sor Fiord section, on southwest Ellesmere Island, arctic Canada. **Cavanophyllum uyenoi** sp. n. also occurs in the slightly younger Zlichovian **Polygnathus** aff. **perbonus** conodont unit in the Sor Fiord section.*

## Introduction

Until 1982, the only formal description of Devonian corals from the Canadian arctic islands was Loewe's (1913) work on material collected by Per Schei, between 1898 and 1902, when he was the geologist on the Second Norwegian Arctic Expedition.

Collections, very much larger than Per Schei's, are now at hand awaiting systematic study. Taxonomic investigation of all the species and genera represented is an enormous task, which will require several, if not many years to complete. As an example of how complicated coral taxonomy has become, it may be pointed out that Loewe described corals now regarded as species of **Lekanophyllum** and **Taimyrophyllum**. In Loewe's day only four species had been established that would be assigned to these genera today. In contrast, there are presently more than 60 species assignable to **Lekanophyllum** and about 15 assignable to **Taimyrophyllum**. Thus, there has been an increase from four, to more than seventy-five species, that have to be considered in taxonomic work on representatives of these two genera alone. The present work is a small contribution toward a complete study of the large Devonian coral faunas of the Canadian arctic islands.

## Biostratigraphy

With the exceptions of the Pragian Koneprusy facies of Czechoslovakia, and the Seigenian to Emsian **Pleurodictyum** bearing beds of Belgium and Germany, corals are rare in the stratotype regions of the standard European Lower Devonian stages. If it were possible to establish intercontinental correlations on the basis of coral distributions - and, in fact, it is not (Oliver and Pedder, 1979, Table 1) - it would still be impossible to do so between either arctic Canada and Belgium and Germany, or between arctic Canada and Czechoslovakia.

In view of this situation, ages of Early Devonian corals from arctic Canada are established best by conodonts, because this enigmatic, but nevertheless time-sensitive, group of fossils has been isolated from coral-bearing strata of the Arctic Islands, as well as from the more pelagic Lower Devonian facies of Czechoslovakia. For an outline of the conodont succession and zonation of the Sor Fiord and Blue Fiord region of southwest Ellesmere Island, and their temporal relationship to the standard European stages, readers are referred to the work of Uyeno and Klapper (1980).

**Taimyrophyllum nolani beaumannense** and **Radiastraea pulchra** come from about 25 to 30 m above the base of the Blue Fiord Formation in the Sor Fiord region. Uyeno and Klapper (1980) showed that **Polygnathus dehiscens** ranges from the upper part of the Eids Formation, to at least 141 m above the base of the overlying Blue Fiord Formation in the Blue and Sor fiords region. Some of the **dehiscens** Zone belongs to the Pragian, but by far the greater part is evidently Zlichovian (Schönlaub, 1979). Therefore, it is safe to assume that **Taimyrophyllum nolani beaumannense** and **Radiastraea pulchra** derive from the early Zlichovian part of the **dehiscens** Zone.

The specimen of **Cavanophyllum uyenoi** from GSC locality C-12498 is probably also from the early Zlichovian part of the **dehiscens** Zone, because of the similarity between the faunas from C-12498 and C-12501, and the knowledge that C-12498 is very low in the Blue Fiord Formation. However, specimens of the same species from GSC locality C-12424, which include the holotype, are referred to the slightly younger Zlichovian **Polygnathus** aff. **perbonus** conodont unit. This is done, despite their position 27.4 m below the first proven occurrence of **Polygnathus** aff. **perbonus** in the section, on the grounds that comparison of Uyeno and Klapper's (1980) figures 8.2 and 8.3, implies that the very brief range of **P.** aff. **perbonus** in the Sor Fiord section is probably merely a teilzone within the upper part of the full range of the taxon in the region.

Family SPONGOPHYLLIDAE Dybowski, 1873
Subfamily PTENOPHYLLINAE Wedekind, 1923

Genus **Taimyrophyllum** Chernyshev, 1941

**Taimyrophyllum** Chernyshev, 1941, p. 12, 53.

**Eddastraea** Hill, 1942a, p. 147, 148.

Type species of **Taimyrophyllum**. **Taimyrophyllum speciosum** Chernyshev, 1941, p. 12, 13, 53, 54, text-fig. 1, Pl. 1, figs. 1-3; Pl. 2, figs. 1-3; Pl. 5, fig. 5. Lower Devonian; holotype from 40 km above the mouth of Tareya River, other material from 65 km above the mouth of Tareya River, southwest Taimyr, U.S.S.R. Chernyshev maintained that the species is restricted to the base of the Lower Devonian in the type area, whereas Kravtsov (1963, p. 10) pointed out that it is confined, in the type area, to unit 3 of the Tareya Suite; that is, to the Zlichovian Daksanski Beds of subsequent terminology (Cherkesova et al., 1968).

Type species of **Eddastraea**. **Phillipsastraea grandis** Dun in Benson, 1918, p. 379, Pl. 35, figs. 4, 5. Loomberah Limestone; precise locality data not published, but probably from Portion 58, Parish of Loomberah, County of Parry, New South Wales, Australia. Currently, the Loomberah Limestone is regarded as a member of the Silver Gully Formation, and is likely to be of Dalejan age.

Diagnosis. Astreoid, thamnasterioid, or weakly pseudocerioid, ptenophyllinid corals with well developed septa in the dissepimentarium.

Description. Corallum massive, astreoid to thamnasterioid, rarely weakly pseudocerioid (term defined by Scrutton, 1968, p. 192). Septa strong, in two orders, although the two orders are indistinguishable in the dissepimentarium. Major septa typically, but not invariably, rhopaloid and rotated about the axis; minor septa restricted to dissepimentarium and outer region of the tabularium. Some species have a weak, discontinuous pseudotheca of septal or trabecular origin. Dissepiments numerous, forming flat to conspicuously everted dissepimentarial surfaces; innermost dissepiments highly inclined towards the axis, commonly quite vertical. Tabulae incomplete, closely spaced and abutting the dissepimentarium at a high angle, so that the tabularium and dissepimentarium are sharply differentiated. Outer tabularial surfaces commonly slope towards the axis; tabularial surfaces may be either concave, or convex about the axial septal whorl.

Remarks. The genus **Aphroidophyllum** and its type species, **A. howelli**, from the Eifelian Hume Formation, District of Mackenzie (holotype from Lac à Jacques), were established by Lenz (1961, p. 505, 506, Pl. 3, figs. 1, 2) for a coral that closely resembles **Taimyrophyllum**, but has exceptionally thin and peripherally withdrawn septa. It is accepted tentatively as a separate genus from **Taimyrophyllum**, pending further studies.

Some species of **Taimyrophyllum** have been referred to either **Phillipsastrea** d'Orbigny, 1849 (often misspelled **Phillipsastraea**), or **Billingsastraea** Grabau, 1917. **Phillipsastrea** has been revised by Scrutton (1968, p. 210-231). It differs from **Taimyrophyllum** in having fanned and commonly rhipidacanthate trabeculae, and fusiform septa that are generally neither rhopaloid nor axially rotated. It has, also, at least some horseshoe dissepiments and less closely spaced tabulae. **Billingsastraea**, which was discussed by Oliver (1976, p. 89), is an indefinable genus, possibly based on a Silurian species of **Arachnophyllum**.

Species composition. The following species belong to **Taimyrophyllum**: **Phillipsastraea grandis** Dun in Benson, 1918; **Taimyrophyllum speciosum** Chernyshev, 1941; **Phillipsastraea callosa** Hill, 1942a; **Eddastraea expansa** Hill, 1942b sensu Strusz, 1966; **Billingsastraea stirps** Crickmay, 1960; **Taimyrophyllum gracillum** Zheltonogova in Khalfin, 1961 (in the absence of a contrary statement, the trivial name is assumed to be an arbitrary combination of letters) (holotype subsequently figured as **T. sibiricum** Soshkina sp. n. by Soshkina and Dobrolyubova, 1962); **T. triadorum** Pedder, 1964; **T. vescibalteatum** Pedder, 1964; **T. colymense** Bul'vanker, 1965; **T. nolani** Merriam, 1974a; **Billingsastraea**(?) sp. T. Merriam, 1974b; **T. magnum** Tsyganko, 1977.

**Taimyrophyllum salairicum** and **T. altaicum**, listed by Ivaniya (1958, p. 197), and **T. crassiseptatum**, listed by Cherepnina (in Ivaniya et al., 1974, p. 8), appear to be nomina nuda.

**Taimyrophyllum carinatum** Bul'vanker, 1958, is probably a species of **Aphroidophyllum**. **Taimyrophyllum araxicum** Sayutina, 1965, is a Frasnian species of **Endophyllum** from the Transcaucasus. A Lochkovian coral from Kazakhstan, identified as **Taimyrophyllum**? sp. by Sytova and Ulitina (1966, p. 247, Pl. 48, fig. 3) and subsequently referred to **Aksarlinia concavotabulata** Kaplan by Kaplan (in Sytova and Kaplan, 1975), is considered to be a species of the cystiphyllid genus **Mazaphyllum**.

Taimyrophyllum nolani Merriam, 1974

**Phillipsastraea verneuili** Milne Edwards and Haime; Loewe, 1913, p. 12-14 (in part), Pl. 3, figs. 1a, b; Pl. 4, figs. 1a, b.

**Phillipsastraea scheii** Loewe, 1913, p. 12-14 (in part), Pl. 4, figs. 3a, b.

**Phillipsastraea gigas** Billings; Loewe, 1913, p. 14, Pl. 4, fig. 2.

**Taimyrophyllum nolani** Merriam, 1974a, p. 44, 45 (in part?), Pl. 9, figs. 1, 2?, 3-5, 6?; Pl. 10, figs. 1- 5?, 6, 7?

not **Phillipsastrea verneuili** Milne Edwards and Haime, 1851, p. 447, 448, Pl. 10, fig. 5 [=**Billingsastraea verneuili** = **Arachnophyllum(?) verneuili**].

not **Phillipsastraea gigas** (Owen); Billings, 1859, p. 128 [=**Asterobillingsa** sp.].

Remarks. Material comprising the type series of **T. nolani** came from three localities in Nevada, and probably includes more than one species or subspecies. The holotype (USNM 166451 - Merriam, 1974a, Pl. 9, figs. 3-5; Pl. 10, fig. 6) and one of the paratypes (USNM 166452 - Merriam, 1974a, Pl. 9, fig. 1) are from Merriam's locality M1349, near Reef Point on Lone Mountain. This locality is not listed in Merriam's published locality registers, nor is there record of any other species from it. Merriam cited the stratigraphic occurrence of **T. nolani** as unit 4 of the Nevada Formation, but his geological map of Lone Mountain (Merriam, 1974a, fig. 5; 1974b, fig. 3) places M1349 on undifferentiated dolomite, overlying unit 2 of the Nevada Formation. This suggests that the type horizon of **T. nolani** may be in the upper dolomitic part of the Coils Creek Member, McColley Canyon Formation, of Murphy and Gronberg's (1970) nomenclature. The upper part of the Coils Creek Member has yielded **Carinagypa aseptata** (Johnson and Kendall, 1976, p. 1114, text-fig. 4), **Elythina** sp. (Murphy and Gronberg, 1970, p. 130) and conodonts of the **serotinus** Zone (Klapper and Johnson, 1977, p. 43, fig. 5). If the holotype of **T. nolani** is from this general level, that is to say, from the lower part of Johnson's Nevada Devonian interval 14 (Johnson et al., 1980, p. 84, fig. 5), its age would be Dalejan.

Three paratypes (USNM 166453, 166476, 166477 - Merriam, 1974a, Pl. 9, fig. 2; Pl. 10, figs. 1-3) are from Merriam's locality M1344, and another (USNM 166475 - Merriam, 1974a, Pl. 9, fig. 6; Pl. 10, figs. 4, 5, 7) is from M1350. M1344 is only about 1.4 km west-northwest of M1349, the type locality of **T. nolani**, but is separated from it by a fault of considerable left lateral separation. The other locality, M1350, is about 17.5 km north of M1349, on Pyramid Hill in the Roberts Mountains. Paratypes from these localities appear to have derived from the **kockelianus** Zone of the Denay Limestone (Johnson and Oliver, 1977, p. 1466), which corresponds to Johnson's Nevada intervals 17 and 18, and should be Eifelian (Weddige, 1977, p. 341-344). Compared with the holotype and topotypic paratype, the possibly younger paratypes are smaller, have fewer and shorter septa, and a less everted dissepimentarium, all of which foster a suspicion that they may not be consubspecific, or even conspecific, with the holotype and topotypic paratype.

A coral, that is probably a subspecies of **Taimyrophyllum nolani**, occurs in the Bird Fiord Formation (probably Dalejan) on North Kent Island, Blubber Point (=Spakkassen locality of Loewe, 1913) and Goose Fiord; all in the general area of southwest Ellesmere Island. Loewe (1913, p. 12-14, Pl. 3, figs. 1a, b; Pl. 4, figs. 1a-3c) assigned representatives of this form in Schei's collection to three species of **Phillipsastrea.** One was identified as **P. gigas** Billings; the other two were considered to be identical with specimens from Michigan figured by Rominger (1877, Pl. 38, figs. 1, 2) as **Strombodes alpenensis** n. sp. and **Phillipsastrea verneuili** Milne Edwards and Haime (referred to as **Phillipsastraea verneuilli** Milne Edwards).

The caption to Rominger's Plate 38 stated that figure 1 is **Strombodes alpenensis** and that figure 2 is **Phillipsastrea verneuili.** Individual figures are not numbered on Rominger's plates. Loewe assumed that the upper left-hand figure on the plate is figure 1 and that the upper right-hand figure is figure 2. Since the upper right-hand figure appears to be of the new species, Loewe concluded that there is a mix-up of names in Rominger's work, and that the specimen apparently attributed to **Strombodes alpenensis** in the plate caption is really **Phillipsastrea verneuili.** Thus, he considered **Strombodes alpenensis** to be a junior synonym of **Phillipsastrea verneuili,** and proposed **P. scheii** as a nomen novum for the specimen illustrated in figure 1 (upper right-hand figure) of Rominger's Plate 38.

However, Loewe overlooked the explicit statement, given at the beginning of the plate section of Rominger's work, that, contrary to Loewe's assumption, in all plates, the upper right-hand figure is figure 1 and the upper left-hand figure is figure 2. Rominger stated on page 129 of his work that figure 2 of Plate 38 represents two silicified fragments of **P. verneuili.** This confirms that the upper left-hand figure is figure 2, because it is the only illustration on the plate that depicts two specimens.

In reality, then, there is no mix-up in Rominger's names and **Phillipsastrea scheii** is an unnecessary taxon. Nevertheless, since Loewe included Ellesmere Island specimens of **Taimyrophyllum nolani** in **P. scheii,** to avoid any future confusion, the original specimen of Rominger's Plate 38, figure 1 (upper right-hand figure) is chosen, here, as the lectotype of **P. scheii.** This specimen is registered number 8576 in the University of Michigan, Museum of Paleontology Collection, and is from the Givetian Four Mile Dam Formation. It is also the holotype of **Strombodes alpenensis** Rominger and is considered (Stumm, 1969; Oliver, 1978) to be a species of **Iowaphyllum.**

**Taimyrophyllum nolani beaumannense** subsp. n.

Plate 9.1a, figures 1-4

Type series. Holotype, GSC 68829, from GSC loc. C-12501. Paratypes, GSC 68830, 68831, also from GSC loc. C-12501.

Diagnosis. Subspecies of **Taimyrophyllum nolani** distinguished by its smaller size (adult corallite diameter 8 to 15 mm) and fewer septa (14x2 to 18x2).

Description. Corallum thamnasterioid, discoidal to subhemispherical, typically with height of less than 8 cm, and diameter of less than 16 cm. Diameter of adult corallites 8 to 15 mm. Calicular platforms prominently elevated around the perimeter of the calicular pit. Calices shallow, depressed in the centre.

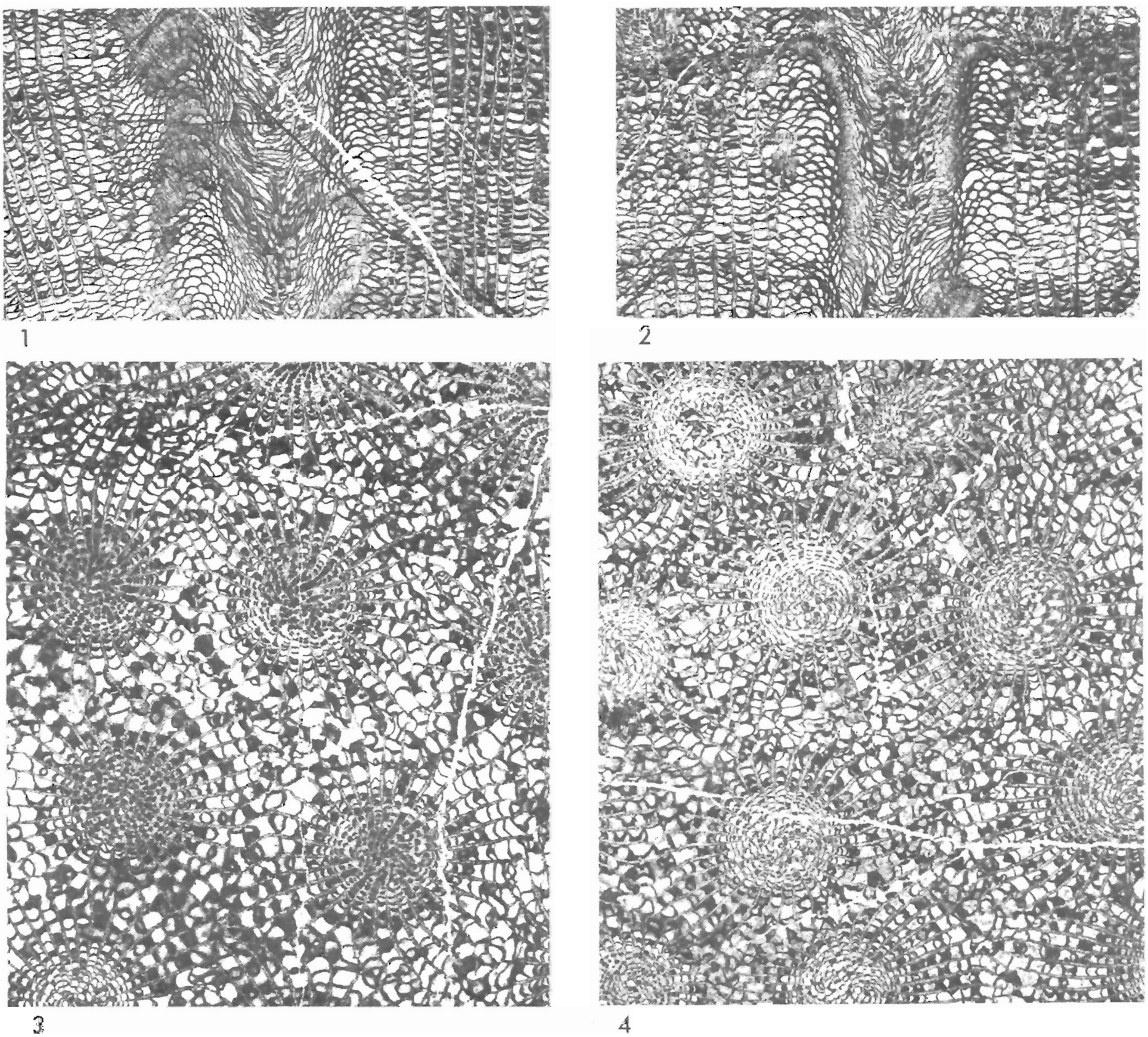


**PLATE 9.1a**

Figures 1-4. **Taimyrophyllum nolani beaumannense** subsp. n.

1, 3. Paratype, GSC 68830, longitudinal and transverse thin sections, X3; GSC loc. C-12501.

2, 4. Holotype, GSC 68829, longitudinal and transverse thin sections, X3; GSC loc. C-12501.

Septa radially and strongly developed in two orders, although major and minor septa are indistinguishable in the dissepimentarium. They commonly number 15x2 to 17x2 in adult corallites, the known range being 14x2 to 18x2. At the periphery of the corallite most touch, or are confluent with a septum of an adjacent corallite. Locally, deflected septal ends, a few of which are bifurcated, and isolated septal fragments form a weak and very discontinuous partition between corallites; but nowhere is this tendency sufficiently pronounced to form a pseudocerioid corallum. Septa tend to be crenulate near the periphery, and thickened in the inner region of the dissepimentarium; they bear fine to moderately prominent zigzag carinae throughout, including the tabularium, where they are flanged and rhopaloid. Minor septa typically extend into the tabularium for a distance equal to about one half of the radius of the tabularium. Periaxial rotation of the major septa produces a broad axial whorl. Trabeculae, which are fine, with a diameter in the order of 0.1 mm, are broadly fanned in the elevated region of the dissepimentarium. They are probably monacanthate, but preservation is inadequate to be certain of this.

Dissepiments are abundant; toward the periphery they tend to be relatively larger and less inflated than in the prominently elevated inner region of the dissepimentarium, where they are strongly inflated. The innermost dissepiments are highly inclined and, on the whole, small but elongate. Diameter of tabularium is mostly 3.0 to 4.0 mm, with a known maximum of 5.2 mm. Tabulae are incomplete, closely spaced; and abut the dissepimentarium at a high angle. Tabularial surfaces adaxially sloping, forming a deep axial depression.

Remarks. The holotype and paratypes are relatively large examples of the subspecies. The average size of the total known population is distinctly smaller than the holotype and topotypic paratype of **Taimyrophyllum nolani nolani**, which have corallite diameters of as much as 20 mm, and as many as 20x2 septa.

The subspecific name derives from Beaumann Fiord, off the coast of Ellesmere Island.

Family CYATHOPHYLLIDAE Dana, 1846
Subfamily STERICTOPHYLLINAE Pedder, 1965

Remarks. Hill (1981, p. 297) questionably synonymized Mictophyllidae Hill, 1940 and Sterictophyllidae Pedder, 1965 with the Cyathophyllidae. **Mictophyllum**, the type genus of the Mictophyllidae, is related closely to **Tabulophyllum**, so that in Hill's 1981 classification, the Mictophyllidae should be synonymous with the Endophyllidae Torley, 1933. The Sterictophyllidae is demoted here to subfamily rank, and used to accommodate cyathophyllid genera with thickened septa.

Genus **Cavanophyllum** Pedder, 1965

**Loomberaphyllum** Pedder, 1965, p. 213, 214.

**Cavanophyllum** Pedder, 1965, p. 215, 216.

Type species of **Cavanophyllum**. **Mictophyllum trochoides** Hill, 1940, p. 265, 266, Pl. 11, figs. 7-10. Lower Middle Devonian; Cavan, Murrumbidgee River, New South Wales, Australia. The type horizon is in the Cavan Bluff Limestone and, also, is in the late Pragian to early Zlichovian **dehiscens** Zone.

Type species of **Loomberaphyllum**. **Loomberaphyllum pustulosum** Pedder, 1965, p. 214, 215, Pl. 32, figs. 8, 9; Pl. 34, figs. 7, 9. Loomberah Limestone Member, Silver Gully Formation, probably Dalejan, possibly Eifelian; Portion 58, Parish of Loomberah, County of Parry, New South Wales, Australia.

Diagnosis. Solitary sterictophyllinid corals, lacking a peripheral septal stereozone.

Description. Corallum solitary, trochoid to subcylindrical. Calicular platform narrow. Wall of calice sloping. Septa numerous, long, in two orders, slightly pinnate about a shortened cardinal septum. Other protosepta generally not identifiable in mature stage. In the inner and middle regions of the dissepimentarium, septa are smooth to faintly carinate, and to a point, increase in thickness towards the periphery; where there is considerable dilation, it spreads to dissepimentarial surfaces. In the peripheral region of the dissepimentarium, septa attenuate to some degree, and become markedly more carinate. In this outermost region of the corallum, septa may degenerate into more than one lamella, and become retiform. Trabeculae are long, commonly coarse, monacanths. They may be wavy or flexed, and are mostly contiguous, except at the periphery, where they tend to separate, making the septa carinate in this region. Dissepiments abundant, mostly relatively small, but well inflated; some of the innermost dissepiments grade to tabellae. Tabulae incomplete, commonly forming axially and periaxially elevated tabularial floors.

Remarks. Jell and Hill (1969, p. 8) placed **Loomberaphyllum** in **Peripaedium** Ehrenberg, 1834 and recognized **Peripaedium** as a subgenus of **Cyathophyllum** Goldfuss, 1826. Subsequently Hill (1981, p. 304) restored **Peripaedium** to full generic rank and only questionably synonymised **Loomberaphyllum** with it. **Cyathophyllum turbinatum** Goldfuss, which is the type species of **Peripaedium**, has been revised by Birenheide (1963, p. 390-393, Pl. 48, fig. 13; Pl. 58, figs. 49-52). It has very thin septa with abundant, delicate carinae throughout the dissepimentarium, and is not congeneric with **Loomberaphyllum.**

Jell and Hill (1969, p. 9) and Hill (1981, p. 304, 305) regarded **Cavanophyllum** as a synonym of **Sterictophyllum** Pedder, 1965. Undeniably the two genera are closely related, but **Sterictophyllum** has a peripheral septal stereozone.

When **Loomberaphyllum** and **Cavanophyllum** were first studied by the writer, they did not appear to be closely related. Now, more material suggests that they are congeneric. **Loomberaphyllum** has page priority, but Recommendation 24A of the International Code of Zoological Nomenclature recommends that the first reviser "should select the name that will best ensure stability and universality of nomenclature". In this case, **Cavanophyllum** is the more appropriate name, because it has been used in primary literature in recent years, whereas **Loomberaphyllum** has not.

Species composition. The following species pertain to **Cavanophyllum: Mictophyllum trochoides** Hill, 1940; **Loomberaphyllum pustulosum** Pedder, 1965; **L. impensum** Pedder, 1965; **Cavanophyllum** sp. n. Pedder and Klapper, 1977, **C. uyenoi** sp. n.

**Cyathophyllum cailliaudi** Barrois, 1889, may also belong to the genus, but is inadequately described and figured, and cannot be assigned to any genus with certainty at present.

### **Cavanophyllum uyenoi** sp. n.

Plate 9.1b, figures 5-10

**Cavanophyllum** sp.; Pedder in Jackson et al., 1978, p. 152, Pl. 41, figs. 2, 4.

Type series. Holotype, GSC 68832, from GSC loc. C-12424. Paratypes, GSC 68833, also from GSC loc. C-12424, and GSC 46121, from GSC loc. C-12498.

Diagnosis. Small species of **Cavanophyllum** (maximum known mean diameter 31 mm) with 33x2 to 35x2 septa at maturity. Calice wall and dissepimentarial surfaces gently sloping towards axis. Septa moderately thickened and weakly carinate in the inner dissepimentarium; near the periphery, they become much more carinate, but do not degenerate into more than one lamella, nor are they retiform. Dissepiments small to medium sized.

Description. Corallum solitary, trochoid to ceratoid; some specimens show rejuvenescences, but none is known to have produced offsets. Maximum known length about 60 mm; greatest mean diameter 31 mm. Calice shallow, about 12 mm deep in adult stages. Calicular wall slopes towards the axis at a low angle, and is not clearly differentiated from the narrow calicular platform. Exteriors are abraded in the type series. Where preserved, the wall is 0.2 to 0.4 mm thick. It carries narrow, shallow septal furrows, broad, more or less flat interseptal ridges, and fine growth rings.

Arrangement of the septa is radial in the counter quadrants, and just sufficiently pinnate in the cardinal quadrants to produce a narrow fossula. At a diameter of 12 mm, in one of the paratypes, the septal count is 31x2. At full diameter, the septal count increases to as much as 35x2. Most of the major septa extend to, or almost to the axis. At certain levels in one of the paratypes (GSC 46121) they are rotated to form a weak axial whorl. Adaxial ends of the major septa may be slightly expanded. Minor septa just penetrate the tabularium. In the inner and central parts of the dissepimentarium, both orders of septa are weakly carinate and moderately dilated. At certain distances from the axis, the dilation extends on to dissepimentarial surfaces. In the outer two or three millimetres of the dissepimentarium, septa generally attenuate somewhat and become much more carinate. Trabeculae monacanthate, coarse, with diameters of about 0.2 to 0.3 mm. At the periphery they are mostly separate from each other and make angles of 60° to 70° with the horizontal; adaxially they become contiguous and their angle of inclination decreases; they are also flexed in the charactophylloid manner (term defined by Pedder, 1972, p. 698).

Dissepiments well inflated, variable in size, although none is large, abundant, generally forming 10 to 15 rows in the distal region of the corallum. Dissepimentarial surfaces gently inclined inwards near the periphery, becoming more steeply inclined towards the axis. Innermost dissepiments may grade to peripheral tabellae. Tabulae mostly incomplete. Tabularial surfaces tend to be elevated periaxially and more or less flat in the axial region; a few are slightly depressed in the axial region.

Remarks. **Cavanophyllum uyenoi** is closer to an unnamed species, figured from the Cranswick Formation of Yukon Territory (Pedder and Klapper, 1977, Figures 43.8, 9, 11, 13; Pedder in Jackson et al., 1978, Pl. 38, figs. 1, 3, 6), than it is to any of the named species assigned to the genus. The unnamed species from the Cranswick Formation, which is slightly younger (**inversus** Zone of the Zlichovian Stage), is larger (greatest diameter more than 45 mm), has many more septa (as many as 51x2), and has a locally everted and wider dissepimentarium that includes some unusually large dissepiments for the genus.

The trivial name given to the new species is a patronym for T.T. Uyeno, whose conodont work has dated the Blue Fiord Formation in the vicinity of the type section.

Family DISPHYLLIDAE Hill, 1939
Subfamily PARADISPHYLLINAE Jell, 1969

Genus **Radiastraea** Stumm, 1937

**Radiastraea** Stumm, 1937, p. 439.

Type species. **Radiastraea arachne** Stumm, 1937, p. 439, 440, Pl. 53, fig. 13; Pl. 55, figs. 8a, b. Basal 152 m of the Nevada Limestone; Lone Mountain, 28 km northwest of Eureka, Nevada, U.S.A. In current terminology, the type stratum is in the Zlichovian **Eurekaspirifer pinyonensis** Zone of the Bartine Member, McColley Canyon Formation (Murphy and Gronberg, 1970; Oliver and Johnson, 1977, p. 110).

Diagnosis. Predominantly thamnasterioid to astreoid, rarely aphroid or pseudocerioid, paradisphyllinid corals.

Description. Corallum massive, usually astreoid or thamnasterioid, less commonly just aphroid or pseudocerioid (term defined by Scrutton, 1968, p. 192). Major septa of variable length; in species having long septa, the major septa may extend to the axial region and form a whorl; in species with short major septa, they may be reduced to isolated trabeculae in the periaxial region. Minor septa generally only just penetrate the tabularium. The two orders of septa are indistinguishable normally in the dissepimentarium. Septa may be smooth, but more commonly are carinate; zigzag carinae predominate over crossbar carinae. Trabeculae monacanthate, essentially vertical in the outer dissepimentarium, and inwardly radiating in the inner dissepimentarium. Dissepiments typically horizontal at and near the periphery, becoming steeply inclined and smaller adaxially; in some species, dissepimentarial surfaces are elevated immediately exterior of the tabularium. Tabulae variable in shape, mostly incomplete. Tabularial surfaces most commonly flat to gently concave peripherally, outwardly inclined periaxially, and depressed, flat, or elevated axially.

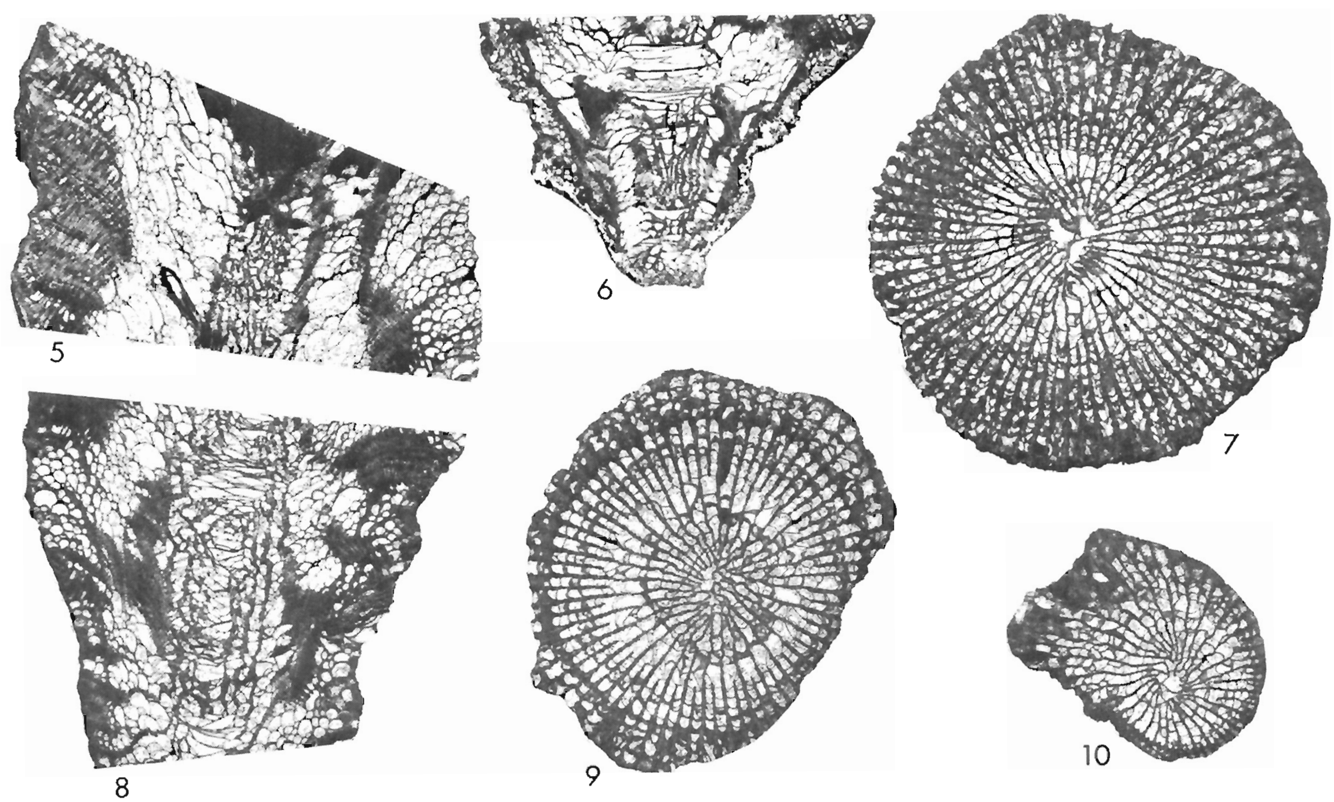


**PLATE 9.1b**

Figures 5-10. **Cavanophyllum uyenoi** sp. n.

5, 9. Paratype, GSC 68833, longitudinal and transverse thin sections, X2; GSC loc. C-12424.

6. Paratype, GSC 46121, longitudinal thin section, X2; GSC loc. C-12498.

7, 8, 10. Holotype, GSC 68832, transverse and longitudinal thin sections, X2; GSC loc. C-12424.

Remarks. This genus was discussed by Pedder and McLean (1976, p. 135-137) who reported Pridolian and probable Pridolian occurrences on Cornwallis and Devon islands.

**Radiastraea** is not easily separated from species of **Phillipsastrea** that have few horseshoe dissepiments. However, such species, which are abundant in some Australian Lower Devonian and Eifelian beds, have a more everted inner dissepimentarium, and a correspondingly narrower and more symmetrical zone of trabecular divergence.

As pointed out previously (Pedder and McLean, 1976, p. 135), **Radiastraea** likely evolved from Silurian species of **Arachnophyllum** by acquisition of lamellar septa. It is also likely that it gave rise to at least some species of **Phillipsastrea** by modification of the inner dissepimentarium.

Species composition. The following species are assigned to the genus: **Smithia verrilli** Meek, 1867; **Phillipsastraea affinis** Billings, 1874; **Billingsastraea billingsi** var. **nevadensis** Stumm, 1937 (raised to species rank by Merriam, 1940, on caption to Plate 12); **Radiastraea arachne** Stumm, 1937; **Billingsastraea trichomisca** Crickmay, 1960; **B. tapetiformis** Crickmay, 1960; **Radiastraea** spp. n. Pedder and McLean, 1976; **Billingsastraea zinzilbania** Erina, 1978; **Radiastraea norrisi** Pedder, 1980; **R. pulchra** sp. n.

### **Radiastraea pulchra** sp. n.

Plate 9.1c, figures 11-16

**Radiastraea** sp. n.; Pedder in Jackson et al., 1978, p. 154, Pl. 42, figs. 5, 7.

Type series. Holotype, GSC 68834, from GSC loc. C-12501. Paratypes, GSC 68835, also from GSC loc. C-12501, and GSC 46127, 68836, 68837, all from GSC loc. C-12498.

Diagnosis. Small species of **Radiastraea** with corallites of 5.0 to 7.5 mm diameter. Septa poorly differentiated, commonly heavily dilated, numbering 15x2 to 18x2 in adult corallites. Major septa mostly withdrawn from the tabularium, which is occupied only by broad tabulae and short, isolated monacanths. Monacanths tufted locally in the dissepimentarium.

Description. Corallum thamnasterioid, discoidal, small, height and diameter not known to exceed 4 cm and 10 cm, respectively. Mean diameter of adult corallites 5.0 to 7.5 mm. Calicular platform narrow, flat, or slightly elevated around the calicular pit. Calicular pit 2.5 to 3.0 mm deep, and 2.5 to 3.5 mm in diameter.

Septa radially arranged around the tabularium in two, poorly differentiated orders, commonly numbering 16x2 or 17x2 (full range 15x2 to 18x2) per adult corallite. Peripherally, they touch, or only just fail to touch, a septum of an adjacent corallite; some are confluent with a septum of an adjacent corallite. Adaxially, minor septa terminate at the inner margin of the dissepimentarium; major septa terminate just inside the tabularium, leaving most of it free of septa, apart from short isolated monacanths. Septa of both orders are normally strongly carinate with some yardarm, as well as zigzag carinae. In many specimens, septa and carinae are strongly dilated in the inner and middle regions of the dissepimentarium. Trabeculae monacanthate, locally tufted, with diameter of as much as 0.3 mm. They are vertically directed in the outer region of the dissepimentarium and fanned close to the tabularium.

Dissepiments abundant, predominantly small, especially those situated close to the tabularium, but well inflated. Dissepimentarial floors more or less flat in the outer region of the corallite, becoming adaxially inclined around the tabularium. In some specimens, the dissepimentarial floors are elevated in a ring just outside the tabularium. Diameter of the tabularium 2.5 to 3.5 mm. Tabulae broad, many being quite complete. Tabularial surfaces varying from gently concave, through essentially flat, to gently convex.

Remarks. Of the previously named species of **Radiastraea**, only **R. tapetiformis** (Crickmay) is as small as **R. pulchra**. Despite the similarity in size, the species are not likely to be confused. **R. tapetiformis** has fewer septa (normally 13x2 or 14x2 and only rarely as many as 15x2) and its septa extend much further into the tabularium. They are also less carinate and finer, because the monacanths are not tufted.

The trivial name is the Latin adjective, **pulcher, pulchra, pulchrum**, meaning beautiful, pretty, fine, etc.

### Locality Register

GSC locality C-12424. Blue Fiord Formation, 180.2-181.5 m above the base of the formation exposed in the section, 881.1-882.4 m below top of the formation; **Polygnathus** aff. **perbonus** conodont unit, Zlichovian. Sor Fiord section, southwest Ellesmere Island, District of Franklin; base of section 77°17'12"N latitude, 85°07'00"W longitude; top of section 77°15'48"N latitude, 85°03'30"W longitude. Collected by A.E.H. Pedder, 1971.

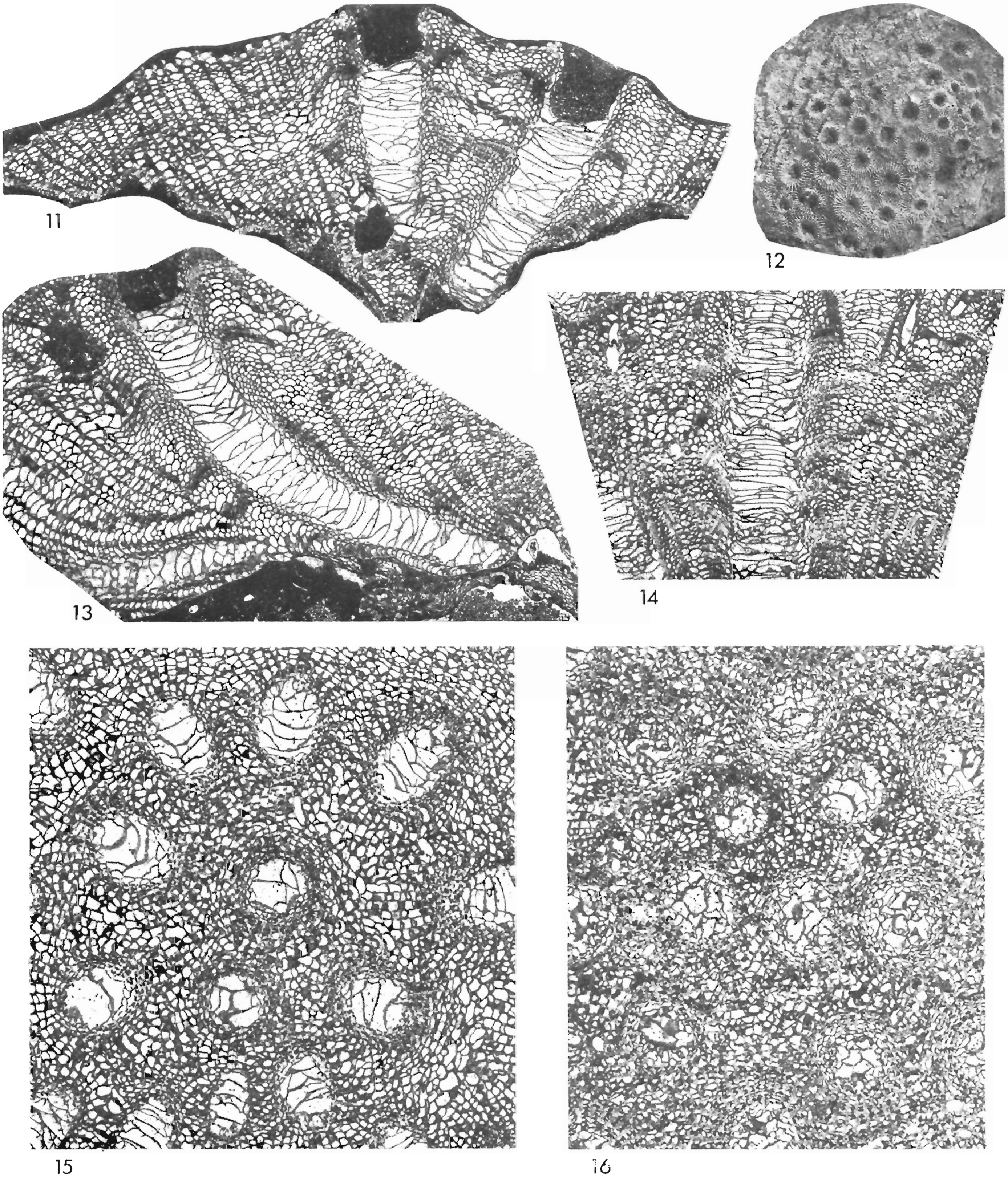


**PLATE 9.1c**

Figures 11-16. **Radiastraea pulchra** sp.n.

11. Paratype, GSC 68836, longitudinal thin section, X4; GSC loc. C-12498.

12. Paratype, GSC 68837, exterior view, X1; GSC loc. C-12498.

13, 15. Holotype, GSC 68834, longitudinal and transverse thin sections, X4; GSC loc. C-12501.

14, 16. Paratype, GSC 68835, longitudinal and transverse thin sections, X4; GSC loc. C-12501.

**Ferestromatopora** sp. (identified by C.W. Stearn), **Alveolites** sp., **Embolophyllum** sp., **Cavanophyllum uyenoi** Pedder.

GSC locality C-12498. Talus and in-place collection from isolated outcrop of Blue Fiord Formation; probably **dehiscens** Zone, possibly **Polygnathus** aff. **perbonus** conodont unit, certainly Zlichovian. About 16 km west of the head of Sor Fiord, Ellesmere Island, District of Franklin; 77°17'30"N latitude, 85°05'40"W longitude. Collected by A.E.H. Pedder, 1971.

**Receptaculites** sp., **Favosites** sp., **Aulopora** sp., **Aulocystis** sp., **Mesophyllum ellesmerense** Pedder and McLean, **M. kirki** (Stumm), **Dohmophyllum** sp., **Cavanophyllum uyenoi** Pedder, **Radiastraea pulchra** Pedder, **Spongonaria loewei** (Stumm), **S. richardsonensis** Crickmay, **Fistulipora** sp., **Petrocrania** sp., **Cortezorthis** sp. cf. **C. maclareni** Johnson and Talent, **Schizophoria** sp., **Leptaena** sp. (broad sense), undet, stropheodontid brachiopods, **Eoschuchertella** sp., **Parachonetes** sp. cf. **P. macrostriatus** (Walcott), **Carinagypa** sp., **Athyrhynchus loriei** Jones, **Oligoptycherhynchus** sp. aff. **O. ellipticus** (Schnur), **Carinatrypa** sp., **Atrypa** sp. cf. **A. nevadana** Merriam, **Nucleospirifer** sp., **Cyrtina** sp., **Howellella** sp., **Fimbrispirifer**(?) sp. cf. **F.**(?) **pseudoscheii** Brice.

GSC locality C-12501. Blue Fiord Formation, approximately 27-28 m above base; **dehiscens** Zone, early Zlichovian part. First gorge northeast of Sor Fiord section, southwest Ellesmere Island, District of Franklin; 77°17'40"N latitude, 85°07'00"W longitude. Collected by A.E.H. Pedder, 1971.

**Thecostegites** sp., **Taimyrophyllum nolani beaumannense** Pedder, **Radiastraea pulchra** Pedder.

## References


Barrois, C.
1889: Faune du calcaire d'Erbray (Loire Inférieure); Société Géologique du Nord, Mémoires, tome 3, p. 1-348.

Benson, W.N.
1918: The geology and petrology of the Great Serpentine Belt of New South Wales. Part vii. The geology of the Loomberah district and a portion of the Goonoo Goonoo Estate. With two palaeontological appendices by F. Chapman, F.R.M.S., A.L.S., Palaeontologist to the National Museum, Melbourne; Linnean Society of New South Wales, Proceedings, v. 42, pt. 2, p. 320-360, 363-394.

Billings, E.
1859: On the fossil corals of the Devonian rocks of Canada West; The Canadian Journal of Industry, Science, and Art, new ser., no. 20, p. 97-140.

1874: On some of the fossils of the Gaspé series of rocks; Geological Survey of Canada, Paleozoic fossils, v. 2, pt. 1, p. 1-64.

Birenheide, R.
1963: **Cyathophyllum**- und **Dohmophyllum**-Arten (Rugosa) aus dem Mitteldevon der Eifel; Senckenbergiana lethaea, Band 44, p. 363-458.

Bul'vanker, E.Z.
1958: Devonskie chetyrekhluchevye korally okrani Kuznetskogo basseyna; Vsesoyuznyy Nauchno-Issledovatel'skiy Geologicheskiy Institut (VSEGEI), Leningrad, text 212 p. and atlas.

1965: Pervye dannye o devonskikh rugozakh severo-vostoka SSSR: in Rugozy paleozoya SSSR, eds. B.S. Sokolov and A.B. Ivanovskiy; Akademiya Nauk SSSR, Sibirskoe Otdelenie, Institut Geologii i Geofiziki, Izadatel'stvo Nauka, p. 54-58.

Cherkesova, S.V., Patrunov, D.K., Smirnova, M.A., Kuz'min, A.M., Kravtsov, A.G., and Nekhorosheva, L.V.
1968: Tareyskiy nizhnedevonskiy opornyy razrez (Tsentral'nyy Taymyr); Nauchno-Issledovatel'skiy Institut Geologii Arktiki, Uchenye Zapiski, Paleontologiya i Biostratigrafiya, vyp. 22, p. 5-35.

Chernyshev, B.B.
1941: Siluriyskie i nizhnedevonskie korally basseyna reki Tarei (yugo-zapadnyy Taymyr); Arkticheskogo Nauchno-Issledovatel'skogo Instituta, Trudy, tom 158, p. 9-64.

Crickmay, C.H.
1960: The older Devonian faunas of the Northwest Territories; Evelyn de Mille Books, Calgary, 21 p.

Erina, M.V.
1978: Rugozy; in Atlas paleontologicheskikh tablits. Prilozhenie k Putevoditelyu ekskursiy; Polevaya sessiya mezhdunarodnoy podkomissii po stratigrafii devona Samarkand, SSSR, 1978, ed. B.S. Sokolov and V.G. Gar'kovets; Tashkent, p. 15-20.

Hill, D.
1940: The Lower Middle Devonian rugose corals of the Murrumbidgee and Goodradigbee Rivers, N.S.W.; Royal Society of New South Wales, Journal and Proceedings, v. 74, p. 247-276.

1942a: The Devonian rugose corals of the Tamworth district, N.S.W.; Royal Society of New South Wales, Journal and Proceedings, v. 76, p. 142-164.

1942b: Middle Palaeozoic rugose corals from the Wellington district, N.S.W.; Royal Society of New South Wales, Journal and Proceedings, v. 76, p. 182-189.

1981: Treatise on invertebrate paleontology. Part F. Coelenterata. Supple-ment 1. Rugosa and Tabulata, ed. Curt Teichert; Geological Society of America and University of Kansas Press, Boulder and Lawrence, v. 1, p. i-xl, 1-378, v. 2, p. i, ii, 379-762.

Ivaniya, V.A.
1958: Biostratigraficheskoe raschlenenie devona Kuzbassa po korallam Rugosa; Uchenye Zapiski Tomskogo Gosudarstvennogo Universiteta imeni. V.V. Kuybysheva, no. 32, p. 194-204.

Ivaniya, V.A., Cherepnina, S.K., and Yaroshinskaya, A.M.
1974: Korally rugozy i mshanki iz nizhnego i srednego devona Zapadnoy Sibiri; in Materialy po stratigrafii i paleontologii Zapadnoy Sibiri, ed. V.A. Ivaniya; Tomskogo Ordena Trudovogo Krasnogo Znameni Gosudarstvennogo Universiteta imeni V.V. Kuybysheva, Trudy, tom 227, p. 3-15.

Jackson, D.E., Lenz, A.C., and Pedder, A.E.H.
1978: Late Silurian and Early Devonian graptolite, brachiopod and coral faunas from northwestern and arctic Canada; The Geological Association of Canada, Special Paper 17.

Jell, J.S. and Hill, D.
1969: Devonian corals from the Ukalunda district, north Queensland; Geological Survey of Queensland, Publication 340, Palaeontological Papers, no. 16.

Johnson, J.G. and Kendall, G.W.
1976: Late Early Devonian brachiopods and biofacies from central Nevada; Journal of Paleontology, v. 50, p. 1113-1128.

Johnson, J.G. and Oliver, W.A., Jr.
1977: Silurian and Devonian coral zones in the Great Basin, Nevada and California; The Geological Society of America, Bulletin, v. 88, p. 1462-1468.

Johnson, J.G., Klapper, G., and Trojan, W.R.
1980: Brachiopod and conodont successions in the Devonian of the northern Antelope Range, central Nevada; Geologica et Palaeontologica 14, p. 77-116.

Khalfin, L.L.
1961: Biostratigrafiya paleozoya Sayano-Altayskoy gornoy oblasti. Tom II. Sredniy paleozoy; Sibirskogo Nauchno-Issledovatel'skogo Instituta Geologii Geofiziki i Mineral'nogo Syr'ya (SNIIGGIMS), Trudy, vyp. 20 (imprint 1960).

Klapper, G., with contributions by Johnson, D.B.
1977: Lower and Middle Devonian conodont sequence in central Nevada; in Western North America: Devonian, eds. M.A. Murphy, W.B.N. Berry and C.A. Sandberg; University of California, Riverside Campus Museum Contribution 4, p. 33-54.

Kravtsov, A.G.
1963: Rannedevonskie chetyrekluchevye korally s reki Tarei (Tsentral'nyy Taymyr): Nauchno-Issledovatel'skiy Institut Geologii Arktiki, Uchenye Zapiski, Paleontologiya i Biostratigrafiya, vyp. 3, p. 5-49.

Lenz, A.C.
1961: Devonian rugose corals of the lower Mackenzie Valley, Northwest Territories; in Geology of the Arctic, Proceedings of the First International Symposium on Arctic Geology, ed. G.O. Raasch; University of Toronto Press, v. 1, p. 500-514.

Loewe, S.
1913: Die devonischen Korallen von Ellesmereland; in Report of the Second Norwegian Arctic Expedition in the "Fram" 1898-1902, Videnskabs-Selskabet i Kristiania, v. 4, no. 30, p. 1-23.

Meek, F.B.
1867: Remarks on the geology of the valley of Mackenzie River, with figures and descriptions of fossils from that region, in the Museum of the Smithsonian Institution, chiefly collected by the late Robert Kennicott, Esq.; The Chicago Academy of Sciences, Transactions, v. 1, p. 61-114.

Merriam, C.W.
1940: Devonian stratigraphy and paleontology of the Roberts Mountains region, Nevada; Geological Society of America, Special Paper 25.

1974a: Middle Devonian rugose corals of the central Great Basin; United States Geological Survey, Professional Paper 799 (imprint 1973).

1974b: Lower and Lower Middle Devonian rugose corals of the central Great Basin; United States Geological Survey, Professional Paper 805.

Milne Edwards, H. and Haime, J.
1851: Monographie des polypiers fossiles des terrains palaeozoiques; Archives du Muséum d'Histoire Naturelle, tome 5, v+502 p.

Murphy, M.A. and Gronberg, E.C.
1970: Stratigraphy and correlation of the Lower Nevada Group (Devonian) north and west of Eureka, Nevada; The Geological Society of America, Bulletin, v. 81, p. 127-136.

Oliver, W.A., Jr.
1976: Noncystimorph colonial rugose corals of the Onesquethaw and Lower Cazenovia Stages (Lower and Middle Devonian) in New York and adjacent areas; United States Geological Survey, Professional Paper 869.

1978: **Iowaphyllum** (rugose coral) from the Upper Devonian of Arizona; United States Geological Survey, Journal of Research, v. 6, p. 797-805.

Oliver, W.A., Jr. and Johnson, J.G.
1977: Notes on Upper Silurian and Devonian coral zones in the Great Basin; in Western North America: Devonian, ed. M.A. Murphy, W.B.N. Berry and C.A. Sandberg; University of California, Riverside Campus Museum Contribution 4, p. 107-111.

Oliver, W.A., Jr. and Pedder, A.E.H.
1979: Rugose corals in Devonian stratigraphical correlation; in The Devonian System, ed. M.R. House, C.T. Scrutton and M.G. Bassett; Special Papers in Palaeontology 23, p. 233-248.

Pedder, A.E.H.
1964: Correlation of the Canadian Middle Devonian Hume and Nahanni Formations by tetracorals; Palaeontology, v. 7, p. 430-451.

1965: A revision of the Australian Devonian corals previously referred to **Mictophyllum**; Royal Society of Victoria, Proceedings, v. 78, p. 201-220.

1972: Species of the tetracoral genus **Temnophyllum** from Givetian/Frasnian boundary beds of the District of Mackenzie, Canada; Journal of Paleontology, v. 46, p. 696-710.

1980: Devonian corals of late Eifelian age from the Ogilvie Formation of Yukon Territory; Canadian Journal of Earth Sciences, v. 17, p. 594-616.

Pedder, A.E.H. and Klapper, G.
1977: Fauna and correlation of the type section of the Cranswick Formation (Devonian), Mackenzie Mountains, Yukon Territory; in Report of Activities, Part B, Geological Survey of Canada, Paper 77-1B, p. 227-234.

Pedder, A.E.H. and McLean, R.A.
1976: New records and range extensions of seven rugose coral genera in Silurian strata of northwestern and arctic Canada; in Report of Activities, Part C, Geological Survey of Canada, Paper 76-1C, p. 131-141.

Rominger, C.
1877: Lower Peninsula, 1873-1876, accompanied by a geological map. Part II. Palaeontology. Fossil corals; Geological Survey of Michigan, v. 3, pt. 2, 161 p.

Sayutina, T.A.
1965: Kolonialnye devonskie rugozy Zakavkaz'ya; Paleontologicheskiy Zhurnal, 1965, 4, p. 4-10.

Schönlaub, H.P.
1979: Austria. Activities 1978 - Project report of Austrian Working Team; Ludlow Research Group, Bulletin 26, p. 5, 6.

Scrutton, C.T.
1968: Colonial Phillipsastraeidae from the Devonian of south-east Devon, England; The British Museum (Natural History), Bulletin, Geology, v. 15, p. 181-281.

Soshkina, E.D. and Dobrolyubova, T.A.
1962: Otryad Evenkiellida; in Osnovy paleontologii, tom 2. Gubki, arkheotsiaty, kishechnopolostnye, chervi, ed. B.S. Sokolov; Izdatel'stvo Akademii Nauk SSSR, Moskva, p. 333-339.

Strusz, D.L.
1966: Spongophyllidae from the Devonian Garra Formation, New South Wales; Palaeontology, v. 9, p. 544-598.

Stumm, E.C.
1937: The Lower Middle Devonian tetracorals of the Nevada Limestone; Journal of Paleontology, v. 11, p. 423-443.

1969: Devonian bioherms of the Michigan Basin; The University of Michigan. Contributions from the Museum of Paleontology, v. 22, p. 241-247.

Sytova, V.A. and Kaplan, A.A.
1975: Tetrakorally; in Kharakteristika fauny pogranichnykh sloev silura i devona Tsentral'nogo Kazakhstana, ed. V.V. Menner; Materialy po geologii Tsentral'nogo Kazakhstana, tom 12, p. 61-76.

Sytova, V.A. and Ulitina, L.M.
1966: Rugozy isen'skoy i biotarskoy svit; in Stratigrafiya i fauna siluriyskikh i nizhnedevonskikh otlozheniy Nurinskogo sinklinoriya, ed. G.A. Khokhaeva; Materialy po geologii Tsentral'nogo Kazakhstana, tom 6, p. 198-253.

Tsyganko, V.S.
1977: Novyy srednedevonskiy vid roda **Taimyrophyllum** Pay-Khoya; in Novye vidy drevnikh rasteniy i bespozvonochnykh SSSR, vyp. 4, ed. G.A. Stukalina; Akademiya Nauk SSSR. Paleontologicheskiy Institut, Moskva, p. 34, 35.

Uyeno, T.T. and Klapper, G.
1980: Summary of conodont biostratigraphy of the Blue Fiord and Bird Fiord formations (Lower-Middle Devonian) at the type and adjacent areas, southwestern Ellesmere Island, Canadian Arctic Archipelago; in Current Research, Part C, Geological Survey of Canada, Paper 80-1C, p. 81-93.

Weddige, K.
1977: Die Conodonten der Eifel-Stufe im Typusgebeit und in benachbarten Faziesgebieten; Senckenbergiana lethaea, Band 58, p. 271-419.

10. PROBABLE DALEJAN (EARLY DEVONIAN) CYSTIPHYLLID CORALS FROM BIRD FIORD FORMATION OF ELLESMERE ISLAND

Project 680093

A.E.H. Pedder
Institute of Sedimentary and Petroleum Geology, Calgary

*Pedder, A.E.H., Probable Dalejan (Early Devonian) cystiphyllid corals from Bird Fiord Formation of Ellesmere Island; in Current Research, Part C, Geological Survey of Canada, Paper 82-1C, p. 83-90, 1982.*

**Abstract**

*Two new species, **Lekanophyllum retiforme** and **L. rugulosum**, are described from Blubber Point, southwest Ellesmere Island. **L. retiforme** is the commonest coral in the Bird Fiord Formation of this area, but, because of its unusual morphology, invariably has been misidentified in previous literature.*

## Introduction

Cystiphyllid corals occur abundantly in many Lower and Middle Devonian sequences. Several important studies of the family have appeared in recent years, especially in the Soviet Union, Germany, and Canada. However, reduction of septal apparatus in the Cystiphyllidae makes taxonomic study of them both difficult and contentious, so that opinions regarding their systematic classification differ widely. For example, Birenheide (1964, 1978) referred all cystiphyllid species from large coral faunas of Germany to two genera and two subgenera, whereas the classification proposed by Hill (1981), would place the same species in seven genera and twelve subgenera.

In recent Canadian works (McLean, 1976; Jackson et al., 1978; Pedder and McLean, in press), a more or less central position has been taken concerning Devonian cystiphyllid taxonomy. The same position is maintained here. If Birenheide's taxonomic scheme were followed, both new species would be assigned to **Mesophyllum.** In contrast, one, possibly two new genera would be required for them, if the degree of generic fragmentation shown in Hill's systematics were upheld.

I am grateful to Brian Jones and Quentin Goodbody, University of Alberta, for the opportunity to study material that provided type specimens for the new species, and to David Worsley, University Palaeontological Museum, Oslo, for the opportunity to study Loewe's (1913) specimens of **Lekanophyllum retiforme.**

## Biostratigraphy

Brian Jones and Quentin Goodbody are studying the stratigraphy and age of the Bird Fiord Formation in the extreme southwest part of Ellesmere Island, south of Schei Syncline. For now, it is sufficient to note that the new species of **Lekanophyllum** are associated with a coral and brachiopod fauna, that at Goose Fiord, is accompanied by conodonts of the Dalejan **serotinus** Zone.

## Systematic Paleontology

Type specimens and locality numbers referred to in this paper are registered in the Paleontological Collections, Department of Geology, The University of Alberta, Edmonton, Canada, T6G 2E3. UA and PCC are abbreviations for The University of Alberta and Paleontological Collections Catalogue.

The morphological terminology used to describe the new corals is identical to that used by Pedder and McLean (in press). It differs from Hill's (1981, p. F6-F36) only in the term presepiment, which denotes peripheral vesicles that separate septal crests from the outer wall. A presepiment is equivalent to a lonsdaleoid dissepiment in Hill's terminology, and to Praesepiment and Wandblasse of German literature.

Family CYSTIPHYLLIDAE Milne Edwards and Haime, 1850

Subfamily DIGONOPHYLLINAE Wedekind, 1923

Genus **Lekanophyllum** Wedekind, 1924

**Lekanophyllum** Wedekind, 1924, p. 29-34 [in part, includes a species of **Mesophyllum**].

**Lekanophyllum** Wedekind; Pedder and McLean, in press [includes synonymy].

Type species. **Lekanophyllum punctatum** Wedekind, 1924, p. 30, 34, figs. 36-38. Junkerberg Formation, Eifelian; Auberg, Gerolsteiner Mulde, Germany (Birenheide, 1968, p. 23).

Diagnosis. See Pedder and McLean, in press.

Included species. The following seventeen species should be added to the forty-five forms listed by McLean (1976, p. 19):

**Atelophyllum tongmuense** Zhang in Jia et al., 1977. Dongganglíng Formation, Givetian, Guangxi, China.

**Zonodigonophyllum guanziyaoense** Kong in Kong and Huang, 1978; **Atelophyllum planotabulatum** Kong in Kong and Huang, 1978; **A. puanense** Kong in Kong and Huang, 1978; **A tenue** Kong in Kong and Huang, 1978. Guanziyao Formation, Eifelian, Guizhou, China.

**Atelophyllum baculum** Kong in Kong and Huang, 1978; **A. houershanense** Huang in Kong and Huang, 1978; **A. jiangzhaiense** Kong in Kong and Huang, 1978; **A. longdongshuiense** Kong in Kong and Huang, 1978; **Dialithophyllum (Protodialithophyllum) quiannanense** Kong in Kong and Huang, 1978; **D. (P.) pinghuangshanense** Kong in Kong and Huang, 1978; **Zonodigonophyllum vesiculosum** Yu and Liao in Kong and Huang, 1978 (=**Z. longdongshuiense** Yu and Liao, 1978). Longdongshui Formation, Eifelian, Guizhou, China.

**Atelophyllum gigantum** Kong in Kong and Huang, 1978. Dushan Formation Givetian, Guizhou, China.

**Atelophyllum beichuanense** He, 1978; **A. intermedium** He, 1978. Dalejan or Eifelian, Sichuan, China.

**Lekanophyllum pustulosum** Pedder and McLean (in press). Blue Fiord Formation, Dalejan part, Ellesmere Island, Arctic Canada.

In addition to these species, **Atelophyllum vesisolens** Kong in Kong and Huang, 1978, from the Eifelian Longdongshui Formation of Guizhou, should be added to McLean's (1976, p. 19, 20) list of doubtful species of **Lekanophyllum.**

Remarks. One of the species doubtfully attached to the genus by McLean (1976, p. 20) was **Pseudodigonophyllum notabile** Tsyganko. This has become the type species of the genus **Septiphyllum** Tsyganko (1978, p. 11), which now should be added to the possible synonyms of **Lekanophyllum.**

### Lekanophyllum retiforme sp. n.

Plate 10.1a, b, c, figures 1-21

**Cyathophyllum nepos** Hall; Loewe, 1913, p. 6, 7, Pl. 1, figs. 1a-d.

**Mesophyllum (Actinocystis) robustum** (Hall); Loewe 1913, p. 12, Pl. 2, figs. 2a, b.

Acanthophyllid; McLaren, 1963, p. 327.

Bethanyphyllids; McLaren, 1963, p. 327.

not **Cyathophyllum robustum** Hall, 1876, Pl. 22, figs. 1-9, 14 [=**Bethanyphyllum robustum** (Hall)].

not **Cyathophyllum nepos** Hall, 1876, Pl. 22, figs. 10, 11 [unrecognizable without sections of type specimen, but not a cystiphyllid coral].

Type series. Holotype, UA 3946, UA loc. PCC 92068. Paratypes, UA 3947-3949, UA loc. PCC 92068, and UA 3950, 3951, UA loc. PCC 92070.

Diagnosis. Solitary species of **Lekanophyllum** with maximum mean diameter of about 35 mm. Septal apparatus well developed, principally as two orders of septal crests, numbering 36x2 to 44x2 in fully grown specimens, and dilated to incorporate lateral dissepiments. A few isolated carinae and trabeculae occur in the peripheral region of the dissepimentarium; isolated spines and sclerenchymal layers develop periodially in the interior region of the corallum. Dissepiments and presepiments abundant and small.

Description. Corallum solitary, commonly trochoid, rarely turbinate, not consistently curved in respect to the cardinal-counter plane, generally rejuvenated or stabilized to a subcylindrical form in late stages. Large specimens attain a length of 60 mm and diameter of about 35 mm. Calice mostly in the form of an inverted cone, but variable, and may have an everted margin. Cardinal fossula present in tabularium, not extended to the periphery of the corallum. Outer wall poorly preserved in material from type region; exterior marked by transverse growth ridges and, locally, by subdued septal grooves and interseptal ridges.

The outer marginarium is abraided and crushed in most specimens examined. Where preserved, the outer wall is 0.05 to 0.3 mm thick; its shape reflects the numerous minor contractions and expansions of the corallum. In the peripheral region, septal apparatus comprises isolated spines, some highly carinate fragments of septal crests and a few discrete carinae. In the inner dissepimentarium and outer tabularium, slender monacanthate trabeculae are fused radially to form two distinct orders of variably carinate, lamellar septa; thickened regions of both orders of septa incorporate lateral dissepiments, so that the septal apparatus is retiform in places. Adaxial ends of minor septa commonly deflect towards an adjacent major septum and, in some specimens, many of the minor and major septa are contratingent. Adaxial ends of major septa are more variable. Some simply attenuate towards the axis, or coalesce with periodically developed axial sclerenchyme; others expand or become fusiforme, as viewed in transverse section. A few short septal spines may be present in the axial region. The cardinal septum is normally shorter than adjacent major septa; septal arrangement is only weakly pinnate about it. Septa number 36x2 to 44x2 in full size coralla.

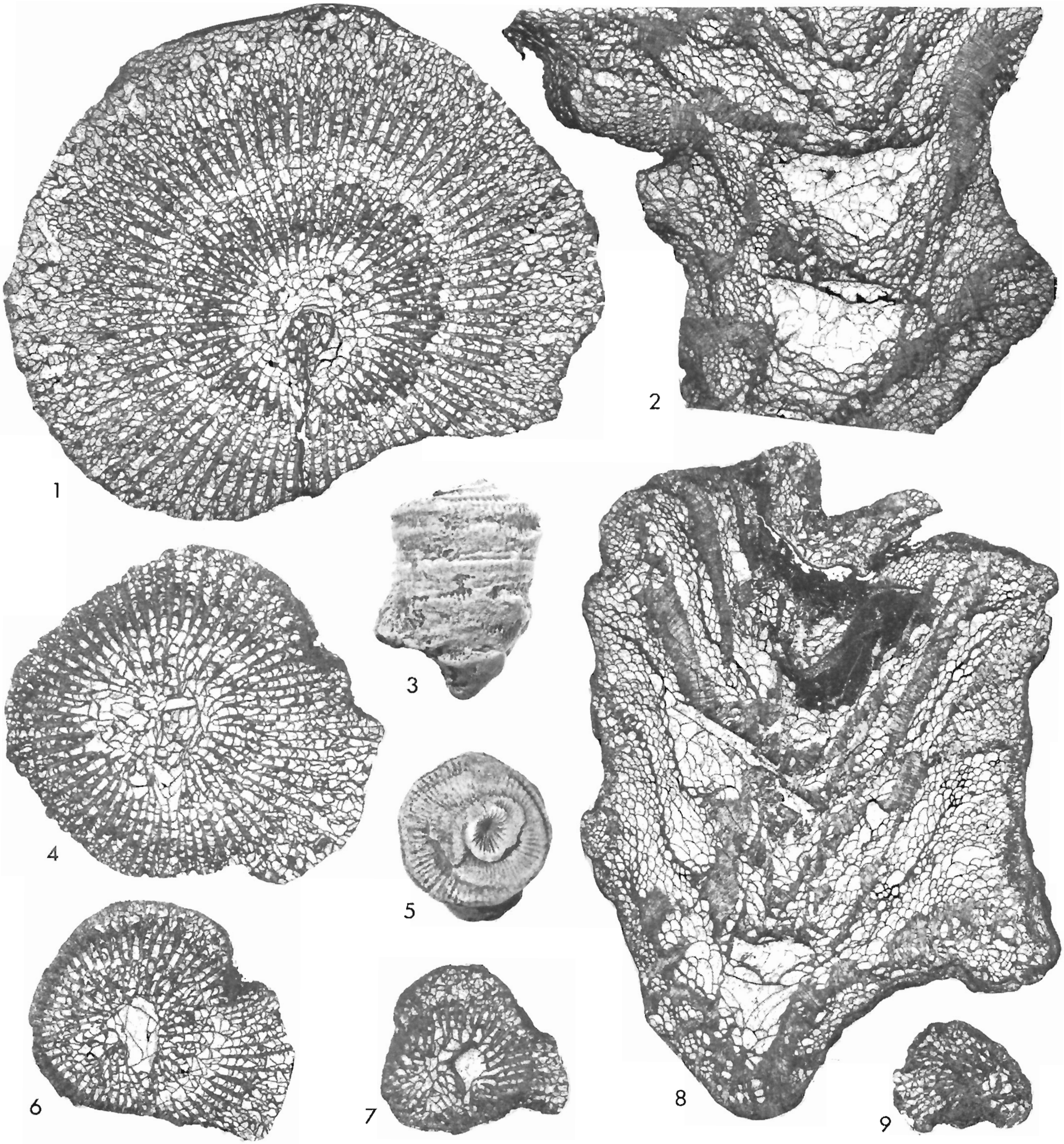


**PLATE 10.1a**

Figures 1-9. **Lekanophyllum retiforme** sp. n.

1, 2. Holotype, UA 3946, transverse and longitudinal sections, X3; UA loc. PCC 92068.

3, 5, 8. Paratype, UA 3949, exterior views before sectioning, X1, longitudinal section, X3; UA loc. PCC 92068.

4, 6, 7, 9. Paratype, UA 3947, transverse sections, X3; UA loc. PCC 92068.

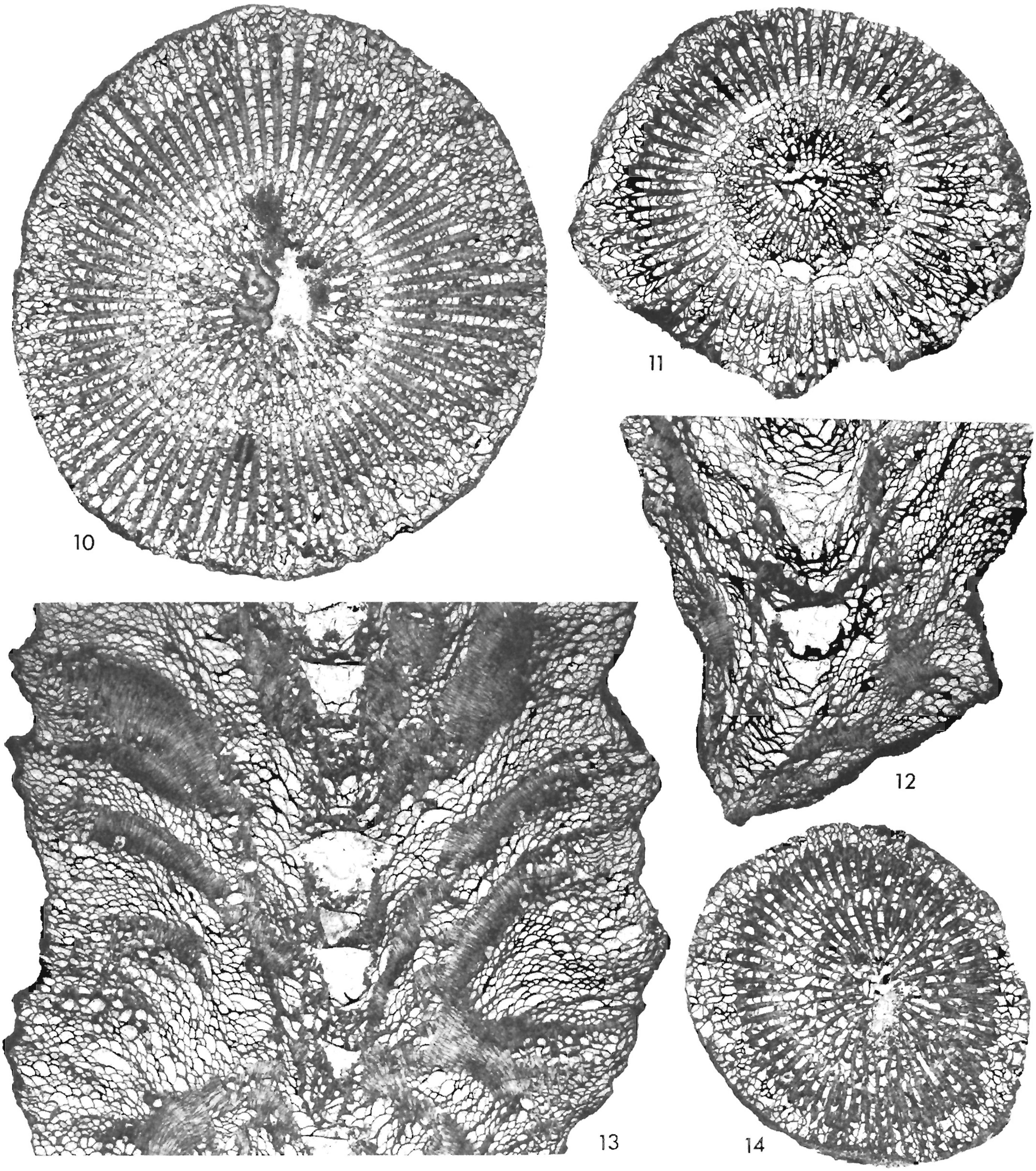

**PLATE 10.1b**

Figures 10-14. **Lekanophyllum retiforme** sp. n.

10, 13, 14. Paratype, UA 3950, transverse and longitudinal sections, X3; UA loc. PCC 92070.

11, 12. Paratype, UA 3951, transverse and longitudinal sections, X3; UA loc. PCC 92070.

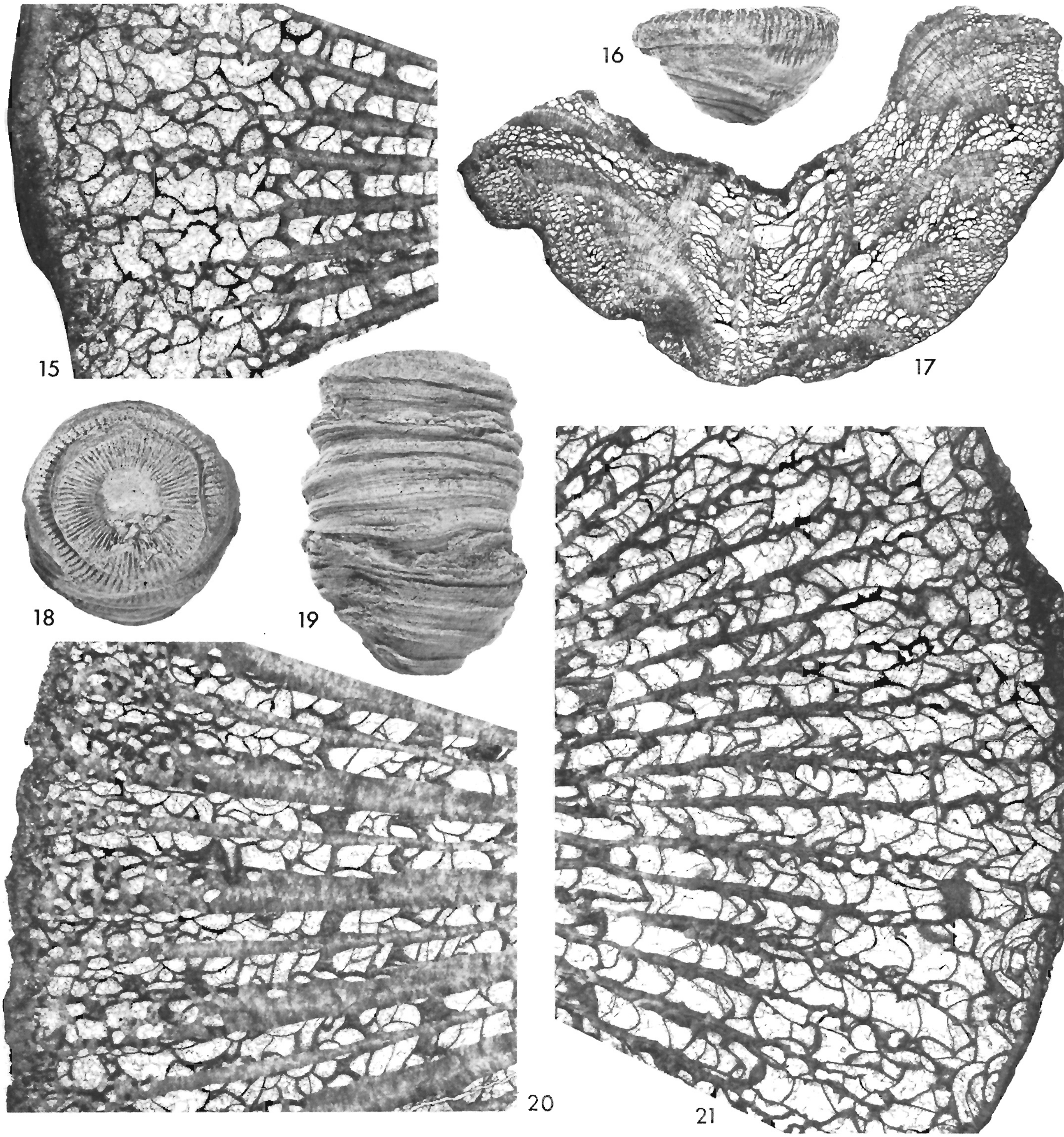

**PLATE 10.1c**

Figures 15-21. **Lekanophyllum retiforme** sp. n.

15. Paratype, UA 3949, part of transverse section, X10; UA loc. PCC 92068.

16, 17, 20. Paratype, UA 3948, exterior view before sectioning, X1, longitudinal thin section, X3, part of transverse section, X10; UA loc. PCC 92068.

18, 19. Paratype, UA 3950, exterior views before sectioning, X1; UA loc. PCC 92070.

21. Paratype, UA 3947, part of transverse section, X10; UA loc. PCC 92068.

Presepiments and dissepiments, including many lateral dissepiments, are small, and commonly form 15 to 20 rows in expanded regions of adult corallites. Peripheral dissepimentarial surfaces may be flat, everted, or inwardly sloping. Diameter of the tabularium is generally greatest in the cardinal-counter plane, and its axial depression is generally elongated in the same plane. Following a significant rejuvenescence, the next tabula is complete, but above this, and below the next rejuvenescence, the tabularium consists of numerous vesicular tabellae that laterally tend to merge imperceptibly with dissepiments.

Remarks. The unusually well developed major and minor septa, and numerous lateral dissepiments distinguish **Lekanophyllum retiforme** from all, but one, of the previously described species now attributed to **Lekanophyllum**. The exception being **L. crassiseptatum**, described by Bul'vanker (1958, p. 72, 73, Pl. 33, figs. 1a-2; Pl. 36, fig. 3) from the Givetian Safonov Beds of the Kuznets Basin. This species is distinguished from **L. retiforme** by having fewer (28x2 to 37x2) septa, larger dissepiments, and, apparently, in lacking discrete peripheral carinae.

**Lekanophyllum retiforme** is the most abundant coral in the Bird Fiord Formation south of the Schei synclinal axis, and accounts for about 30 per cent of the total coral fauna of the formation in this region.

The trivial name is the Latin adjective **retiformis**, from **rete**, meaning a net, and **forma**, meaning shape. It refers to the distinctive septal morphology of the species.

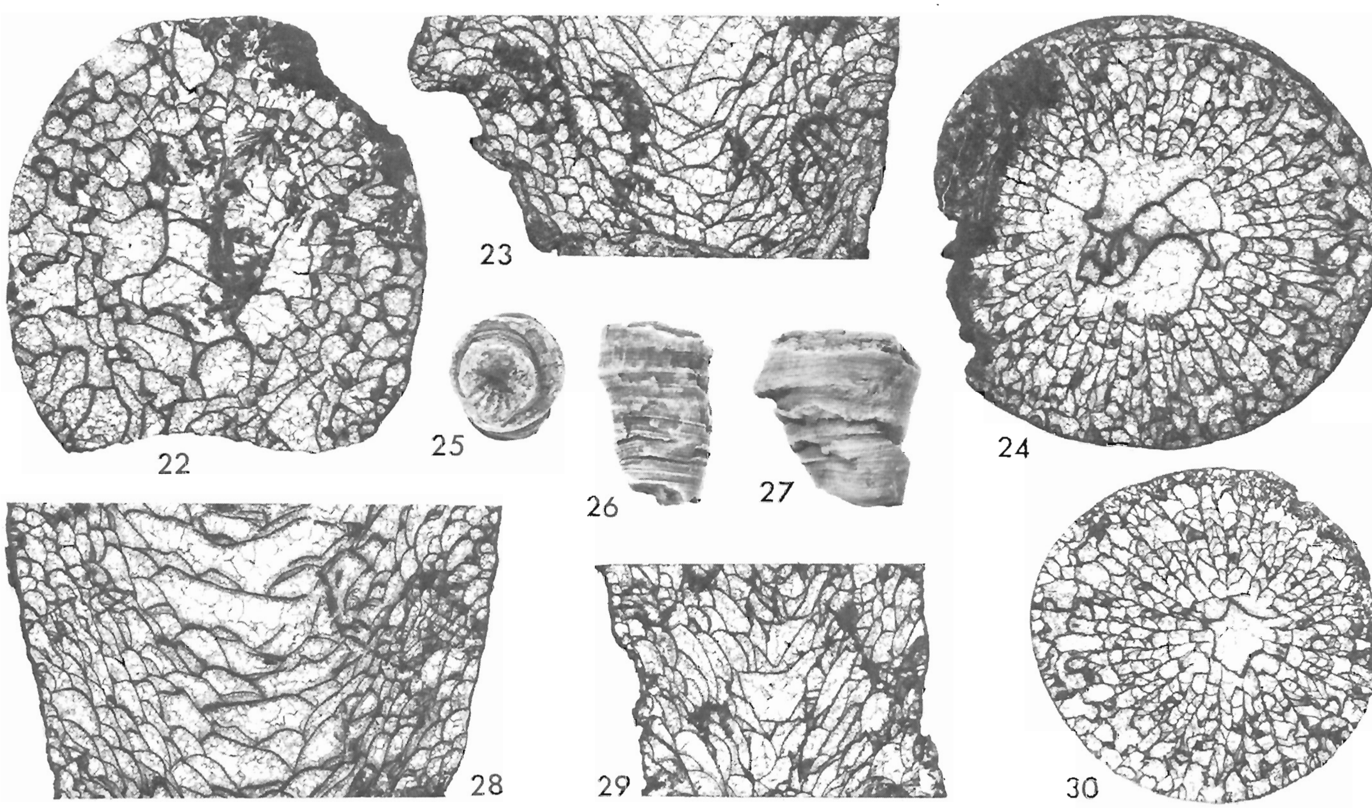


**PLATE 10.1d**

Figures 22-30. **Lekanophyllum rugulosum** sp. n.

22. Paratype, UA 3954, transverse section, X3; UA loc. PCC 92070.

23, 24, 27. Holotype, UA 3952, longitudinal and transverse sections, X3, exterior view before sectioning, X1; UA loc. PCC 92068.

25, 26, 29, 30. Paratype, UA 3953, exterior views before sectioning, X1, longitudinal and transverse sections, X3; UA loc. PCC 92068.

28. Paratype, UA 3955, longitudinal section, X3; UA loc. PCC 92070.

**Lekanophyllum rugulosum** sp. n.

Plate 10.1d, figures 22-30

Type series. Holotype, UA 3952, UA loc. PCC 92068. Paratypes, UA 3953, UA loc. PCC 92068, and UA 3954, 3955, UA loc. PCC 92070.

Diagnosis. Solitary species of **Lekanophyllum** with a maximum known mean diameter of 21 mm. Septal apparatus radially arranged, extremely variable. In some specimens it consists of as many as 27 thin, lamellar and very finely carinate major septa and only slightly fewer minor septa; in others, it is reduced to mere fragments of septal crests and fine, isolated spines. Presepiments and dissepiments moderate to relatively large size. Sclerenchymal thickening absent from both vertical and horizontal skeletal elements.

Description. Corallum solitary. Earliest growth form unknown, later stages ceratoid to cylindrical with marked changes in diameter, including pronounced rejuvenescences in some specimens. Observed maximum mean diameter 21 mm. Although none of the type specimens is complete, it is unlikely that any was significantly longer than 27 mm. Calice unknown. Exterior of outer wall marked only by fine, transverse growth lines.

An outer wall, 0.05 to 0.2 mm thick, entirely covers the exterior of the corallum. Septal apparatus extremely variable, comprising very thin, somewhat sinuous, finely, but abundantly carinate septal crests, and isolated spines. In specimens that have a well developed septal apparatus, there are 25 to 27 radially arranged major septa. These extend from the periphery, or only a slight distance inside it, to within 2 mm of the axis. Minor septa are also well developed in these specimens, although a few are represented only by fine, peripherally situated spines. In specimens that have weakly developed septal apparatus, major septa are mostly discontinuous and much withdrawn from the periphery. Minor septa are either entirely supressed, or reduced to peripheral spines and a few fragmentary lamellae. A few fine septal spines develop in the tabularium of specimens having well developed septal apparatus; such spines are extremely rare in specimens having poorly developed septal apparatus. The fine septal structure is difficult to discern, but appears to lack trabeculae.

Presepiments and dissepiments are moderate to relatively large in size, and inwardly inclined, except over expanded parts of the marginarium, where they tend to be flat lying. Lateral dissepiments extremely rare. Typically, the dissepimentarium comprises four to eight rows of dissepiments, but is not clearly differentiated from the tabularium. Vesicular tabellae and a few, more or less complete tabulae construct the tabularium.

Remarks. The small size and very variable, thin and finely carinate septa distinguish this from other species of the genus. **Lekanophyllum bizonatum**, described by Kravtsov (1966, p. 45, 46, Pl. 8, figs. 3a, b; Pl. 9, fig. 1) as **Pseudomicroplasma bizonata**, from the Pragian Lower Val'nev Horizon of Novaya Zemlya, and **L. pustulosum** Pedder and McLean (in press), from the Dalejan part of the Blue Fiord Formation of Ellesmere Island, seem to be the least dissimilar of previously described species. Compared with the new species, **L. bizonatum** has thicker, less carinate and more numerous (38 at 19 to 21 mm diameter) major septa, and much smaller dissepiments. **L. pustulatum** is larger (maximum diameter 32 mm) than **L. rugulosum**, and has less carinate, more sinuous and more numerous (as many as 34) major septa, and more abundant dissepiments.

The trivial name is the Latin adjective **rugulosus**, meaning with small wrinkles or creases. It refers to the peculiar septal morphology of the species.

## Locality Register

UA locality PCC 92068. Bird Fiord Formation, 375.5 m above base (=top of Blue Fiord Formation), 125.5 m above top of gypsiferous siltstone unit in the lower part of the Bird Fiord Formation at this locality; **serotinus** Zone or younger, probably Dalejan. Blubber Point, southwest Ellesmere Island, District of Franklin; 76°36'N latitude, 89°35'W longitude. Collected by Q. Goodbody, 1981. Brachiopods identified by Brian Jones.

**Favosites** sp., **Cladopora** sp., **Oculipora**(?) sp., **Lekanophyllum retiforme** Pedder, **L. rugulosum** Pedder, **Taimyrophyllum** sp. (including form named **Phillipsastraea scheii** by Loewe, 1913), **Cavanophyllum** sp. n., **Schizophoria sulcata** Johnson and Perry, indeterminate strophomenid brachiopod, **Phragmostrophia latior** (Meyer)?, **Capularostrum repetitor** Johnson and Perry, **Spinatrypa** sp., **Perryspirifer scheii** (Meyer), "**Elythina**" **sverdrupi** Brice, indeterminate bivalves.

UA locality PCC 92070. Bird Fiord Formation, 385 m above base (=top of Blue Fiord Formation), 135 m above top of gypsiferous siltstone unit in the lower part of the Bird Fiord Formation at this locality; **serotinus** Zone or younger, probably Dalejan. Same locality and collection data as UA loc. PCC 92068. Brachiopods identified by Brian Jones.

**Cladopora** sp., **Alveolites** sp., **Oculipora** (?) sp., **Syringopora** sp., **Lekanophyllum retiforme** Pedder, **L. rugulosum** Pedder, **Taimyrophyllum** sp. (including form named **Phillipsastraea scheii** by Loewe, 1913), **Cavanophyllum** sp. n., undetermined cyathophyllid coral, **Schizophoria sulcata** Johnson and Perry, indeterminate strophomenid brachiopod (same as in PCC 92068), **Phragmostrophia latior** (Meyer)?, **Spinatrypa** sp. (same as in PCC 92068), **Perryspirifer scheii** (Meyer), "**Elythina**" **sverdrupi** Brice.

## References


Birenheide, R.

1964: Die "Cystimorpha" (Rugosa) aus dem Eifeler Devon; Abhandlungen der Senckenbergischen Naturforschenden Gesellschaft 507, p. 1-120.

1968: Die Typen der Sammlung Wedekind aus der Gattung **Plasmophyllum** (Rugosa; Mitteldevon); Senckenbergiana lethaea, Band 49, p. 1-37.

1978: Leitfossilien. No. 2. Rugose Korallen des Devon; Gebruder Borntraeger, Berlin, Stuttgart, vi + 265 p.

Bul'vanker, E.Z.

1958: Devonskie chetyrekhluchevye korally okrani Kuznetskogo basseyna; Vsesoyuznyy Nauchno-Issledovatel'skiy Geologicheskiy Institut (VSEGEI), Leningrad, text 212 p. and atlas.

Hall, J.

1876: Illustrations of Devonian fossils: Gasteropoda, Pteropoda, Cephalopoda, Crustacea and corals of the Upper Helderberg, Hamilton and Chemung Groups; Geological Survey of the State of New York, Albany, 7 p.

He, Yuan-xiang

1978: Rugosa; in Atlas of fossils of southwest China. Sichuan Volume. Part 1. From Sinian to Devonian (in Chinese), ed. Chengdu Institute of Geology and Mineral Resources; Geological Publishing House, Peking, p. 98-179, 555-568.

Hill, D.

1981: Treatise on invertebrate paleontology. Part F. Coelenterata. Supplement 1. Rugosa and Tabulata, ed. Curt Teichert; Geological Society of America and University of Kansas Press, Boulder and Lawrence, v. 1, p. i-xl, 1-378, v. 2, p. i, ii, 379-762.

Jackson, D.E., Lenz, A.C., and Pedder, A.E.H.

1978: Late Silurian and Early Devonian graptolite, brachiopod and coral faunas from northwestern and Arctic Canada; The Geological Association of Canada, Special Paper, no. 17.

Jia Hui-zhen, Xu Shou-yong, Kuang Guo-dun, Zhang Bu-fei, Zuo Zi-bi, and Wu Jin-shu

1977: Anthozoa; in Atlas of the paleontology of central and southern China, v. 2. Late Paleozoic Era (in Chinese), ed. Geological Science Research Institute, Hubei and others; Geological Publishing House, Peking, p. 109-270, 764-789.

Kong Lei and Huang Yun-ming

1978: Tetracoralla; in Atlas of the paleontology of the southwestern regions of China, v. 1. Cambrian to Devonian (in Chinese), ed. Guizhou Stratigraphy and Paleontology Work Team; Geological Publishing House, Peking, p. 35-161, 739-759.

Kravtsov, A.G.

1966: Rannedevonskie i eyfel'skie chetyrekhluchevye korally yuzhnogo ostrova Novoy Zemli (val'nevskiy gorizont); Nauchno-Issledovatel'skiy Institut Geologii Arktiki, Uchenye Zapiski, Paleontologiya i Biostratigrafiya, vyp. 16, p. 22-63.

Loewe, S.

1913: Die devonischen Korallen von Ellesmereland; in Report of the Second Norwegian Arctic Expedition in the "Fram" 1898-1902, Videnskabs-Selskabet i Kristiania, v. 4, no. 30, p. 1-23.

McLaren, D.J.

1963: Southwestern Ellesmere Island betwen Goose Fiord and Bjorne Peninsula; in Y.O. Fortier et al., Geology of the north-central part of the Arctic Archipelago, Northwest Territories (Operation Franklin); Geological Survey of Canada, Memoir 320, p. 310-338.

McLean, R.A.

1976: Middle Devonian cystiphyllid corals from the Hume Formation, northwestern Canada; Geological Survey of Canada, Bulletin 274.

Pedder, A.E.H. and McLean, R.A.

Lower Devonian cystiphyllid corals from North America and eastern Australia with notes on the genus **Utaratuia**; Geologica et Palaeontologica 16. (in press)

Tsyganko, V.S.

1978: Novyy rod devonskikh rugoz; Akadamii Nauk SSSR, Komi filiala Institut Geologii, Trudy, vyp. 25, p. 10-13.

Wedekind, R.

1924: Das Mitteldevon der Eifel. Eine biostratigraphische Studie. I Teil. Die Tetrakorallen des unteren Mitteldevon; Schriften der Gesellschaft zur Beforderung der gesampten Naturwissenschaften zu Marburg, Band 14, Heft 3, vii + 93 p.

Yu Chang-min and Liao Wei-hua

1978: Middle Devonian rugose corals of Longdongshui Member, Houershan Formation from Dushan district, Guizhou (Chinese with English summary); Memoirs of Nanjing Institute of Geology and Palaeontology, Academia Sinica, no. 12.

11.

# RECENT DISCOVERIES OF JURASSIC FOSSILS IN THE LOWER SCHIST DIVISION OF CENTRAL YUKON

Project 760042

T.P. Poulton and D.J. Tempelman-Kluit[1]
Institute of Sedimentary and Petroleum Geology, Calgary

*Poulton, T.P. and Tempelman-Kluit, D.J., Recent discoveries of Jurassic fossils in the Lower Schist Division of central Yukon; in Current Research, Part C, Geological Survey of Canada, Paper 82-1C, p. 91-94, 1982.*

### Abstract

*Recent discoveries of* ***Buchia*** *and* ***Cardioceras*** *species confirm the Jurassic age of the Lower Schist Division in central Yukon. The lithologies, sedimentary structures, and succession confirm the correlation of the Lower Schist with the Kingak Formation of northern Yukon. They further suggest the correlation of Keno Hill Quartzite of the North Klondike area with Neocomian quartzites of northern Yukon. The Keenan Quartzite of east-central Alaska, in a paleogeographic position between west-central and northern Yukon, must also represent the same unit.*

## Introduction

The presence of Jurassic rocks in central Yukon was established in 1961 with the discovery of Middle Jurassic ammonites in the North Klondike area (Green and Roddick, 1962, p. 13; map unit 19). Formerly, these strata had been assigned to the Yukon Group and had been assigned a Precambrian age on the basis of metamorphic grade and the apparent lack of fossils. The discovery, of **Arctocephalites** and **Cadoceras?** species (GSC loc. 47219; see Tempelman-Kluit, 1970, p. 96), was in black shale near the top of map unit 19 of Green and Roddick (1962). This unit is now known to comprise several thrust-repeated intervals and to involve Paleozoic through Cretaceous rocks. Its fossil-bearing upper beds comprise a thin slice of Triassic and Jurassic rocks, thrust over probable Cretaceous rocks to the north and themselves covered structurally by Precambrian or Cambrian rocks (Tempelman-Kluit, 1970). Subsequently, **Cardioceras** sp. and **Cardioceras**(?) sp. were found in 1965 at two localities in the same thin slice of argillaceous rocks (GSC locs. 68091, 70444; see Frebold et al., 1967).

The Lower Schist Division and overlying Keno Hill Quartzite, far to the east of North Klondike area, are hosts to the lead-zinc-silver veins at Keno Hill (Boyle, 1965). They were similarly regarded as Precambrian until Green and Roddick (1962) recognized the Jurassic age for what appeared to be equivalent rocks to the west in North Klondike area. These two units extend westward from Keno Hill to the North Klondike area (Fig. 11.1), where they dominate the thrust sheet below that containing the previously discovered Jurassic fossils mentioned above.

The correlation of the fossiliferous shale of the upper, thin, thrust slice in the North Klondike area with the westerly outcrop of the Lower Schist Division in the underlying thrust sheet was suggested earlier, although the tentative nature of the correlation was emphasized by assigning the two argillaceous units to different map-units (Tempelman-Kluit, 1970, units 11 and 12; Green and Roddick, 1962, units 17 and 17a). Uncertainty regarding the correlation stemmed from the absence of a quartzite above the argillaceous unit in the higher thrust slice that could be correlated with the Keno Quartzite.

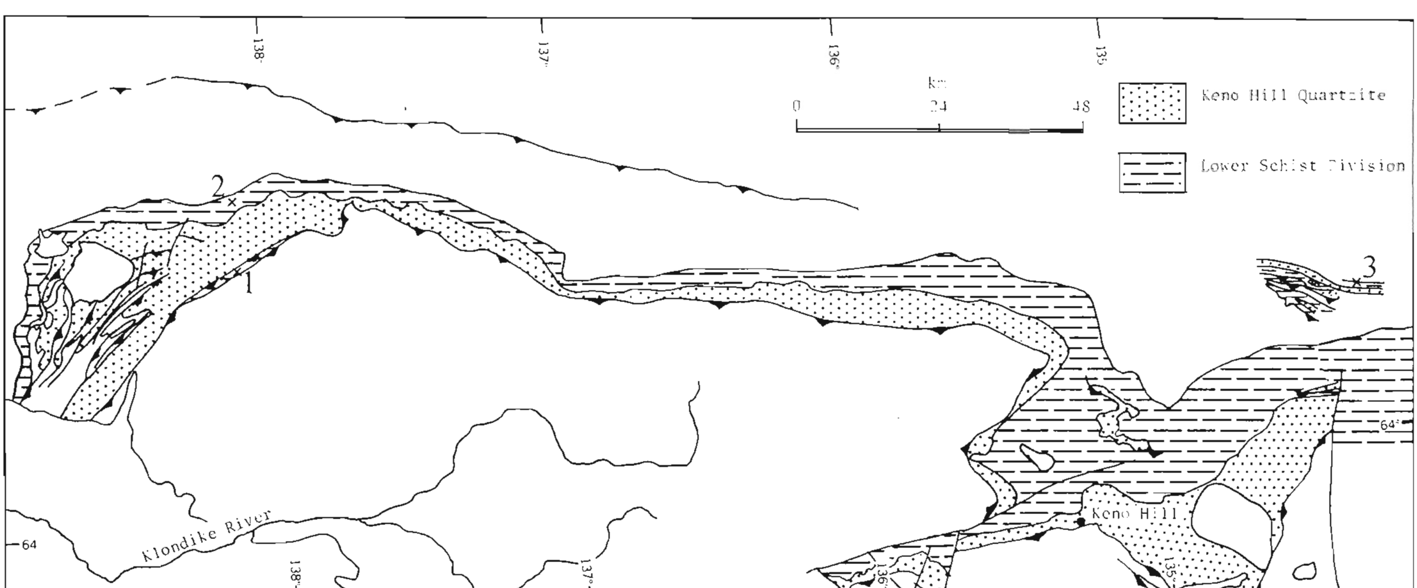


***Figure 11.1.*** *Index Map, adapted from Tempelman-Kluit (1970, 1981), showing fossil localities: 1) Fossils described by Frebold et al. (1967); 2)* ***Cardioceras*** *sp. of this report (GSC loc. C-95380); 3)* ***Buchia*** *sp. (GSC locs. 97519, 97520).*

[1]Department of Indian and Northern Affairs, Whitehorse


***Figure 11.2***

*Lower Schist Division (recessive) and overlying Keno Hill Quartzite (resistant bluffs), west of Dempster Highway, south of North Fork Pass. X marks the* ***Cardioceras*** *locality (GSC loc. C-95380).*

Recently Blusson (1978, p. 77) indicated the lithological similarity of the Lower Schist and Keno Hill Quartzite in Keno Hill area to part of the Paleozoic succession in eastern Yukon and treated them as Late Paleozoic.

The newly discovered Jurassic fossil occurrences described in this paper, occur within the Lower Schist Division in the northerly, structurally lower thrust slices, confirming the age and the correlations suggested earlier (e.g. Tempelman-Kluit, 1970). The Keno Hill Quartzite is still not dated directly.

### Fossil Occurrences

The fossils found in 1961 and 1965 and described by Frebold et al. (1967) occur in siliceous concretions in grey and black, graphitic phyllite with minor, thin siltstone and fine-grained sandstone laminae, about 100 m above the base of the Lower Schist (Fig. 11.1, loc. 1).

In the Nash Creek area in 1980 (Fig. 11.1, loc. 3), E.T. Tozer collected unidentifiable belemnites and, higher in the section, **Buchia** (s. lato) ex gr. **concentrica** (Sowerby) **-mosquensis** (von Buch), which were identified by J.A. Jeletzky. Jeletzky (personal communication) indicated a possible Late Oxfordian to Early Portlandian, and most likely a Late Oxfordian to Early Kimmeridgian age, and pointed out the correlation with the lower part of the Husky Formation of northern Yukon. The fossils were found in small outcrops surrounded by Holocene alluvium within a broad, recessive belt north of the main outcrop area of the Lower Schist Division. These outcrops lie along strike east of a complex, thrust repeated Paleozoic and Mesozoic succession, which is host to the Blue Lite Tungsten Skarn showing (Tempelman-Kluit, 1981). Their position within the Lower Schist Division and their relation to the Keno Hill Quartzite is uncertain, but the fossils provide further evidence of the age of the Lower Schist. The locality (GSC locs. 97519, 97520) is on the southeast side of Rackla River, 1000 m southeast of the mouth of the stream draining Kathleen Lakes at the first bend below that stream.

Poulton collected **Cardioceras** sp., from about 100 m below the top of a black, very soft, carbonaceous phyllite which occurs about 150 m below the top of the Lower Schist Division, in the col between two ridges southeast of North Fork Pass, in the north Klondike area. The locality (GSC loc. C-95380; Fig. 11.1, loc. 2) is in northeastern Tombstone Range, near the Dempster Highway, at the head of a small tributary entering North Klondike River from the east, at Latitude 64°30'40"N and Longitude 138°08'N. The upper 150 m of the Lower Schist here contain increasingly abundant planar-laminated and strongly bioturbated sandstone beds upward toward the massive, resistant bluffs of the Keno Hill Quartzite (Fig. 11.2).

### Paleogeographic Setting

The Lower Schist Division and the Keno Hill Quartzite occur in thrust slices which have been transported northward over cratonic terranes in which the Proterozoic and Paleozoic successions are similar to those in the transported sheets. They are thus tied to the craton stratigraphically and paleogeographically. The structural and stratigraphic trends of these pericratonic strata are truncated on the southwest by the Tintina transcurrent fault, along which 450 km of right-lateral displacement is recognized (see also Tipper et al., 1981). Because the Lower Schist Division is pericratonic and not an extra-cratonic, allochthonous unit as is the case in other regions farther southwest, its distribution constrains modelling of the Jurassic shorelines of northwestern North America.

No significant lithological differences distinguish the Lower Schist Division from its northern Yukon equivalents, the Kingak and Husky formations. The sandstones in its upper part, furthermore, are virtually identical with those in the southern exposures of the Kingak in Ogilvie Mountains. The central and northern Yukon Jurassic rocks were probably deposited in physical continuity with one another. Poulton (in press; and in Poulton et al., 1982) showed that the northern Yukon Lower Jurassic through lower Upper Jurassic facies trends and shorelines ran southwest from western Mackenzie Delta, curving southward along its west side near the Yukon-Alaska border. The shelf in pre-Late Oxfordian times must have passed around a promontory, forming the northwest corner of the continent in north central Yukon, and south of it formed an east-trending re-entrant in which were deposited strata of the Lower Schist Division (Fig. 11.3).

Such a restricted distribution probably did not characterize the immediately younger rocks, however. The Husky Formation in northern Yukon is markedly transgressive over the limits of the older Jurassic rocks.

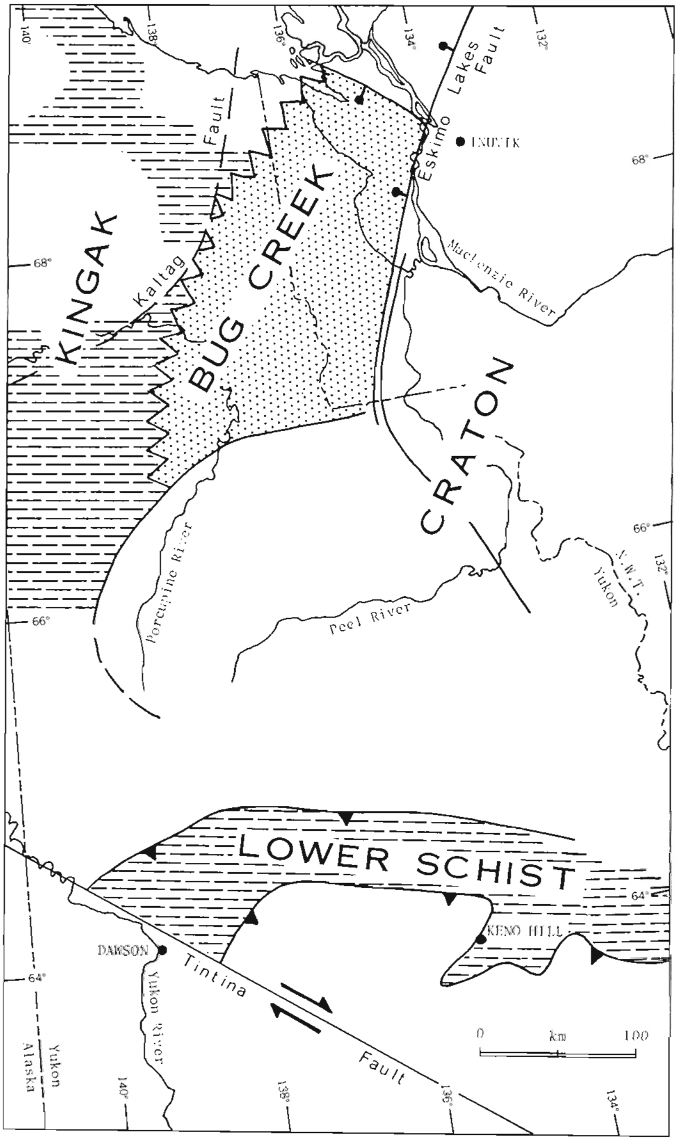


*Figure 11.3. Paleogeographic-tectonic configuration of Lower Oxfordian and older Jurassic rocks of northern and central Yukon Territory.*

Oxfordian or Kimmeridgian microfossils identify Husky equivalents in shale on the north side of Peel River, in northern Hart River map area (W. Brideaux, personal communication; D.K. Norris, in press). Therefore, the promontory that characterized pre-Late Oxfordian Jurassic time was apparently largely if not entirely submerged by Kimmeridgian time.

In an earlier interpretation, Jeletzky (1975) had considered that the northern and central Yukon Jurassic strata were directly connected depositionally by an intracratonic trough – the "Porcupine Plain – Richardson Mountains Trough". Young (1975) showed that Jurassic rocks are absent in Eagle Plain, and interpreted an arch there instead – "Eagle Arch" – separating the northern and central Yukon Jurassic occurrences.

Tempelman-Kluit (1970) indicated the similarity of the Keno Hill Quartzite to Lower Cretaceous units in the Kandik River area of east-central Alaska, named the K^^ an Quartzite (Brabb, 1969), and to the Valanginian to Hauterivian quartzite units of northern Yukon Territory. These units are all lithologically identical and were presumably deposited in continuity.

## Taxonomic Description

**Cardioceras** sp. aff. **C. mountjoyi** Frebold
Figure 11.4a, b

aff. **Cardioceras mountjoyi** Frebold (Frebold et al., 1959, p. 22, 23, Pl. III, Fig. 3, 4).

### Description

The maximum preserved diameter is 9 cm. At least the last one-third of the last whorl is non-septate. The inner whorls are not exposed.

The smallest growth stage preserved has a whorl height of 2 cm. The umbilical wall is steep and high, and carries extensions of the primary ribs. The umbilical edge is abruptly rounded. The lower part of the flank is flat, except for the ribs, and slopes gently outward to a maximum conch

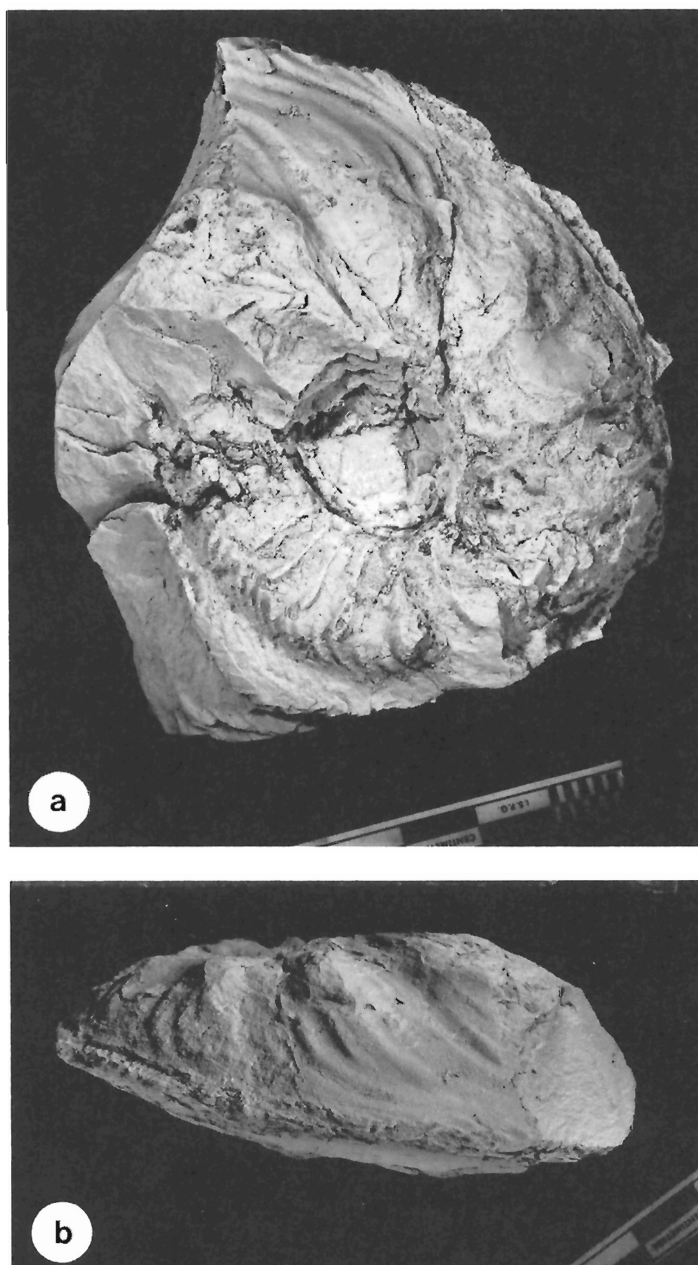


***Figure 11.4a, b.*** ***Cardioceras*** *sp. aff.* ***C. mountjoyi*** *Frebold. Lateral and ventral (only one half of shell preserved) views of figured specimen GSC 68650 from GSC locality C-95380.*

thickness halfway up its height. This part of the flank is ornamented with strong, moderately widely-spaced, rectiradiate primary ribs, that are swollen to prominent bullae halfway up the flank. The ventral half of the flank drops off to the carinate venter which is not preserved. Finer secondary ribs, about three to each primary, are inclined moderately forward. They are barely perceptible near the keel.

Adorally, the strength and spacing of the primaries and the strength of the bullae increase markedly. On the adoralmost part preserved, strong, widely-spaced swellings are the dominant ornament. The spaces between the swellings carry finer corrugations. The strong forward inclination of these may be due partly to tectonic compression. These corrugations and the secondary ribs arising from the tubercles swing forward strongly on the ventral one third of the flank, become nearly spiral in their orientation on the concave part of the flank adjacent to the keel, and then become more upright on the keel itself. At this preserved growth stage the maximum width is near the umbilicus.

The suture pattern cannot be traced.

### Discussion

The single specimen is not sufficiently distinctive to warrant detailed comparison with other species. However, in the overall character, the strength and spacing of the ribs, the prominent bullae where the ribs subdivide, and the ratio of primaries to secondaries, the specimen most closely resembles **Cardioceras mountjoyi** Frebold from the Fernie Formation of Alberta. Some other specimens of **Cardioceras** from northern Yukon have been compared with **C. cordatum** (J. Sowerby) and **C. alphacordatum** Spath (Frebold et al., 1967). Specimens previously collected in the North Klondike area were identified as **Cardioceras** sp. indet. (Frebold et al., 1967).

### Repository

The figured specimen, GSC 68650, is stored in the Type Collection, Geological Survey of Canada, 601 Booth Street, Ottawa, Ontario.

### References


Blusson, S.L.
1978: Regional geologic setting of lead-zinc deposits in Selwyn Basin, Yukon; in Current Research, Part A, Geological Survey of Canada, Paper 78-1A, p. 77-80.

Boyle, R.W.
1965: Geology, geochemistry, and origin of the lead-zinc-silver deposits of the Keno Hill-Galena Hill area; Geological Survey of Canada, Bulletin 111.

Brabb, E.E.
1969: Six new Paleozoic and Mesozoic formations in east-central Alaska; United States Geological Survey, Bulletin 1247-I.

Frebold, H., Mountjoy, E.W., and Reed, R.
1959: The Oxfordian beds of the Jurassic Fernie Group, Alberta and British Columbia; Geological Survey of Canada, Bulletin 53.

Frebold, H., Mountjoy, E.W., and Tempelman-Kluit, D.
1967: New occurrences of Jurassic rocks and fossils in central northern Yukon; Geological Survey of Canada, Paper 67-12.

Green, L.H.
1972: Geology of Nash Creek, Larsen Creek and Dawson map-areas, Yukon Territory; Geological Survey of Canada, Memoir 364.

Green, L.H. and Roddick, J.A.
1962: Dawson, Larsen Creek and Nash Creek map-areas, Yukon Territory; Geological Survey of Canada, Paper 62-7.

Jeletzky, J.A.
1975: Jurassic and Lower Cretaceous paleogeography and depositional tectonics of Porcupine Plateau, adjacent areas of northern Yukon and those of Mackenzie District, Northwest Territories; Geological Survey of Canada, Paper 74-16.

Norris, D.K.
Hart River map-area (116H); Geological Survey of Canada, map. (in press)

Poulton, T.P.
Paleogeographic and tectonic implications of the Lower and Middle Jurassic facies patterns in northern Yukon Territory and adjacent Northwest Territories; Proceedings, 3rd International Symposium on the Geology of the Arctic; Canadian Society of Petroleum Geologists, Memoir. (in press)

Poulton, T.P., Leskiw, K., and Audretsch, A.P.
1982: Stratigraphy and microfossils of the Jurassic Bug Creek Group of northern Richardson Mountains, northern Yukon and adjacent Northwest Territories; Geological Survey of Canada, Bulletin 325.

Tempelman-Kluit, D.J.
1970: Stratigraphy and structure of the "Keno Hill Quartzite" in Tombstone River-Upper Klondike River map-areas, Yukon Territory; Geological Survey of Canada, Bulletin 180.

1981: Blue Lite; in D.J. Tempelman-Kluit (compiler): Yukon Geology and exploration 1979-80; Indian and Northern Affairs Canada, p. 243-244.

Tipper, H.W., Woodsworth, G., and Gabrielse, H. (co-ordinators)
1981: Tectonic assemblage map of the Canadian Cordillera and adjacent parts of the United States of America; Geological Survey of Canada, Map 1505A.

Young, F.G.
1975: Stratigraphic and sedimentologic studies in northeastern Eagle Plain, Yukon Territory; in Report of Activities, Part B, Geological Survey of Canada, Paper 75-1B, p. 309-319.

12.

# *CECILIAPHYLLUM*, A NEW CHARACTOPHYLLID CORAL GENUS FROM THE UPPER DEVONIAN (LATE FRASNIAN) OF BRITISH COLUMBIA

Project 680093

R.A. McLean[1]
Institute of Sedimentary and Petroleum Geology, Calgary

*McLean, R.A.* ***Ceciliaphyllum,*** *a new charactophyllid coral genus from the Upper Devonian (late Frasnian) of British Columbia; in Current Research, Part C, Geological Survey of Canada, Paper 82-1C, p. 95-98, 1982.*

***Abstract***

***Ceciliaphyllum,*** *with type species* ***C. bastillense*** *sp. nov., is described from strata equivalent to the Ronde Member of the Southesk Formation at Surprise Pass, east-central British Columbia. At present, similar forms are known only from the Frasnian of Poland.*

## Introduction

Rugose corals belonging to the family Charactophyllidae, occurring in Middle Devonian strata of western Canada, have been studied in some detail (Pedder, 1972, 1982). However, the family has not been recognized previously in the Upper Devonian of the region, where its representatives are the commonest solitary corals present. The two most widespread charactophyllid genera in the Upper Devonian of western Canada are **Temnophyllum** Walther, 1928, and **Hunanophrentis** Sun, 1958. Collections made by the writer during the 1981 field season revealed the presence of another, undescribed, charactophyllid genus, the description of which is the subject of the present contribution.

The remainder of the large rugose coral fauna of the Frasnian of western Canada (over 100 species) is currently being studied by the writer in conjunction with A.E.H. Pedder of the Geological Survey of Canada.

Acknowledgments

I wish to thank A.E.H. Pedder for critical comments on the manuscript. Figure 12.1 was drafted by D. Brink. Photography was the work of W. Sharman of the Institute of Sedimentary and Petroleum Geology, Calgary.

## Biostratigraphy

The stratigraphy of the early Frasnian Flume Formation of the Wallbridge Mountain – Surprise Pass area (Fig. 12.1) was described by Maurin and Raasch (1972), but the younger Frasnian strata of the area have received little attention. A more detailed review of the stratigraphy of the area is in progress. For the present, it is simply noted that the carbonate unit at Surprise Pass, from which the material of **Ceciliaphyllum** described below was obtained, contains a diverse and well preserved rugose coral fauna. Elsewhere in the Rocky Mountains of British Columbia and Alberta, this fauna is representative of the carbonates of the upper unit of the Ronde Member of the Southesk Formation and equivalent beds, and also of the Kakisa Formation of the southern Northwest Territories. These strata contain the youngest Devonian coral faunas in western Canada and are overlain by units bearing early Famennian brachiopods (Sassenach, Palliser, and Trout River formations; Sartenaer, 1969).

## Systematic Paleontology

Morphological terminology used in this paper is basically that employed by Hill (1981). An addition is the term "intraseptal dissepiments" introduced by Wrzolek (1981), and discussed further below.

Family CHARACTOPHYLLIDAE Pedder, 1972

Genus **Ceciliaphyllum** gen. nov.

Derivation of name. After Cecilia Lake, in the region of the type locality.

Type species. **Ceciliaphyllum bastillense** sp. nov.

Diagnosis. Solitary charactophyllid coral with patellate corallum and peripherally everted dissepimentarium. Septa degenerate to isolated trabeculae or groups of trabeculae peripherally and become naotic; irregular lateral projections from septa are common, but true carinae apparently are not developed. Dissepiments are mainly small, globose, becoming more elongate peripherally where layers are everted; intraseptal and lateral dissepiments may be common, especially peripherally. Tabularium is narrow with arched series of tabulae.

[1] Amoco Canada Petroleum Co. Ltd., 444 – 7 Avenue S.W., Calgary, Alberta, T2P OY2

Discussion. The new genus is distinguished from other representatives of the Charactophyllidae (see Pedder, 1972; 1982) by its patellate growth form and eversion of the dissepimentarium with peripheral breakdown of the septa. Development of lateral projections on the septa of **Ceciliaphyllum** is a common feature of the charactophyllids, and is represented to varying degrees in the type species of **Charactophyllum, C. nanum** (Hall and Whitfield), as discussed by Watkins (1959, p. 82, Pl. 16, fig. 20) and Pedder (1982, p. 563). These projections do not appear to be normal carinae, but irregular extension of the coarse trabeculae from the plane of the septum. Species referrable to **Temnophyllum** Walther, 1928 **sensu lato** (see Pedder, 1972, p. 700) show closest similarities to **Ceciliaphyllum** in such septal structure, and also in extensive development of lateral dissepiments. **"Neostringophyllum" pronini** Soshkina, 1951, in particular, shows such features (Soshkina, 1951, Pl. 10, fig. 1-5) and was designated type species of a new genus, **Piceaphyllum**, by Rozkowska (1979). From the variability shown by this and related species, and in particular by the considerable variation shown in the very large assemblages from western Canada examined by the writer, it would seem preferable to consider **"N." pronini** as an extreme end member of the morphological scope of **Temnophyllum,** differing primarily from **Ceciliaphyllum** in lacking the everted dissepimentarium and patellate growth form.

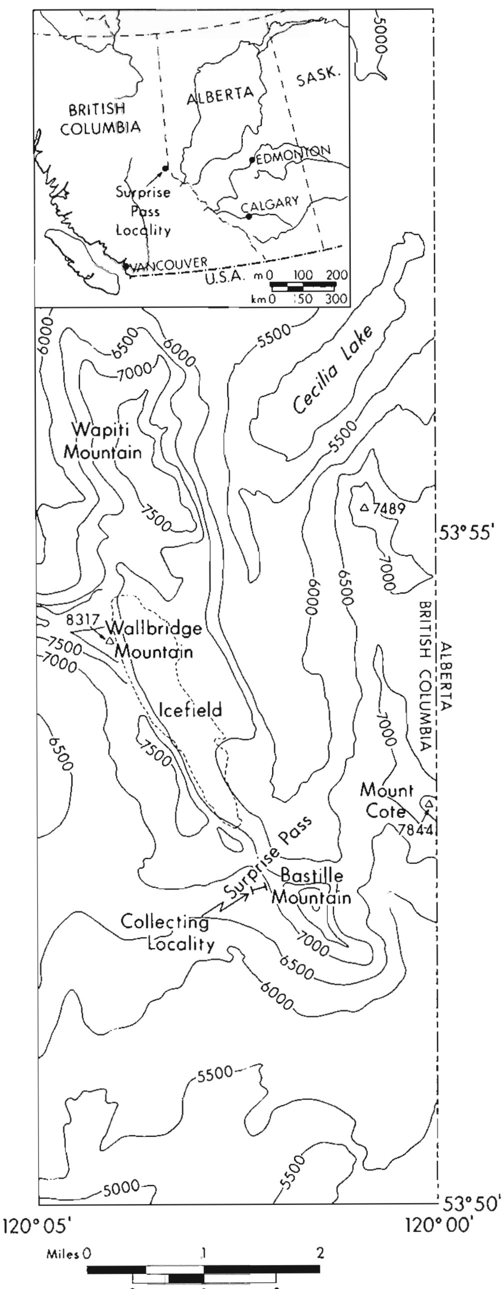


*Figure 12.1. Map of Wallbridge Mountain area, British Columbia, showing Surprise Pass collecting locality.*

The form described as **Craterophyllum ? humile** by Rözkowska (1979) from strata of the late Frasnian **gigas** zone of the Holy Cross Mountains, Poland, shows close similarities to **C. bastillense** and may be congeneric. It has a comparable growth form to **C. bastillense** and the peripheral septal structure appears similar (Rozkowska, 1979, p. 17, fig. 2a, b). According to Rozkowska, however, the septa do not extend into the tabularium, and the tabulae are more widely spaced and more complete. Although an adequate transverse section of the Polish species has not been illustrated, it is likely that it is a representative of **Ceciliaphyllum.** It shows some homeomorphic similarities to the Silurian cyathophyllid **Craterophyllum** Foerste, 1909 (see review of that genus by McLean, 1977, p. 16), but, like **C. bastillense,** is better grouped with the Charactophyllidae.

Some similarities to **Ceciliaphyllum** are exhibited by **Cyathophyllum diffusum** Wrzolek, 1981, also from strata of the late Frasnian **gigas** zone of the Holy Cross Mountains, Poland. It has a similar everted dissepimentarium, narrow tabularium and peripheral septal degeneration. However, **"C." diffusum** appears to have more complex septal structure, with development of extensive carinae or very long individual trabeculae (e.g. Wrzolek, 1981, Pl. 2, fig. 1, 2) throughout the dissepimentarium, and somewhat of a meshwork appearance, caused by mixing of trabeculae, carinae and lateral and intraseptal dissepiments in transverse section (Wrzolek, 1981, Pl. 2, fig. 1a; Pl. 5, fig. 1a), although the illustrations are not particularly clear. A few longer trabeculae are shown peripherally in the longitudinal section of the holotype of **Ceciliaphyllum bastillense** (Plate 12.1, fig. 2), but never to the extent developed in **"C." diffusum.** It is possible the two species may be congeneric, but further material of **C. bastillense** and more clearly illustrated transverse sections of **"C". diffusum** would be necessary to confirm this. Whatever the generic affinities of the Polish species may be, it does not appear to belong to **Cyathophyllum,** which is characterized by slender septa, with very well developed carinae and fine trabeculae (Birenheide, 1963, 1978).

Wrzolek (1981, p. 171) also introduced the term "intraseptal dissepiments" for those small dissepiments developed in the plane of a septum, the individual trabeculae either piercing the layers of these dissepiments or being interrupted by them. Such dissepiments are commonly developed in many diverse genera, such as the Silurian **Craterophyllum** and **Kymocystis,** and Devonian chonophyllids such as **Endophyllum** and **Iowaphyllum** and cystiphyllids including **Lekanophyllum** and **Digonophyllum.** Intraseptal dissepiments are generally developed peripherally in coralla of these genera, where septa tend to break down to individual trabeculae or groups of trabeculae. In parts of the corallum where the septa are more complete, the intraseptal dissepiments frequently become lateral dissepiments (see Plate 12.1, fig. 1, 3). Intraseptal dissepiments are a characteristic feature of **Ceciliaphyllum.**

**Ceciliaphyllum bastillense** sp. nov.

Plate 12.1, figures 1-5

Derivation of name. After Bastille Mountain, on whose flanks the type material was collected.

Material. Holotype GSC 68819, Ronde Member equivalent, Southesk Formation, approximately 81 m below top. South side of Surprise Pass, between Wallbridge and Bastille Mountains, British Columbia (see Fig. 12.1), 53°52'22"N latitude, 120°02'15"W longitude. Paratypes GSC 68820, 68821, same horizon and locality. Collected by R.A. McLean, 1981.

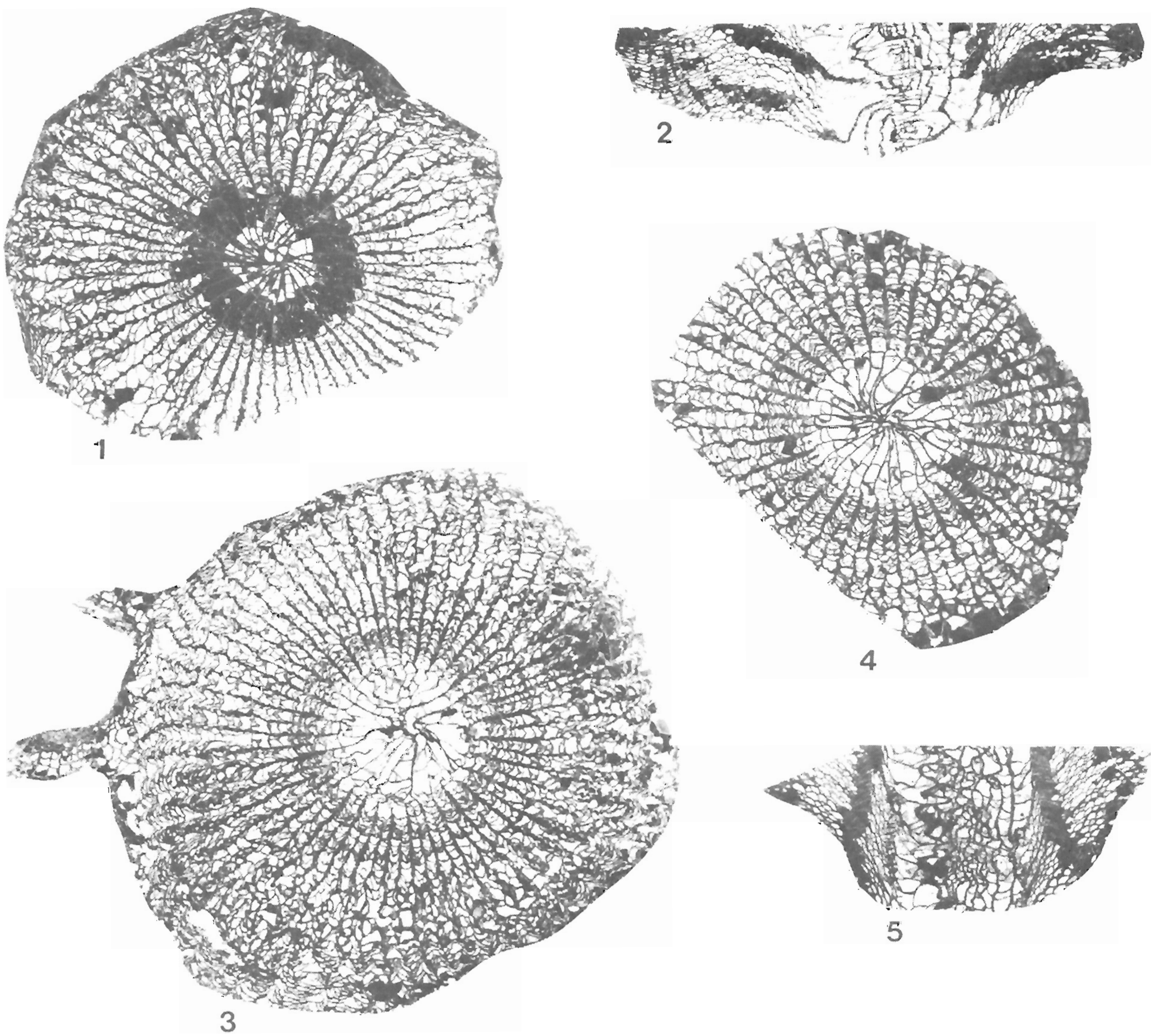


**PLATE 12.1**

Figures 1-5. **Ceciliaphyllum bastillense** gen. et sp. nov., x2.

1, 2. Holotype, GSC 68819, transverse and longitudinal sections; Surprise Pass, British Columbia.

3. Paratype, GSC 68820, transverse section; same locality.

4, 5. Paratype, GSC 68821, transverse and longitudinal sections, peripheral regions not preserved; same locality.

Diagnosis. As for genus.

Description. Corallum solitary, with one specimen (GSC 68820, Plate 12.1, fig. 3) showing a possible small calical offset. Coralla are patellate, but available material is fragmentary and height to width ratio cannot be accurately determined. Corallite diameter reaches 42 mm in the most complete specimen. Septal number ranges from 58-62, major septa extending to corallite axis where they are irregularly twisted, and minor septa barely extending into tabularium. Peripherally septa become naotic, being reduced to irregularly spaced, isolated trabeculae, or groups of trabeculae, enclosed by rows of intraseptal dissepiments. Convex side of intraseptal dissepiments is directed towards corallite margin in everted parts of corallite. More complete, adaxial portions of septa are variably lined by small lateral dissepiments. Nodes are unevenly developed on sides of septa, reflecting irregular projections of the generally coarse trabeculae. Septa show weak to moderate fusiform dilation in dissepimentarium, becoming very slender in tabularium. Dissepimentarium is broad, with dissepiments mainly small, globose to weakly elongate, in broadly flattened layers, which are variably everted at corallite periphery. Tabularium is narrow, about 0.3 of diameter of corallite, comprising arched series of well spaced, incomplete tabulae and tabellae.

Remarks. Similarities to **Ceciliaphyllum ? humile** (Rozkowska, 1979) and **Ceciliaphyllum ? diffusum** (Wrzolek, 1981) from the late Frasnian of Poland have been noted above under the discussion of the genus. No other described species shows any close similarities to **C. bastillense.**

## References


Birenheide, R.

1963: **Cyathophyllum** – und **Dohmophyllum** – Arten (Rugosa) aus dem Mitteldevon der Eifel; Senckenbergiana lethaea, Band 44, p. 363-458.

1978: Leitfossilien No. 2. Rugose Korallen des Devon; Gebrüder Borntraeger, Berlin, Stuttgart, vi + 265 p.

Hill, D.

1981: Treatise On Invertebrate Paleontology. Part F. Coelenterata. Supplement 1. Rugosa and Tabulata, ed. C. Teichert; Geological Society of America and University of Kansas Press, Boulder and Lawrence, v. 1, p. i-xl, 1-378, v. 2, p. i, ii, 379-762.

McLean, R.A.

1977: Early Silurian (Late Llandovery) rugose corals from western North Greenland; Grønlands Geologiske Undersøgelse, Bulletin 121, 46 p.

Maurin, A.F. and Raasch, G.O.

1972: Early Frasnian stratigraphy, Kakwa – Cecilia Lakes, British Columbia, Canada; Notes et mémoires, Compagnie Française des Pétroles (Total), No. 10, 80 p.

Pedder, A.E.H.

1972: Species of the tetracoral genus **Temnophyllum** from Givetian/Frasnian boundary beds of the District of Mackenzie, Canada; Journal of Paleontology, v. 46, p. 696-710.

Pedder, A.E.H. (cont.)

1982: **Chostophyllum**, a new genus of charactophyllid corals from the Middle Devonian of western Canada; Journal of Paleontology, v. 56, p 559-582.

Rozkowska, M.

1979: Contributions to the Frasnian tetracorals from Poland; Paleontologica Polonica, No. 40, p. 3-56.

Sartenaer, P.

1969: Late Upper Devonian (Famennian) rhynchonellid brachiopods from western Canada; Geological Survey of Canada, Bulletin 169, 269 p.

Soshkina, E.D.

1951: Pozdnedevonskie korally rugosa, ikh systematika i evolyutsiya. Trudy paleontologicheskogo Instituta, tom 34, 122 p.

Watkins, J.L.

1959: On the identity of the Devonian rugose coral genus **Diversophyllum** with **Tabulophyllum**, and notes on the genus **Charactophyllum**; Journal of Paleontology, v. 33, p. 81-82.

Wrzolek, T.

1981: Rugose coral **Cyathophyllum diffusum** sp. n. from the Frasnian deposits of the Holy Cross Mts.; Acta Geologica Polonica, v. 31, p. 169-175.

13. **TWO SAPPHIRINE LOCALITIES IN THE KRAMANITUAR COMPLEX, BAKER LAKE REGION, DISTRICT OF KEEWATIN**

Project 800008

Mikkel Schau
Precambrian Geology Division

*Schau, M., Two sapphirine localities in the Kramanituar complex, Baker Lake region, District of Keewatin; in Current Research, Part C, Geological Survey of Canada, Paper 82-1C, p. 99-102, 1982.*

### Abstract

*Sapphirine-enstatite-garnet-biotite rocks with alteration products occur within the granulite suite in the Kramanituar complex, north and east of Baker Lake. Estimates of metamorphic pressures and temperatures from geobarometry and geothermometry methods are contradictory; it is suggested that the presence or absence of quartz, may play an important, though as yet unspecified, part in yielding these inconsistent estimates of metamorphic conditions.*

## Introduction

The 60 km by 30 km Kramanituar complex (Unit 5, Schau et al., 1982; Schau and Ashton, 1979, 1980; Schau and Hulbert, 1977), located at the east end of Baker Lake, N.W.T., consists of a granulite suite and a meta-anorthositic gabbroic suite of late Archean age (Schau, 1980). The granulite suite consists of rocks composed mainly of various proportions of garnet, orthopyroxene, clinopyroxene, hornblende, antiperthitic plagioclase, and less abundant quartz, perthite, biotite and aluminosilicates, yielding generally basic to intermediate granulites. Layers composed almost wholly of bytownite or orthopyroxene, or felsic granulites, serve as marker horizons that show the structure to be a large extremely flattened anticline-syncline pair. Within the granulite suite rusty weathering, pale greenish blue, mica-bearing, poikiloblastic, garnetiferous rocks occur which, in thin section, are seen to contain sapphirine. Two localities from the complex are described below.

## Chemical Petrology

Localities A and B contain the same initial mineral assemblage. Thin sections are dominated by large inclusion-bearing garnet, set in a matrix of, and containing, biotite, enstatite, sapphirine, and minor calcic plagioclase and trace to accessory amounts of spinel, rutile, and zircon. The sapphirine locally contains small inclusions of spinel and especially near enstatite grains has a very fine wormy intergrowth of unidentified mineral(s). At most, but not all, contacts of sapphirine and enstatite small subidioblastic garnets are present.

Later very fine grained alteration products, in veins and along some grain boundaries, have obscured some textural relations. Phlogopite veinlets which cut across the earlier biotite occur throughout the thin section of the locality A specimen. The specimen from locality B, near a fault zone, contains a variety of brownish alteration products including intergrown amesite and white mica, corundum, chloritized biotite and other fine grained alteration products with low birefringence and moderate relief.

Polished thin sections from each locality were prepared and some mineral phases were analyzed with the electron microprobe; the results are summarized in Table 13.1.

## Discussion

Sapphirine localities are relatively rare in the northern portion of the Churchill Structural Province. Incomplete sampling may be the main reason that there is an apparent trend connecting the few known localities. A slightly arcuate east-west line links occurrences on Baffin Island at Lake Harbour and Pritzler Harbour (W.L. Davison, personal communication, 1973; Fraser et al., 1978), and northern New Quebec (Taylor, 1980), Somerset Island (Giquère, 1972), Daly Bay (Gordon, 1980) and Baker Lake (this study) on the mainland.

The petrogenetic implications of sapphirine-bearing assemblages are difficult to assess. Herd (1973) notes that they generally occur in granulite and amphibolite grade rocks which have undergone metasomatism.

Higgins et al. (1979), suggested that sapphirine with a greater magnesia-silica (2:2:1 variety) content is more stable at higher pressures and lower temperatures than that with more alumina (7:9:3 variety). If the analyses of Table 13.1 are recast in the manner suggested by Higgins et al. (1979) they have the form shown below. Based on 5 analyses of sapphirine from locality A varies between

$$(Mg_{3.3},\ Fe^{+2}_{0.4},\ Al_{4.1},\ Fe^{+3}_{0.4})\ (Si_{1.6}\ Al_{4.4})O_{20} \quad \text{and}$$

$$(Mg_{3.2},\ Fe^{+2}_{0.2},\ Al_{4.0},\ Fe^{+3}_{0.5})\ (Si_{1.5}\ Al_{4.5})O_{20}$$

Sapphirine from locality B (based on 9 analyses) is quite similar

$$(Mg_{3.2}\ Fe^{+2}_{0.4},\ Al_{4.0}\ Fe^{+3}_{0.4})\ (Si_{1.6}\ Al_{4.4})O_{20} \quad \text{and}$$

$$(Mg_{3.2}\ Fe^{+2}_{0.5},\ Al_{4.1}\ Fe^{+3}_{0.3})\ (Si_{1.6}\ Al_{4.4})O_{20}$$

These compositions are near the low silica (7:9:3) type and thus might indicate their formation under high temperatures and low pressures. Higgins et al. (1979) also calculated the relative distribution of magnesium and iron in sapphirine and enstatite. They concluded that the ratio $K_D = ((Fe^{+2}/Mg)$ sapphirine/$(Fe^{+2}/Mg)$ orthopyroxene) was relatively constant having a value of 0.65. If the structural mineral formulae derived above are used to calculate the $Fe^{+2}/Mg$ ratio in sapphirine, it varies between 0.06 to 0.16 whereas the Fe/Mg in enstatite is relatively constant (0.25-0.28); this gives rise to a large variation in $K_D$, (0.25 to 0.64). This range is only in part due to rounding errors; perhaps the method of assigning the ferrous/ferric ion ratio is not particularly precise; the sapphirine and enstatite, though apparently related by some reaction which yielded garnet, may not be in equilibrium with each other; or the presence of aluminum in both sapphirine and enstatite may affect the $K_D$ as calculated by Higgins et al. (1979).

Associated with sapphirine are minerals often used to estimate the pressures and temperatures at which they formed. Two such pairs are garnet – biotite and aluminous enstatite – garnet. If coexistence in a thin section with no reaction relations between the phases is a sufficient

Table 13.1

Analyses of selected minerals

Locality A (SMB S604c)

North shore of main Bowells Islands on Chesterfield Inlet near Cross Bay

| | INITIAL ASSEMBLAGES | | | | | ALTERATION | |
|---|---|---|---|---|---|---|---|
| | Poorly Zoned? Sapphirine | | Poorly Zoned Orthopyroxene | | Garnet | Early Biotite | Late Biotite |
| | from a | to b | from a | to b | | | |
| $SiO_2$ | 13.42 | 12.35 | 50.58 | 51.59 | 40.69 | 37.40 | 37.41 |
| $TiO_2$ | nf | nf | 0.11 | 0.10 | 0.02 | 3.07 | 2.86 |
| $Al_2O_3$ | 59.94 | 61.96 | 8.29 | 7.28 | 22.36 | 16.14 | 16.55 |
| $Cr_2O_3$ | nf | nf | 0.01 | 0.04 | 0.03 | nf | 0.01 |
| Fe as FeO | 7.66 | 7.27 | 13.69 | 12.96 | 19.21 | 13.45 | 9.53 |
| MnO | nf | nf | 0.05 | 0.05 | 0.31 | nf | nf |
| MgO | 18.43 | 17.62 | 27.78 | 28.88 | 16.56 | 16.93 | 20.34 |
| CaO | nf | nf | nf | nf | 1.38 | 0.09 | 0.12 |
| $Na_2O$ | nf | nf | nf | nf | nf | nf | 0.44 |
| $K_2O$ | nf | nf | nf | nf | nf | 8.41 | 8.03 |
| SUM | 99.45 | 99.20 | 100.51 | 100.90 | 100.56 | 95.49 | 95.29 |

Locality B (SMA 8-7001)

North shore of Chesterfield Inlet southwest of Tagiuk Lake

| | INITIAL ASSEMBLAGES | | | | ALTERATION | | | | |
|---|---|---|---|---|---|---|---|---|---|
| | Sapphirine | | Orthopyroxene | Garnet | Early Biotite | Later Biotite | Chloritized Biotite | Chlorite (Amesite) | Mainly Corundum |
| | from a | to b | | | | | | | |
| $SiO_2$ | 13.73 | 13.51 | 50.41 | 40.81 | 37.37 | 38.48 | 28.69 | 18.12 | 1.23 |
| $TiO_2$ | 0.02 | 0.05 | 0.06 | 0.02 | 3.58 | 3.57 | 0.03 | 0.03 | nf |
| $Al_2O_3$ | 60.13 | 60.27 | 8.38 | 23.22 | 14.78 | 15.23 | 19.47 | 37.82 | 91.22 |
| $Cr_2O_3$ | nf | nf | nf | 0.02 | 0.01 | nf | nf | 0.02 | nf |
| Fe as FeO | 8.03 | 7.78 | 13.18 | 19.88 | 12.26 | 8.93 | 11.21 | 9.16 | 0.74 |
| MnO | 0.03 | nf | 0.02 | 0.22 | nf | nf | nf | 0.03 | nf |
| MgO | 18.24 | 18.26 | 28.61 | 16.00 | 16.76 | 19.11 | 24.10 | 19.74 | 1.53 |
| CaO | nf | nf | nf | 0.23 | 0.03 | 0.02 | 0.12 | nf | 0.68 |
| $Na_2O$ | nf | nf | nf | 0.51 | 0.40 | nf | nf | nf | nf |
| $K_2O$ | nf | nf | nf | 0.01 | 9.56 | 9.74 | 1.03 | nf | nf |
| SUM | 100.18 | 99.87 | 100.66 | 100.41 | 94.86 | 95.48 | 84.65 | 84.92 | 95.40 |

Locality C

Garnet Biotite pair from Quartz-bearing rock
(SMA 6-0017) see Schau and Hulbert (1977)
for details

| | Garnet | | Biotite | |
|---|---|---|---|---|
| | from a | to b | from a | to b |
| $SiO_2$ | 39.30 | 38.48 | 39.95 | 37.62 |
| $TiO_2$ | 0.06 | 0.08 | 3.86 | 3.86 |
| $Al_2O_3$ | 22.15 | 21.83 | 17.96 | 18.20 |
| $Cr_2O_3$ | 0.11 | 0.06 | 0.02 | 0.06 |
| Fe as FeO | 27.16 | 27.21 | 12.23 | 11.48 |
| MnO | 0.28 | 0.25 | nf | nf |
| MgO | 10.22 | 9.48 | 14.43 | 15.51 |
| CaO | 0.92 | 1.49 | 0.10 | 0.09 |
| $Na_2O$ | 0.31 | 0.17 | 0.16 | 0.41 |
| $K_2O$ | nf | nf | 8.99 | 9.16 |
| SUM | 100.51 | 99.05 | 97.70 | 96.39 |

Analysis by M. Bonardi, GSC Laboratories; nf = not found

Table 13.2

Ratios derived from mineral analyses

| | Ferry-Spear distribution coefficient | $Al^{VI}/Al^{IV}$ in biotite* | Fe/Mg in garnet |
|---|---|---|---|
| Sapphirine-bearing | | | |
| Locality A | 0.58 | 0.35 | 0.65 |
| Locality B | 0.57 | 0.36 | 0.70 |
| Quartz-bearing | | | |
| Locality C | | | |
| ranges from a | 0.33** | 0.43 | 1.49 |
| to b | 0.26 | 0.55 | 1.61 |

* Calculated using 21 charges provided on elements on two sites (excluding the potash)

** Calculated using garnet a-biotite a and garnet b-biotite b.

indication of equilibrium between the minerals at one stage of their history, then using the methods of Ferry and Spear (1978) to calculate the temperature and Perkins et al., (1981) to calculate the pressure, one derives an estimate of about 30 kb at about 1575°C is obtained.

These conclusions are mutually contradictory. Sapphirine cannot be a low pressure variety and also be formed at 30 kb. The garnet-biotite and aluminous enstatite estimate is rather high compared to those derived for granulite terranes elsewhere. Newton and Perkins (1982) for instance indicate that many granulites give estimates near 9 kb and 800°C, values less than half those derived above.

One possible factor in the anomalous results is that bulk composition of the rock is very low in silica and is instead potassic, magnesian, and aluminous. Perhaps the presence of sapphirine and the absence of quartz has modified the activity of various components (such as silica) in the mineral assemblage.

To test this possibility a garnet-biotite pair (Locality C, Table 13.1) from a quartz-perthite-garnet-biotite-sillimanite-graphite rock was chosen. The two rocks types, i.e. the sapphirine-bearing and the quartz-bearing granulites, are thought to have a similar metamorphic history, hence similar distributions of iron and magnesium between biotite and garnet are the expected result. The calculations for the quartz-bearing rock yields a Ferry and Spear (1978) distribution coefficient of K=0.33 compared to K=0.58 for the sapphirine-bearing rock.

Comparisons of various ratios in each of the rocks analyses are shown in Table 13.2.

The differences in the Ferry Spear distribution coefficient between quartz-bearing and quartz absent parageneses may be due to variations in water activity or fluid compositions leading to variations in (OH) or ferric/ferrous iron ratios in biotite between the localities or more likely due to differences in bulk composition. Note the differences in the Fe/Mg ratios in the garnet and the variation in the proportion of aluminum present on the octahedral site of the biotite; the higher ratio present in the more siliceous rock.

Charlu et al. (1975), have suggested that extreme caution should be used in applying experimental data derived from synthetic pyrope to natural garnet solid solutions. Perhaps this geothermometer is an example where this caution is necessary.

If the anomalous relations described here are due to local inhomogeneities arising as a result of incomplete back reactions occurring as the granulites moved toward the surface, perhaps with more detailed work it will be possible to trace the later metamorphic history of the unit. The fine grained alteration products may well hold the necessary clues to this endeavour. The samples have been transferred to R.K. Herd who will pursue such a detailed study.

The mode of origin of such potassic, magnesian and aluminous rocks requires that they form isochemically from very unusual rocks such as alteration pipes with chlorite-alunite associations as suggested by Schreyer (1982). Alternatively they may form by metasomatic processes such as adding alkali rich fluids associated with a pegmatite to a chlorite schist (Herd, 1973). Iron-rich layers, some pyrrhotite-bearing, are common near Tagiuk Lake, to the east of the sapphirine localities. The hypothesis that the sapphirine localities are within metamorphosed alteration pipes of granulite grade will be actively pursued in the continuing petrographic study of rocks in the vicinity of Tagiuk Lake.


### Acknowledgments

Thanks to Ken Ashton whose persistent curiosity is directly responsible for the discovery of these localities and to R.K. Herd for introducing the writer to the world of sapphirine. E. Froese commented on an earlier draft of the paper and his help is much appreciated. The mistakes are those of the author.


### References


Charlu, T.V., Newton, R.C., and Kleppa, O.J.
1975: Enthalpies of formation at 970°K of compounds in the system $MgO-Al_2O_3-SiO_2$ from high temperature solution calorimetry; Geochimica et Cosmochimica Acta, v. 39, p. 1487-1497.

Ferry, J.M. and Spear, F.S.
1978: Experimental calibration of the partitioning of Fe and Mg between biotite and garnet; Contributions to Mineralogy and Petrology, v. 66, p. 113-117.

Fraser, J.A., Heywood, W.W., and Mazurski, M.A.
1978: Metamorphic map of the Canadian Shield; Geological Survey of Canada, Map 1475A.

Giquère, J.F.
1972: Coexisting pyroxenes in some granulite facies gneisses from Somerset Island; Canadian Mineralogist, v. 11, p. 548-551.

Gordon, T.M.
1980: Geology of the Daly Bay Complex, District of Keewatin; Program with Abstracts, v. 5, GAC-MAC, p. 56.

Herd, R.K.
1973: Sapphirine and kornerupine occurrences within the Fiskenaesset complex; Grønlands Geologiske Undersøgelse Rapport no. 51, p. 65-71.

Higgins, J.B., Ribbe, P.H., and Herd, R.K.
1979: Sapphirine I. Crystal chemical contributions; Contributions to Mineralogy and Petrology, v. 68, p. 349-356.

Newton, R.C. and Perkins, D. III.
1982: Thermodynamic calibration of geobarometers based on the assemblages garnet-plagioclase-orthopyroxene-(clinopyroxene)-quartz; American Mineralogist, v. 67, p. 203-222.

Perkins, D. III, Holland, T.J.B., and Newton, R.C.
1981: The $Al_2O_3$ contents of enstatite in equilibrium with garnet in the system $MgO-Al_2O_3-SiO_2$ at 15-40 Kbar and 900°-1600°C; Contributions to Mineralogy and Petrology, v. 78, p. 99-109.

Schau, M.
1980: Zircon ages from a granulite-anorthosite complex and a layered gneiss complex northeast of Baker Lake, District of Keewatin; in Loveridge, W.D., Rubidium-Strontium and Uranium-Lead Isotopic Age Studies, Report 3, in Current Research, Part C, Geological Survey of Canada, Paper 80-1C, p. 237-238.

Schau, M. and Ashton, K.E.
1979: Granulite and plutonic complexes northeast of Baker Lake, District of Keewatin; in Current Research, Part A, Geological Survey of Canada, Paper 79-1A, p. 311-316.

1980: Geological map of the granulite and anorthosite complex at the southeast end of Baker Lake, 56D1, 56C4, parts of 55M16 and 55N13; Geological Survey of Canada, Open File 712.

Schau, M. and Hulbert, L.
1977: Granulites, anorthosites and cover rocks northeast of Baker Lake, District of Keewatin; in Report of Activities, Geological Survey of Canada, Paper 77-1A, p. 399-407.

Schau, M., Tremblay, F., and Christopher, A.
1982: Geology of Baker Lake map area, District of Keewatin: a process report; in Current Research, Part A, Geological Survey of Canada, Paper 82-1A, p. 143-150.

Schreyer, W.
1982: Fuchsite aluminum silicate rocks in Archean greenstone belts; Geologische Rundschau, Band 71, p. 347-360.

Taylor, F.C.
1980: Two sapphirine localities in New Quebec; Canadian Mineralogist, v. 18, p. 373-374.

## CHEMICAL FORMS OF COPPER IN FALLEN SNOW

Project 740081


M.H. Timperley[1] and I.R. Jonasson
Resource Geophysics and Geochemistry Division


It has been proposed (Jonasson, 1973; Jonasson and Allan, 1972) that trace metals can move upwards from soils overlying mineralized ground into fallen snow cover. The migration mechanism was considered to be ionic movement upwards via pellicular water (films) on packed ice crystallites. The possibility that chelates of fulvic or humic acids were involved was not discounted.

This work attempts to establish the chemical forms of copper in snow gathered from the same rural sample sites described in the previous study (Jonasson, 1973).

Snow samples (A and B) were collected at two locations over mineralized ground from a depth of 5 to 15 cm above ground level in snow cover approximately 1 m deep. Both samples were thawed and filtered through acid-washed glass wool. The pH of A and B (25°C) were 5.2 and 5.4 respectively. Total dissolved solids and dissolved volatile solids were 4.6 mg/L and 1.7 mg/L in A, and 7.3 mg/L and 3.0 mg/L in B; total dissolved organic carbon was less than 1 mg/L in each sample.

Total analysis, using a Perkin Elmer Heated Graphite Atomizer, gave 30 ± 5 ug/L copper in A and 34 ± 5 ug/L copper in B. A cupric ion specific electrode (Orion 94-29-00) with a double-junction reference electrode (Orion 90-02-00) showed activities equivalent to 20 ± 3 ug/L of cupric ion in A and 25 ± 4 ug/L in B relative to standards at pH 5. Standard addition of a cupric sulphate solution at pH 5 to the snow samples and subsequent determination of cupric ion (electrode) showed that, within analytical error, all the added copper remained as the cupric ion for a period of at least 48 hours.

These results indicate that between 50 and 90 per cent of the copper present in the snow existed as the cupric ion. This situation is consistent with a simple pH controlled system rather than an equilibrium between copper and organic ligands. The predominant equilibria between copper and water involve the species $(Cu(OH))^+$, and from equilibrium data (Sillen and Martell, 1964) the ratio of this species to total copper at pH 5 is approximately 0.04, confirming the predominance of cupric ion as was observed.

Copper-organic acid chelates of the type expected to occur in soil leachates have pK values greater than about 8 and consequently would remain essentially undissociated at pH 5, i.e., no cupric ion would be detected. If pH is the only factor involved, then the same equilibrium should predominate in the soil leachate.

Approximately 500 g of fresh soil from below the snow sample sites was shaken with one litre of water for 12 hours. After centrifuging (100 g for 60 minutes) the supernate showed a total copper concentration (Heated Graphite Atomizer) of 100 ± 5 µg/L, a pH of 7.8 and cupric ion activity equivalent to 38 ± 5 µg/L (relative to standards at pH 5).

At pH 7.8, the ratio of cupric ion to total copper is calculated to be approximately 0.5 (assuming $(Cu(OH))^+$, is the only other species of significance) which is in reasonable agreement with the result obtained, 0.38 ± 0.07.

It is concluded that in the system studied, copper exists predominantly as both the cupric ion and the $(Cu(OH))^+$ species in the soil leachate. On ablation from the soil surface, these ions move up into the snow via pellicular water where in the lower pH environment (presumably controlled by atmospheric $CO_2$; $(HCO_3^-)$ = 0.25 and 0.75 mg/L for A and B respectively) dissociation occurs to produce a predominance of cupric ions. The presence of cupric ions at pH 5 and 7.8 is believed to discount copper chelation as a significant transport mechanism in the present system.


### Acknowledgment

We appreciate the help of Alice I. MacLaurin with the analytical work.


### References


Jonasson, I.R.
1973: Migration of trace metals in snow; Nature, v. 241, no. 5390, p. 447-448.

Jonasson, I.R. and Allan, R.J.
1972: Snow: a sampling medium in hydrogeochemical prospecting in temperate and permafrost regions; in Geochemical Exploration, 1972, ed. M.J. Jones, Proceedings, 4th International Symposium Geochemical Exploration (London, U.K.), p. 161-176.

Sillen, L.G. and Martell, A.E.
1964: Stability constants; Chemical Society, London, Special Publication, v. 17, 754 p.


[1]Department of Scientific and Industrial Research, Taupo, New Zealand


*From: Scientific and Technical Notes in Current Research, Part C; Geol. Surv. Can., Paper 82-1C*

## CORING OF FROZEN POND SEDIMENTS, EAST-CENTRAL ELLESMERE ISLAND: A PROGRESS REPORT

Project 750063

W. Blake, Jr.
Terrain Sciences Division

### Introduction

The program of coring frozen pond sediments, initiated in 1978, has been continued in succeeding field seasons. The aim at first was to sample shallow ponds below the limit of Holocene marine submergence in order to obtain chronological and paleoecological information. The region is characterized by steep and rough terrain and, unlike other parts of Ellesmere Island (cf. Blake, 1975), the few pockets of raised beaches are generally lacking in driftwood, hence dating the basal organic pond sediment was one way of studying the pattern of emergence. The work has been expanded, in 1981 and 1982, to include ponds at higher elevations (Fig. 1). These ponds also freeze to the bottom each winter, and they cannot be sampled with conventional lake coring equipment because the basal organic sediments never thaw. This note summarizes highlights of field results obtained since 1978, when a preliminary report was issued (Blake, 1978). Laboratory work is under way on various facets of a number of cores, but this is not expected to be completed for several years.

### Methods and Equipment

The coring unit used continues to be a SIPRE (CRREL)-type auger powered by a 3.4 h.p. gasoline motor and equipped with a reduction gear box (Stihl model 4308; Fig. 2). New 7.6 cm-diameter coring barrels of stainless steel have been available since 1981, thus removing the danger of sample contamination by paint chipping off the normal mild steel barrels. As in older models, the removable teeth are of tungsten carbide so that it is possible to cut through pebbles and cobbles. The 1 m-long aluminum extension rods used earlier have been replaced by heavier duty magnesium-zirconium rods of the same length. Increments up to 40 cm in length can be accommodated in the core barrel, although in practice the effective length is restricted to about 30 cm because of the accumulation of cuttings in the top of the barrel above the core.

Additional information about the Stihl motor unit and associated coring equipment is given in the detailed report by Veillette and Nixon (1980), but a few modifications to equipment deserve mention here:

1. The handle attached to the motor has been cut in half and the two pieces may be unbolted and detached for shipping in a box measuring 33x69x76 cm instead of 53x64x122 cm.
2. Ancillary equipment used routinely now includes a 23 cm-long aluminum wedge designed to attach to the extension rods. This wedge is useful for breaking off the core downhole in cases where this is not done while coring is under way.
3. The core retriever (Fig. 3), which also attaches to the extension rods, is used to recover core increments from deeper than approximately 70 cm (arm length). Instead of the usual pieces of spring steel at the base for gripping the core, the modified core retriever is equipped with four pivoted teeth set in a ring (all of stainless steel). The tips of these teeth protrude about 1 mm when the teeth are folded in, and when the retriever is rotated in a counterclockwise direction, the teeth bite into the frozen sediment, enabling recovery of the core. The advantages of this design over the spring steel blades are: (a) shorther increments can be retrieved and (b) the increased strength allows removal of heavy, long core increments of inorganic sediments.

Whenever possible a four-man team operated the coring unit, but on trips by Bell 206B helicopter to more distant sites, only three persons could be accommodated, as the coring unit occupied the middle section of the back seat.

After recovery, measurement of core length, and brief notes on stratigraphy, each core increment was wrapped individually in thin aluminum foil, the top and bottom were marked, and the core was placed in a plastic bag. The cores were either stored in the shade (below 0°C) or were packed directly in an insulated metal box (Coleman 40-quart size). At base camp the insulated boxes were kept in a hollowed-out snowbank. After transport to Resolute via Twin Otter aircraft the insulated boxes were stored in a freezer, and en route to Montreal by commercial aircraft the boxes were placed in the unheated belly of the plane.

In Ottawa subsampling is done on a diamond saw mounted inside a walk-in freezer. The increment to be used for an age determination is allowed to thaw, and if samples for diatom and pollen analysis have not been extracted from the core in frozen state, they are taken at this stage. In some cases the entire increment is examined for insect remains and plant macrofossils, then it is oven-dried and sieved through a #18 screen (1.00 mm mesh). Any additional plant macrofossils, pebbles, etc. that are retained on the screen are saved, and the <1.00 mm fraction is utilized for dating. Usually a 3 to 5 cm-long increment provides sufficient material for a radiocarbon age determination.

### Results

During May 1978 cores of frozen sediment were recovered from five ponds on the Cape Herschel peninsula (Blake, 1978). Over the next four years additional, longer, cores were collected at two of these sites ('Moraine pond' and 'Camp pond'), and 13 other ponds were sampled. The locations of the ponds are indicated in Figure 1 and details of the coring sites are listed in Table 1.

In the laboratory a permanent record of most cores, expecially those that are to be sampled for dating or for paleoecological analysis, is made in the form of X-rays. Figure 4 illustrates two increments from a 146 cm-long core taken in Skraeling Island pond on May 26, 1981. Near-basal organic detritus from 83 to 87 cm below the ice/sediment interface gave an age of 6650 ± 70 years (GSC-3391). A small amount of organic matter was present in the next lower increment, at 87 to 91 cm depth, but the main characteristic of this horizon was the sharp increase in inorganic material and corresponding decrease in noncarbonate carbon (from 22% at 83.0 to 83.5 cm depth to 2% at 86.5 to 87.0 cm depth); one gneissic cobble cut through by the corer had dimensions that exceeded 4x2x2 cm (cf. Fig. 4).

An age in the range of 6600 to 6700 years for the onset of organic accumulation seems reasonable in view of the fact that the surface of the pond (Fig. 5) is at an elevation of 76 m above high tide level (based on levelling from the ice foot), i.e., as shown below, at an elevation such that the sea <u>may</u> have encroached into the basin in early Holocene time, although unequivocal evidence of such a transgression has not been found. Some 18 km to the west-southwest of Skraeling Island well preserved **Mya truncata** valves (at 50 m elevation) in deltaic sediments near the head of Alexandra Fiord are 7000 ± 70 years old (GSC-3288). Contemporaneous sea level was an unknown amount higher; prominent terraces cut into the delta are 15 and 20 m above the level at which the shells occurred (all elevations at this site were measured with a Wallace and Tiernan surveying altimeter).

From: *Scientific and Technical Notes in Current Research, Part C; Geol. Surv. Can., Paper 82-1C*

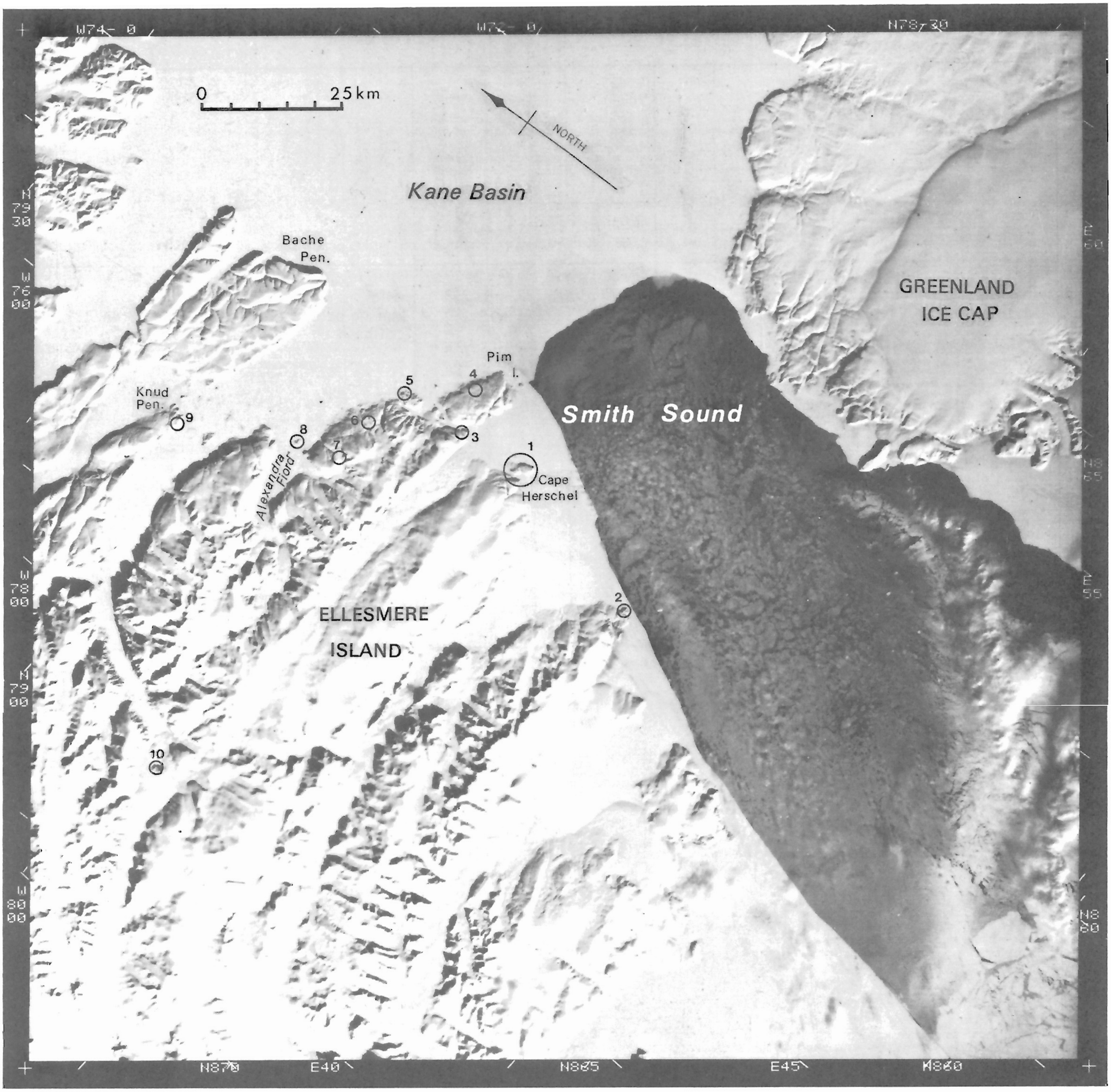


*Figure 1.* LANDSAT image showing sites where cores of frozen sediment have been recovered (refer to Table 1). Note the development of the North Water in Smith Sound on April 4, 1973. Image E-10255-18054, spectral band 7.

Table 1

Summary of core sites and frozen sediment cores

| Locality (number refers to Figure 1) | Elevation m a.s.l. | Snow thickness (cm) — At time of best coring results | Ice thickness (cm) — At time of best coring results | Maximum length of core recovered (cm) | Remarks |
|---|---|---|---|---|---|
| 1. Pond in col, C. Herschel plateau | 135 | 15 | 25 | 223 | |
| 1. Moraine pond, C. Herschel | 82 | 137 | 103 | 585 | Marine pelecypod shells in sand within 1.5 m of base |
| 1. Camp pond, C. Herschel base | 58 | 8 | 19 | 139 | |
| 1. Willow pond, C. Herschel | 8 | 13 | 24 | 84 | |
| 1. Beach ridge lagoon, Elison Pass | 25 | 25 | 19 | 27 | |
| 1. Pond in stream valley, west of C. Herschel peninsula | 135 | 40 | 10 | 43 | |
| 2. C. Isabella | 180 | 0 | 36 | 63 | No appreciable amount of organic sediment |
| 3. Rice Strait pond | 105 | 30 | 16 | 185 | |
| 4. Pond, north slope Pim Island | 285 | 30 | 15 | 155 | No appreciable amount of organic sediment |
| 5. C. Rutherford pond | 165 | 5 | 30 | 51 | |
| 6. Saate Glacier pond | 325 | 25 | 15 | 62 | |
| 7. Pond in col, valley SE of Alexandra Fiord | 525 | 12 | 28 | 73 | No appreciable amount of organic sediment |
| 8. Skraeling Island pond | 76 | 38 | 1 | 162 | |
| 9. South shore Knud Peninsula | 80 | 10 | 25 | 15 | No appreciable amount of organic sediment |
| 10. Stygge Glacier nunatak pond | 340 | 10 | 77 | 348 | Unfrozen saline layer at varying depth, 1.7 to 2.2 m |

***Figure 2.*** *Coring underway with the Stihl motor unit at 'Willow Pond', north side of Cape Herschel peninsula. An 84 cm-long core was collected at this site, 8 m a.s.l. Pim Island is in the distance. May 25, 1981. GSC 203670-0*

**Figure 3.** *Detail of the core retriever and a section of core from 'Moraine pond' at Cape Herschel. Note the score marks made by the teeth as the retriever was pushed down over the core. May 19, 1981. GSC 203670-P*

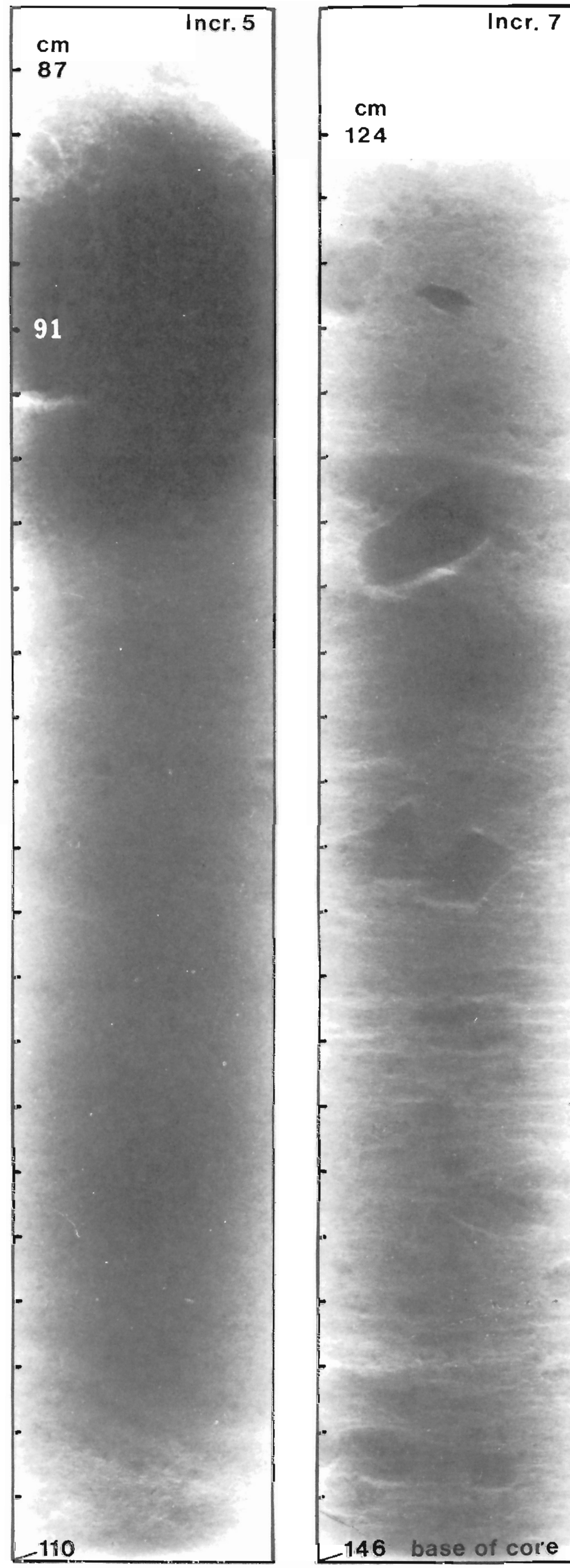


**Figure 4**

*X-radiographs of core 1 (1981) from Skraeling Island pond. At the top of Increment 5, dark greyish brown (2.5Y 4/2) organic sediment at 83 to 87 cm depth gave an age of 6650 ± 70 years (GSC-3391). The basal organic sediment is visible at the 87 cm mark as it passes into pebbles and cobbles which make up much of the zone (with less water) down to 93 cm. Below that level, grey (5Y 5/1) sand with a few pebbles occurs. Increment 7 shows the basal section of the core composed of light olive grey (5Y 6/2) sand with numerous pebbles.*

***Figure 5.*** *View westward of Skraeling Island and Alexandra Fiord. The location of the pond is indicated with an arrow. May 27, 1981. GSC 203670-S*

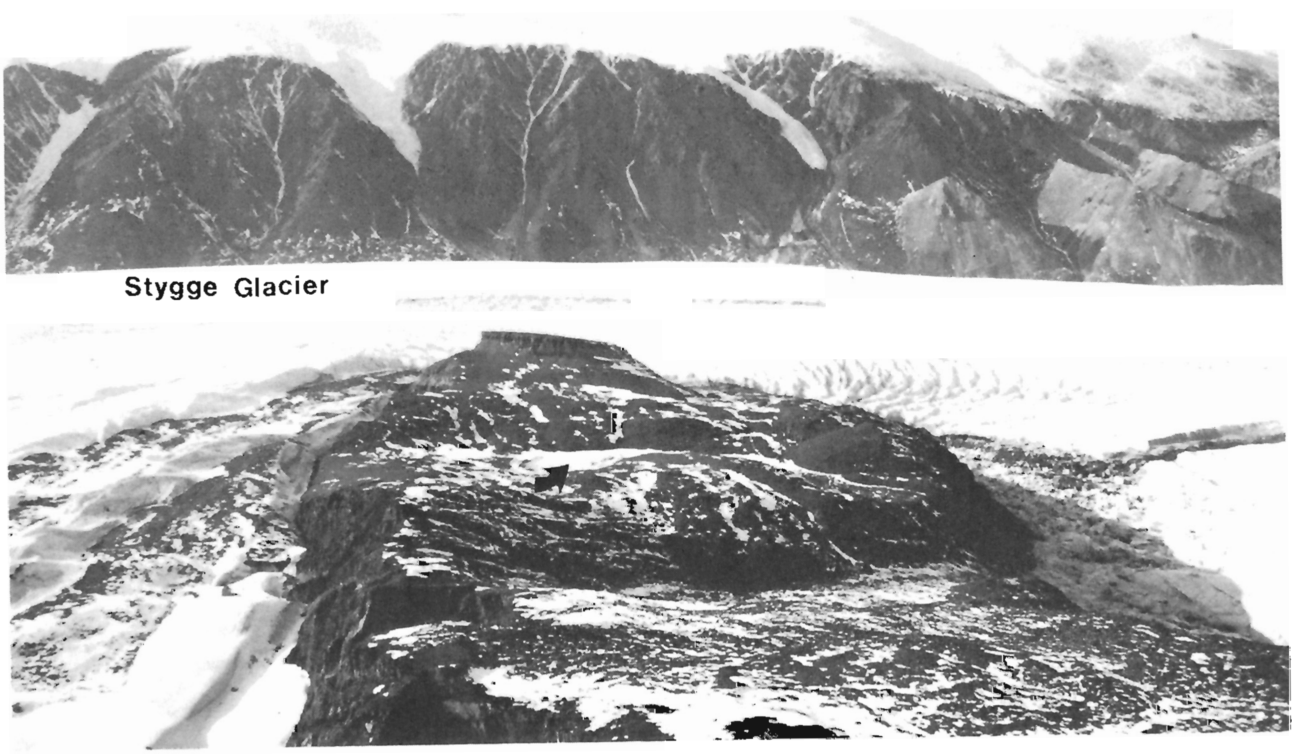


***Figure 6.*** *View north along Stygge Glacier nunatak. Note the dolomite capping the hilltop north of the pond (arrow). May 27, 1981. GSC-203670-Q*

The longest core collected was obtained in 1981 from a moraine-dammed pond at 82 m a.s.l. on the north side of the Cape Herschel peninsula. In earlier attempts to core the pond we had been misled by the snow that drifted into this hollow; hence we drilled too close to the southern edge and the cores recovered were only approximately 140 cm (1978) and 170 cm (1979) in length. The 1979 hole was marked by a stake, and its position was surveyed later that summer. From this reference point, a new hole was drilled in 1981 nearer to the centre of the pond and a 585 cm-long core was recovered; a large cobble/boulder or bedrock prevented further penetration. Ice was encountered at several horizons in the hole, but most interesting was the fact that marine shell fragments were recovered from the sandy core cuttings somewhere in the zone between 450 and 550 cm. The sample was too small for dating, but it may be that this shell-bearing sand is the same facies that outcrops to the northwest along the stream draining the pond; there **Macoma calcarea** occurs with **Mya truncata**, the latter dated at 7210 ± 90 years (GSC-2525, 52 m a.s.l.; Blake, 1978).

Two other coring sites are worthy of mention. In 1982 a small pond near the north coast of Pim Island was cored as there are no large lakes on this part of the island. It was hoped that suitable material for radiocarbon dating could be obtained to supplement the sediment cores that have been recovered from three lakes in the southern part of the island (Blake, 1981). After several attempts encountered rocks immediately under the ice, a hole was drilled to 155 cm, at which depth either bedrock or a boulder prevented further penetration. Although only a few centimetres of organic material were present at the top, this core does show that at least 150 cm of till is present at this locality, and it will allow analysis of an unweathered sample. In general the till cover on Pim Island and Cape Herschel is thin (in many places <30 cm), and large areas are characterized by exposed bedrock. At a depth of 120 cm a well polished and striated dolomite cobble (7x5x4.5 cm) was neatly cut through by the corer.

The pond on Stygge Glacier nunatak (Fig. 6) is unusual in that it is the only one cored where an unfrozen layer was encountered at depth. Salinity measurements on the fluid which melted out of the increments at 176.5 to 181 cm and 181 to 188 cm depth (Increments 10 and 11, Core 1, 1981) gave values of 19‰ and 13.5‰, respectively. Presumably the zone in which fluid is most concentrated is even more saline. The pale yellow (5Y 7/4) viscous fluid has an exceptionally strong and penetrating odour, and on evaporation crystals of halite form. Similar salinities were recorded in a brackish water pool (the sea enters at high tide) near the northwest tip of the Cape Herschel peninsula, but none of the higher ponds cored in that area – ponds known to have been submerged in Holocene time – exhibits unfrozen saline layers. There is no indication that trapped marine waters are present in the pond (at 340 m a.s.l.) on Stygge Glacier nunatak, nor is there any evidence, such as marine shells in till on the surrounding slopes, to indicate that sediment from the seabottom has been dragged to this elevation by an advance of Stygge Glacier.

One feature of Stygge Glacier nunatak which distinguishes it from other sites where frozen sediments have been cored is the presence of a capping of dolomite on the hilltop north of the pond. The dolomite overlies the crystalline basement, here consisting of retrograded orthopyroxene granite (Frisch and Morgan, in press). It is possible that some evaporites are present in the sedimentary sequence as well, such as those reported by Christie (1967a) from the Bache Peninsula region, and if so these rocks may well be the source of the salts that are now concentrated in the pond below. An analysis of the surface water collected at the west end of the pond (in a moat <5 m wide) at the same time that the frozen sediments near the centre of the pond first were cored (May 29, 1981) gave values for dissolved sodium, chloride, and sulphate (9.1, 12.6, and 17.4 mg/L, respectively; NAQUADAT Detailed Report, Water Quality Branch, Environment Canada, Calgary) that are higher than normal for ponds and lakes above the limit of Holocene marine submergence on the Shield rocks in the region (cf. Environment Canada, in press).

In addition, at the eastern end of the same pond, the ground in places has a coating of gypsum crystals, and similar efflorescences (mainly thenardite) are known from many areas of the Arctic (e.g., Christie, 1967b; Davies, 1974; Tedrow, 1977). Nichols (1969) reported a variety of surface efflorescences in Inglefield Land, Greenland; for instance, bands composed mainly of NaCl occurred on the slopes of a dissected delta. Watts (1981) reported efflorescences of sodium salt, including thenardite, adjacent to a pond close to sea level on the north shore of Knud Peninsula, and the writer has also collected at this site. One possible source that Watts suggested for the salts was the Paleozoic sequence exposed nearby, and in this sense the site is similar to Stygge Glacier nunatak. Sea spray (cf. Gorham, 1958) would not seem to be a source of the salts at Stygge Glacier nunatak, for the site is not subject to moisture laden winds in the way that Cape Herschel is. The latter site, because of the sea spray carried over the peninsula by the northerly and southerly winds in the area of the North Water (cf. Fig. 1; Ito, 1981), has one of the highest corrosion rates in the Arctic (Biefer, 1980).

### Acknowledgments

Generous logistical support, without which this work would not have been possible, has been provided by the Polar Continental Shelf Project (G.D. Hobson, Director). The Project's field staff in Resolute has been helpful at all times, and a particular debt is owed to Emile Gravelle for the care he has taken with storing and shipping the frozen cores. Many people have participated in the Cape Herschel project, and all have contributed to its success. In addition to the individuals mentioned in the 1978 report on coring, I would like to thank especially my colleague F.M. Nixon; the longer cores obtained in 1981 and 1982 are directly attributable to his expertise in frozen ground coring techniques. Those responsible for the major share of assistance in the arduous work of drilling were O. Salvigsen (Norsk Polarinstitutt) and G.M. MacDonald (Scarborough College) in 1981, and R.L. Christie (Institute of Sedimentology and Petroleum Geology, Calgary) in 1982. General assistance was provided by Anne Snider (née Baker) in 1981 and by Louise Légère in 1982. K.R. Meleskie and D. Lusk of the Non-Destructive Testing Laboratory, CANMET, provided access to their X-ray equipment and darkroom facilities. The GSC's Instrument Development Shop (R.J. Thibedeau, Head) has constructed several new items of coring equipment; their assistance is gratefully acknowledged. Mineral identifications (X-ray diffraction) have been carried out by A.C. Roberts of the Mineralogy Section. D.A. Hodgson provided helpful comments on the manuscript.

## References


Biefer, G.J.
1980: Survey of atmospheric corrosivity in the Canadian Arctic; Canada Centre for Mineral and Energy Technology, Physical Metallurgy Research Laboratories Report MRP/PMRL 80-13 (TR), 28 p.

Blake, W., Jr.
1975: Radiocarbon age determinations and postglacial emergence at Cape Storm, southern Ellesmere Island, Arctic Canada; Geografiska Annaler, v. 57A, p. 1-71.

1978: Coring of Holocene pond sediments at Cape Herschel, Ellesmere Island, Arctic Archipelago; in Current Research, Part C; Geological Survey of Canada, Paper 78-1C, p. 119-122.

1981: Lake sediment coring along Smith Sound, Ellesmere Island and Greenland; in Current Research, Part A; Geological Survey of Canada, Paper 81-1A, p. 191-200.

Christie, R.L.
1967a: Bache Peninsula, Ellesmere Island, Arctic Archipelago; Geological Survey of Canada, Memoir 347, 63 p.

1967b: Reconnaissance of the surficial geology of northeastern Ellesmere Island, Arctic Archipelago; Geological Survey of Canada, Bulletin 138, 50 p.

Davies, W.E.
1974: Geological and limnological factors of cold deserts; in Polar Deserts and Modern Man, ed. T.L. Smiley and J.H. Zumberge; University of Arizona Press, Tucson, Arizona, p. 53-61.

Environment Canada
Detailed surface water quality data, Northwest Territories, 1977-1979; Inland Waters Directorate, Western and Northern Region, Water Quality Branch. (in press)

Frisch, T. and Morgan, W.C.
Geology, Prince of Wales Mountains, Ellesmere Island; Geological Survey of Canada, Map 1572A. (in press)

Gorham, E.
1958: The influence and importance of daily weather conditions in the supply of chloride, sulphate and other ions to fresh waters from atmospheric precipitation; Philosophical Transactions of the Royal Society of London, Series B, Biological Sciences, v. 241, no. 679, p. 147-178.

Ito, H.
1981: On the mechanics of the fast ice in the North Water area; Zurcher Geographische Schriften (Geographisches Institut, Eidgenössische Technische Hochschule, Zurich), Heft 2, 93 p.

Nichols, R.L.
1969: Geomorphology of Inglefield Land, North Greenland; Meddelelser om Grønland, Bd. 188, nr. 1, 109 p.

Tedrow, J.C.F.
1977: Soils of the Polar Landscapes; Rutgers University Press, New Brunswick, New Jersey, 638 p.

Veillette, J.J. and Nixon, F.M.
1980: Portable drilling equipment for shallow permafrost sampling; Geological Survey of Canada, Paper 79-21, 35 p.

Watts, S.H.
1981: Near-coastal and incipient weathering features in the Cape Herschel - Alexandra Fiord area, Ellesmere Island, District of Franklin; in Current Research, Part A; Geological Survey of Canada, Paper 81-1A, p. 389-394.

# AMBIENT pH LEVELS IN ENVIRONMENTAL SAMPLES FROM THE HIGH ARCTIC

Project 750063

R. McNeely
Terrain Sciences Division

## Introduction

There has been an increasing awareness of the long-range transport of pollutants in the atmosphere. Observations of an "arctic haze" have become more frequent in recent years (Kerr, 1979, 1981; Heintzenberg et al., 1981) and concerns about acidic precipitation in sensitive terrains are becoming increasingly valid. During the 1981 field season, as an adjunct to the Cape Herschel Project (Ellesmere Island; Blake, 1978), a variety of media (precipitation – rain, mixed snow and rain, and rime frost; and surface waters – ponds and lakes) was sampled to provide baseline limnological information. The sites sampled are outlined in Figure 1. Because the pH of water samples may change during storage, especially poorly buffered samples, the pH of each sample was measured in the field as soon as possible after collection. A subsequent measurement of pH was performed in the laboratory after the samples had been stored for up to six months.

## Methods

The rain and mixed precipitation samples were collected at Cape Herschel base camp (site 15) either in a standard, copper rain gauge or in stainless steel trays. All collectors were thoroughly rinsed with distilled water and air-dried prior to each precipitation event. The rain or melted snow samples were transferred to clean polyethylene bottles for shipment to the laboratory. The surface water samples were collected in clean 1 L polyethylene bottles.

A portion of each sample was transferred to a clean beaker and the pH measured. Both field and laboratory pH values were measured potentiometrically. The field measurements were made with a portable "Digi-Sense" pH meter buffered at pH 4 and 7 for each measurement. The laboratory measurements of pH and total alkalinity were carried out in the Water Quality Branch laboratories in Calgary and Burlington on portions of the water samples that had been stored at room temperature in tightly capped polyethylene bottles (Environment Canada, 1979).

## Results and Discussion

Table 1 lists thirty-six data pairs of pH measurements on different media. Also included in the table are total alkalinity values which are indicators of the potential buffering capacity in the samples. Because the majority of the surface water samples were taken on Precambrian terrane (Christie, 1962), they exhibited low (<25 mg/L) alkalinities. The precipitation samples had alkalinities of 2 mg/L or less except for one sample which had a value of 12.7 mg/L – this sample may have had a small quantity of extraneous "calcareous material" entrained in it at the time of sampling which subsequently reacted with the sample enhancing both its alkalinity and pH. Except for four samples (including the one noted above), the differences between field and laboratory pH measurements were less than one unit and usually (>75%) the differences were less than or equal to 0.5 pH units. Although there were measurable differences between the field and laboratory pH on individual samples, the average pH values were not statistically different at the 95 per cent confidence limit ($t = 1.74$ for $df = 35$) for the whole data set (field/lab = 6.4/6.8) because of the large variability between samples. Because this data set is composed of paired – field and laboratory – measurements the most valid comparison of the data is made using a paired "t" test. A significant and measurable difference was evident between the field and laboratory measurements for the complete data set as well as for the surface water samples considered separately; but contrary to Jervis' (1979) observations on precipitation in Washington State the precipitation samples from Cape Herschel did not exhibit a significant difference ($t = 1.64$ for $df = 9$) upon storage even though the differences were measurable. The surface water samples with alkalinities greater than 25 mg/L did not exhibit a significant difference between the field and laboratory measurements either ($t = 1.01$ for $df = 8$). The minimal change of the Cape Herschel samples during storage may be a consequent of the purity of the water samples.

The average pH of the precipitation samples (pH = 5.7) and the average pH of the surface water samples with low alkalinities (pH = 6.1) also showed no statistical difference ($t = 1.23$ for $df = 9, 16$). Surface waters with alkalinities greater than 25 mg/L had an average pH (7.8) significantly different ($t = 10.53$ for $df = 9, 8$) from that of the precipitation in the region.

Table 2 indicates that the more poorly buffered samples (total alkalinity <25 mg/L) increased in pH during storage, whereas samples with elevated alkalinity values decreased slightly in pH during storage.

Seven of the field pH measurements were less than the equilibrium pH of carbon dioxide in water, and thus acidic, but none of the laboratory values of pH was less than 5.6.

## Conclusions

Although the averages of the field and laboratory pH values for these samples were not significantly different, the differences on individual samples were measurable and significantly different when analyzed by a paired "t" test ($t = 2.65$ for $df = 35$). If only laboratory measurements of pH had been made, then all samples would have exhibited pH values greater than 5.6 – the equilibrium pH of carbon dioxide in water – and thus would have been judged to be nonacidic, but four field measurements on precipitation samples were slightly acidic and three surface water samples were slightly to moderately acidic. Therefore field measurements of pH would appear to be essential to detect gradual changes in the acidity of atmospheric precipitation which might result from anthropogenic inputs or natural sources or phenomena. Because precipitation and low-alkalinity surface waters had similar pH values and many of the surface waters may be ombrogenic, changes in the acidity of the atmospheric aerosol in this region of the High Arctic might have a significant influence on many of the local ponds and lakes.

## Acknowledgments

I am indebted to J.A. Snider for competently performing the field pH measurements essential for this report. Special thanks are due to W.D. Gummer and F. Philbert (Water Quality Branch, Environment Canada) for providing the laboratory services in the Calgary and Burlington laboratories, respectively. My personal thanks are also extended to W. Blake, Jr. (project leader) who kindly provided logistical field support through the Polar Continental Shelf Project and subsequently encouraged the development of this report.

*From: Scientific and Technical Notes in Current Research, Part C; Geol. Surv. Can., Paper 82-1C*

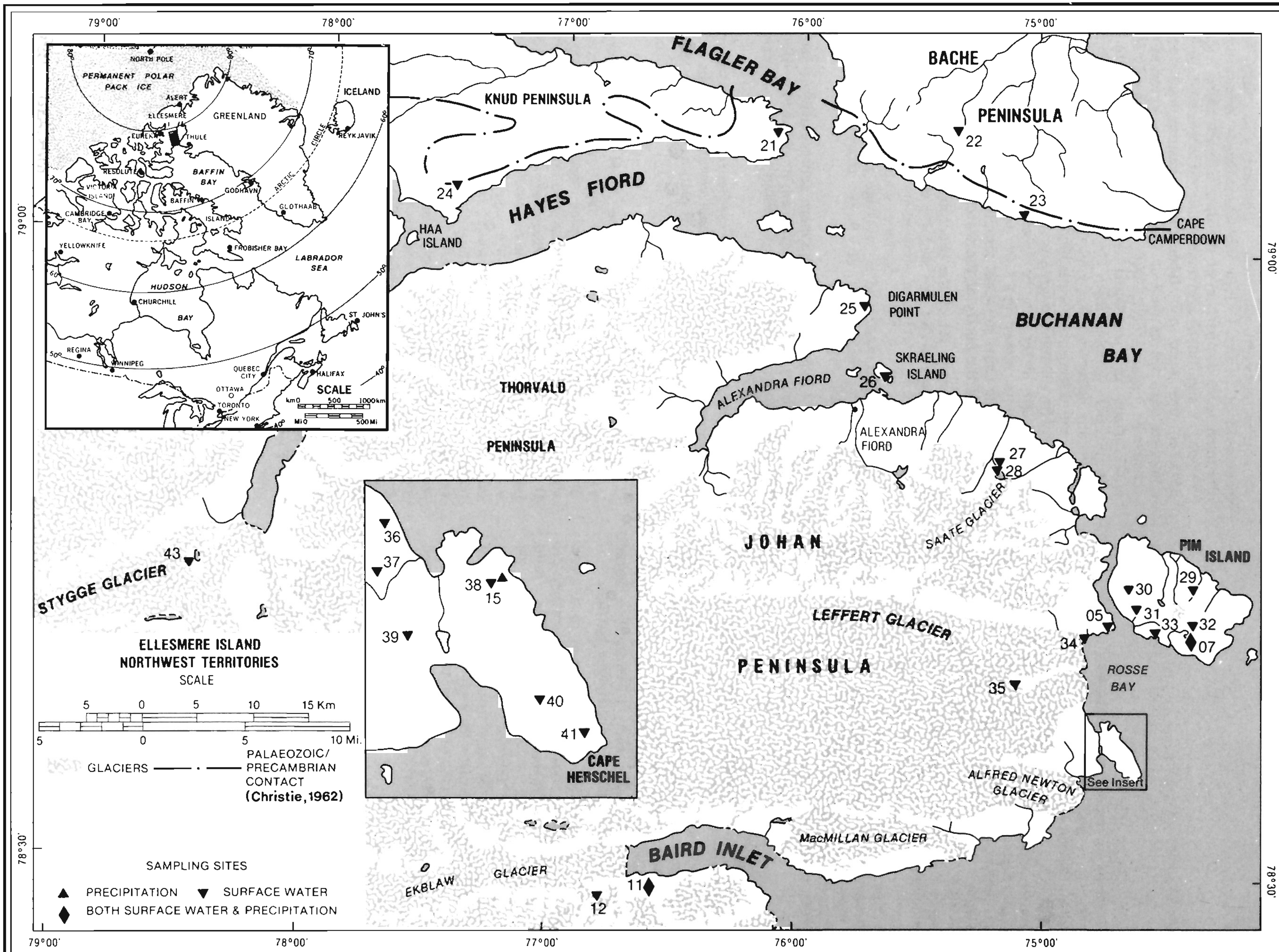


*Figure 1.* Map of study area showing sampling sites.

Table 1

pH Data Pairs for Different Media

| Collection Date | Site No. (cf. Fig. 1) | Field No. | Alkalinity (mg/L) | pH (units) Field | Lab | ΔpH (L-F) |
|---|---|---|---|---|---|---|
| Precipitation - Rain | | | | | | |
| June 29-30 | 15 | 21-1 | 1.4 | 5.8 | 6.1 | +0.3 |
| June 29-30 | 15 | 21-2 | 0.9 | 5.5* | 6.0 | +0.5 |
| June 29-30 | 15 | 22 | 1.9 | 5.2* | 5.8 | +0.6 |
| July 14-15 | 15 | 33 | 1.9 | 6.3 | 6.1 | -0.2 |
| July 15-16 | 15 | 34 | 1.9 | 5.7 | 5.9 | +0.2 |
| July 24 | 15 | 42 | 1.9 | 6.4 | 5.8 | -0.6 |
| Precipitation - Mixed Snow and Rain | | | | | | |
| June 3 | 15 | 3 | 12.7 | 5.2* | 7.8 | +2.6 |
| July 16-17 | 15 | 35 | 1.6 | 6.0 | 6.0 | 0.0 |
| July 14-17 | 15 | 37 | 1.9 | 6.1 | 6.1 | 0.0 |
| Rime Frost | | | | | | |
| June 5 | 32 | 6 | 2.0 | 4.8* | 6.1 | +1.3 |
| | | Average (n = 10): | | 5.7 ± 0.5† | 6.1 ± 0.6 | 0.6 |
| Surface Water - Alkalinity <25mg/L | | | | | | |
| June 17 | 05 | 6 | 4 | 6.6 | 6.4 | -0.2 |
| June 4 | 07 | 4 | 23 | 6.8 | 6.7 | -0.1 |
| June 23 | 11 | 19 | 1 | 6.2 | 6.1 | -0.1 |
| June 25 | 12 | 20 | < 1 | 6.0 | 6.1 | +0.1 |
| June 11 | 24 | 12 | 22 | 7.0 | 7.6 | +0.6 |
| June 11 | 25 | 14 | 9 | 6.3 | 6.6 | +0.3 |
| June 16 | 26 | 15 | 9 | 6.3 | 6.5 | +0.2 |
| June 18 | 27 | 17 | 6 | 6.1 | 6.8 | +0.7 |
| June 19 | 28 | 18 | < 1 | 5.8 | 6.6 | +0.8 |
| June 6 | 30 | 8 | 11 | 4.3* | 7.2 | +2.9 |
| June 8 | 31 | 9 | 5 | 5.9 | 6.3 | +0.4 |
| June 5 | 32 | 5 | 9 | 4.1* | 6.7 | +2.6 |
| June 6 | 33 | 7 | 3 | 6.2 | 6.3 | +0.1 |
| July 21 | 34 | 38 | 14 | 6.9 | 7.6 | +0.7 |
| July 3 | 35 | 26 | 2 | 5.5* | 5.9 | +0.4 |
| July 28 | 37 | 46 | 5 | 6.4 | 6.2 | -0.2 |
| July 26 | 39 | 45 | 2 | 6.4 | 6.9 | +0.5 |
| | | Average (n = 17): | | 6.1 ± 0.8 | 6.6 ± 0.5 | 0.6 |
| Surface Water - Alkalinity >25mg/L | | | | | | |
| June 11 | 21 | 13 | 75 | 7.5 | 7.3 | -0.2 |
| June 9 | 22 | 11 | 55 | 7.7 | 7.3 | -0.4 |
| June 9 | 23 | 10 | 136 | 7.4 | 8.3 | +0.9 |
| July 4 | 29 | 27 | 33 | 8.0 | 7.9 | -0.1 |
| July 25 | 36 | 43 | 112 | 8.0 | 7.8 | -0.2 |
| July 14 | 38 | 32 | 120 | 8.3 | 8.0 | -0.3 |
| July 22 | 40 | 40 | 43 | 7.7 | 7.4 | -0.3 |
| July 22 | 41 | 39 | 32 | 7.6 | 7.3 | -0.3 |
| May 29 | 43 | 1 | 29 | 7.7 | 7.4 | -0.3 |
| | | Average (n = 9): | | 7.8 ± 0.3 | 7.6 ± 0.4 | 0.3 |
| All Surface Waters – Average (n = 26): | | | | 6.6 ± 1.1 | 7.0 ± 0.7 | 0.5 |
| All Samples – Average (n = 36): | | | | 6.4 ± 1.0 | 6.8 ± 0.7 | 0.6 |

* pH value less than the equilibrium pH (5.6) of carbon dioxide in pure water at atmospheric pressure.

† mean pH $(\bar{x}) = \frac{1}{n}\sum_{i=1}^{n} x_i$ ± standard deviation $(s_x) = \sqrt{\dfrac{\Sigma x^2 - \dfrac{(\Sigma x)^2}{n}}{n-1}}$

Table 2

Changes in Sample pH During Storage

| Alkalinity (mg/L) | Decrease No. | Decrease (%) | Decrease Av. Change | Increase No. | Increase (%) | Increase Av. Change | No Change No. | No Change (%) | No Change Av. Change |
|---|---|---|---|---|---|---|---|---|---|
| <25 | 6 | (22) | 0.2 | 19 | (71) | 0.8 | 2 | (7) | 0.0 |
| >25 | 8 | (89) | 0.3 | 1 | (11) | 0.9 | - | - | - |

## References


Blake, W., Jr.
1978: Coring of Holocene pond sediments at Cape Herschel, Ellesmere Island, Arctic Archipelago; in Current Research, Part C; Geological Survey of Canada, Paper 78-1C, p. 119-122.

Christie, R.L.
1962: Geology, Alexandra Fiord, Ellesmere Island, District of Franklin; Geological Survey of Canada, Map 9-1962.

Environment Canada
1979: Analytical Methods Manual; Inland Waters Directorate, Water Quality Branch, Ottawa.

Heintzenberg, J., Hansson, H.-C., and Lannefors, H.
1981: The chemical composition of arctic haze at Ny-Alesund, Spitsbergen; Tellus, v. 33, p. 162-171.

Jervis, T.R.
1979: Rainfall acidity: natural variance and subsequent time dependence of pH; Atmospheric Environment, v. 13, p. 1601.

Kerr, R.A.
1979: Global pollution: is the arctic haze actually industrial smog?; Science, v. 205, p. 290-293.

1981: Pollution of the arctic atmosphere confirmed; Science, v. 212, p. 1013-1014.

# RUBIDIUM-STRONTIUM AND URANIUM-LEAD ISOTOPIC AGE STUDIES

# ÉTUDES DES DATATIONS ISOTOPIQUES PAR LES MÉTHODES RUBIDIUM-STRONTIUM ET URANIUM-PLOMB

Rb-Sr and U-Pb Isotopic Age Studies, Report 5

Compiled by W.D. Loveridge

CONTENTS

# INTRODUCTION

W.D. Loveridge

The following papers present the results of 10 U-Pb isotopic age studies on zircon and 6 Rb-Sr isotopic age studies on whole-rock samples. These age determination projects are joint research studies by field geologists of the Geological Survey of Canada and members of the staff of the Geochronology Section, typically initiated by the field geologists in an attempt to solve specific geological problems. In many cases the results are known to the geologist in question but not to the geological community at large. In some instances preliminary reference has been made in scientific reports to the resultant ages but the analytical data and other details have not been published.

This current group of papers is the third in a series to be presented in "Current Research, Part C" and includes both current geochronological studies and older, presently inactive studies that have not been previously published.

## U-Pb Age Studies on Zircon Concentrates

The preparation of zircon concentrates and analytical procedures for U-Pb age determination work was discussed by Sullivan and Loveridge (1980). The U-Pb results presented in this group of papers were determined during the period 1975 to 1982 and consist of studies of three or more zircon fractions from each sample. In some cases the geological age may be simply determined from the upper intersection with the concordia curve by a chord through the analytical points. In other cases, however, the pattern of analytical points is more complex and a considerable amount of interpretation may be required to derive the geological history from the observed results.

Concordia intercept ages are calculated by a computer program which first determines the parameters of the chord through a least squares linear regression and then finds the intercepts by an iterative method. The uncertainties associated with concordia intercept ages of chords are based on the standard error of the slope of these chords. These uncertainties are determined from the intersection with concordia of hypothetical chords with slopes equal to that of the original chord plus and minus its standard error, projected from a point which is the average of the analytical points and are expressed at the 95 per cent confidence level.

The uranium decay constants used are: $^{238}U$, $1.55125 \times 10^{-10} a^{-1}$ and $^{235}U$, $9.8485 \times 10^{-10} a^{-1}$ as recommended by the IUGS Subcommission on Geochronology (Steiger and Jaeger, 1977). Descriptions of zircon concentrates are by R.D. Stevens.

## Rb-Sr Whole-Rock Isochron Studies

The analytical work leading to the Rb-Sr age results published in this collection of papers was performed from 1980 to 1982. Analytical procedures have progressed and been modified over the years, but are based on those described by Wanless and Loveridge (1972). The analytical uncertainty to be associated with the isotopic ratios has also changed with time, and is listed individually in each data table.

All whole-rock isochron data were subjected to regression analysis using the program published by Brooks et al. (1972). The published ages and initial $^{87}Sr/^{86}Sr$ ratios and their associated errors (95 per cent confidence interval) are those determined by the York 1 portion of the program. The value obtained for the Mean Square of Weighted Deviates (MSWD) from the McIntyre portion of the program is used to classify the linear array of experimental points as an isochron or an errorchron. In the terminology of Brooks et al. (1972) an errorchron is the result of regression of data that possess scatter in excess of experimental error whereas the data points forming an isochron are collinear within experimental error. Thus the excess scatter of points forming an errorchron is attributable not to lack of laboratory precision, but to the complex history of the suite of rocks under investigation. Such complexities might include partial resetting of the Rb-Sr systematics of the suite by subsequent metamorphic, hydrothermal or deformational events, inhomogeneity of $^{87}Sr/^{86}Sr$ ratio at the time of emplacement, or members of the suite not having been initially cogenetic.

Recent advances in the field of mass spectrometry have caused the distinction between isochrons and errorchrons to become less well defined. The remarkable precision in isotope ratio measurement available in modern mass spectrometers is now greater than the inherent accuracy of Rb-Sr systematics in many geological systems; some suites of rock studies will yield errochrons by the criteria of Brooks et al. (1972) even though they may have apparently satisfied the geological requirements for development of isochrons. In studies of this nature, it is necessary to employ geological or other geochronological criteria to determine whether or not the age result obtained is representative of the event studied. We have still used the terminology of Brooks et al. in most Rb-Sr contributions to this publication because the precision associated with these experimental results is not sufficient to warrant its abandonment.

In particular, regression results obtained at the current level of precision (0.014% in $^{87}Sr/^{86}Sr$ ratio at the 95 per cent confidence level) which do not meet the Brooks et al. criteria for isochrons would be errorchrons even if the precision were improved. Brooks et al. (1972, p. 557) pointed out that the uncertainties associated with errorchron results at a given confidence interval contain none of the predictive aspects that characterize true confidence intervals. For an isochron with error figures given at the 95 per cent confidence level, 19 of 20 repeats of the isochron should give results which would fall within those error figures. This is not the case with an errorchron; it is possible that no repeats would fall within the stated error limits. Therefore the error limits associated with errorchrons may be indicative of the uncertainty in the age and initial ratio results, but are by no means definitive. For this reason the error limits associated with errorchron results are mentioned only in the text but omitted from the diagrams to prevent inadvertent misuse by the casual reader.

The $^{87}Rb$ decay constant used in this series of papers is $1.42 \times 10^{-11} a^{-1}$ as recommended by the IUGS Subcommission on Geochronology (Steiger and Jaeger, 1977). Previously published Rb-Sr ages referred to in these papers have been adjusted to the constants recommended by the subcommission. Analytical uncertainties presented in the papers are at the 95 per cent confidence level.

I would particularly like to thank O. van Breemen and R.D. Stevens for critically reading all papers in this section and J. MacManus for drafting many of the diagrams.

## References


Brooks, C., Hart, S.R., and Wendt, I.
1972: Realistic use of two error regression treatments as applied to rubidium-strontium data; Reviews of Geophysics and Space Physics, v. 10, no. 2, p. 551-577.

Steiger, R.H. and Jaeger, E.
1977: Subcommission on Geochronology: Convention on the use of decay constants in geo- and cosmochronology; Earth and Planetary Science Letters, v. 36, no. 3, p. 356-362.

Sullivan, R.W. and Loveridge, W.D.
1980: Uranium-lead age determination on zircon at the Geological Survey of Canada; current procedures in concentrate preparation and analysis; in Loveridge, W.D., Rubidium-strontium and uranium-lead isotopic age studies, Report 3; in Current research, Part C, Geological Survey of Canada, Paper 80-1C, p. 161-246.

Wanless, R.K. and Loveridge, W.D.
1972: Rubidium-strontium isochron age studies, Report 1; Geological Survey of Canada, Paper 71-23.

# 1. THE DEADMAN'S BAY PLUTON, NORTHEASTERN NEWFOUNDLAND; U-Pb STUDY OF ZIRCON REVEALS A GRENVILLIAN COMPONENT

K.L. Currie, W.D. Loveridge, and R.W. Sullivan

*Currie, K.L., Loveridge, W.D., and Sullivan, R.W., The Deadman's Bay pluton, northeastern Newfoundland; U-Pb study of zircon reveals a Grenvillian component; in Rb-Sr and U-Pb Isotopic Age Studies, Report 5, in Current Research, Part C, Geological Survey of Canada, Paper 82-1C, p. 119-124, 1982.*

**Abstract**

*A U-Pb study of zircon from the Deadman's Bay pluton yields a linear trend of highly discordant data points suggesting an age of emplacement between 353 + 12/-17 Ma (lower concordia intercept) and 430 ± 2 Ma ($^{207}Pb/^{206}Pb$ age of the largest grained, hand picked, clear zircon fraction), in agreement with previous K-Ar ages from the area. The upper intercept is poorly defined at about 1150 Ma indicating a Grenvillian component. Possible sources of the Grenvillian component may be the surrounding gneisses or a postulated Precambrian crust existing to the east of the study area prior to emplacement of the pluton.*

## Geological Setting

The Deadman's Bay pluton (Fig. 1), the largest in northeastern Newfoundland, forms a roughly semicircular mass some 40 km across, bounded to the north by the Atlantic Ocean, and on other sides by older gneisses and foliated granites. The pluton, remarkably homogeneous for so large a body, consists of a coarse grained matrix of quartz, biotite and oligoclase, in which are set subhedral masses of pink potash feldspar up to 10 cm across. These megacrysts commonly form 20 to 50 per cent of the volume. The megacrysts locally exhibit crude lamination, occur in cross-cutting dykes, and decrease in size and number toward the margins of the pluton. Despite such evidence of igneous derivation, other observations show that some megacrysts must have a metasomatic origin in part. Most megacrysts contain inclusions of matrix minerals in the same texture and relative proportions as the matrix, suggesting that the megacrysts overgrew the matrix. Inclusions in the pluton also contain megacrysts, and megacrysts grow across the margins of late aplitic dykes. On the western boundary of the pluton, megacrysts occur in wall rocks as well as the pluton. These, and other considerations suggested to Currie et al. (1979) that the pluton underwent a long and complex development.

Structurally, the pluton is one of the youngest Acadian plutons in this part of Newfoundland (Jayasinghe and Berger, 1976). Presumably, this final emplacement is responsible for the young K-Ar ages of 342 ± 14* and 359 ± 15* Ma obtained from this pluton (Wanless et al., 1965, 1972). However there are several indications of older activity. Fairbairn and Berger (1969) obtained some inconclusive Rb-Sr data compatible with an age near 600 Ma, while Cormier (quoted in Jayasinghe and Berger, 1976), obtained a poor Rb-Sr isochron of 580 ± 120 Ma, using some of the same samples. Berger and Naylor (1974) obtained a discordant zircon date of 510 Ma for $^{207}Pb/^{206}Pb$, with younger ages of 404 Ma for $^{207}Pb/^{235}U$ and 385 Ma for $^{206}Pb/^{238}U$.

The present study was intended to clarify some of the early history of the Deadman's Bay pluton. A single large block of about 30 kilograms of freshly blasted material was collected (Fig. 1) from a road cut near Lumsden, Newfoundland. This material appeared in hand specimen to be completely fresh and unaltered. The megacrysts here form about 35 per cent of the volume, and locally display both plagioclase around k-feldspar, and k-feldspar around plagioclase rims. Microscopically the quartz is markedly strained and polygonized. The accessory minerals comprise magnetite, sphene, apatite and zircon, with very small amounts of white mica on some of the plagioclase grains. In thin section, the zircons are mostly slender, waterclear, doubly terminated prisms, but some of the larger zircons exhibit a darker, cloudy, rather rounded core.

## Analytical Procedures and Results

Techniques for the concentration of zircon, separation into distinct fractions of differing physical characteristics, and the extraction and analysis of lead and uranium are described in Sullivan and Loveridge (1980). Analytical results are listed in Table 1 and displayed on a concordia diagram (Fig. 2). A description of the zircon morphology of the fractions as analyzed is presented in the Appendix.

The five fractions analyzed yielded data points forming a linear trend; one data point (no. 3, Fig. 2) falls somewhat above the trend suggested by the other four points. We interpret the linear trend as a mixing line between a small Precambrian component possibly present in all zircon crystals studied and a much larger Paleozoic component. A chord of lower concordia intercept 353 + 12/-15 Ma and upper intercept 1148 + 157/-144 Ma may be fitted to the four approximately collinear data points. Due to the extreme discordance of the experimental points, the upper intercept age is strongly model dependant so that the value obtained represents only a minimum age for the Precambrian component. The lower intercept age of 353 + 12/-15 Ma, when considered in the context of the K-Ar ages of 342 ± 14 and 359 ± 15 Ma obtained on biotite from other samples of this pluton (op. cit.), might be regarded as a reasonable estimate of the age of emplacement. However, this picture is complicated by a 400 ± 13 Ma, K-Ar age on biotite from the same sample that yielded the zircon of this study (Stevens et al., 1982, p. 47).

Fraction number 3 was hand picked to include only members of the clear zircon population (without evident cores; see Appendix and Fig. 3). Translucent zircons (often with visible cores, Fig. 3) were excluded from fraction 3 but hand picked exclusively to form fraction 5. The data point for fraction 3 falls above the apparent mixing line defined by the other four points and provides independent evidence that the 353 Ma lower intercept may not precisely define the age of emplacement of the pluton. Results from this carefully hand picked fraction would be expected to yield the best estimate of the age of emplacement as it is composed of the largest grain size of clear euhedral zircon crystals showing no cores or fractures, separated in this study. It also has the lowest uranium content and should thereby have been least susceptible to recent lead loss. From this point of view, the $^{207}Pb$-$^{206}Pb$ age of 430 ± 2 Ma for fraction 3 might be regarded as the best estimate for the age of emplacement.

* Recalculated using revised decay constants (Steiger and Jaeger, 1977).

However, the results for fraction 2 (which is morphologically similar to fraction 3 but of smaller grain size) clearly fall on the mixing line defined by the other sample points. Since fraction 2 apparently contains a small Precambrian component it is probable that fraction 3 does so as well. Thus the $^{207}Pb$-$^{206}Pb$ age for fraction 3 (430 Ma) must be regarded as a maximum for the age of emplacement.

Conversely, fractions 4 and 5 contain much higher uranium contents than the other three fractions with grains from fraction 5 being frequently fractured as well. These fractions might be expected to have suffered recent lead loss due to their metamict nature. Thus the 353 Ma lower intercept age through these points must be considered a minimum age for emplacement. We interpret these results as bracketing the age of emplacement between an upper limit of 430 ± 2 Ma and a lower limit of 353+12/-15 Ma.

Four of the five data points fall at the extreme lower end of the chord. This implies that the bulk of the zircon material crystallized between 350 and 430 Ma about miniscule Precambrian zircon "seeds". Only in the largest size fraction is the Precambrian component greater than 10%. Radiogenic lead components of the four smaller size fractions are generally low, 20 to 40 ppm or about 6% of the corresponding uranium contents. This would also be true for the largest size fraction (no. 1) except that the isotopic abundance of $^{208}Pb$ in this zircon material is exceptionally high at about 52%. It is evident from the results in Table 1 that the $^{208}Pb$ abundances of all the zircon fractions correlate with the relative position on the chord; without exception the zircons lowest on the chord have the smaller $^{208}Pb$ abundances. This implies that the source of the high $^{208}Pb$ radiogenic lead is in the

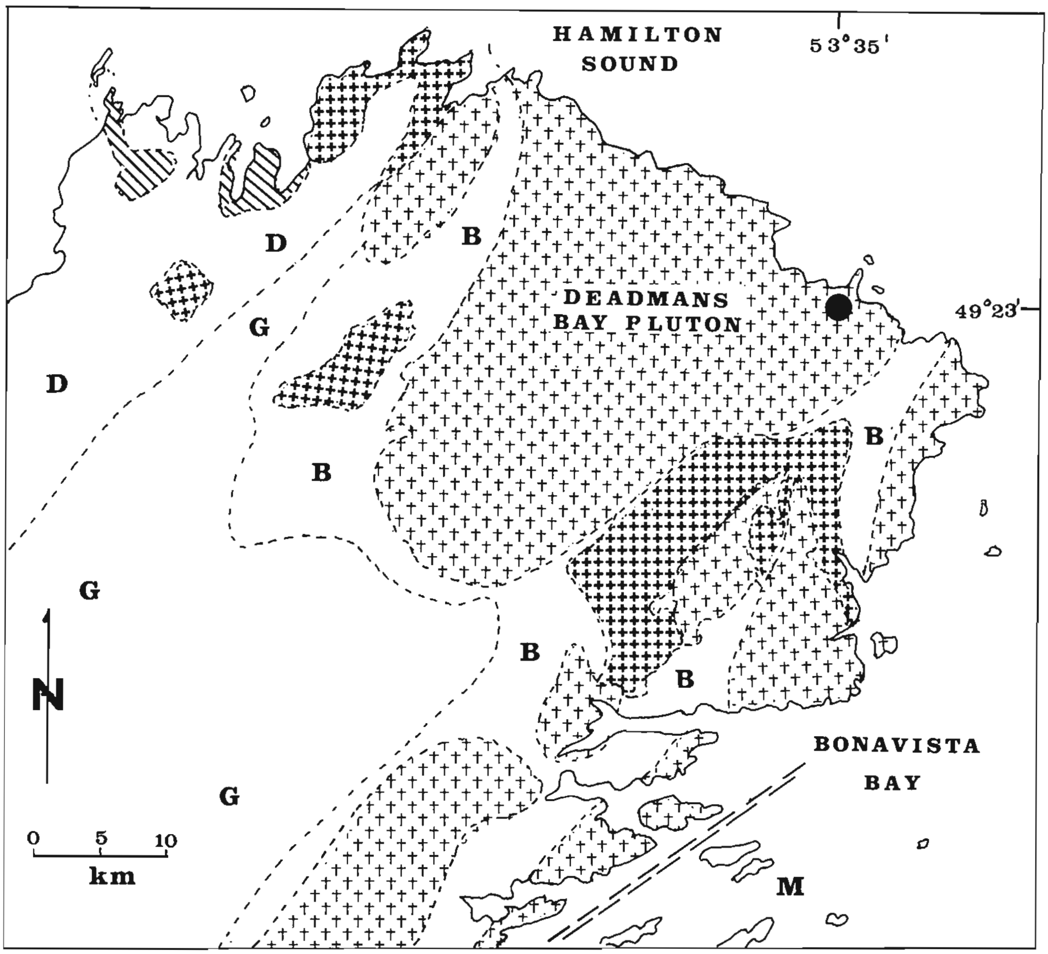


*B – Bonavista Bay gneiss complex*
*G – Gander Group (metamorphosed psammites and pelites of Cambro(?)-Ordovician age*
*M – late Precambrian sedimentary and volcanic rocks of the Avalon zone*
*D – Davidsville Group (mainly pelitic rocks of Ordovician age)*
*diagonal hachuring – tonalites, probably of Silurian age*
*light crosses – megacrystic granites of various ages.*
*heavy crosses – biotite granite, biotite-muscovite granite, leucogranite and migmatite, mainly of Silurian or Devonian age*

*Sample site is shown by a solid circle. Geology modified after Jayasinghe and Berger (1976).*

***Figure 1.*** *Geological setting of the Deadman's Bay pluton, northeastern Newfoundland.*

Table 1

Analytical data for U-Pb analyses of zircon,
Deadman's Bay pluton, northeastern Newfoundland

| Fraction number | | 1 | 2 | 3 | 4 | 5 |
|---|---|---|---|---|---|---|
| Fraction size, μm | | +149 | -62+44 | -149+105 | -62+44 | -149+105 |
| Magnetic or nonmagnetic | | - | nm | nm | mag | mag |
| Characteristic | | - | - | clear | - | translucent |
| Weight, mg | | 5.55 | 4.63 | 4.35 | 4.61 | 2.90 |
| Total Pb, ng | | 154.0 | 41.50 | 23.71 | 49.04 | 34.19 |
| Pb blank, % | | 1.3 | 2.6 | 2.1 | 2.2 | 3.6 |
| Observed | $^{206}Pb/^{204}Pb$ | 1107 | 697.0 | 1397 | 1288 | 1549 |
| *Abundances | $^{204}Pb$ | 0.0504 | 0.1006 | 0.0377 | 0.0425 | 0.0087 |
| ($^{206}Pb$ = 100) | $^{207}Pb$ | 7.1123 | 7.1361 | 6.0893 | 6.1910 | 5.5886 |
| | $^{208}Pb$ | 117.43 | 13.243 | 10.564 | 9.565 | 4.498 |
| Radiogenic Pb, ppm | | 65.06 | 26.62 | 20.01 | 35.74 | 44.65 |
| " " % | | 98.4 | 94.2 | 97.7 | 97.4 | 99.4 |
| Uranium, ppm | | 421.8 | 430.2 | 328.7 | 601.3 | 828.2 |
| Atomic ratios | $^{206}Pb/^{238}U$ | 0.080103 | 0.062349 | 0.061651 | 0.060818 | 0.057192 |
| | $^{207}Pb/^{235}U$ | 0.70542 | 0.48789 | 0.47106 | 0.46740 | 0.43069 |
| | $^{207}Pb/^{206}Pb$ | 0.063866 | 0.056749 | 0.055412 | 0.055735 | 0.054614 |
| Ages, Ma | $^{206}Pb/^{238}U$ | 497 | 390 | 386 | 381 | 359 |
| | $^{207}Pb/^{235}U$ | 542 | 403 | 392 | 389 | 364 |
| | $^{207}Pb/^{206}Pb$ | 737 | 482 | 429 | 442 | 396 |

*Corrected for Pb Blank

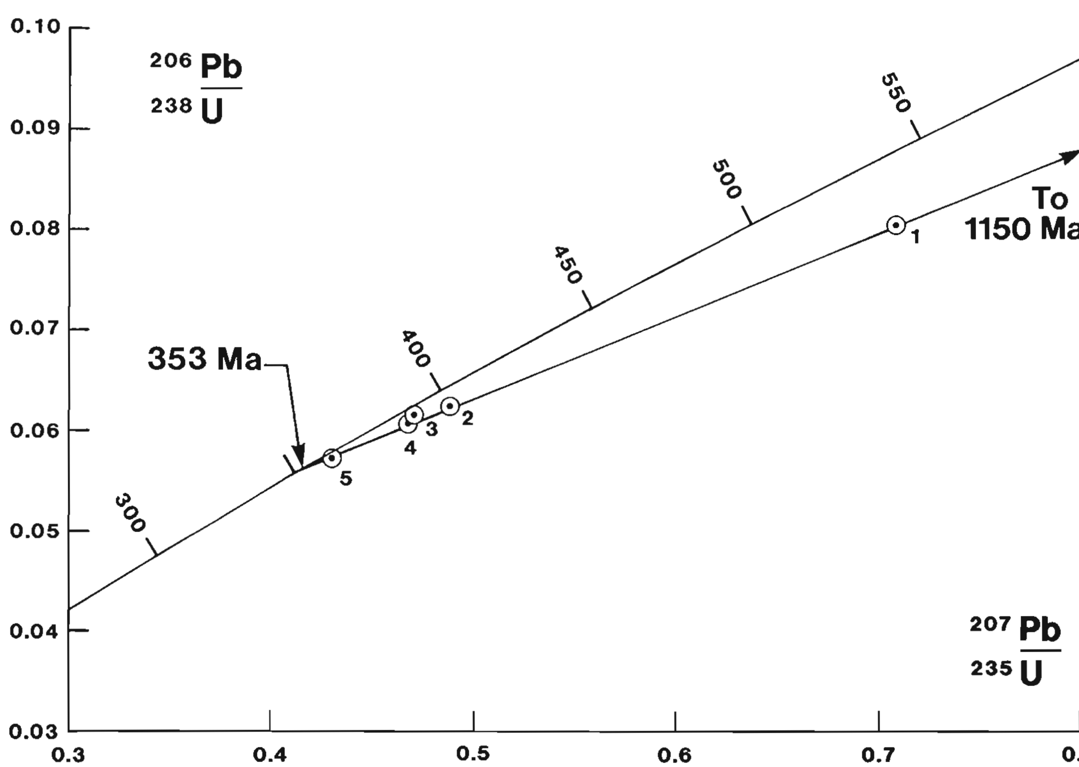


*Figure 2.* *Concordia diagram showing the results of U-Pb analyses of five zircon fractions from the Deadman's Bay pluton, northeastern Newfoundland.*

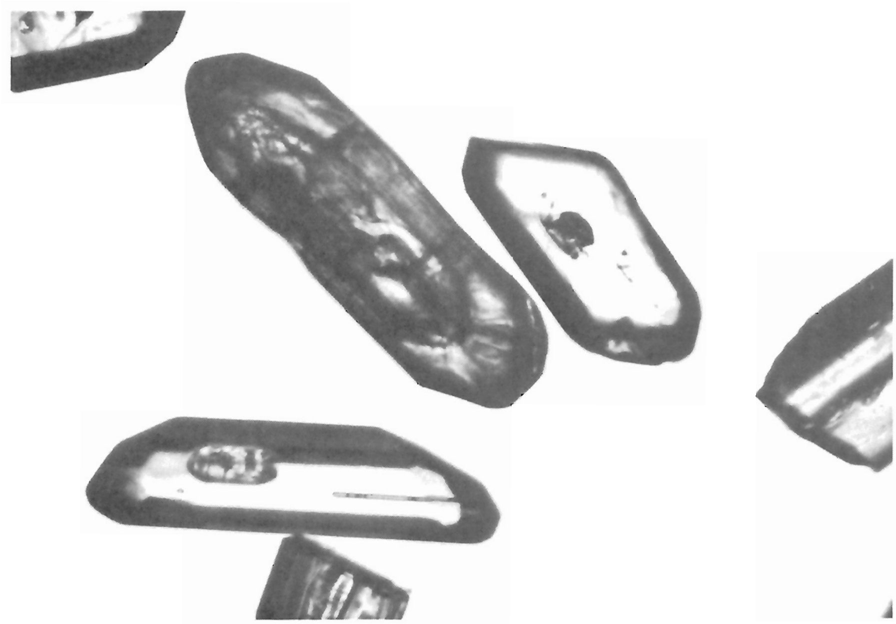

***Figure 3***

*Photomicrograph of zircon crystals from the Deadman's Bay pluton showing a semi-translucent crystal with a visible core flanked by two clear crystals with inclusions (x100).*

Precambrian zircon component. Ultimately, it may be possible to employ this unusual isotopic composition to identify the source rocks of the Precambrian component.

The results of this study suggest that the Rb-Sr measurements of Fairbairn and Berger (1969) and Cormier (quoted in Jayasinghe and Berger, 1976) produced inconclusive results due to the hybrid nature of the pluton. Since they did not obtain isochrons of age between 350 and 430 Ma with elevated initial $^{87}Sr$-$^{86}Sr$ ratios, it is probable that the Rb-Sr systems throughout the pluton were inhomogeneous at the time of emplacement. The data point for the U-Pb result on zircon by Berger and Naylor (1974) falls just below point no. 2 on our concordia plot (Fig. 2).

## Interpretation

The results of this study do not precisely define the age of emplacement for the Deadman's Bay pluton, but bracket it between maximum and minimum ages of 430 ± 2 and 353 ±12/-15 Ma. K-Ar dates on three samples from the pluton fall inside this range within their analytical uncertainties. The regional significance of these relatively young dates has recently been discussed by Currie and Pajari (1981). Four of the five points on the chord tend to cluster near the lower intercept, suggesting the bulk of the zircon crystallized during this late event. However, all zircon studied, particularly the largest size fraction, appears to contain a significant fraction of a very different zircon material of much greater age. The correct interpretation of the source of this older zircon is somewhat speculative at present, but all the plausible possibilities are of great interest. Three possibilities seem most likely. (a) The older zircon is relict from inclusions of the surrounding gneisses. Repeated suggestions have been made that these gneisses (Bonavista Bay gneiss complex of Blackwood, 1978) are of Precambrian age, but this is the first hard evidence. If this interpretation is accepted, then a floor existed in the eastern part of the Gander zone which was both a source and a substratum for the later sedimentary events discussed by Currie et al. (1979). (b) As a variant of the above hypothesis, it might be supposed that the Deadman's Bay pluton developed by anatexis of the gneiss complex, and that the older zircons are "restite" fragments. This hypothesis has the same consequences as the first, but is a somewhat stronger assumption. (c) It might be supposed that the older zircons are detrital material acquired by the pluton from the Late Precambrian or Early Paleozoic sedimentary rocks in the surroundings. The known transport directions in this region are from east to west (Currie et al., 1979). Hence this hypothesis implies the presence of Precambrian crust somewhere to the east of the Deadman's Bay pluton during the Late Devonian or Carboniferous. The exact location of this exposed basement is unknown, but it could be the long-sought basement to the Avalon zone of Newfoundland.

## References


Berger, A.R. and Naylor, R.S.
1974: Isotopic dates on zircons from the Deadman's Bay pluton, northeastern Newfoundland, and their geological implications; Geological Association of Canada, 27th Annual Meeting, St. Johns, Newfoundland, Program with Abstracts, p. 9.

Blackwood, R.F.
1978: Northeastern Gander Zone, Newfoundland; Mineral Development Division, Newfoundland Department of Mines and Energy, Report of Activities for 1977, p. 72-79.

Currie, K.L. and Pajari, G.E.
1981: Peraluminous anatectic granites from the Carmanville area, northeastern Newfoundland; Canadian Mineralogist, v. 19, p. 147-161.

Currie, K.L., Pajari, G.E., and Pickerill, R.K.
1979: Tectono-stratigraphic problems in the Carmanville area, northeastern Newfoundland; in Current Research, Part A, Geological Survey of Canada, Paper 79-1A, p. 71-76.

Fairbairn, H.W. and Berger, A.R.
1969: Preliminary geochronological studies in northeastern Newfoundland; Massachusets Institute of Technology Progress Report, 1969, p. 19-20.

Jayasinghe, N.R. and Berger, A.R.
1976: On the plutonic evolution of the Wesleyville area, Bonavista Bay, Newfoundland; Canadian Journal of Earth Sciences, v. 13, no. 11, p. 1560-1570.

Steiger, R.H. and Jaeger, E., compilers
1977: Subcommission on Geochronology: Convention on the use of decay constants in geo- and cosmochronology; Earth and Planetary Science Letters, v. 36, no. 3, p. 356-362.

Stevens, R.D., Delabio, R.N., and Lachance, G.R.
1982: Age determinations and geological studies, K-Ar isotopic ages, Report 15; Geological Survey of Canada, Paper 81-2, p. 47.

Sullivan, R.W. and Loveridge, W.D.
1980: Uranium-lead age determinations on zircon at the Geological Survey of Canada: current procedures in concentrate preparation and analysis; in Loveridge, W.D., Rubidium-strontium and uranium-lead isotopic age studies, Report 3; in Current Research, Part C, Geological Survey of Canada, Paper 80-1C, p. 161-246.

Wanless, R.K., Stevens, R.D., Lachance, G.R., and Rimsaite, J.Y.H.
1965: Age determinations and geological studies, Part 1-Isotopic ages, Report 5, Geological Survey of Canada, Paper 64-17 (Part 1), p. 126.

Wanless, R.K., Stevens, R.D., Lachance, G.R., and Delabio, R.N.
1972: Age determinations and geological studies, K-Ar isotopic ages, Report 10; Geological Survey of Canada, Paper 71-2, p. 91-92.

## APPENDIX

Description of zircon concentrate, Deadman's Bay pluton.
Latitude 49°23'N, longitude 53°35'W

The initial concentrate was composed mainly of two distinct zircon populations (Fig. 3), one being clear and simple, and the other being semi-translucent and complex with obvious cores and fractures. In the larger grain sizes Frantz separation effectively separated these two populations, the clear being relatively nonmagnetic and the semitranslucent being relatively magnetic. All crystals had a very fresh appearance, but embayments, dumbell shapes and other evidence of modification were commonly observed. Three size fractions were selected for analysis and detailed examination and two of these were split into relatively magnetic and nonmagnetic pairs.

Fraction 1. A hand picked +149 μm fraction consisted of 100% zircon crystals and fragments ranging from clear and colourless to light tan and cloudy-translucent. Very prominent elongated bubble inclusions and distinctive black inclusions were also observed in some crystals. The bubble inclusions were mostly clear, but some contained red-orange or black material. This fraction was not magnetically separated.

Fraction 2. The -62+44 μm fraction was separated into relatively nonmagnetic (fraction 2) and magnetic (fraction 4) cuts. The nonmagnetic material of fraction 2 was essentially similar to the nonmagnetic -149+105 μm cut, fraction 3.

Fraction 3. A hand picked -149 + 105 μm, nonmagnetic fraction consisted of 100% clear, euhedral zircon crystals and fragments, generally with a slightly rounded appearance. Colour varied from almost colourless to light tan-purple and elongation ranged from about 2:1 up to 6:1. Many crystals showed bubble inclusions in transmitted light and most of the bubbles were somewhat to greatly elongated parallel to crystal length, though an outstanding few had such inclusions slightly elongated in a direction approximately at right angles to crystal length.

Fraction 4. The magnetic -62 + 44 μm cut comprised 95% clear, colourless, euhedral crystals plus 5% with varying amounts of red-orange material; up to 20% contained distinct black inclusions.

Fraction 5. The relatively magnetic -149 + 105 μm fraction also was hand picked to yield 100% euhedral zircon crystals of a generally translucent character with light brownish colour. Crystal terminations varied from sharp to somewhat rounded and elongation averaged about 3:1 but ranged up to a rare 6:1. Distinct zoning was observed in many, and dark rims on clearer cores were common. The latter were frequently fractured and some contained dark inclusions and large bubble inclusions.

## 2. A U-Pb AGE ON ZIRCON FROM DYKES FEEDING BASAL RHYOLITIC FLOWS OF THE JUMPING BROOK COMPLEX, NORTHWESTERN CAPE BRETON ISLAND, NOVA SCOTIA

K.L. Currie, W.D. Loveridge, and R.W. Sullivan

*Currie, K.L., Loveridge, W.D., and Sullivan, R.W., A U-Pb age on zircon from dykes feeding basal rhyolitic flows of the Jumping Brook complex, northwestern Cape Breton Island, Nova Scotia; in Rb-Sr and U-Pb Isotopic Age Studies, Report 5, in Current Research, Part C, Geological Survey of Canada, Paper 82-1C, p. 125-128, 1982.*

***Abstract***

*U-Pb studies have yielded a concordia intercept age of 439 ± 7 Ma on zircon from dykes which feed basal rhyolite flows of the Jumping Brook complex, Cape Breton Island, Nova Scotia. Biotite from the same specimen yielded a K-Ar age of 369 ± 9 Ma. These two results are consistent with a cyclic history for this part of the Cape Breton Highlands through late Precambrian and early Paleozoic time.*

### Geological Setting

The Cape Breton Highlands form a block of crystalline rocks some 100 by 50 km. Pioneer geologists considered the crystalline rocks to be of Precambrian age (Fletcher, 1885), but radiometric age determinations obtained by Neale (1963) showed granitic rocks of Devonian age to be present. More recent work by Cormier (1972) found granitic rocks of Late Precambrian to Early Cambrian (540-570 Ma)[1] and Ordovician age (450 Ma)[1]. The history of the highlands appears to be long and complex (Wiebe, 1972; Currie, 1975). The most promising clues to unravelling this history lie in the supracrustal sequences which rest on the very complex gneisses of the central highlands. During the past decade various workers have shown that at least two series of supracrustal rocks form a discontinuous fringe around the highlands (Wiebe, 1972; Neale and Kennedy, 1975; Currie, 1975; Jamieson, 1981). The older sequence locally contains marble and quartzite units, and is almost everywhere at amphibolite grade, locally containing kyanite. Near the town of Cheticamp this sequence is clearly intruded by a granodiorite pluton (Fig. 1) yielding a Rb-Sr isochron age of 530 ± 44 million years (Cormier, 1972; recalculated by Keppie and Smith, 1978). The older supracrustal sequence must therefore be older than the Late Precambrian or Early Cambrian age of the granodiorite. The older composite gneisses thus appear to be Precambrian, as generally assumed, although their exact age remains uncertain.

North of Cheticamp (Fig. 1), a younger supracrustal sequence lies unconformably upon the granodiorite (Currie, in press). The sequence consists of basal bimodal volcanics overlain by black pelite with a volcanogenic component, and capped by greywacke. The metamorphic grade is extremely variable, ranging from sub-greenschist along the shore, to high amphibolite farther inland, but the metamorphism is uniformly of low to moderate pressure type (andalusite-bearing). These rocks, termed the Jumping Brook complex (Currie, in press), have been complexly folded and faulted, so that different parts of the sequence tend to be juxtaposed. However lithological and structural correlatives have been traced around much of the Cape Breton Highlands (Wiebe, 1972; Neale and Kennedy, 1975; Jamieson, 1981). The sequence has been metamorphosed only once, presumably during the Devonian Acadian Orogeny. Since it is younger than the 530 Ma granite, and older than the Devonian, the sequence must belong, sensu lato, to the lower Paleozoic, but its exact age, and hence its possible correlatives, were unknown prior to the present study.

Samples for age determination were collected from dykes occurring on a cliff face at Grande Falaise, in Cape Breton Highlands National Park, about 10 km northeast of Cheticamp (Fig. 1). The dykes cut the 530 Ma granite, and feed basal rhyolitic flows of the Jumping Brook complex.

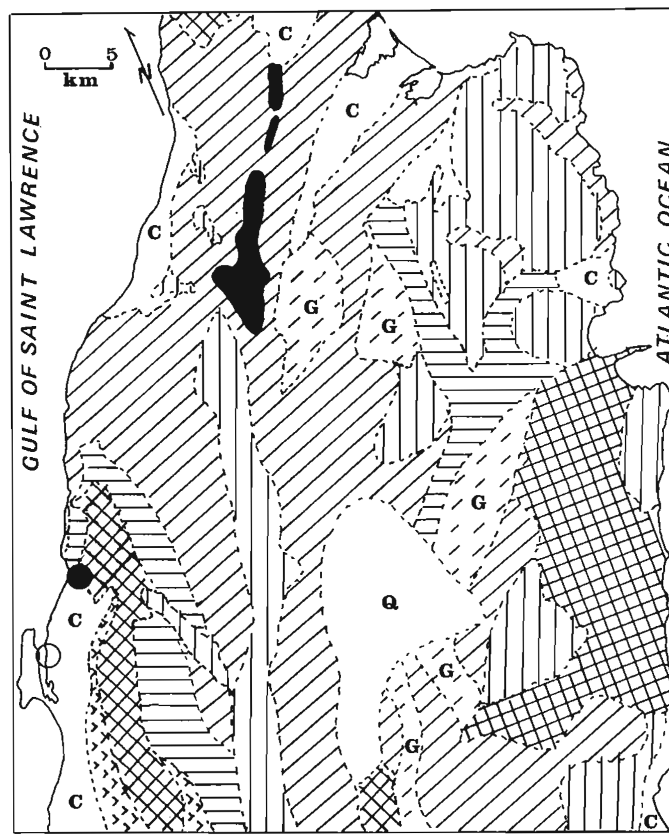


*Figure 1. Geological sketch map of northwestern Cape Breton Island.*

*Solid black – anorthosite and amphibolite (basement)*

*Diagonal hatching – basement and reactivated basement (Composite gneiss)*

*G – Precambrian sedimentary cover on basement*

*Cross hatched – pre-Ordovician Plutons*

*Horizontal ruling – Jumping Brook complex and equivalents*

*Vertical ruling – middle Ordovician and younger plutons*

*v's – Fisset Brook Formation*

*C – Carboniferous sedimentary rocks*

*Q – Quaternary cover*

*Open circle – town of Cheticamp*

*Solid circle – sample location (46°40.5'N, 60°57.8'W).*

[1]Recalculated using $^{87}Rb$ decay constant = $1.42 \times 10^{-11}\ a^{-1}$.

Table 1

Analytical data, zircon fractions from dykes feeding basal rhyolite flows of the Jumping Brook complex, northwestern Cape Breton Island

| Fraction number | | 1 | 2 | 3 |
|---|---|---|---|---|
| Fraction size, μm | | -149+105 | +149 | -149+105 |
| Magnetic or nonmagnetic | | nm | - | mag |
| Weight, mg | | 2.36 | 1.58 | 2.46 |
| Total Pb, ng | | 45.38 | 26.48 | 41.02 |
| Pb blank, % | | 2.2 | 2.6 | 2.4 |
| Observed | $^{206}Pb/^{204}Pb$ | 484.9 | 297.9 | 290.9 |
| * Abundances | $^{204}Pb$ | 0.1650 | 0.2872 | 0.2977 |
| ($^{206}Pb$ = 100) | $^{207}Pb$ | 7.967 | 9.761 | 9.911 |
| | $^{208}Pb$ | 30.546 | 32.757 | 33.571 |
| Radiogenic Pb, ppm | | 44.35 | 43.19 | 53.00 |
| " " % | | 91.4 | 85.4 | 85.0 |
| Uranium, ppm | | 681.8 | 705.8 | 893.1 |
| Atomic ratios | $^{206}Pb/^{238}U$ | 0.057850 | 0.055255 | 0.053385 |
| | $^{207}Pb/^{235}U$ | 0.44345 | 0.42450 | 0.40995 |
| | $^{207}Pb/^{206}Pb$ | 0.055591 | 0.055716 | 0.055690 |
| Ages, Ma | $^{206}Pb/^{238}U$ | 362.6 | 346.7 | 335.3 |
| | $^{207}Pb/^{235}U$ | 372.7 | 359.3 | 348.8 |
| | $^{207}Pb/^{206}Pb$ | 436.1 | 441.1 | 440.1 |

* Corrected for Pb Blank

The dykes have been moderately metamorphosed and fractured, and now exhibit a felsitic texture, with visible minute flakes of biotite. In hand specimen the rocks appear fresh and homogeneous, with a moderate cataclastic foliation. In thin section the minerals are fresh, but strongly strained and fractured. The specimen dated was a single block of about 25 kilograms spanning the entire width of a 30 cm dyke. The zircons in thin section were water clear elongated prisms, with rather rounded terminations.

## Analytical Procedures and Results

Techniques for the concentration of zircon and the extraction and analysis of lead and uranium are described in Sullivan and Loveridge (1980). Analytical results are listed in Table 1 and displayed on a concordia diagram (Fig. 2). A description of the zircon morphology of the fractions as analyzed is presented in the Appendix.

The three fractions analyzed yielded data points which form a closely spaced collinear grouping to the right of the concordia curve between 300 and 400 Ma (Fig. 2). Linear regression of these results yields a chord with an upper concordia intercept of 429 Ma and a slightly negative lower intercept ($^{206}Pb/^{238}U = -0.00136$). Such a chord does not lead to a satisfactory interpretation in terms of age due to the negative lower intercept. The data points are also well fitted by a chord originating at the origin and intersecting the concordia at 439 ± 7 Ma. This age is equivalent to the average of the $^{207}Pb$-$^{206}Pb$ ages for the three fractions and the analytical uncertainty of ± 7 Ma is twice the standard error of the mean of these ages. Thus, we interpret these results as indicating an age of emplacement of 439 ± 7 Ma for the rhyolite flows of the Jumping Brook complex, since the data points cluster near the upper end of the chord and the morphology (see Appendix) is consistent with an igneous volcanic origin.

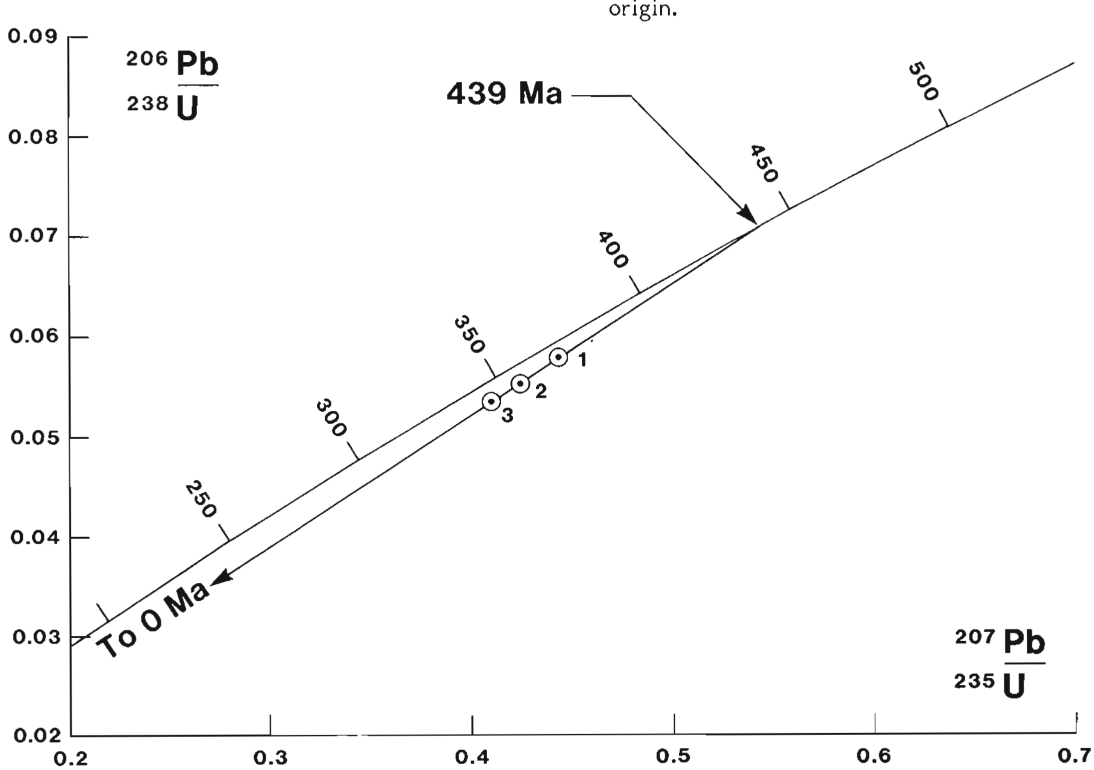


*Figure 2. Concordia diagram showing the results of analyses of three zircon fractions from dykes feeding basal rhyolite flows of the Jumping Brook complex, northwestern Cape Breton Island.*

Biotite from the same specimen yielded a K-Ar age of 363 ± 9 Ma (Wanless et al., 1979, p. 56). This result is interpreted as indicating the time that the biotite passed its argon blocking temperature.

## Interpretation

These two ages, when combined with previous results, go a long way toward unravelling the history of this part of the Cape Breton Highlands, suggesting a cyclic history throughout late Precambrian and early Paleozoic time.

The youngest cycle consists of the Upper Devonian Fisset Brook Formation of bimodal volcanics, with a Rb-Sr isochron age of 370 ± 20 Ma (Cormier and Kelly, 1964, recalculated by Keppie and Smith, 1978), which is overlain by the clastic Mississippian Horton Group. The age of the Fissett Brook Formation is essentially identical to the K-Ar age of 363 ± 9 Ma obtained on biotite from the Jumping Brook complex, and to several dates obtained by Neale from the young granites of this region. The similarity in dates shows that the Highlands must have been very rapidly uplifted and unroofed following metamorphism and plutonism, presumably along the complex set of steeply dipping mylonite zones which bound this region.

An older cycle, including the rocks dated in this study commenced with emplacement of granite (448 ± 37 Ma for the Cape Smoky pluton according to Keppie and Smith, 1978). The bimodal volcanics of the Jumping Brook complex (439 ± 7 Ma), appear to follow this emplacement as closely as the Fisset Brook follows the Acadian plutons, while the subsequent sedimentary part of the Jumping Brook complex compares to the Horton and younger groups.

Remnants of a third cycle occur in the granodiorite complex, which is cut by bimodal acid and basic dykes older than the Jumping Brook complex. Surficial manifestations of this activity have not been found, presumably because they have been destroyed by erosion.

All of these sequences have well known equivalents elsewhere in Atlantic Canada. The oldest cycle appears to be of Late Precambrian age, and hence equivalent to the "Avalonian" volcanics of southeastern Cape Breton Island. Bimodal volcanic rocks at or near the base of the Carboniferous section are well known from several parts of the Maritime Provinces (Kelley and Mackasey, 1965). Bimodal volcanics of known or suspected Silurian age occur at several other points in the Atlantic Provinces, notably the Springdale volcanics of Newfoundland (Whalen and Currie, 1982), and in the Cobequid Highlands of Nova Scotia (Donahoe and Wallace, 1979).

## References


Cormier, R.F.
1972: Radiometric ages of granitic rocks, Cape Breton Island, Nova Scotia; Canadian Journal of Earth Sciences, v. 9, no. 9, p. 1074-1086.

Cormier, R.F. and Kelly, D.G.
1964: Absolute age of the Fisset Brook Formation and the Devonian-Mississippian boundary, Cape Breton Island, Nova Scotia; Canadian Journal of Earth Sciences, v. 1, no. 3, p. 159-166.

Currie, K.L.
1975: Studies of granitoid rocks in the Canadian Appalachians; in Report of Activities, Part A, Geological Survey of Canada, Paper 75-1A, p. 265-270.

Paleozoic supracrustal rocks near Cheticamp, Nova Scotia; Maritime Sediments and Atlantic Geology, v. 18 (in press).

Donahoe, H.V. and Wallace, P.I.
1979: The new geological map of the Cobequid Highlands, Nova Scotia; Nova Scotia Department of Mines, Report 80-1, p. 211-219.

Fletcher, H.
1885: Report on geology of northern Cape Breton; Geological Survey of Canada, Report of Progress, 1882-84, Part H.

Jamieson, R.A.
1981: Geology of the Crowdis Mountain volcanics, southern Cape Breton Highlands; in Current Research, Part C, Geological Survey of Canada, Paper 81-1C, p. 77-81.

Kelley, D.G. and Mackasey, W.O.
1965: Basal Mississippian volcanic rocks in Cape Breton Island, Nova Scotia; Geological Survey of Canada, Paper 64-34.

Keppie, J.D. and Smith, P.K.
1978: Compilation of isotopic age data of Nova Scotia; Nova Scotia Department of Mines, Report 78-4.

Neale, E.R.W.
1963: Pleasant Bay Map-area; Geological Survey of Canada, Map 1119A.

Neale, E.R.W. and Kennedy, M.J.
1975: Basement and cover rocks at Cape North, Cape Breton Island, Nova Scotia; Maritime Sediments, v. 11, p. 1-4.

Sullivan, R.W. and Loveridge, W.D.
1980: Uranium-lead age determinations on zircon at the Geological Survey of Canada; current procedures in concentrate preparation and analysis; in Loveridge, W.D., Rubidium-strontium and uranium-lead isotopic age studies, Report 3; in Current Research, Part C, Geological Survey of Canada, Paper 80-1C, p. 161-246.

Wanless, R.K., Stevens, R.D., Lachance, G.R., and Dilabio, R.N.
1979: Age determinations and geological studies, K-Ar isotopic ages, Report 14; Geological Survey of Canada, Paper 79-2.

Whalen, J.B. and Currie, K.L.
1982: Volcanic and plutonic rocks in the Rainy Lake area, Newfoundland; in Current Research, Part A, Geological Survey of Canada, Paper 82-1A, p. 17-22.

Wiebe, R.A.
1972: Igneous and tectonic events in northeastern Cape Breton Island, Nova Scotia; Canadian Journal of Earth Sciences, v. 9, no. 10, p. 1262-1277.

## APPENDIX

Description of zircon concentrates as analyzed,
feeder dykes, Jumping Brook complex, northwestern Cape Breton Island.
Latitude 46°40.5'N, longitude 60°57.8'W

The analyzed fractions of these samples were of 100% pure zircon in the form of euhedral to slightly rounded crystals and crystal fragments of light tan colour varying from clear to translucent. Some crystals showed evidence of concentric zoning and many contained small inclusions or internal cracks. Most crystals were moderately elongated with a maximum observed length-to-breadth ratio of 4.3:1. The magnetic fraction differed from the nonmagnetic only in having slightly more abundant opaque inclusions.

# 3. A U-Pb ZIRCON AGE FOR THE CREIGHTON GRANITE, ONTARIO

M.J. Frarey, W.D. Loveridge, and R.W. Sullivan

*Frarey, M.J., Loveridge, W.D., and Sullivan, R.W., A U-Pb zircon age for the Creighton Granite, Ontario; in Rb-Sr and U-Pb Isotopic Age Studies, Report 5, in Current Research, Part C, Geological Survey of Canada, Paper 81-1C, p. 129-132, 1982.*

**Abstract**

*A U-Pb, upper concordia intercept age of 2333 + 33/-22 Ma on zircon from the Creighton Granite (near Sudbury, Ontario) is interpreted as the time of magmatic intrusion of the Creighton and Murray granites. This result establishes these intrusions as pre-Nipissing diabase and provides a minimum age for deposition of the Huronian Supergroup.*

## Geological Setting

The Creighton Granite and Murray Granite are relatively small felsic plutons that lie immediately south of the south range of the Sudbury Nickel Irruptive near the city of Sudbury. Separated by less than two kilometres and of similar composition and texture, they are considered to be cogenetic and coeval; they may be joined at depth. The age, origin, and relationship of the intrusions to other rocks and to the geological history of the area have frequently been the subject of discussion. The two bodies intrude steeply inclined, mainly volcanic, lowermost strata of the Huronian Supergroup, namely, the Elsie Mountain, Stobie, and Copper Cliff formations of the Elliot Lake Group. The Creighton pluton is cut by small mafic dykes of uncertain affiliation, by the norite and Copper Cliff offset dyke of the Irruptive, by olivine diabase dykes of the Sudbury swarm, and by small felsic dykes of uncertain age (Card, 1968; Innes, 1978).

The Creighton and Murray plutons range in composition from granite to oligoclase granodiorite but mainly consist of porphyritic and nonporphyritic quartz monzonite. According to Dutch (1979), the Creighton consists, in decreasing abundance, of quartz, oligoclase, perthitic microcline and biotite, with epidote, hornblende, and zircon as minor constituents. The pluton is strongly foliated in many places; this foliation formed either during diapiric emplacement (Dutch, 1979) or, more likely, during both emplacement and subsequent regional deformation (Card, 1979). The sample from which the zircons were separated was coarse grained, porphyritic and moderately biotitic. It was taken from a fairly large, homogeneous outcrop area on Highway 536 about 2 kilometres northwest of the town of Lively, in Snider Township (Fig. 1).

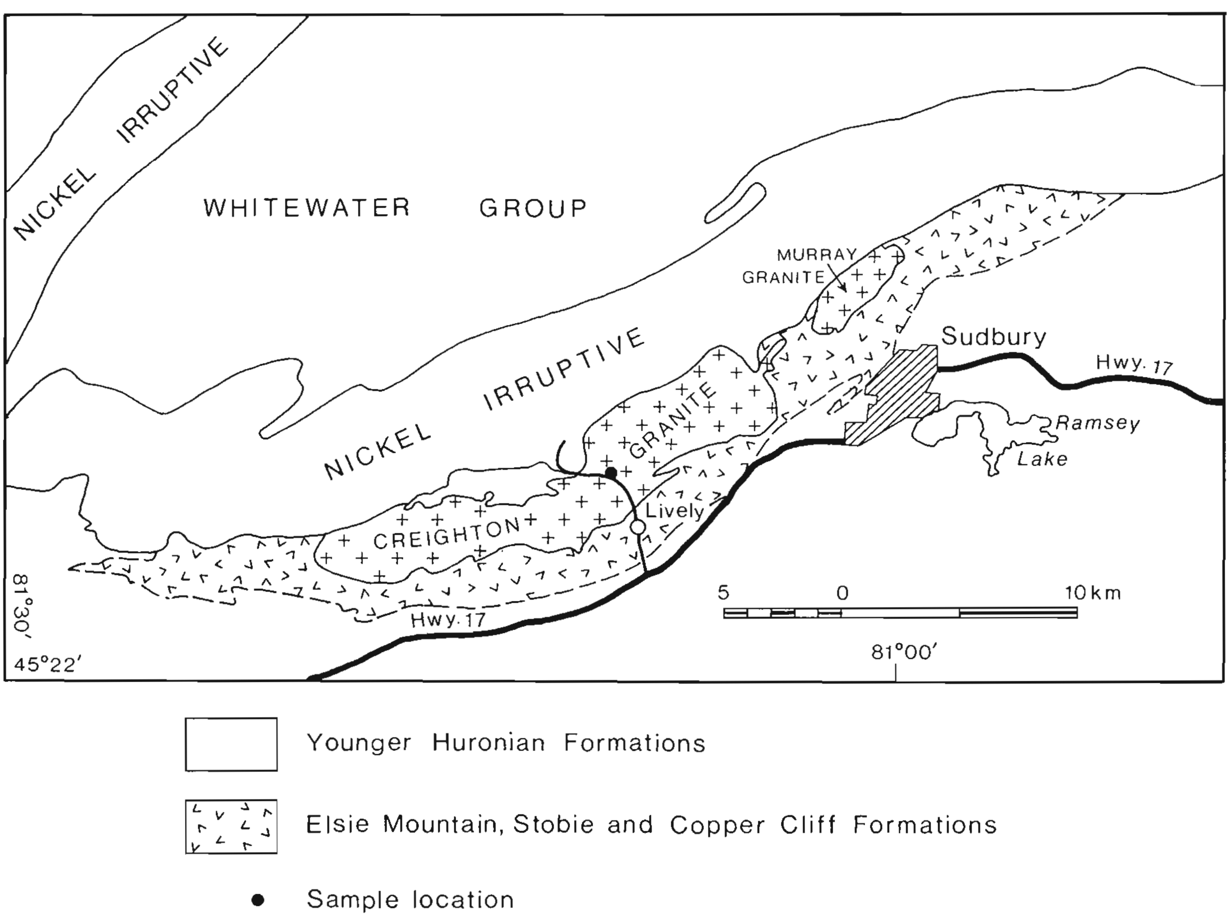


***Figure 1.*** *Geological sketch map of the Sudbury area showing the sample location.*

Table 1

Analytical data, zircon fractions from the Creighton Granite

| Fraction number | | 1 | 2 | 3 |
|---|---|---|---|---|
| Fraction size, µm | | -105+74 | -149+105 | -149+105 |
| Magnetic or nonmagnetic | | nm | nm | mag |
| Weight, mg | | 1.55 | 0.92 | 2.38 |
| Total Pb, ng | | 113.3 | 67.43 | 189.2 |
| Pb Blank, % | | 1.1 | 1.8 | 0.7 |
| Observed | $^{206}Pb/^{204}Pb$ | 1670 | 1368 | 1394 |
| *Abundances | $^{204}Pb$ | 0.04049 | 0.04079 | 0.06021 |
| ($^{206}Pb$ = 100) | $^{207}Pb$ | 15.348 | 15.302 | 15.544 |
| | $^{208}Pb$ | 14.377 | 12.744 | 13.890 |
| Radiogenic Pb, ppm | | 238.9 | 198.4 | 240.8 |
| " " % | | 98.0 | 97.9 | 97.0 |
| Uranium, ppm | | 549.8 | 463.6 | 585.3 |
| Atomic ratios | $^{206}Pb/^{238}U$ | 0.39494 | 0.39417 | 0.37733 |
| | $^{207}Pb/^{235}U$ | 8.0749 | 8.0316 | 7.6847 |
| | $^{207}Pb/^{206}Pb$ | 0.14828 | 0.14777 | 0.14770 |
| Ages, Ma | $^{206}Pb/^{238}U$ | 2146 | 2142 | 2064 |
| | $^{207}Pb/^{235}U$ | 2239 | 2235 | 2195 |
| | $^{207}Pb/^{206}Pb$ | 2326 | 2320 | 2319 |

*Corrected for Pb blank

Previous attempts to date these intrusions have not yielded consistent or definitive results. Five whole-rock Rb-Sr isochron ages have ranged from 2095 ± 60 Ma to 2242 Ma (recalculated values by C.H. Stockwell, 1982): his average of the five (Stockwell, 1982, p. 50) is 2165 Ma. A more definitive U-Pb age for the intrusions is desirable, particularly since a subdivision of the Aphebian Era, based in part on this event, has recently been proposed (Stockwell, 1982).

### Analytical Procedures and Results

Techniques for the concentration of zircon and the extraction and analysis of lead and uranium are described in Sullivan and Loveridge (1980). Analytical results are listed in Table 1 and displayed on a concordia diagram (Fig. 2). A description of the zircon morphology of the fractions as analyzed is presented in the Appendix. The three fractions analyzed yielded data points, collinear within analytical uncertainity, defining a chord which cuts the concordia curve at 2333 + 33/-22 and 195 + 429/-195 Ma.

### Interpretation and Significance

The U-Pb age of 2333 + 33/-22 is taken to be the time of magmatic intrusion of the Creighton and Murray granites. The significance of the age is as follows:

1. It conclusively establishes the intrusions as pre-Nipissing Diabase. Previously this was uncertain because of the lack of field relationships and the lack of a definitive age for the felsic intrusions.

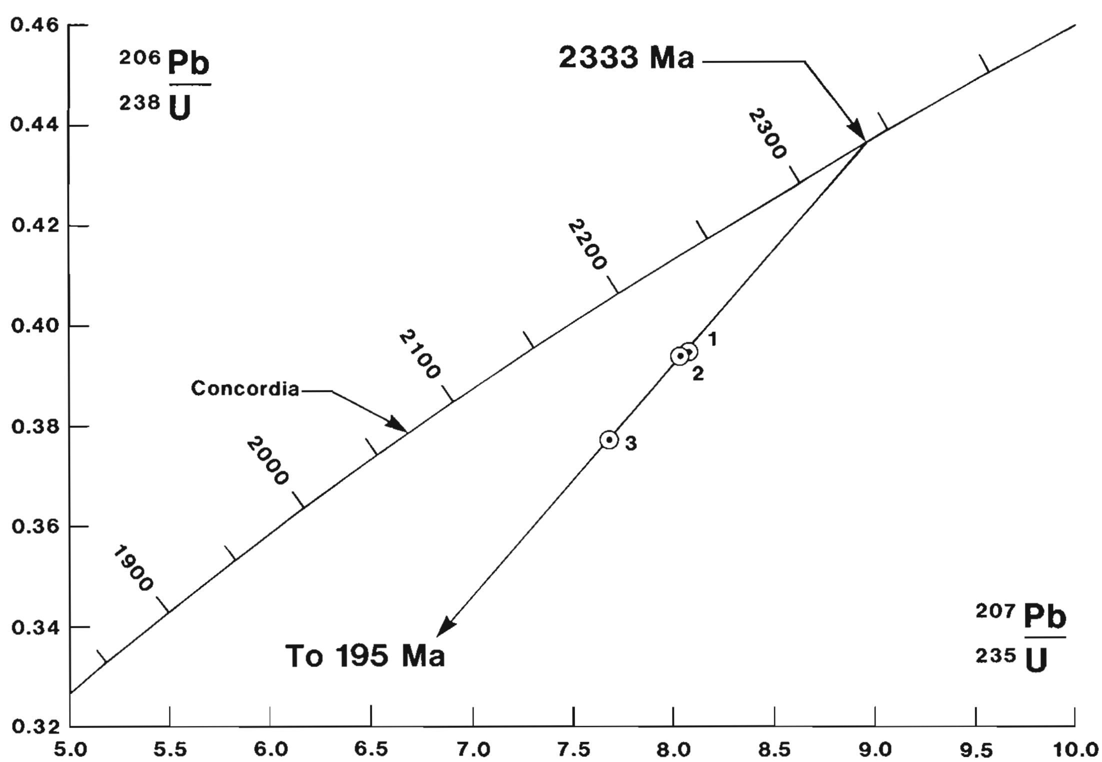


*Figure 2.* *Concordia diagram showing the results of analyses of zircon concentrates from the Creighton Granite.*

2. The intrusions are regarded as syn- or post-kinematic with respect to the earliest deformation of the Huronian Supergroup. Since there is no evidence of a major break in Huronian deposition in the Sudbury-Lake Huron region, or of separate deformation or plutonism affecting lower and upper parts of the supergroup, the age indicates that the entire supergroup was deposited prior to 2333 Ma. Previously, the minimum age was set by the isotopic age of the Nipissing Diabase, about 2115[1] Ma (Van Schmus, 1965; Fairbairn et al., 1969).
3. The U-Pb age thus indicates that the Rb-Sr age of about 2240[1] Ma obtained from sediments of the Gowganda Formation (Fairbairn et al., 1969) is a minimum and not a true age of Huronian sedimentation.

### References


Card, K.D.

1968: Geology of Denison-Waters area, Ontario; Ontario Department of Mines, Geological Report 60, 63 p.

1979: The Creighton pluton, Ontario: an unusual example of a forcefully emplaced intrusion: Discussion; Canadian Journal of Earth Sciences, v. 16, no. 11, p. 2181-2182.

Dutch, S.I.

1979: The Creighton pluton, Ontario: an unusual example of a forcefully emplaced intrusion; Canadian Journal of Earth Sciences, v. 16, no. 2, p. 333-349.

Fairbairn, H.W., Hurley, P.M., Card, K.D., and Knight, C.

1969: Correlation of radiometric ages of Nipissing diabase and metasediments with Proterozoic orogenic events in Ontario; Canadian Journal of Earth Sciences, v. 6, no. 3, p. 489-497.

Innes, D.G.

1978: McKim Township, District of Sudbury; Ontario Geological Survey, Preliminary Map P-1978, Ontario Geological Survey publication index no. P-01978 PRECAM.

Stockwell, C.H.

1982: Proposals for time classification and correlation of Precambrian rocks and events in Canada and adjacent areas of the Canadian Shield; Geological Survey of Canada, Paper 80-19, Part 1: A time classification of Precambrian rocks and events, 135 p.

Sullivan, R.W. and Loveridge, W.D.

1980: Uranium-lead age determinations on zircon at the Geological Survey of Canada: current procedures in concentrate preparation and analysis; in Loveridge, W.D., Rubidium-strontium and uranium-lead isotopic age studies, Report 3; in Current Research, Part C, Geological Survey of Canada, Paper 80-1C, p. 161-246.

Van Schmus, R.

1965: The geochronology of the Blind River-Bruce Mines area, Ontario, Canada; Journal of Geology, v. 73, no. 5, p. 755-780.


[1] Recalculated using $^{87}Rb$ decay constant = $1.42 \times 10^{-11}$ $a^{-1}$.

## APPENDIX

Description of zircon concentrates, Creighton Granite

The initial concentrate consisted of mainly euhedral zircon ranging from more or less clear but mottled, through cloudy-milky, to brown translucent. Many crystals exhibited combinations of various domains from any part of this range and a few crystals were observed to have clear overgrowths on their ends. Transmitted light examination of the less translucent grains showed the presence of rod inclusions and parallel linear features which may indicate zonal growth. Many grains showed irregular, "knobby" sides indicative of resorption or irregular growth, whereas a few other elongated ones appear to have been bent into a distinctly curved form. Rare parallel twins were observed and occasional apparently dislocated and offset terminations may be real or an artifact of resorption along internal fractures. Crystal form was mainly short prismatic with an average elongation of 2.7:1, but distinctly elongated (5.1:1) individuals were noted.

The relatively magnetic and nonmagnetic fractions visibly differed only in that the magnetic carried more black speck inclusions and surface attachments and was generally slightly less translucent than the nonmagnetic, the latter appearing darker and more altered.

# 4. U-Pb ISOTOPIC AGES OF ZIRCON FROM THE JURASSIC PLUTONIC SUITE, HOTAILUH BATHOLITH, NORTH-CENTRAL BRITISH COLUMBIA

R.G. Anderson, W.D. Loveridge, and R.W. Sullivan

*Anderson, R.G., Loveridge, W.D., and Sullivan, R.W., U-Pb isotopic ages of zircon from the Jurassic plutonic suite, Hotailuh Batholith, north-central British Columbia; in Rb-Sr and U-Pb Isotopic Age Studies, Report 5, in Current Research, Part C, Geological Survey of Canada, Paper 82-1C, p. 133-137, 1982.*

**Abstract**

*Zircons from the potassic marginal phase, in western exposures of the Three Sisters pluton, yield essentially concordant U-Pb isotopic ages of 170 ± 1 Ma which are consistent with the K-Ar isotopic ages for hornblende and biotite from the same sample. These data, in concert with K-Ar isotopic data and detailed intrusive relations suggest intrusion of the Three Sisters pluton may have occurred during an interval of 10-20 million years and that the western parts of the pluton apparently cooled quickly. Isotopic U-Pb and K-Ar analytical data suggest that the McBride River pluton probably crystallized around 166 ± 8 Ma (intersection with concordia of chord through data points and origin) and that the older K-Ar isotopic age may be due to excess Ar.*

## Geological Setting

The Hotailuh Batholith is a composite intrusion comprising plutonic suites of Triassic and Jurassic ages. Relationships with intrusive and overlying rocks of about the same age provide a minimum age constraint for the emplacement of the Triassic plutonic suite (pre-Karnian or Norian (Late Triassic) for most of the suite) and intrusive and metamorphic relationships provide maximum age constraints for emplacement of the Jurassic plutonic suite (post Toarcian (late Early Jurassic) for the Three Sisters pluton; and post Karnian or Norian for the McBride River, Pallen Creek and Tanzilla plutons). Detailed lithological descriptions of plutons in and around the Hotailuh Batholith and intrusive relations involving the Triassic plutonic suite, Mesozoic volcanics and sediments and Jurassic plutonic suite are given in Anderson (1978, 1979, 1980).

The Jurassic plutonic suite consists of batholithic (Three Sisters and McBride River plutons; see Fig. 1) and satellitic (Snowdrift Creek, Pallen Creek and Tanzilla plutons) intrusions. This paper gives results of U-Pb isotopic analyses of zircon from a sample of each of the Three Sisters pluton, potassic marginal phase, and the McBride River pluton.

The Three Sisters pluton is heterogeneous and composite, with common mafic inclusions, rare foliation, and an expanded compositional suite represented in five, sequentially intruded, mafic to felsic phases ranging from hornblende gabbro of the mafic phase to hornblende-biotite quartz syenite of the potassic marginal phase.

In contrast to the Three Sisters pluton, the McBride River pluton is homogeneous and massive, contains rare mafic inclusions, and comprises siliceous hornblende-biotite granodiorite or quartz monzodiorite.

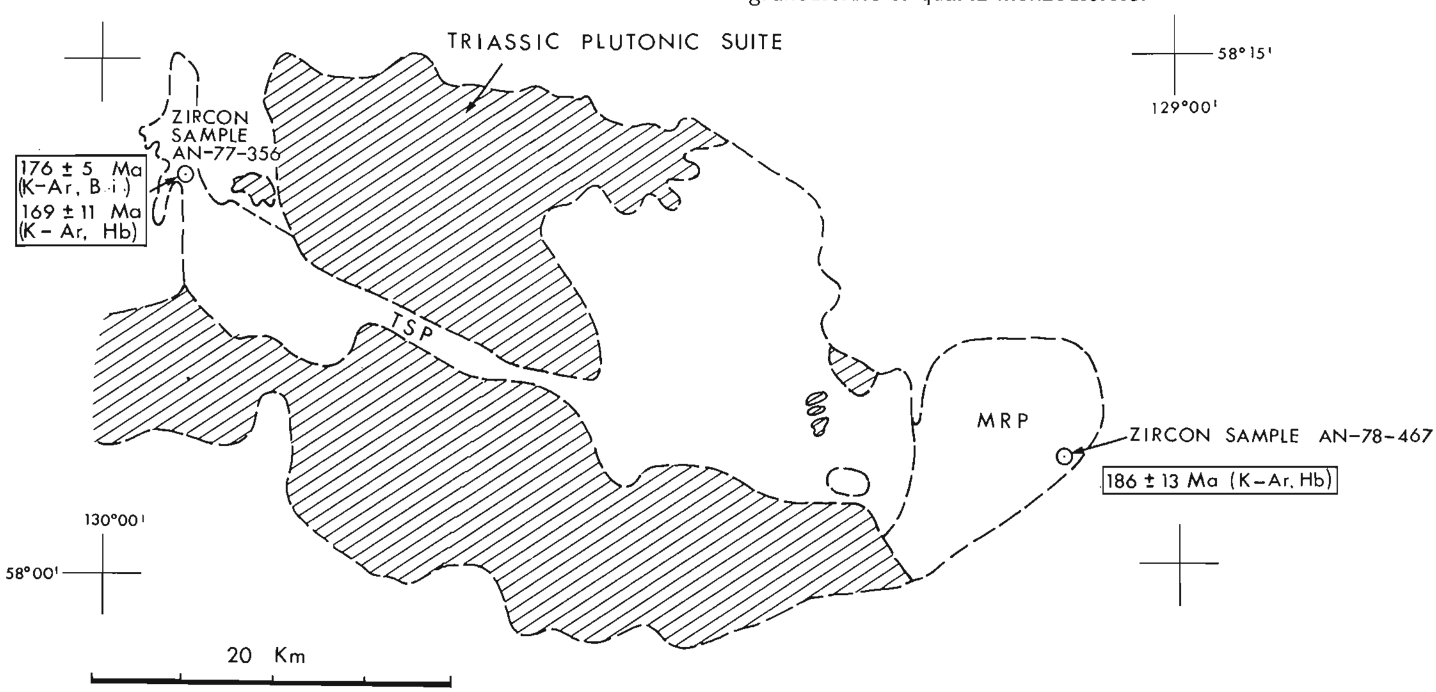


***Figure 1.*** *Location of analyzed samples in the Three Sisters and McBride River plutons of the Jurassic plutonic suite and available K-Ar isotopic data for the samples (see Stevens et al., 1982, GSC 80-2, 80-3, and 80-11). Ruled areas are the Triassic plutonic suite. Abbreviations are: Bi = biotite; Hb = hornblende; MRP = McBride River pluton; and TSP = Three Sisters pluton.*

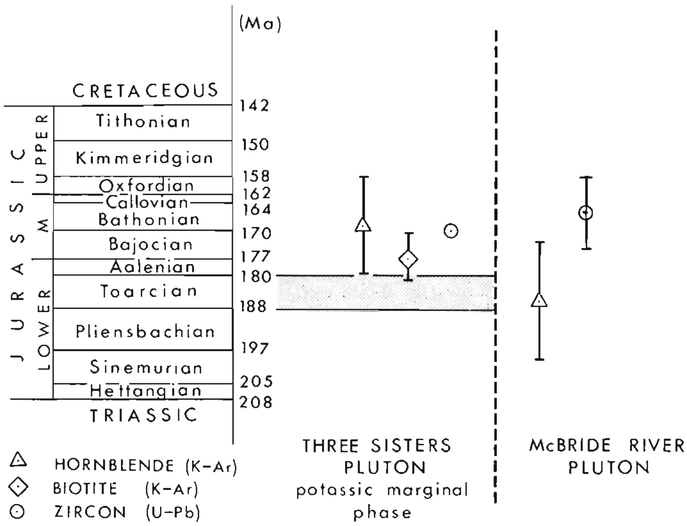


***Figure 2.*** *Plot of K-Ar mineral and U-Pb zircon isotopic ages for the Three Sisters pluton, potassic marginal phase (sample AN-77-356) and McBride River pluton (sample AN-78-467) compared to Armstrong's (1978, 1981) time scale. The U-Pb isotopic age for the Three Sisters pluton is the average of $^{206}Pb/^{238}U$ and $^{207}Pb/^{235}U$ ages for all fractions. The U-Pb isotopic age for the McBride River pluton is the concordia intercept age (Fig 3). Sources for the K-Ar isotopic ages are the same as for Figure 1. Shaded area is the estimated age (and maximum stratigraphic age) for the eastern part of the Three Sisters pluton.*

## K-Ar Isotopic Dating

Potassium-argon isotopic ages for the Jurassic plutonic suite range from 142 to 208 Ma (R.D. Stevens, personal communication, 1982). Most of the Three Sisters pluton in the northeastern part of the batholith is thought to have been intruded at about 180-188 Ma based on the oldest K-Ar isotopic ages, stratigraphic constraints on maximum emplacement age and the revised Jurassic time scale of Armstrong (1978, 1981). In the west, K-Ar isotopic ages range from 161 to 176 Ma and for the sample submitted for zircon U-Pb isotopic analysis, concordant K-Ar hornblende (169 ± 11 Ma; Stevens et al., 1982, GSC 80-3) and biotite (176 ± 5 Ma; Stevens et al., 1982, GSC 80-2) isotopic ages were determined (see Fig. 2). A single K-Ar hornblende age of 186 ± 13 Ma (Stevens et al., 1982, GSC 80-11) was determined for the McBride River pluton sample submitted for zircon U-Pb isotopic analysis.

## Analytical Procedures and Results

Analytical methods used in concentration of zircon, analysis of lead and uranium and computation of U-Pb isotopic ages are detailed in Sullivan and Loveridge (1980) and Loveridge (1980). Common lead corrections were made assuming a model age of 185 Ma for both samples (Stacey and Kramers, 1975). Analytical results are given in Table 1 and Figures 2 and 3. Descriptions of rock samples and zircon fractions are given in the Appendix.

The lead contamination levels associated with the analyses of the three zircon fractions from the McBride River pluton sample, AN-78-467, were relatively high due to the very low amounts of lead obtained from these samples for

Table 1

Analytical data, zircon fractions from the Three Sisters pluton, potassic marginal phase and the McBride River pluton

| Sample | | AN-77-356 | | | | AN-78-467 | | |
|---|---|---|---|---|---|---|---|---|
| Unit | | Three Sisters Pluton, Potassic Marginal Phase | | | | McBride River Pluton | | |
| Location (Lat., Long.) | | 58°11'30"N; 129°55'00"W | | | | 58°03'00"N; 129°06'30"W | | |
| Fraction Number | | 1 | 2 | 3 | 4 | 1 | 2 | 3 |
| Fraction size (μm) | | -105+74 | -105+74 | +149 | +149 | -74+62 | +74 | +105 |
| Magnetic/nonmagnetic | | NM | M | NM | M | NM | | |
| Weight (mg) | | 2.10 | 2.15 | 5.47 | 4.05 | 1.38 | 3.04 | 2.03 |
| Total Pb (ng) | | 40.60 | 95.95 | 76.54 | 111.6 | 5.47 | 9.27 | 8.29 |
| Pb Blank (%) | | 2.6 | 2.1 | 2.6 | 1.7 | 18.3 | 10.8 | 12.1 |
| Observed | $^{206}Pb/^{204}Pb$ | 2096 | 1982 | 285 | 2768 | 196.1 | 386.5 | 328.3 |
| Abundances* | $^{204}Pb$ | 0.0050 | 0.0221 | 0.3050 | 0.0085 | 0.1546 | 0.0655 | 0.0862 |
| ($^{206}Pb$ = 100) | $^{207}Pb$ | 5.0511 | 5.3103 | 9.4552 | 5.0953 | 7.195 | 5.097 | 6.214 |
| | $^{208}Pb$ | 13.117 | 14.437 | 23.425 | 16.018 | 20.70 | 16.67 | 16.93 |
| Radiogenic Pb | (ppm) | 52.91 | 120.6 | 32.64 | 97.75 | 11.35 | 9.92 | 8.20 |
| Radiogenic Pb | (%) | 99.69 | 98.64 | 83.14 | 99.48 | 91.1 | 96.1 | 94.8 |
| Uranium (ppm) | | 1958 | 4469 | 1217 | 3539 | 487.8 | 444.9 | 376.1 |
| Atomic ratios: | $^{206}Pb/^{238}U$ | 0.02664 | 0.02645 | 0.02656 | 0.02660 | 0.02251 | 0.02173 | 0.02134 |
| | $^{207}Pb/^{235}U$ | 0.1829 | 0.1818 | 0.1821 | 0.1823 | 0.1528 | 0.1481 | 0.1456 |
| | $^{207}Pb/^{206}Pb$ | 0.04978 | 0.04986 | 0.04973 | 0.04970 | 0.04922 | 0.04944 | 0.04947 |
| Ages (Ma): | $^{206}Pb/^{238}U$ | 169.5 | 168.3 | 169.0 | 169.3 | 143.5 | 138.5 | 136.1 |
| | $^{207}Pb/^{235}U$ | 170.5 | 169.6 | 169.9 | 170.0 | 144.3 | 140.3 | 138.0 |
| | $^{207}Pb/^{206}Pb$ | 184.8 | 188.3 | 182.2 | 181.2 | 158.2 | 168.9 | 170.2 |

*After subtraction of Pb blank.

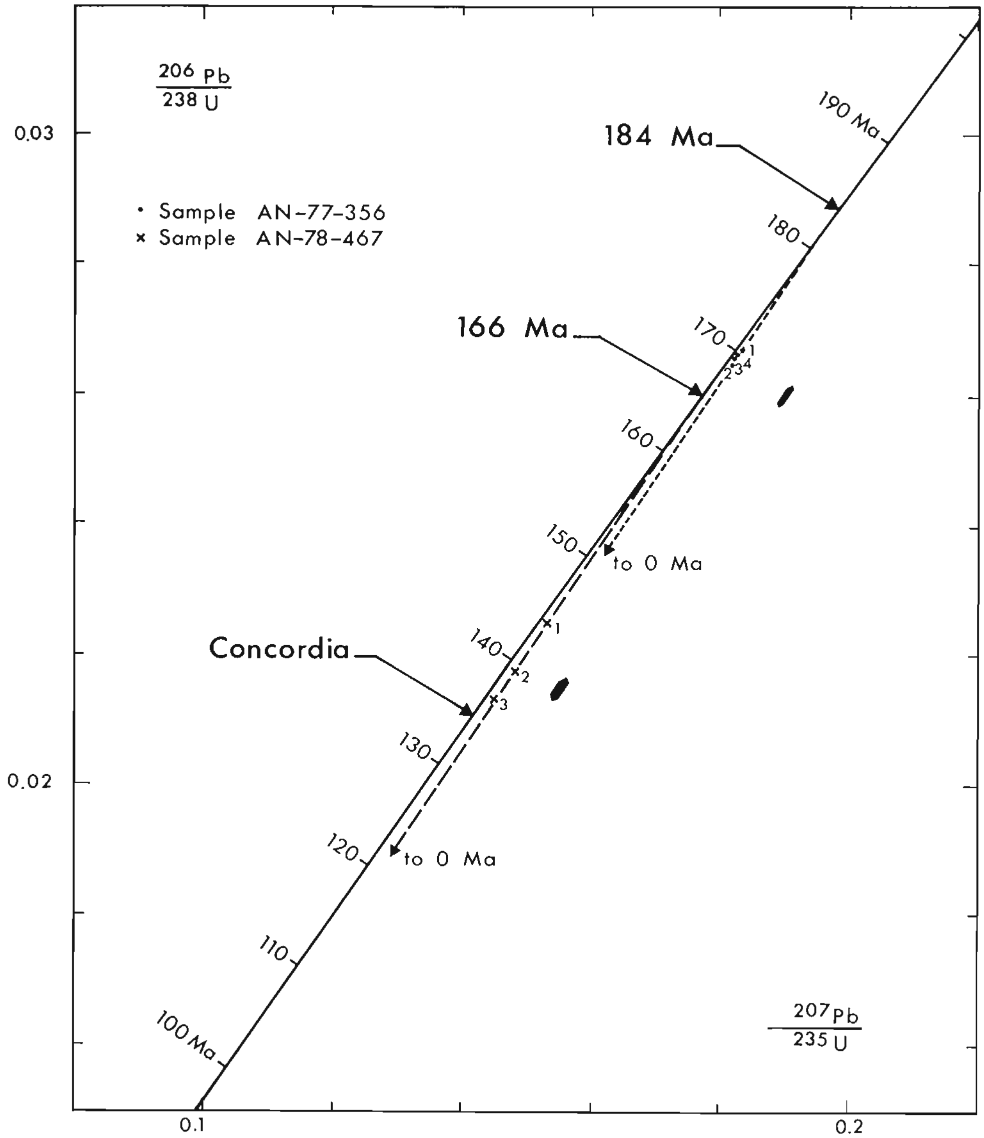


***Figure 3***

*Concordia plot for: sample AN-77-356, Three Sisters pluton, potassic marginal phase (dots); and sample AN-78-467, McBride River pluton (crosses). Numbers refer to fraction numbers in Table 1. Shaded symbols are analytical error polygons. Dashed lines are chords through origin and data ("best fit" line forced through origin for McBride River pluton) whose upper concordia intercepts give average $^{207}Pb/^{206}Pb$ "age".*

analysis (5 to 9 ng). For this reason, the analytical uncertainties in the measured $^{207}Pb/^{206}Pb$ ratios, ±0.30%, are approximately twice normal. Lead levels were satisfactorily high in the Three Sisters pluton zircon fractions and relative contamination levels correspondingly low.

Discussion

The U-Pb isotopic ages for individual fractions of sample AN-77-356 (Three Sisters pluton, potassic marginal phase) differ by less than 1 per cent and are essentially concordant at 170 Ma (Fig. 3). A chord through the data cluster of points in Figure 3 and the origin has an upper concordia intercept of 184 Ma, the average of the $^{207}Pb/^{206}Pb$ "ages". Although it is intriguing to compare this age, 184 ± 5 Ma ($2\sigma$ uncertainity derived from standard error of the mean), with the estimated cooling age for the northeastern portion of the Three Sisters pluton (180-188 Ma) described previously, in view of the concordant U-Pb ages (average of fractions is 169.6 ± 1 Ma), the $^{207}Pb/^{206}Pb$ "age" probably has no significance. The U-Pb isotopic age of 170 Ma for the sample from the western Three Sisters pluton, potassic marginal phase compares closely with the K-Ar isotopic ages determined from the same sample (Fig. 2). If the zircon U-Pb isotopic ages date the time of crystallization, the western exposures of the Three Sisters pluton apparently cooled rapidly through the argon retention temperatures for biotite and hornblende. At this locality, the present level of exposure is near the roof of the intrusion and supports the hypothesis of rapid cooling. Further, comparison of the crystallization age of the western Three Sisters pluton (170 Ma) with estimated emplacement age of the pluton in the east (180-188 Ma) suggests diachronous intrusion of the Three Sisters pluton from east to west over a period of 10-20 million years.

The three zircons fractions from the sample of the McBride River pluton yield increasingly discordant U-Pb isotopic ages with increasing fraction size (0.6 per cent difference in U-Pb ages in fraction 1 compared with 1.4 per cent difference in ages in fraction 3). As shown in Figure 3 the data lie off the concordia curve but are very nearly concordant within the analytical error. A chord through the data yields an upper concordia intercept of about 155 Ma but leads to a negative lower intercept and so is an inappropriate solution for discordancy in the U-Pb ages. A "best fit" chord forced through the origin and the data points has an upper concordia intercept of 166 ± 8 Ma (Fig. 3: $2\sigma$ uncertainity derived from the standard error of the mean of the $^{207}Pb/^{206}Pb$ "ages"). This age is barely concordant within analytical uncertainity with the single K-Ar determination (186 ± 13 Ma; see Fig. 2). The U-Pb isotopic ages fall within a limited range of 136 to 144 Ma, averaging 140 Ma, but probably reflect lead loss and likely have no physical significance. A distinction between the apparent U-Pb ages and the concordia intercept age is important because there is no stratigraphic constraint on the minimum emplacement age and only a loose stratigraphic constraint on the maximum emplacement age for the McBride River pluton. The pluton is lithologically, petrographically and geochemically similar to part of the Snowdrift Creek pluton north of the Hotailuh Batholith which has yielded a single K-Ar biotite isotopic age of 147 ± 5 Ma (Stevens et al., 1982, GSC 80-1); and if there is a major period of plutonism around 145-150 Ma, it may have been responsible for an apparent "event" around 150-155 Ma which selectively reset some of the K-Ar isotopic ages of the Jurassic plutonic suite. More geochronological work is warranted to confirm a reliable emplacement and/or cooling age for the McBride River pluton. We currently interpret these results as indicating that emplacement of the McBride River pluton occurred at 166 ± 8 Ma and that the K-Ar age of 186 ± 13 Ma may be anomalously old due to the presence of excess argon.

## Conclusions

Uranium-lead isotopic analyses of zircon separates from samples of the western Three Sisters pluton, potassic marginal phase suggest that this intrusion crystallized about 170 Ma. The U-Pb isotopic age is concordant with the available K-Ar isotopic ages for the same sample and these data suggest rapid cooling in the western outcrops of the pluton and, together with K-Ar isotopic data in the eastern part of the pluton, imply emplacement of the pluton from east to west over a period of 10-20 million years. Results of U-Pb isotopic analyses of zircons from the eastern McBride River pluton suggest that emplacement of the pluton probably occurred 166 ± 8 Ma ago.

## References


Anderson, R.G.

1978: Preliminary report on the Hotailuh Batholith: its distribution, age and contact relationships in the Cry Lake, Spatsizi and Dease Lake map-areas, north-central British Columbia; in Current Research, Part A, Geological Survey of Canada, Paper 78-1A, p. 29-31.

Anderson, R.G. (cont.)

1979: Distribution and emplacement history of plutons within the Hotailuh Batholith in the Cry Lake and Spatsizi map-areas, north-central British Columbia; in Current Research, Part A, Geological Survey of Canada, Paper 79-1A, p. 393-395.

1980: Satellitic stocks, volcanic and sedimentary stratigraphy, and structure around the northern and western margins of the Hotailuh Batholith, north-central British Columbia; in Current Research, Part A, Geological Survey of Canada, Paper 80-1A, p. 37-40.

Armstrong, R.L.

1978: Pre-Cenozoic Phanerozoic time-scale—computer file of critical dates and consequences of new and in-progress decay-constant revisions; American Association of Petroleum Geologists, Studies in Geology, no. 6, p. 73-91.

1981: Late Triassic-Early Jurassic time scale calibration in British Columbia; in Numerical Dating in Stratigraphy, ed. G.S. Odin, John Wiley & Sons, p. 509-513.

Loveridge, W.D.

1980: Introduction; in Rb-Sr and U-Pb Isotopic Age Studies, Report 3; in Current Research, Part C, Geological Survey of Canada, Paper 80-1C, p. 163.

Stacey, J.S. and Kramers, J.D.

1975: Approximation of terrestrial lead evolution by a two stage model; Earth and Planetary Science Letters, v. 26, p. 207-221.

Stevens, R.D., DeLabio, R.N., and Lachance, G.R.

1982: Age determinations and geological studies; Geological Survey of Canada, Paper 81-2, p. 3-4.

Sullivan, R.W. and Loveridge, W.D.

1980: Uranium-lead age determinations on zircon at the Geological Survey of Canada: current procedures in concentrate preparation and analysis; in Rb-Sr and U-Pb Isotopic Age Studies, Report 3; in Current Research, Part C, Geological Survey of Canada, Paper 80-1C, p. 164.

## APPENDIX

Petrographic description of rocks and analyzed zircon separates

Description of Rock Samples

Sample AN-77-356 (Three Sisters pluton, potassic marginal phase)

Massive, equigranular, medium-grained hypidiomorphic quartz monzonite containing alkali feldspar (47.5%), andesine (28.6%), quartz (11.6%), hornblende (7.9%), biotite (3.2%) and accessory allanite (0.7%), magnetite (0.3%), clinopyroxene (0.1%), zircon (0.1%) and apatite (<0.1%).

Sample AN-78-467 (McBride River pluton)

Massive, equigranular, medium-grained hypidiomorphic granodiorite containing andesine (53.5%), quartz (21.1%), alkali feldspar (15.8%), biotite (4.5%), hornblende (3.9%), and accessory titanite (0.6%), magnetite (0.5%), zircon (<0.1%) and monazite (<0.1%).

Description of Analyzed Zircon Concentrates

The following size, magnetic and petrographic criteria allowed hand picking of the fractions to provide a totally pure concentrate.

Sample AN-77-356 (Three Sisters pluton, potassic marginal phase)

(a) Fractions 1 and 3 (see Table 1)

Nonmagnetic splits of both size fractions (-105+74 μm and +149 μm) contain clear to very pale tan, euhedral, prismatic zircons (plus fragments) with sharp terminations and uncommon faint zoning, black speck inclusions and bubble inclusions or cracks (especially prevalent in the larger zircons).

(b) Fractions 2 and 4 (see Table 1)

Magnetic splits of both size fractions (-105+74 μm and +149 μm) are predominantly brown to purple and transparent, euhedral, prismatic and more or less sharply terminated grains (or fragments of the same type) and are characterized by pronounced, concentric zoning uncommonly about a visible rounded core. Although the cores may indicate a xenocryst origin, the transparent, euhedral, sharply terminated nature of both fractions indicates that the zircons are products of primary crystallization from a magma.

Sample AN-78-467 (McBride River pluton)

(a) Fractions 1, 2, and 3 (see Table 1)

In all three fractions analyzed, the sample consisted of 100% zircon crystals of generally euhedral, well terminated shape. The coarser material was very light straw coloured, while the finest fraction was essentially colourless. Nearly all crystals were clear and of fresh appearance, though rod and bubble inclusions were commonly present. A few crystals contained distinct, relatively large cavities of irregular shapes but elongated parallel to the main crystal axis. Grain shape ranged from equant to elongated (4.8:1 observed maximum).

# 5. U-Pb MEASUREMENTS ON ZIRCON INDICATE MIDDLE PALEOZOIC PLUTONISM IN THE OMINECA CRYSTALLINE BELT, NORTH-CENTRAL BRITISH COLUMBIA

Project 700047

H. Gabrielse, W.D. Loveridge, R.W. Sullivan, and R.D. Stevens

*Gabrielse, H., Loveridge, W.D., Sullivan, R.W., and Stevens, R.D., U-Pb measurements on zircon indicate middle Paleozoic plutonism in the Omineca Crystalline Belt, north-central British Columbia; in Rb-Sr and U-Pb Isotopic Age Studies, Report 5, in Current Research, Part C, Geological Survey of Canada, Paper 82-1C, p. 139-146, 1982.*

### Abstract

*Zircons from foliated granitic sills within two localities of tightly folded upper Proterozoic clastic rocks of the Ingenika Group in the Swannell Ranges, north-central British Columbia, give discordant U-Pb zircon ages indicating Silurian and possibly later plutonic events. These data combined with U-Pb, U-Th-Pb, and K-Ar ages for similar granitic plutons elsewhere in the Cordillera suggest that an ensialic magmatic arc extended intermittently or continuously along the western part of the Cordilleran miogeocline during Siluro-Devonian and perhaps later time. In late Devonian time the arc and related tectonism may have provided a source for turbiditic clastic sediments that were deposited over much of the western part of the Cordilleran miogeocline.*

## Introduction

In the Omineca Crystalline Belt of north-central British Columbia an anticlinorium in Swannell Ranges exposes tightly folded clastic rocks which comprise the oldest strata of the upper Proterozoic Ingenika Group (Fig. 1). In the core of the anticlinorium the rocks have been regionally metamorphosed to kyanite grade but on the flanks of the structure they are commonly below chlorite grade (Fig. 2). Locally, the clastic rocks have been intruded by granitic sills and/or dykes as much as 15 m thick. The granitic rocks are tightly folded with the enclosing metasediments and have one well defined foliation parallel with compositional layering in the metasediments and one parallel with the axial surfaces of nearby folds (Fig. 3).

It has been assumed, generally, that most, if not all, regional metamorphism and most of the plutonism in the northern Omineca Crystalline Belt occurred in the Mesozoic. K-Ar determinations on granitic rocks in the belt commonly indicate mid-Cretaceous, late Cretaceous and rare Cenozoic ages and K-Ar ages of regionally metamorphosed rocks give mainly Cretaceous or early Cenozoic ages. The latter appear to represent a widespread thermal event in regions of greatest Eocene uplift. Thus age determinations on the granitic rocks sampled for this study were expected to provide a maximum date for Mesozoic deformation in the region.

## Petrology

Metasediments in the general area of the granitic rocks are fresh, pervasively cleaved, fine- to medium-grained, silvery-brownish-buff grey, quartz-plagioclase-garnet-biotite-muscovite schist. A typical sample comprises the following modal mineral percentages: quartz (28), plagioclase (8), garnet (4), biotite (23), muscovite (33), chlorite (2), zircon (2) and accessory tourmaline, apatite and opaques. Excellent schistosity imparted by the micas is parallel with the cleavage.

Adjacent to at least one of the sills the host rocks apparently have been hornfelsed over widths of greater than 10 m and comprise fresh, fine- to medium-grained quartz-plagioclase-zoisite-garnet-chlorite-biotite semi-schist with conspicuous light grey poikiloblasts of oligoclase (Fig. 4). Modal percentages of a typical sample are as follows: quartz (37), oligoclase (24), biotite (36), garnet (1), zircon (1) and accessory zoisite, chlorite, opaques, tourmaline and apatite. The rock has typical hornfelsic texture. Foliation in the hornfels indicates that it was affected by the main deformation and regional metamorphism. Apparently, the composition of the hornfels precluded significant mineralogical and textural changes at the grade of superimposed metamorphism.

The granitic rock of the sills and/or dykes is fresh, light creamy grey, medium grained, weakly to moderately foliated, relatively homogeneous, metamorphosed muscovite-biotite quartz monzonite. Modal percentages are as follows: quartz (16), plagioclase (40), microcline (31), biotite (7), muscovite (2), opaques (2), calcite-ankerite (1) and accessory allanite, apatite and zircon. Biotite is only slightly chloritized. Pale straw yellow zircon occurs mainly as inclusions in biotite or close to clusters of biotite flakes. The rocks show minor cataclasis but retain a hypidiomorphic texture.

## K-Ar Age Determinations

Biotites from hornfelsed country rocks and from one of the quartz monzonite bodies (GA-76-89A) gave K-Ar ages of 101 ± 4 Ma and 96.2 ± 3.6 Ma, respectively (Wanless et al., 1979, p. 15). Muscovite from beyond the limits of the hornfels zone gave a K-Ar age of 122 ± 4 Ma (Wanless et al., 1979, p. 16). A K-Ar age of 114 ± 3 Ma was obtained on biotite from the other dyke/sill, GAMA-76-135 (Table 1).

## Zircon Studies: Analytical Considerations, Results and Discussion

General techniques in the concentration of zircon and the extraction and analysis of lead and uranium are described in Sullivan and Loveridge (1980). Techniques specific to these samples are described below. Analytical results are presented in Tables 2 and 3 and displayed on a concordia diagram, Figure 5. Description of the zircon morphology of the two samples and sample locations appear in the appendix.

Samples from two granitic sills with similar lithology, several hundred metres apart, provided zircon for U-Pb study. Sample GAMA-76-135 yielded two families of zircon. One, denoted "clear" consisted of clear, stubby and very rounded grains (Fig. 6a). The other, "translucent", were translucent to opaque, relatively more prismatic, elongate grains with rounded terminations (Fig. 6b). Zircons from GA-76-89A (Fig. 6c), however, were predominantly translucent stubby euhedral crystals with sharp terminations, quite dissimilar from either of the two types from GAMA-76-135.

Five zircon fractions from GA-76-89A were processed and analyzed for U and Pb over a period of years. Initially the zircon concentrate was sieved and the coarsest material (-149 + 105 μm) passed through a Frantz Isodynamic Separator to obtain a relatively more versus less magnetic pair, fractions 4 and 5, Table 2. More recently, three more fractions were similarly processed from the remaining material but were abraded to remove surficial material using a technique originated by Krogh (1982). After abrasion the (originally) -105 + 93 μm fraction was carefully sieved and hand picked to obtain the coarser and finer fractions 1 and 2, Table 2, Figures 5 and 6d. Fraction 3 resulted from hand picking abraded zircon grains originally in the -149 + 105 μm size range.

The results of the U-Pb analyses show the value of the abrasion technique (Fig. 5). The data points for the three abraded fractions (1, 2 and 3) fall on the chord suggested by the two unabraded zircon data points (4 and 5) but are much more concordant, being only about 10% discordant whereas the unabraded fractions are 15 to 20% discordant. The five data points for GA-76-89A are collinear on a concordia plot (Fig. 5) defining a chord which yields an upper intercept age of 429 + 10/-7 Ma and a lower intercept of 126 + 57/-59 Ma. We interpret the upper intercept as the age of formation of the zircons and the primary age of intrusion of the sill. Because the lower intercept age is in agreement with K-Ar ages for regional metamorphism we interpret this as the cause of the discordance, viz. episodic lead loss at 126 Ma.

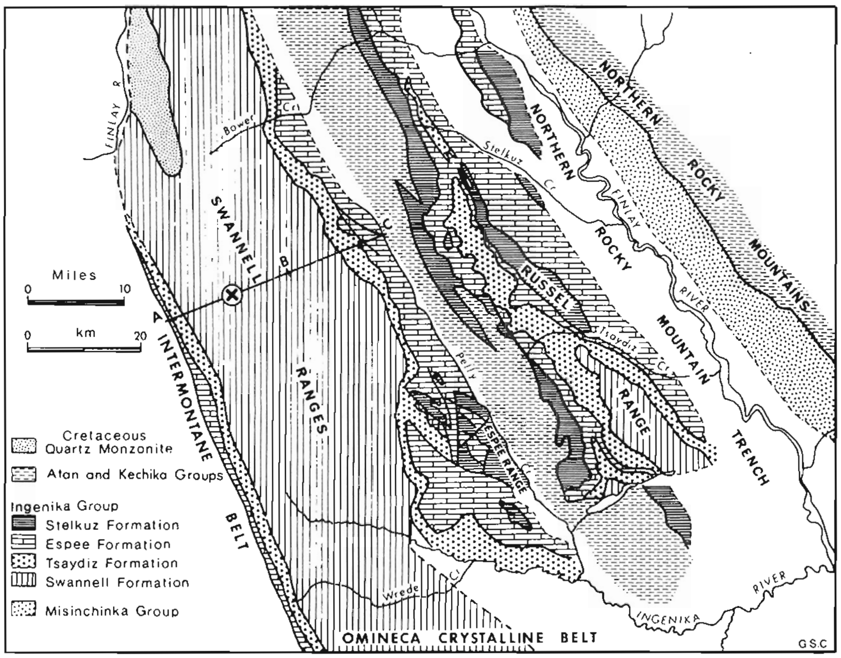


***Figure 1***

*Geological setting of granitic sills and/or dykes in Swannell Ranges and location of structural cross-section in Figure 2.*

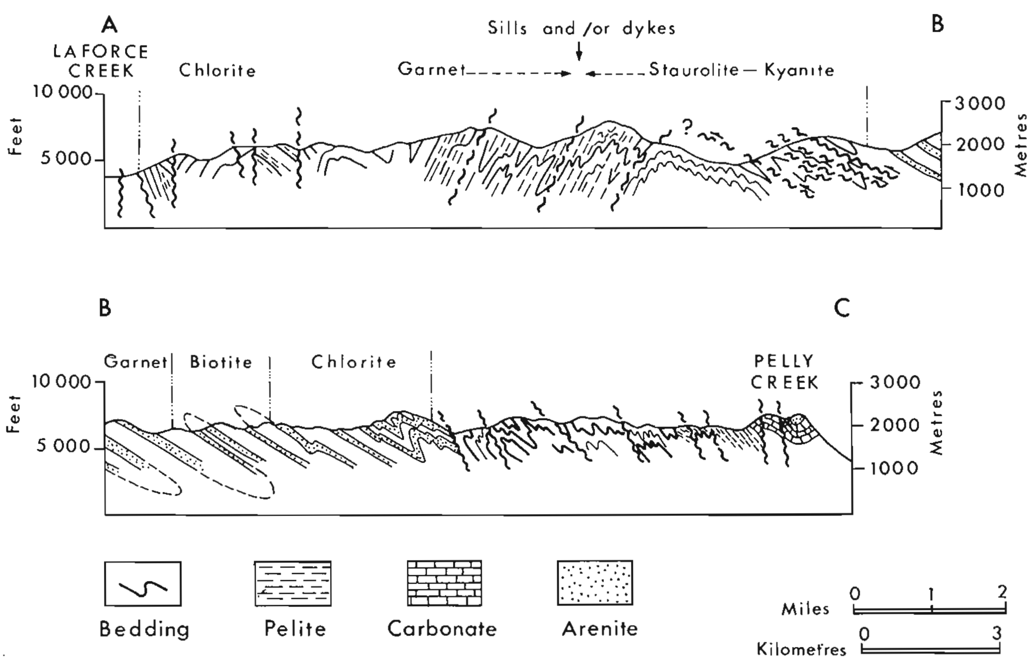


***Figure 2.*** *Structural setting of granitic sills and/or dykes in Swannell Ranges. After Mansy and Dodds, 1976. See Figure 1 for location.*

The uranium content in zircon from GA-76-89A is moderately high (750 to 1350 ppm) and would facilitate episodic lead loss from radiation damaged crystals.

Uranium is concentrated at or near the surface of the zircon crystals as evinced by the difference of up to 54% in uranium content between abraded and unabraded non magnetic zircon fractions. However, the lack of evident internal structure suggests that this is a phenomenon of original zircon formation as opposed to overgrowth of zircon at the time of metamorphism. Diffusive incorporation of uranium at the time of metamorphism is also virtually excluded by the near concordancy of the data points and the relatively constant U/Pb ratios in the abraded and unabraded fractions.

The results obtained from the analyses of GAMA-76-135 provide a radically different case from the classical picture presented by the results of GA-76-89A. Eight zircon fractions from GAMA-76-135 were hand picked for analysis, three from the clear family and five from the translucent. The data points from the five translucent zircon fractions form a linear array on a concordia plot defining a chord of upper intercept 2466 ± 30 Ma and lower intercept 353 ± 10 Ma. The data points are not precisely collinear, yielding a scatter about the chord of up to four times the analytical uncertainty. Unfortunately the abrasion technique was not in use in this laboratory at the time of analysis of zircon from GAMA-76-135.

Because the upper concordia intercept age given by the first four translucent zircon fractions analyzed was unexpectedly high, we felt it prudent to verify these results. Therefore a fifth fraction was carefully concentrated from a reserve portion of the original rock sample of GAMA-76-135. This concentrate also contained the same two families of zircon characteristic of the original concentrate and analysis of a carefully hand picked translucent fraction produced the results presented as fraction 3 in Table 3 and Figure 5, thus confirming the chord defined by the other four translucent data points.

***Figure 3.*** *Folded granitic sill with envelope of metasedimentary rock.*

Table 1

K-Ar age determination

GAMA-76-135, biotite from metagranodiorite; a folded and metamorphosed granitic dyke/sill located just east-southeast of GA-76-89A.

K-Ar age = 114 ± 3 Ma
K = 6.63%, $^{40}Ar/^{40}K$ = 0.00683
radiogenic argon = 48.5%

Concentrate: Biotite – reddish brown with approximately 9% chlorite alteration.

***Figure 4***

*Hornfelsed metasedimentary rocks of Swannell Formation, Ingenika Group. Note conspicuous light grey weathering poikiloblasts of oligoclase.*

Table 2

Analytical results of sample GA-76-89A

| Fraction | | 1 | 2 | 3 | 4 | 5 |
|---|---|---|---|---|---|---|
| Fraction size, µm | | -105 + 93 | -105 + 93 | -149 + 105 | -149 + 105 | -149 + 105 |
| Magnetic or nonmagnetic | | nm | nm | nm | nm | mag |
| Characteristic* | | abr., c | abr., f | abr. | - | - |
| Weight, mg | | 3.13 | 1.75 | 2.79 | 19.06 | 17.37 |
| Total Pb, ng | | 63.1 | 30.9 | 52.9 | 473.6 | 515.8 |
| Pb blank, % | | 1.3 | 2.6 | 3.7 | 0.4 | 0.6 |
| Observed | $^{206}Pb/^{204}Pb$ | 2635 | 1600 | 870 | 4367 | 5526 |
| Abundances† | $^{204}Pb$ | 0.0146 | 0.0143 | 0.0460 | 0.0153 | 0.0070 |
| ($^{206}Pb$ = 100) | $^{207}Pb$ | 5.7436 | 5.7346 | 6.1793 | 5.7299 | 5.6021 |
| | $^{208}Pb$ | 27.677 | 28.125 | 27.842 | 25.505 | 24.705 |
| Radiogenic Pb, ppm | | 62.82 | 58.34 | 63.88 | 78.47 | 89.80 |
| Radiogenic Pb, % | | 99.20 | 99.22 | 97.50 | 99.15 | 99.61 |
| Uranium, ppm | | 843.8 | 748.6 | 892.2 | 1153 | 1350 |
| Atomic ratios: | $^{206}Pb/^{238}U$ | 0.065148 | 0.064838 | 0.063086 | 0.060572 | 0.059438 |
| | $^{207}Pb/^{235}U$ | 0.49676 | 0.49400 | 0.47906 | 0.45993 | 0.45070 |
| | $^{207}Pb/^{206}Pb$ | 0.055299 | 0.055255 | 0.055072 | 0.055067 | 0.054992 |
| Ages, Ma: | $^{206}Pb/^{238}U$ | 407 | 405 | 394 | 379 | 372 |
| | $^{207}Pb/^{235}U$ | 410 | 408 | 397 | 384 | 378 |
| | $^{207}Pb/^{206}Pb$ | 424 | 423 | 415 | 415 | 412 |

*abr = abraded, c = sieved coarser, + 88 µm, f = sieved finer, -88 + 74 µm (after abrasion)

†Corrected for Pb blank

Table 3

Analytical results of sample GAMA-76-135

| Fraction | | 1 | 2 | 3 | 4 | 5 | 6 | 7 | 8 |
|---|---|---|---|---|---|---|---|---|---|
| Fraction size, µm | | +105 | +105 | +74 | -74 + 62 | -62 | +105 | +105 | -88 + 74 |
| Magnetic or nonmagnetic | | nm | - | - | - | - | nm | mag | - |
| Characteristic | | trl. | trl. | trl. | trl. | trl. | clear | clear | clear |
| Weight, mg | | 2.56 | 3.31 | 1.73 | 1.21 | 0.19 | 4.67 | 2.53 | 1.74 |
| Total Pb, ng | | 66.12 | 123.9 | 61.91 | 42.42 | 10.20 | 99.18 | 41.52 | 35.16 |
| Pb Blank, % | | 1.7 | 1.0 | 1.6 | 4.4 | 9.8 | 1.4 | 2.5 | 3.7 |
| Observed | $^{206}Pb/^{204}Pb$ | 2021 | 1510 | 972.6 | 561.5 | 429.6 | 1575 | 1167 | 527.7 |
| Abundances* | $^{204}Pb$ | 0.0196 | 0.0495 | 0.0754 | 0.1006 | 0.0570 | 0.0391 | 0.0398 | 0.1231 |
| ($^{206}Pb$ = 100) | $^{207}Pb$ | 13.685 | 12.140 | 11.325 | 11.130 | 10.086 | 13.606 | 13.606 | 13.380 |
| | $^{208}Pb$ | 14.581 | 13.430 | 13.539 | 14.407 | 13.218 | 17.263 | 17.161 | 19.160 |
| Radiogenic Pb, ppm | | 90.96 | 103.3 | 88.78 | 91.44 | 153.1 | 50.79 | 56.97 | 47.00 |
| Radiogenic Pb, % | | 99.02 | 97.48 | 96.14 | 94.87 | 97.04 | 98.09 | 98.05 | 94.06 |
| Uranium, ppm | | 501.3 | 854.2 | 912.1 | 996.7 | 1766 | 189.4 | 253.9 | 211.4 |
| Atomic ratios: | $^{206}Pb/^{238}U$ | 0.16554 | 0.11397 | 0.093183 | 0.088191 | 0.083522 | 0.24134 | 0.20216 | 0.20344 |
| | $^{207}Pb/^{235}U$ | 3.0657 | 1.8047 | 1.3252 | 1.1884 | 1.0725 | 4.3582 | 3.6484 | 3.2969 |
| | $^{207}Pb/^{206}Pb$ | 0.13431 | 0.11484 | 0.10314 | 0.097723 | 0.093127 | 0.13097 | 0.13088 | 0.11753 |
| Ages, Ma: | $^{206}Pb/^{238}U$ | 988 | 697 | 574 | 545 | 517 | 1394 | 1187 | 1194 |
| | $^{207}Pb/^{235}U$ | 1424 | 1047 | 857 | 795 | 740 | 1704 | 1560 | 1480 |
| | $^{207}Pb/^{206}Pb$ | 2155 | 1877 | 1681 | 1581 | 1490 | 2111 | 2110 | 1919 |

*Corrected for Pb blank

All five points defining the chord are quite discordant, with apparent lead loss/uranium gain ranging from 73 to 93%. Uranium contents are high, ranging from 500 to 1760 ppm, and parallel the degree of discordance, which in turn increases with decreasing grain size. Thus the smallest grains are the most discordant and have the highest uranium contents. Radiogenic lead contents are much more constant, varying from 89 to 153 ppm while common lead contents are low, one to five per cent.

The clear zircon fractions (6, 7 and 8) from GAMA-76-135 yield data points that fall to the left of the chord established by the translucent zircon results, and do not form a linear array (Fig. 5). The three clear zircon fractions contain much less uranium than the translucent zircons on a comparable grain size basis and the data points are less discordant. Yet, if uranium concentration is plotted against degree of discordancy, the clear zircon results fit the trend established by the translucent zircon results. Radiogenic lead contents of the clear zircon fractions are also relatively constant but are about half those of the translucent zircon fractions.

The results obtained from the clear zircon fractions suggest that they are either of the same age or somewhat younger than given by the upper concordia intercept of the translucent zircon chord and have been affected by one or more additional events between that time and 353 Ma.

One interpretation, and the one favoured by the authors for the disparate results obtained on the two samples GAMA-76-135 and GA-76-89A is as follows. The two sills, lithologically similar but with highly dissimilar zircon populations were emplaced at essentially the same time. Proximity, lithology and structure suggest a common magmatic and structural history. The primary age of emplacement is 429 + 10/-7 Ma as determined by the results on GA-76-89A.

However in GAMA-76-135 two families of zircon, one (translucent) of age approximately 2466 Ma, the other (clear) of similar antiquity but of differing U and Pb content and appearing to exhibit a more complex history were incorporated into the magma which was emplaced as that granitic sill. The two families of zircon may have co-existed in the same parent material or may indicate the inclusion of more than one parent material in the synthesis of the magma of the sill. The rounded shapes of the clear zircon family suggest that either their parent material had undergone granulite facies metamorphism (cf. Pidgeon and Bowes, 1972) or the zircons themselves had been rounded due to the abrasion of detrital action in an earlier sedimentary cycle (i.e. they are metasedimentary zircons incorporated from the host rocks); compare clear zircons, Fig. 6a, with mechanically abraded zircons from GA-76-89A, Figure 6d. The latter suggestion is the more probable as the rounded

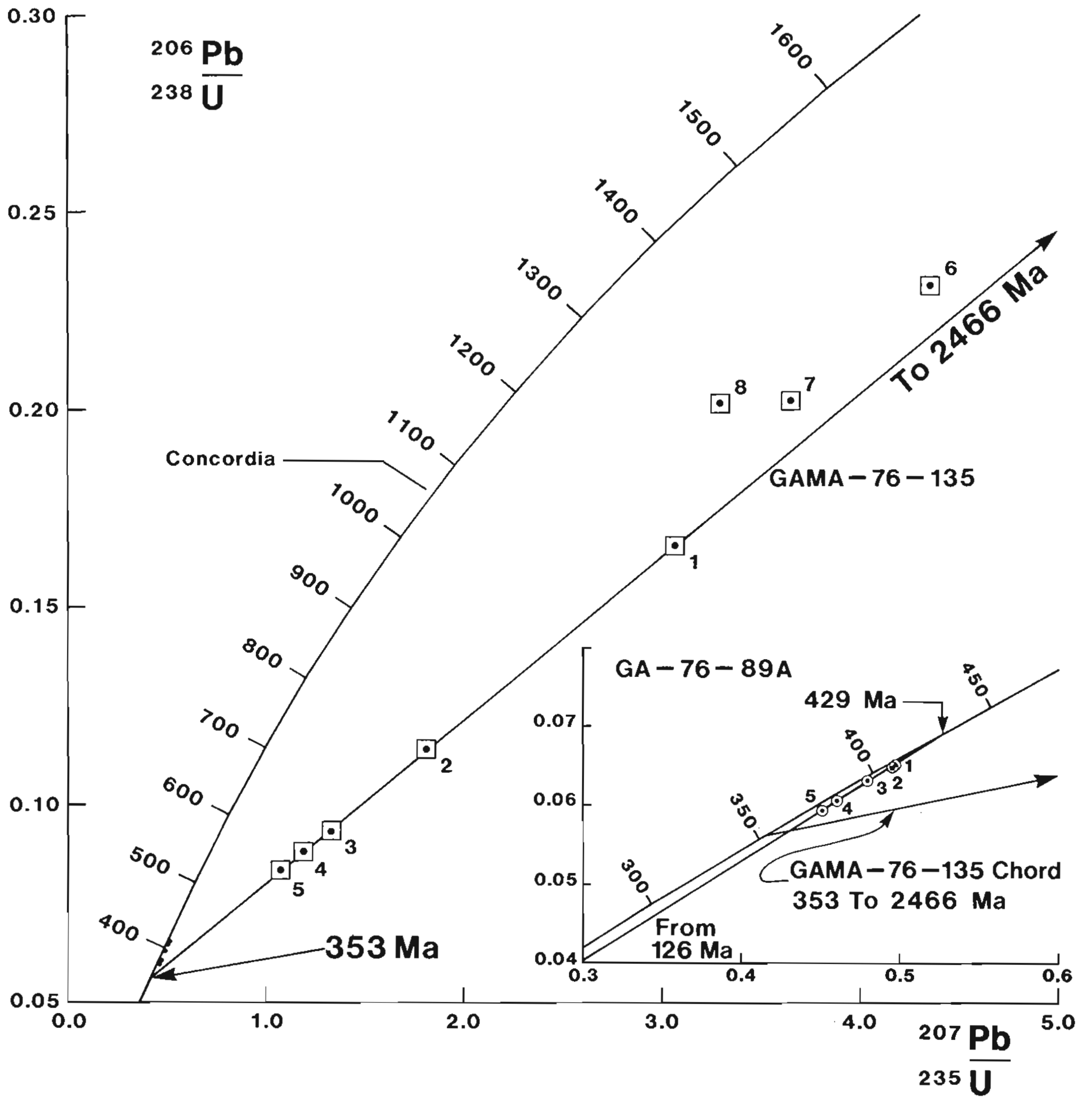


*Figure 5.* *Concordia diagram showing the results of U-Pb analyses of zircon concentrates from GAMA-76-135 (squares) and GA-76-89A (dots, circles on inset).*

shapes do not show the multiplicity of high order facets typical of zircons formed during granulite facies metamorphism.

We propose that the direct relationship between high uranium content, small grain size and high degree of discordance is due to incorporation of uranium by diffusion at about 353 Ma. The degree of discordance of both the translucent and the clear zircons is closely linked to uranium content but shows little proportionality to the (relatively constant) radiogenic Pb contents. Thus the degree of discordance is probably due to gain of uranium rather than loss of lead at about 353 Ma. If ambient uranium were incorporated into the surface of the zircon grains at that time, smaller grains with greater surface to volume ratios would have become proportionately more discordant, as observed. The possibility of uranium gain by zircon growth at that time is probably excluded by the absence of observable growth features.

It is possible, therefore, that the 353 Ma age does not relate to the age of emplacement of the sill, but to a period of uranium gain. If the sill were emplaced at 429 Ma as indicated by the results on GA-76-89A, some lead loss would probably have occurred at that time. The relatively constant radiogenic lead levels observed in the analyzed zircon fractions suggest that lead loss would not have been great. Substantial uranium gain at 353 Ma would then have yielded the observed systematics for the translucent family of zircons; a chord of imperfectly aligned, highly discordant

*Figure 6.* *Photomicrographs of zircon concentrates:*

*a. GAMA-76-135 "clear" (x 100)*
*b. GAMA-76-135 "translucent" (x 100)*
*c. GA-76-89A – note dissimilarity to a and b (x 40)*
*d. GA-76-89A, fraction 1, after abrasion (x 100)*

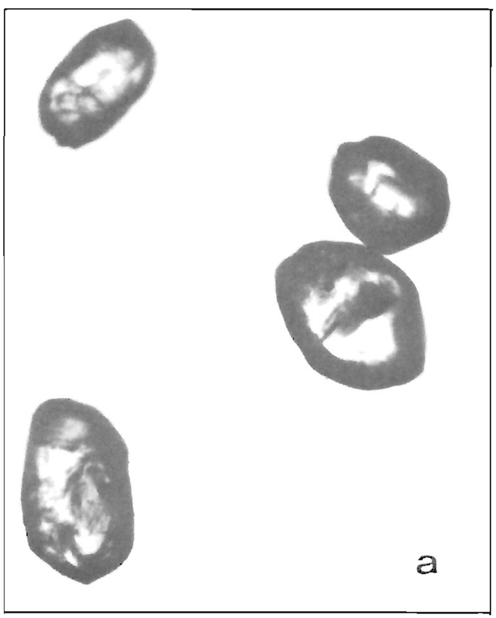


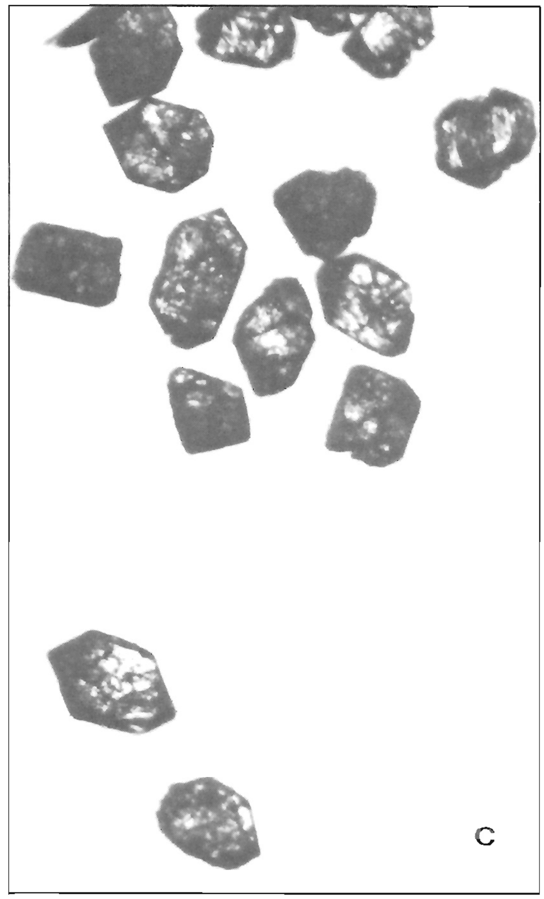


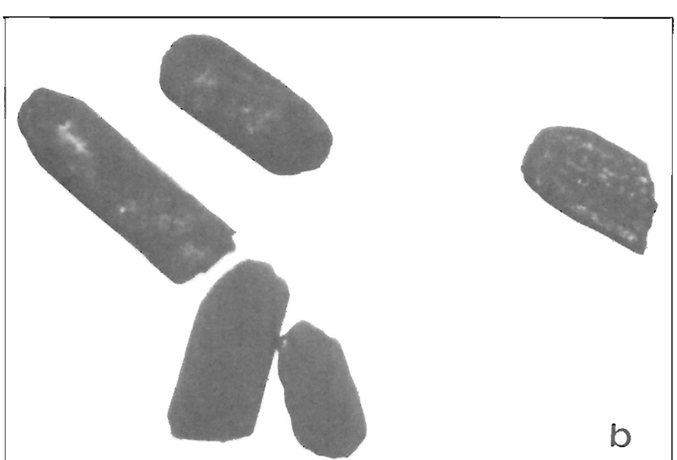


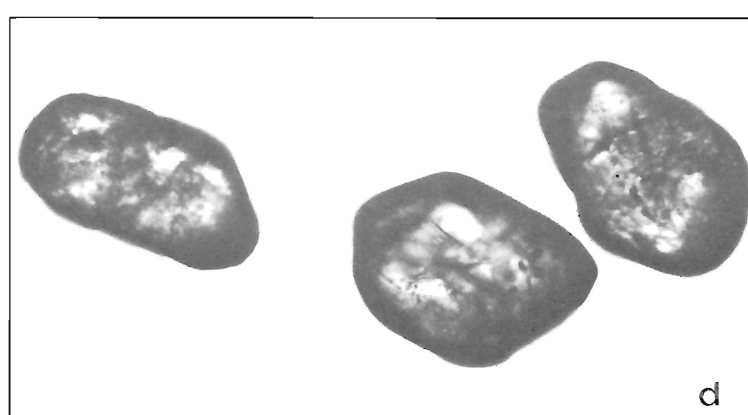

data points with a lower intercept age of 353 Ma and an upper intercept approximately or slightly younger than the original Precambrian age.

Opposing this model is the argument that zircon would have been annealed at the time of emplacement of the sills and would not have been sufficiently metamict to be receptive to surficial gain of uranium (ca.) 80 Ma later at (ca.) 353 Ma. It is, furthermore, possible to achieve the observed systematics through more complex models which do not involve a 353 Ma "event". Nevertheless, we believe that the interpretation based on a period of uranium gain at 353 Ma is the most direct and best suited to the data at hand.

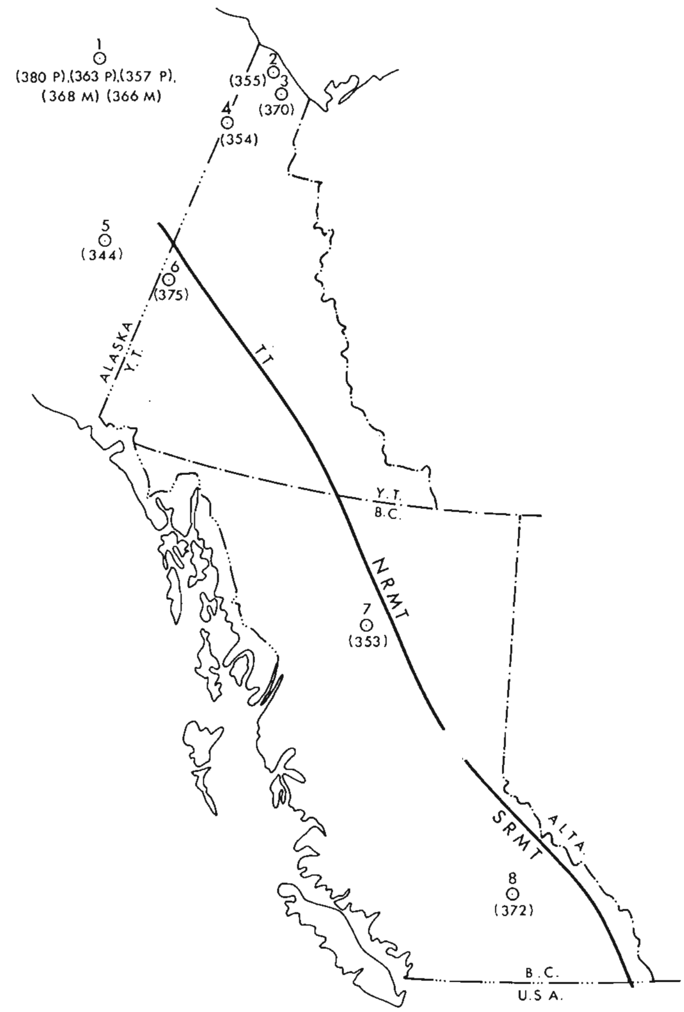


***Figure 7.*** *Cordilleran localities of Devonian granitic rocks suggested by isotopic ages. TT, Tintina Trench; SRMT, Southern Rocky Mountain Trench; NRMT, Northern Rocky Mountain Trench.*

1. *Southern Brooks Range, Dillon et al., 1980. Zircon ages on plutonic (p) and metavolcanic (m) rocks.*
2,3. *Northern Yukon, Baadsgaard et al., 1961, Wanless et al., 1965. K-Ar ages.*
4. *Old Crow batholith, Ziegler, 1969. Rb-Sr age.*
5. *Yukon-Tanana Upland. Aleinikoff et al., 1981. U-Pb zircon age.*
6. *Fiftymile Batholith (Pelly Gneiss), Tempelman-Kluit and Wanless, 1980. U-Pb zircon age.*
7. *Swannell Ranges, Omineca Mountains, this paper. U-Pb zircon age.*
8. *Shuswap region. Okulitch et al., 1975. U-Pb zircon age.*

Alternatively, the two samples GA-76-89A and GAMA-76-135 may represent two different sills, emplaced at different times (429 + 10/-7 and 353 ± 10 Ma respectively). This hypothesis is supported by the radically different characteristics of the zircon from the two samples. Opposing this hypothesis is field evidence (lithology and proximity) which suggests that the two sample locations comprise parts of a single magma series.

## Geological Considerations

The U-Pb age of 429 Ma suggested by zircons from a sample of the granitic sill or dyke, GA-76-89A, seems to have little reflection in the stratigraphy and tectonics of the northern Omineca Belt. During much of the Silurian the region was the site of carbonate or graptolitic shale and siltstone deposition, presumably in a relatively quiescent environment. Noteworthy, however, is a widespread unconformity in Cassiar, Omineca and northern Rocky Mountains at the base of Upper Llandovery (upper Lower Silurian) strata. The lower intercept of 126 Ma is compatible with K-Ar data for regional metamorphism.

The apparent age of uranium gain by sample GAMA-76-135 of 353 Ma, on the other hand, can be related to a time of significant tectonic activity in the region and may be compared with a number of mid to late Devonian ages that have been determined for granitic plutons along the length of the Cordillera (Fig. 7). During the late Devonian a marked change took place in the tectonic regime of the central and northern Cordillera. Typical miogeoclinal carbonate deposits of Middle Devonian age were succeeded by wide-spread fine- to coarse-grained clastic rocks, in many localities represented by thick turbidites (Nilsen, 1981; Gordey et al., 1982; Gabrielse, Dodds and Mansy, 1977; Struik, 1981). They are the first clastic sediments in the history of the Cordilleran miogeocline that were clearly derived from a source other than the North American craton. Chert-pebble conglomerate and chert arenite are distinctive lithologies and were derived from uplift of off-shelf sedimentary strata.

As suggested by Dillon et al. (1980) for the Brooks Range in Alaska, the clastic sedimentary rocks may have been related to an ensialic magmatic arc. A similar arc with related uplift and tectonism in the Canadian Cordillera may have provided a source for the late Devonian to Mississippian clastic wedge deposited in a trough along the outer margin of the northern Cordilleran miogeocline.

## References

Aleinikoff, J.N., Dusel-Bacon, C., Foster, H.L., and Futa, K.
1981: Proterozoic zircon from augen gneiss, Yukon-Tanana Upland, east-central Alaska; Geology, v. 9, no. 10, p. 469-473.

Baadsgaard, H., Folinsbee, R.E., and Lipson, J.
1961: Potassium-argon dates of biotite from Cordilleran granites; Bulletin of the Geological Society of America, v. 72, p. 689.

Dillon, J.T., Pessel, G.H., Chen, J.H., and Veatch, N.C.
1980: Middle Paleozoic magmatism and orogenesis in the Brooks Range, Alaska; Geology, v. 8, no. 7, p. 338-343.

Gabrielse, H., Dodds, C.J., and Mansy, J.L.
1977: Operation Finlay, British Columbia; in Current Research, Part A, Geological Survey of Canada, Paper 77-1A, p. 243-246.

Gordey, S.P., Abbott, J.G., and Orchard, M.J.
1982: Devono-Mississippian (Earn Group) and younger strata in east-central Yukon; in Current Research, Part B, Geological Survey of Canada, Paper 82-1B, p. 93-100.

Krogh, T.E.
1982: Improved accuracy of U-Pb zircon ages by the creation of more concordant systems using an air abraision technique; Geochimica et Cosmochimica Acta, v. 46, p. 637-649.

Mansy, J.L. and Dodds, C.J.
1976: Stratigraphy, structure and metamorphism in northern and central Swannell Ranges; in Report of Activities, Part A, Geological Survey of Canada, Paper 76-1A, p. 91-92.

Nilsen, Tor H.
1981: Upper Devonian and Lower Mississippian redbeds, Brooks Range, Alaska; in Sedimentation and Tectonics in Alluvial Basins; Geological Association of Canada, Special Paper 23, p. 187-219.

Okulitch, A.V., Wanless, R.K., and Loveridge, W.D.
1975: Devonian plutonism in south-central British Columbia; Canadian Journal of Earth Sciences, v. 12, no. 10, p. 1760-1769.

Pidgeon, R.T. and Bowes, D.R.
1972: U-Pb ages of granulites from the Central Region of the Lewisian, northwestern Scotland; Geological Magazine, v. 109, no. 3, p 247-258.

Struik, L.C.
1981: A re-examination of the type area of the Devono-Mississippian Cariboo Orogeny, central British Columbia; Canadian Journal of Earth Sciences, v. 18, no. 12, p. 1767-1775.

Sullivan, R.W. and Loveridge, W.D.
1980: Uranium-lead age determinations on zircon at the Geological Survey of Canada: current procedures in concentrate preparation and analysis; in Rubidium-strontium and uranium-lead isotopic age studies, Report 3; in Current Research, Part C, Geological Survey of Canada, Paper 80-1C, p. 161-246.

Tempelman-Kluit, D.J. and Wanless, R.K.
1980: Zircon ages for the Pelly Gneiss and Klotassin granodiorite in western Yukon; Canadian Journal of Earth Sciences, v. 17, no. 3, p. 297-306.

Wanless, R.K., Stevens, R.D., Lachance, G.R., and Rimsaite, R.Y.H.
1965: Age determinations and geologic studies, Part 1 – Isotopic Ages, Report 5; Geological Survey of Canada, Paper 64-17, p. 22.

Wanless, R.K., Stevens, R.D., Lachance, G.R., and Delabio, R.N.
1979: Age determinations and geological studies, K-Ar Isotopic Ages, Report 14; Geological Survey of Canada, Paper 79-2.

Ziegler, P.A.
1969: The development of sedimentary basins in western and Arctic Canada, Calgary; Alberta Society of Petroleum Geologists.

## APPENDIX

Description of zircon concentrates and locations of GA-76-89A and GAMA-76-135

Sample GA-76-89A (57°05.6'N; 126°16.4'W)

The original zircon concentrate consisted of more than 95% pure euhedral zircon crystals and crystal fragments. Terminations were generally sharp, but most grains had an uneven, 'ragged' appearance. The population ranged from clear and colourless through light brown with reddish hues to translucent. Some crystals showed a tendency to split along their length and some others showed a phenomenon whereby they are divided into two halves of different character. In transmitted light the grains appeared pitted and irregularly fractured, and varied from clear to translucent with dusty inclusions. Approximately 25% were more or less clear and 75% were translucent. Amongst the more ragged crystals some were noteworthy in exhibiting toothed or serrated terminations. Occasional end-to-end twins were also noted. Overall, the grains were quite stubby, almost equidimensional in form. However, elongations range from 1:1 up to about 2.5:1 but with rare cases of up to 3.6:1.

Sample GAMA-76-135 (57°05.6'N; 126°16.4'W)

The concentrate consisted of two distinctly different zircon types, one being generally clear and rounded, and the other being more prismatic and translucent to almost opaque. The clear, rounded grains were of short oval outline with elongation ratios ranging from 1.3:1 to 2.3:1, while the translucents varied from 1.7:1 to more than 3.5:1 with many more in the elongated range.

The clear zircon grains ranged from rounded subhedral to very rounded, from colourless to light yellow, some with a hint of red-orange. Bubble and black speck inclusions were present but not abundant. Grain surfaces commonly appeared under high magnification, to be corroded and pitted. The translucent grains, on the other hand, were more prismatic subhedral, varied from translucent to nearly opaque, and were coloured in various shades of tan with occasional red-orange tints. In transmitted light all appeared more or less opaque, frosty grey to brown, with black speck inclusions. Some grains showed clear domains on their ends and sides and some showed knobby protuberances, both of which may represent overgrowths. No internal structure such as zoning or cores were noted in either the clear or the translucent types.

# 6. A Rb-Sr STUDY OF A DIFFERENTIATED QUARTZ MONZONITE INTRUSION AT RAINY LAKE, CAMSELL RIVER AREA, DISTRICT OF MACKENZIE

S.S. Gandhi and W.D. Loveridge

*Gandhi, S.S. and Loveridge, W.D., A Rb-Sr study of a differentiated quartz monzonite intrusion at Rainy Lake, Camsell River area, District of Mackenzie; in Rb-Sr and U-Pb Isotopic Age Studies, Report 5, in Current Research, Part C, Geological Survey of Canada, Paper 82-1C, p. 147-153, 1982.*

**Abstract**

*A sill-like intrusion at Rainy Lake, Camsell River area, District of Mackenzie, approximately 10 km long and 2 km thick, is differentiated from monzodiorite in the lower part to quartz syenite near the roof. Of seven samples analyzed, four from the lower part and one from the upper part have yielded a Rb-Sr isochron of age 1956 ± 82 Ma, initial $^{87}Sr/^{86}Sr$ 0.7019 ± 0.0010 and MSWD of 1.0.*

## Introduction

A sill-like body at Rainy Lake in the Camsell River area is one of a group of five shallow-seated intrusions in the area near the southeast shore of Great Bear Lake (Hoffman et al., 1976). They are compositionally distinct, ranging from monzodiorite[1] through quartz monzonite to quartz syenite, and are the oldest among the plutons of the Great Bear Batholith (Hoffman and McGlynn, 1977). They occur within an area 75 km long and 20 km wide, well known for uranium and silver veins which are spatially closely associated with them (Fig. 1).

The present study is related to a broader petrochemical and metallogenic investigation of the intrusion at Rainy Lake undertaken by S.M. Roscoe, S.S. Gandhi and N. Prasad at the Geological Survey of Canada, and the 7 samples discussed here are part of a suite of 211 samples collected for the broader petrochemical study.

## General Geology

The quartz monzonitic intrusions near Echo Bay in the north (Fig. 1) are semiconcordant bodies in a varied assemblage of volcanic rocks dominated by basaltic andesite, andesite and intercalated sediments, referred to as the 'Echo Bay Formation' of the 'LaBine Group' as described by Hildebrand (1981b). The intrusions were unroofed prior to deposition of conglomerate of the overlying 'Cameron Bay Formation', which contains boulders of the intrusions (Hildebrand, 1981b), and is in turn overlain by fluvial red arkosic sediments and interbedded tuffs (Kidd, 1933; Mursky, 1973; Hildebrand, 1981b). Mursky (1973, p. 10) regarded these rocks as separated by an erosional interval, represented by an unconformity, from the underlying rocks of the Echo Bay Formation. Hildebrand (1981b, p. 139), however, found that some units of the two formations interfinger in the southern part of the Echo Bay area.

In the Camsell River area, a comparable sequence of sediments, tuffs and flows, unconformably overlying a thick pile of andesitic flows, was mapped as part of the 'Clut cauldron complex' of the LaBine Group by Hildebrand (1981a). At Uranium Point on Balachey Lake, approximately 8 km northwest of Rainy Lake, boulders of quartz monzonitic rock, identical to that of the nearby Balachey Lake intrusion (one of the five shallow seated intrusions discussed above, Fig. 1), are found in a conglomerate at the base of the sequence (Badham, 1972; Hoffman et al., 1976). It is thus apparent that the quartz monzonitic intrusions in the Camsell River area, like those in the Echo Bay area, were unroofed prior to deposition of the younger sequence. Although correlation of the younger sequences of the two areas is uncertain, it is probable that they are not separated significantly in time, considering overall similarities in geology of the two areas. These field relations are important in interpretation of the Rb-Sr age determination.

The sill-like intrusion at Rainy Lake was emplaced below the base of a 3 km thick andesite pile that includes some sedimentary rocks (unit 3, Fig. 2). The rocks are folded about a northwesterly trending synclinal axis located northeast of the intrusion. Dips of beds near the intrusion and of the upper contact are close to 60 degrees. The contact is semiconcordant along a tuffaceous sedimentary unit (unit 2, Fig. 2) at the base of the andesite pile, and is traceable for 10 km. The lower contact is poorly exposed, irregular and truncated by younger granite in the south. Silver-bearing veins of Terra Mine (Fig. 2) occur near the upper contact in the tuffaceous sedimentary unit, and are steeply dipping with easterly strikes (Shegelski, 1973; Badham, 1975).

The sill-like body is 2.0 to 2.5 km thick, located in an area of good outcrop and, because of the steep dip, a section across the body is exposed. It is differentiated from the lower monzodiorite through a transitional quartz monzonitic zone, to the upper quartz syenite, with monzonitic marginal zones (Hoffman et al., 1976; Tirrul, 1976). The texture is dominated by well-developed laths of plagioclase 7 to 10 mm long, with interstitial hornblende, alkali feldspars, quartz, and accessory magnetite, apatite, zircon and titanite. Biotite is present locally. Quartz commonly makes up 5 to 15 per cent of the rock. Granophyric texture is common in the interstitial material. Rocks are altered to a varying degree with plagioclase partially saussuritized, commonly at the core, and chlorite and actinolite are common alteration products of mafic silicates.

Samples for Rb-Sr isotopic age determination were collected in 1978 along a traverse across the sill-like body in the north-central part (Fig. 2), and an additional sample from the decline of Terra Mine was provided by the mine geologist David Brace. Chemical analyses of the seven rocks selected for Rb-Sr isotopic determinations (Table 1) are presented in Table 2. They show calc-alkaline character, as pointed out by Badham (1973). Two of the samples, 4 and 6, show a significant enrichment in soda and a corresponding depletion in potash compared to other samples, a chemical feature prevalent in the upper part of the intrusion. This indicates soda metasomatism, a conclusion supported by the plagioclase composition in sample 6, as determined by microprobe analyses using energy dispersive spectra. These determinations showed compositional ranges of $An_{0.0-3.8}$ and $Ab_{95.9-98.9}$, for both the coarse and interstitial plagioclase, with an average of 10 readings at $An_{0.7}Ab_{98.3}Or_{1.0}$. By comparison the plagioclase composition of sample 1 shows a range of $An_{54.6-41.2}$ and $Ab_{41.1-51.7}$, with an average of 12 readings as $An_{48.7}Ab_{47.4}Or_{3.9}$ (analyses by M. Bonardi, Geological Survey of Canada, Ottawa).

[1]Nomenclature according to Streckeisen, 1976

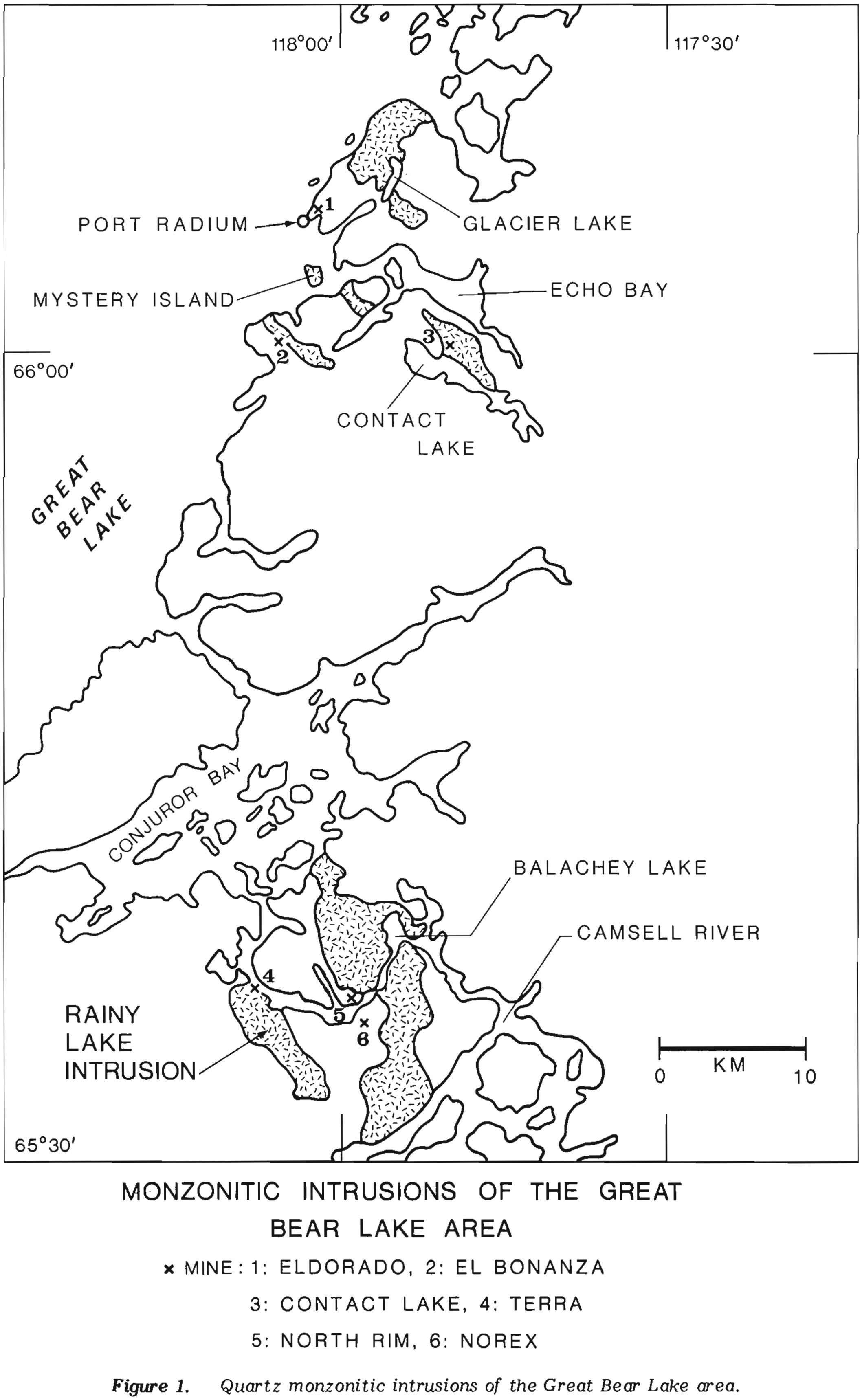


***Figure 1.*** *Quartz monzonitic intrusions of the Great Bear Lake area.*

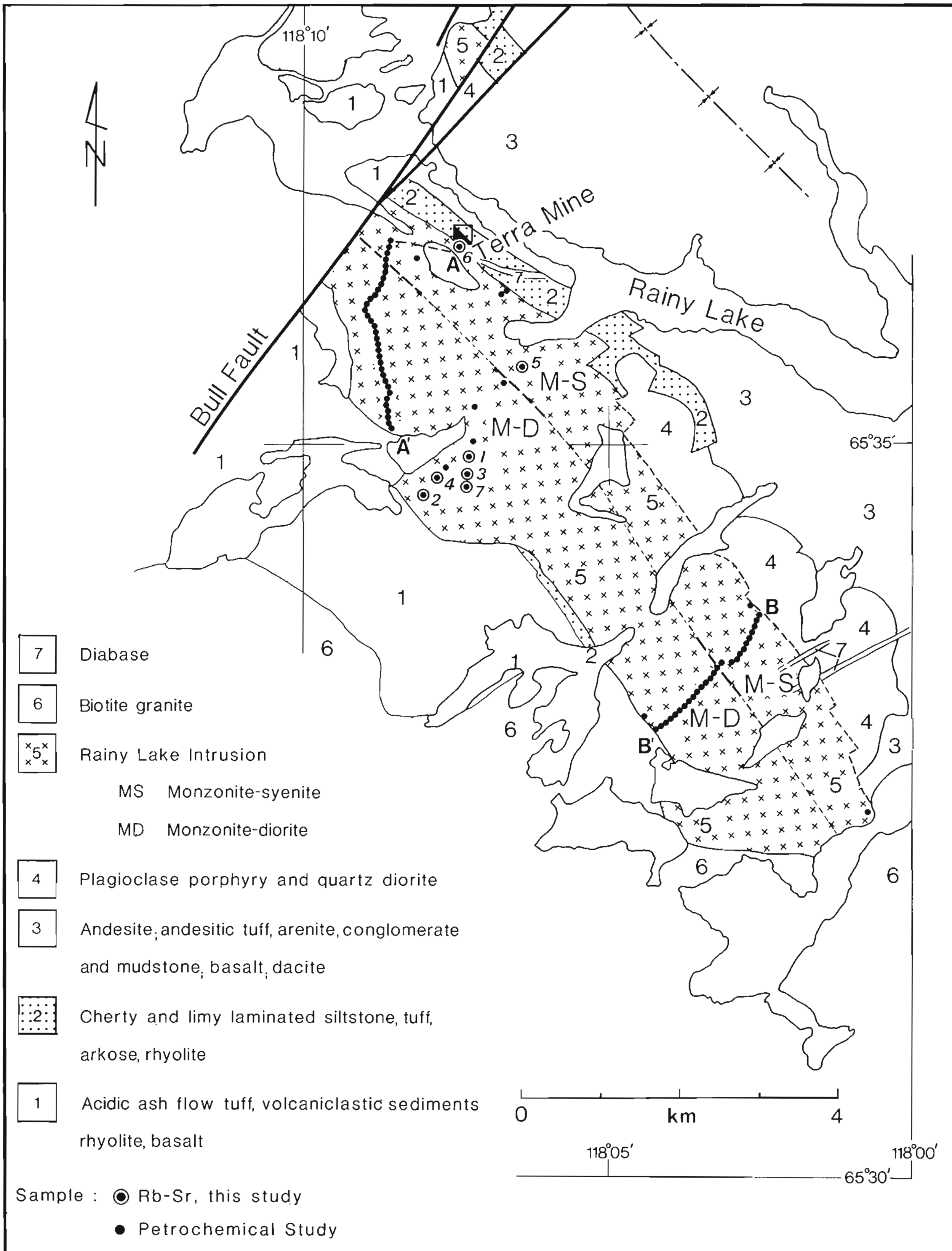


***Figure 2.*** *General geology of the Rainy Lake area and location of samples listed in Table 1. (Modified after Tirrul, 1976 and Hildebrand, 1981a). A-A' and B-B': Sampling traverses for a petrochemical study by S.M. Roscoe, S.S. Gandhi, and N. Prasad.*

## Analytical Techniques, Data and Results

Analytical procedures for Rb-Sr isotopic analyses of whole-rock samples were based on those described by Wanless and Loveridge (1972) with the exception that $^{87}Sr/^{86}Sr$ were obtained only from spiked Sr analyses in this study; no unspiked Sr measurements were performed.

Seven samples were analyzed isotopically and the results are listed in Table 1 and plotted in Figure 3. Five of the seven sample points (1 to 5) are collinear and yield an isochron of age 1956 ± 82 Ma, initial $^{87}Sr/^{86}Sr$ 0.7019 ± 0.0010, and MSWD 1.0. The other two samples (6 and 7) fall somewhat below the trend. The low initial $^{87}Sr/^{86}Sr$ is compatible with mantle derivation of these rocks or indicates that any period of crustal residence prior to final emplacement was minimal.

## Discussion

Three of the 5 samples that define the isochron are diorite-monzodiorite, typical of the lower part of the intrusion from which they come (samples 1, 2 and 3, Tables 1 and 2). Sample 4 is located in their vicinity, and is also similar in composition except that it shows a considerable enrichment in soda and corresponding depletion in potash. This feature is not normal for this part of the intrusion but is characteristic of the upper marginal and quartz syenite zones, as reflected in the composition of sample 6. This deviation in the relative proportion of the alkalis, however, has apparently not affected the isotopic equilibrium of sample 4 which plots on the isochron defined by four other points. Sample 6 on the other hand, plots below the isochron. The reason for this may be additional alteration it may have undergone because of its position close to the roof (approximately 25 m from the contact) and proximity to the mineralization at Terra Mine. Sample 7 which also plots below the isochron, is abnormally high in silica for its position in the vicinity of samples 1 to 4 (Fig. 1). This may be attributable to contact irregularities resulting in localized silica enrichment during differentiation. The fact that this sample plots below the isochron is probably due to later alteration. Sample 5 which lies on the isochron is compositionally typical of the upper quartz syenite zone, but its texture is somewhat different in that the plagioclase crystals are smaller and more closely packed than elsewhere in the intrusion. Textural variations are common in the upper part of the intrusion.

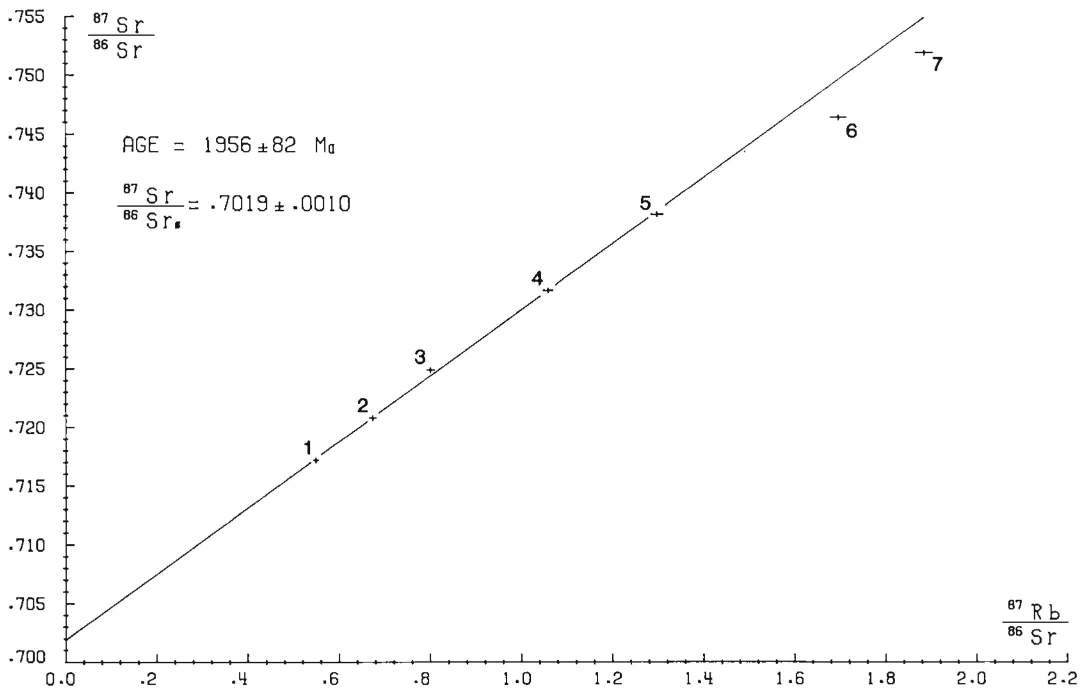


***Figure 3.*** *Rb-Sr isochron plot, quartz monzonite intrusion at Rainy Lake, Camsell River area, District of Mackenzie.*

Table 1

Analytical data, whole-rock sample, quartz monzonite intrusion at Rainy Lake, Camsell River area, District of Mackenzie

| Sample No. | Rb ppm | Sr ppm | $^{87}Sr/^{86}Sr$ | $^{87}Rb/^{86}Sr$ |
|---|---|---|---|---|
| 1 | 128.9 | 678.9 | 0.7172 ± 0.0004 | 0.5489 ± 0.0110 |
| 2 | 142.8 | 612.8 | 0.7208 ± 0.0004 | 0.6737 ± 0.0135 |
| 3 | 137.3 | 496.1 | 0.7249 ± 0.0004 | 0.8001 ± 0.0160 |
| 4 | 66.02 | 180.3 | 0.7317 ± 0.0004 | 1.059 ± 0.021 |
| 5 | 139.8 | 311.4 | 0.7382 ± 0.0004 | 1.298 ± 0.026 |
| 6 | 166.0 | 282.6 | 0.7465 ± 0.0004 | 1.698 ± 0.034 |
| 7 | 152.8 | 234.1 | 0.7520 ± 0.0004 | 1.887 ± 0.038 |

The isochron age of 1956 ± 82 Ma is compatible with the known geological history of the area and published isotopic dates on related rocks younger than the intrusion. Zircon from a younger granite in the Echo Bay area has been dated by the U-Pb method at 1820 ± 30 Ma (Jory, 1964) and a number of determinations using the same method on granites and related felsic volcanic rocks elsewhere in the Great Bear Batholith have yielded results close to 1860 ± 10 Ma according to Van Schmus and Bowring (1980). An ash-flow tuff high in the stratigraphy of the Labine Group at Conjuror Bay, approximately 10 km to the north of Rainy Lake, yielded an U-Pb date on zircon of 1870 ± 10 Ma (Van Schmus and Bowring, 1980; Hildebrand, 1981b, p. 136). As mentioned earlier, the tuffs in the upper part of Labine Group (Cameron Bay Formation) were deposited after the monzonitic intrusions were unroofed. The date on the tuff thus provides a minimum age constraint for the intrusions, which are older by the interval of time required for their unroofing and for deposition of the conglomerate which contains boulders derived from them.

The maximum age of the intrusion is constrained by a zircon U-Pb date of 1920 ± 10 Ma for a gneissic granodiorite that appears to underlie the volcanic rocks of the lower Labine Group at Hottah Lake (Van Schmus and Bowring, 1980). The isochron age of the intrusion at Rainy Lake, taking into account the analytical uncertainty (±82 million years), is not in conflict with this age for the gneissic granodiorite. Between the basement represented by the granodiorite, and the Labine Group, and separated from

Table 2

Chemical analyses of rocks (Table 1) from the quartz monzonite intrusion at Rainy Lake, Camsell River area, District of Mackenzie

| Sample No. / Field No.: GFA- | 1 / -'78-266 | 2 / -'78-271 | 3 / -'78-267 | 4 / -'78-270 | 5 / -'78-273 | 6 / -'78-274 | 7 / -'78-268 |
|---|---|---|---|---|---|---|---|
| Wt. per cent: | | | | | | | |
| $SiO_2$ | 55.40 | 54.50 | 55.40 | 58.10 | 65.00 | 56.90 | 64.10 |
| $TiO_2$ | 0.59 | 0.90 | 0.65 | 0.89 | 0.56 | 0.78 | 0.53 |
| $Al_2O_3$ | 20.90 | 18.60 | 20.60 | 17.70 | 15.10 | 17.20 | 14.70 |
| $Fe_2O_3$ | 2.40 | 2.40 | 1.60 | 0.70 | 1.30 | 2.10 | 2.50 |
| FeO | 3.30 | 5.00 | 3.80 | 5.70 | 3.00 | 3.70 | 3.20 |
| MnO | 0.26 | 0.32 | 0.23 | 0.19 | 0.11 | 0.21 | 0.12 |
| MgO | 2.04 | 2.15 | 2.04 | 2.41 | 2.19 | 3.41 | 1.81 |
| CaO | 5.24 | 5.27 | 4.96 | 3.45 | 3.16 | 3.70 | 3.64 |
| $Na_2O$ | 3.90 | 2.70 | 4.30 | 6.70 | 2.80 | 6.50 | 3.30 |
| $K_2O$ | 4.11 | 4.74 | 3.85 | 1.85 | 4.12 | 1.69 | 4.23 |
| $P_2O_5$ | 0.30 | 0.55 | 0.30 | 0.46 | 0.16 | 0.31 | 0.15 |
| $H_2O_T$ | 1.90 | 2.10 | 2.00 | 1.70 | 1.60 | 1.70 | 1.00 |
| $CO_2$ | 0.10 | 0.00 | 0.10 | 0.10 | 0.20 | 0.70 | 0.10 |
| Cl | 0.08 | 0.12 | 0.13 | 0.07 | 0.04 | 0.07 | 0.08 |
| F | 0.05 | 0.09 | 0.06 | 0.08 | 0.09 | 0.07 | 0.08 |
| S | 0.02 | 0.02 | 0.03 | 0.02 | 0.08 | 0.04 | 0.02 |
| Total | 100.59 | 99.46 | 100.05 | 100.12 | 99.51 | 99.08 | 99.56 |
| ppm: | | | | | | | |
| Ag | nd | nd | nd | nd | nd | nd | nd |
| Cu | 69 | 37 | 76 | 9 | 43 | 5 | 16 |
| Pb | 9 | 31 | nd | 40 | 47 | nd | 7 |
| Zn | 167 | 149 | 205 | 85 | 123 | 89 | 50 |
| Co | 13 | 14 | 12 | 10 | 14 | 11 | 10 |
| Ni | 12 | 8 | 14 | 7 | 30 | 17 | 5 |
| U | 2.5 | 4.0 | 7.3 | 3.7 | 8.3 | 3.0 | 6.5 |
| Th | 7 | 15 | 10 | 13 | 36 | 15 | 24 |
| Specific Gravity | 2.76 | 2.80 | 2.76 | 2.77 | 2.72 | 2.70 | 2.75 |

Notes: $H_2O_T$: Total $H_2O+$ and $H_2O-$

Oxides, F, Cl and S analyses based on X-ray fluorescence and chemical methods by the Analytical Chemistry Section, Geological Survey of Canada, Ottawa

Ag, Cu, Pb, Zn, Co and Ni analyses based on atomic absorption method and Th determinations on X-ray fluorescence method by Bondar-Clegg & Co. Ltd., Ottawa

U analyses using delayed neutron counting method, by Atomic Energy of Canada Ltd., Ottawa

nd: Not detected (detection limit: Ag = 0.1 ppm; Pb = 2 ppm) them by unconformities, is the Conjuror Bay Group (Hildebrand, 1981a) composed of conglomerate, orthoquartzite, basaltic and andesitic flows and tuffs. Allowing for the time required for the deformation and erosion of basement, deposition of the Conjuror Bay Group, followed by erosion and deposition of the lower part of the Labine Group, it is likely that the intrusion at Rainy Lake is close in age to the 1870 ± 10 Ma old tuff rather than the granodiorite. This is not evident from the Rb-Sr date presented here in relation to the two zircon dates, except that the minimum Rb-Sr age of 1874 Ma indicated by the analytical uncertainty, is well within the constraints put by the zircon dates and field relations.

The andesitic volcanic flows and tuffs of Echo Bay Formation at Echo Bay have yielded a Rb-Sr isochron age of 1733 ± 30 Ma[1] with initial $^{87}Sr/^{86}Sr$ 0.7020 ± 0.0030 (Robinson and Morton, 1972). The volcanic rocks are intruded by quartz monzonitic intrusions (Fig. 1) similar to the intrusion at Rainy Lake. Hence the difference between the isochron dates of the volcanic rocks and the intrusion is anomalous. Hildebrand (1981b, p. 147) suggested that the isochron age of 1733 ± 30 Ma may be related to pervasive potash metasomatism in these volcanic rocks which he states is prevalent in the Echo Bay area, and Badham (1973) invoked similar prevalent alkali metasomatism for the potash-rich volcanic rocks of the Camsell River area. The intrusion at Rainy Lake, however, does not show effects of this postulated younger potash metasomatic event.

The initial $^{87}Sr/^{86}Sr$ for the volcanic rocks at Echo Bay, 0.7020 ± 0.0030, is similar to the initial ratio of 0.7019 ± 0.0010 obtained for the intrusion at Rainy Lake. These ratios suggest a mantle origin or only short crustal histories for both magmas. Overall compositional similarities of the intrusion and the volcanics indicate that they are comagmatic (Badham, 1973; Hoffman et al., 1976).

The veins at Terra Mine (Fig. 1), and other similar veins at the Eldorado Mine in the Echo Bay area, are spatially closely associated with the monzonitic intrusions, and some of them intersect the intrusions. They are mineralogically complex, and the main stages observed in their paragenetic sequence are: 1) quartz-hematite pitchblende, 2) Co-Ni arsenides, silver, bismuth, carbonate ± pitchblende, 3) Cu, Pb, and Zn sulphides, sulpharsenides, silver, bismuth, and 4) Cu and Ag sulphides, carbonates. An additional one or two stages involving one or more of the above minerals are recognized in some of the veins (Kidd and Haycock, 1935; Campbell, 1957; Shegelski, 1973; Badham, 1975). Isotopic dating of several pitchblende and galena samples from the veins has been discussed by Thorpe (1974); leads in galena (excepting some that contain a variable radiogenic component) have yielded model ages of 1625 to 1670 Ma[2], whereas pitchblendes have yielded U-Pb dates of 1420 Ma[3] or less[4]. Another pitchblende sample from No. 54 vein at 200 m depth in Terra Mine was analyzed in conjunction with the present study. It contains pitchblende as younger veinlets and aggregates in carbonate-quartz gangue carrying silver and Co-Ni arsenides. Such late stage pitchblende is known in other veins of the Echo Bay – Camsell River area. Analyses of the sample indicate low common Pb, some loss of radiogenic Pb, and a $^{207}Pb/^{206}Pb$ date of 1138 Ma (Sample GFA-78-1; analyses by Geospec Consultants Ltd., Edmonton, Alberta).

The U-Pb isotopic date on the vein and the Rb-Sr isochron age reported here confirm a significant time interval between the intrusion of monzonite and the formation of the veins known from the earlier isotopic studies. The time interval is also apparent from the structural relations which show that the tensional fractures occupied by the vein minerals are subsidiary to the major northeast-trending right lateral strike-slip faults (Campbell, 1957; Badham, 1972) which displace the younger granites that are intrusive into the monzonites.

## Acknowledgments

Field assistance by N. Prasad and C. Lamontagne were very valuable. Discussions with S.M. Roscoe, R.I. Thorpe and R.S. Hildebrand, and critical comments by P.F. Hoffman, all of the Geological Survey of Canada, have been helpful in improvement of the manuscript. The opinions expressed here, however, are the writers'. Courtesies extended by Terra Mine staff in the field were greatly appreciated.

## References

Badham, J.P.N.

1972: The Camsell River – Conjuror Bay area, Great Bear Lake, N.W.T.; Canadian Journal of Earth Sciences, v. 9, no. 11, p. 1460-1468.

1973: Calc-alkaline volcanism and plutonism from the Great Bear Batholith, N.W.T.; Canadian Journal of Earth Sciences, v. 10, no. 8, p. 1319-1328.

1975: Mineralogy, paragenesis and origin of the Ag-Ni, Co arsenide mineralization, Camsell River, N.W.T., Canada; Mineralium Deposita, v. 10, p. 153-175.

Campbell, D.D.

1957: Port Radium Mine: in Structural Geology of Canadian Ore Deposits, 2nd Edn.; Canadian Institute of Mining and Metallurgy, p. 177-189.

Hildebrand, R.S.

1981a: Preliminary geological map of Rainy Lake and White Eagle Falls 1:50,000 sheets; Department of Indian and Northern Affairs, Economic Geology Series Map.

1981b: Early Proterozoic LaBine Group of Wopmay Orogen: Remnant of a continental volcanic arc developed during oblique convergence; in Proterozoic Basins in Canada, ed. F.H.A. Campbell, Geological Survey of Canada Paper 81-10, p. 133-156.

---

[1] Recalculated using $^{87}Rb$ decay constant = $1.42 \times 10^{-11} a^{-1}$

[2] Recalculated using Stacey and Kramers (1975) two stage model for lead isotope evolution.

[3] Recalculated using U decay constants of Jaffey et al., 1971.

[4] A paper by R.G. Miller: "Geochronology of uranium deposits in the Great Bear batholith, Northwest Territories", Canadian Journal of Earth Sciences, v. 19, no. 7, p. 1428-1448, 1982, was received after the present report was completed. He presented 8 new isotopic analyses on pitchblende from the Echo Bay mine and quartz-pitchblende – Cu sulphide – Ni, Co arsenide veins of 'SHORE' claims on Achook Island, 35 km north of Echo Bay, and plotted them (p. 1440) with Jory's (1964) data on 6 pitchblende samples from Echo Bay. Nine of the 14 points on the combined plot yielded a discordia with intersections at 1424 ± 29 and 339 ± 22 Ma. He also noted that two of Jory's samples are virtually concordant and have identical $^{207}Pb/^{206}Pb$ ages of 1419 Ma (revised using uranium decay constants of Jaffey et al., 1971) which stands as the most accurate estimate for the age of the uranium mineralization.

Hoffman, P.F., Bell, I.R., and Tirrul, R.
1976: Sloan River map-area (86K), Great Bear Lake, District of Mackenzie; in Report of Activities, Part A; Geological Survey of Canada Paper 76-1A, p. 353-358.

Hoffman, P.F. and McGlynn, J.C.
1977: Great Bear Batholith: a volcano-plutonic depression; in Volcanic Regimes in Canada, ed. W.R.A. Baragar, L.C. Coleman, and J.M. Hall; Geological Association of Canada, Special Paper 16, p. 170-192.

Jaffey, A.H., Flynn, K.F., Glendenin, L.E., Bentley, W.C., and Essling, A.M.
1971: Precision measurement of half lives and specific activities of $^{235}U$ and $^{238}U$; Physical Review C, v. 4, p. 1889-1906.

Jory, L.T.
1964: Mineralogical and isotopic relations in the Port Radium pitchblende deposit, Great Bear Lake, Canada; unpublished Ph.D. thesis, California Institute of Technology, Pasadena, 275 p.

Kidd, D.F.
1933: Great Bear Lake area, Northwest Territories; Geological Survey of Canada Summary Report, 1932, Part C, p. 1-36.

Kidd, D.F. and Haycock, M.H.
1935: Mineralogy of the ores of Great Bear Lake; Geological Society of America, Bulletin 46, p. 879-960.

Mursky, G.
1973: Geology of the Port Radium map-area, District of Mackenzie; Geological Survey of Canada, Memoir 374, 40 p.

Robinson, B.W. and Morton, R.D.
1972: The geology and geochronology of the Echo Bay area, N.W.T., Canada; Canadian Journal of Earth Sciences, v. 9, no. 2, p. 158-172.

Shegelski, R.J.
1973: Geology and mineralogy of the Terra Silver Mine, Camsell River, N.W.T.; unpublished M.Sc. Thesis, University of Toronto, Toronto, Ontario.

Stacey, J.S. and Kramers, J.D.
1975: Approximation of terrestrial lead isotope evolution by a two stage model; Earth and Planetary Science Letters, v. 26, p. 207-221.

Streckeisen, A.
1976: To each plutonic rock its proper name; Earth Sciences Review, v. 12, p. 1-33.

Tirrul, R.
1976: The geology of the Rainy Lake igneous complex, District of Mackenzie, Northwest Territories; unpublished B.Sc. thesis, Queen's University, Kingston, Ontario, 115 p.

Thorpe, R.I.
1974: Lead isotope evidence for the genesis of silver-arsenide vein deposits of the Cobalt and Great Bear Lake areas, Canada; Economic Geology, v. 69, p. 777-791.

Van Schmus, W.R. and Bowring, S.A.
1980: Chronology of igneous events in the Wopmay Orogen, Northwest Territories, Canada; in Abstracts with Programs, Geological Society of America, v. 12, p. 540.

Wanless, R.K. and Loveridge, W.D.
1972: Rubidium-strontium isochron age studies, Report 1; Geological Survey of Canada, Paper 72-23.

# 7. A Rb-Sr STUDY OF THE ET-THEN GROUP BASALTS, GREAT SLAVE LAKE, DISTRICT OF MACKENZIE

S.S. Gandhi and W.D. Loveridge

*Gandhi, S.S. and Loveridge, W.D., A Rb-Sr study of the Et-Then Group basalts, Great Slave Lake, District of Mackenzie; in Rb-Sr and U-Pb Isotopic Age Studies, Report 5, in Current Research, Part C, Geological Survey of Canada, Paper 82-1C, p. 155-160, 1982.*

***Abstract***

*A Rb-Sr study of 8 drill core samples of basaltic flows, intercalated with gently to moderately dipping conglomerate units of the Et-Then Group, has yielded an errorchron of age 1969 ± 82 Ma, initial $^{87}Sr/^{86}Sr$ of 0.7046 ± 0.0006 and MSWD 3.7. The samples are from a 450 m section of the virtually unmetamorphosed Murky Formation which forms the lower part of the group. The age obtained is greater than published dates for some Aphebian rocks known to be older than the Et-Then Group from their field relations.*

## Introduction

The Et-Then Group in the east arm of Great Slave Lake (Fig. 1) bears many lithological and tectonic similarities to the Martin Formation (Tremblay, 1972, 1973) of the Beaverlodge uranium mining district of northern Saskatchewan, as summarized by Fraser et al. (1970, p. 233). These similarities prompted a few companies to explore, during the late 1970s, for uranium deposits at the base and in the vicinity of the Et-Then Group, in search of vein-type deposits as well as for unconformity-related deposits similar to those associated with the Martin and Athabasca formations in Saskatchewan. One of the companies, S.E.R.U. Nucléaire (Canada) Limitée, explored Preble Island (Fig. 1, 2), and drilled a vertical hole in 1978 to a depth of 765 m that intersected gently dipping conglomeratic units and basaltic flows of the lower part of the Et-Then Group, without reaching the basement. The drill core provided an excellent opportunity to select, for Rb-Sr isotopic age determination, unweathered samples of basalt flows from various stratigraphic levels. The eight samples selected are fine- to medium-grained, massive basalts, dark green in colour excepting one which has a faint reddish colouration due to hematite. Thin sections of the samples analyzed show partial alteration of some of the augite crystals to chlorite and many of the feldspar crystals are saussuritized. The degree of alteration varies from weak to moderate, with more intense alteration near a few microveinlets of calcite in some of the rocks. Sample locations are shown on a simplified drill section based on the log supplied by the company (Fig. 3). Samples containing vesicles or amygdules were rejected.

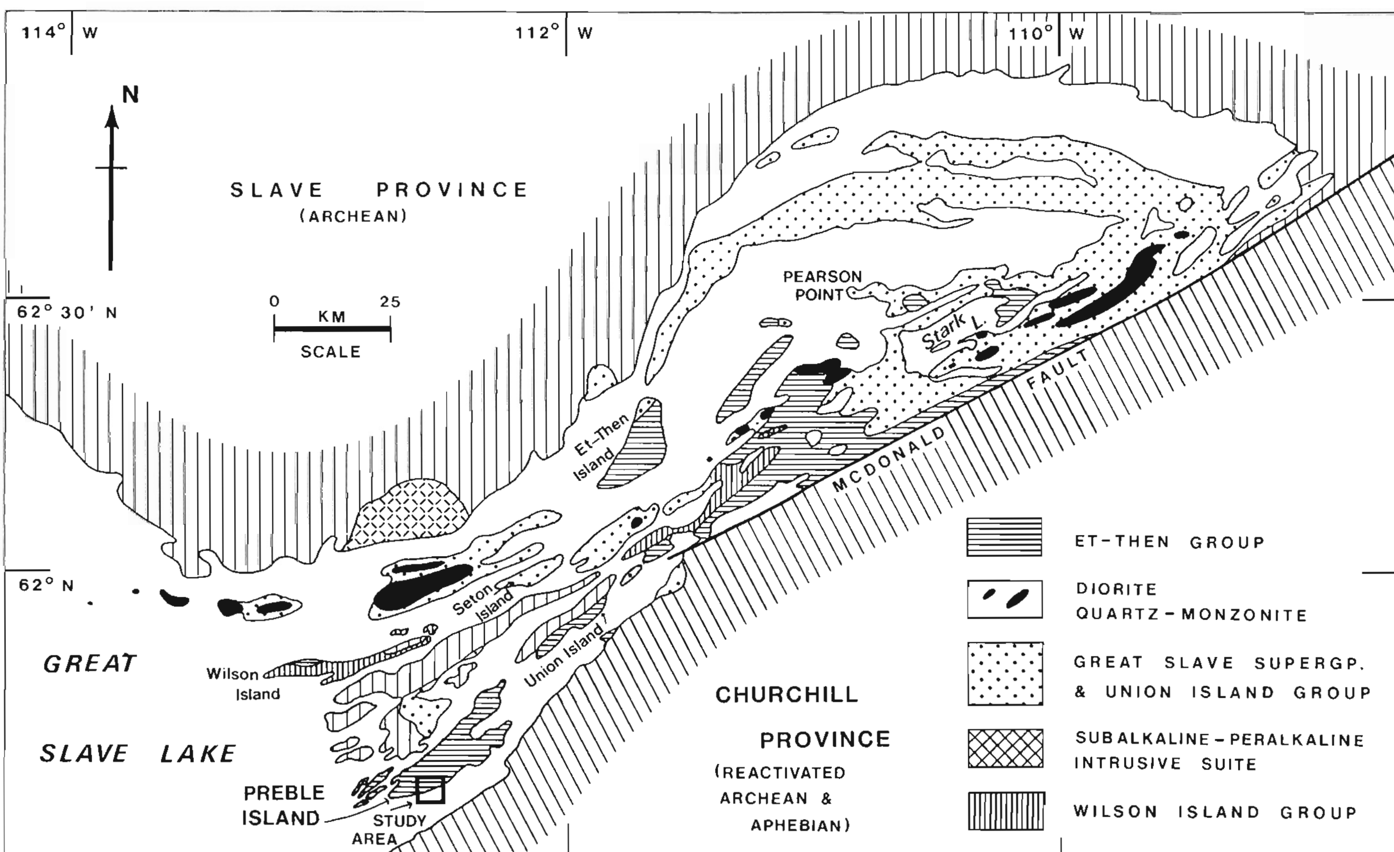


*Figure 1. Generalized geological map of the east arm of Great Slave Lake, District of Mackenzie.*

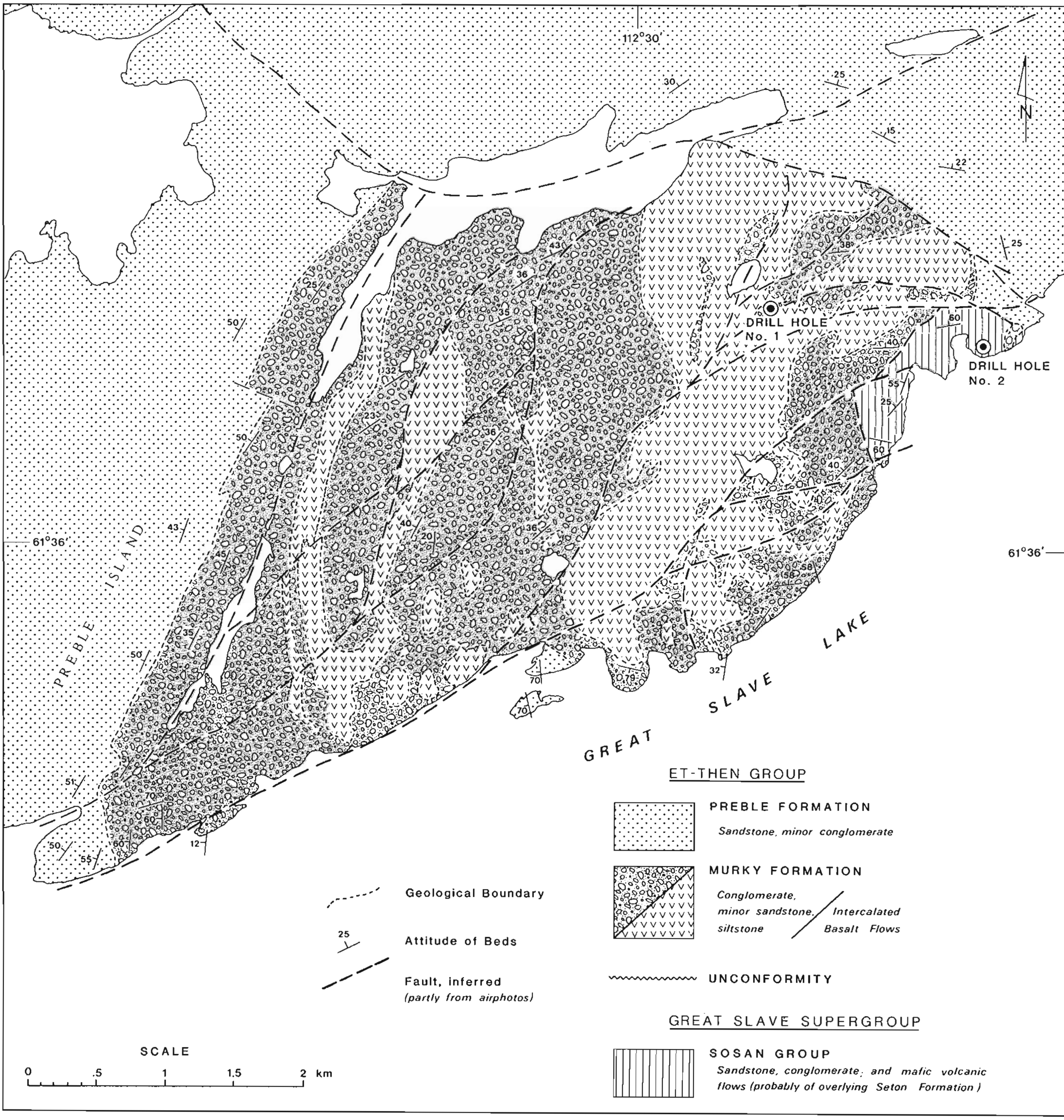


***Figure 2.*** *Geological map of part of Preble Island and location of drill hole no. 1 sampled for this study; based on the map of Preble Island claim group at a scale of 1:23 000 approximately, from S.E.R.U. Nucléaire Canada Limitée, report no. 7805-24, map no. 11, with minor modifications.*

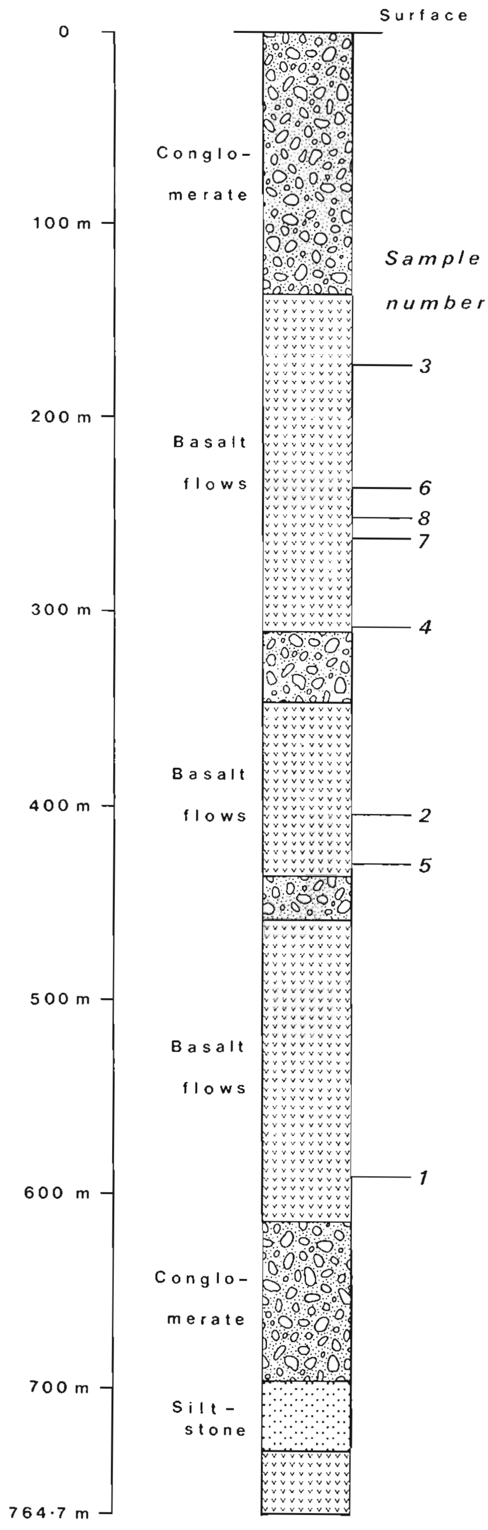


***Figure 3.*** *Drill section, hole no. 1, Preble Island, Great Slave Lake, showing location of samples of basalt flows on which Rb-Sr analyses were performed; simplified from drill log supplied by S.E.R.U. Nucléaire Canada Limitée.*

## Geological Setting

The Et-Then Group includes the youngest of the early Proterozoic sediments preserved in a structural trough along the 200 km length of the east arm of Great Slave Lake (Fig. 1). The group consists of two formations, named and defined by Stockwell (1936a, b); the older Murky Formation and the younger Preble Formation, approximately 1000 m and 3500 m in thickness respectively. The Murky Formation is predominantly a very thick bedded, red to buff, boulder conglomerate in units up to 50 m thick, separated by thin mudcracked red shale and siltstone intervals and caliche horizons (Hoffman, 1968, 1969). Basaltic flows, massive to amygdaloidal and intercalated with the conglomerate units, are found on Preble Island and on the south shore of Great Slave Lake south of Union Island, as first reported by Hoffman (1968, 1977). Those in the latter locality were mapped earlier by Henderson (1939) but were referred to as the "Kahochella Formation" of the older Great Slave Supergroup (Hoffman, 1968). A 20 m thick zone of basaltic flows was discovered during recent exploration by Home Oil Limited farther to the east, west-southwest of Stark Lake near McDonald Fault. Elsewhere within the Murky Formation basaltic flows are not known. Chemical analyses of 4 drill core samples from Preble Island, in an unpublished company report, show that they are continental tholeiitic type.

The Preble Formation is composed predominantly of lithic or arkosic, red or buff, friable sandstone, and has a gradational boundary with the conglomerate of Murky Formation below. At many localities however, the Murky Formation is absent, and the Preble Formation directly overlies rocks older than the Et-Then Group.

The Et-Then Group is a continental red-bed sequence (Chandler, 1980) and some of the basalts have highly oxidized flow tops indicating subaerial extrusion. The Murky Formation is interpreted by Hoffman (1969) and Hoffman et al. (1974), as a fanglomeratic sequence, deposited as alluvial fans growing northwestwards from scarps developed along the northeast-trending boundary fault system (McDonald Fault System) with dextral transcurrent movements (Reinhardt, 1969b; Hoffman et al., 1977). Deposition proceeded contemporaneously with the fault movements. The fine grained northwestern facies is interpreted as lacustrine deposits formed at distal margins of the alluvial fans. The Murky Formation is cut by the main fault and its splays, but there are great changes in thickness across fault lines, and sandstone high in the Preble Formation oversteps several splay faults (Hoffman et al., 1977). The sedimentary structures in the Preble Formation indicate deposition in fining upward fluvial cycles and sedimentary transport to the southwest, although the material may have been derived from the boundary faults (Hoffman, 1969).

The transcurrent faulting continued after deposition of the Preble Formation, with some vertical movements and, locally, overturning of beds, according to Reinhardt (1972, p. 29 and 1969a, p. 180).

The Et-Then Group is intruded by shallowly dipping diabase dykes and sills, which are in turn cut by northwest-trending nearly vertical diabase dykes of the Mackenzie swarm (Stockwell, 1936a, b; Fahrig and Jones, 1969; Irving et al., 1972; McGlynn and Irving, 1978).

## Analytical Techniques, Data and Results

Analytical procedures for Rb-Sr isotopic analyses of whole rock samples were based on those described by Wanless and Loveridge (1972), with the exception that $^{87}Sr/^{86}Sr$ ratios were obtained only from spiked Sr analyses in this study; no unspiked Sr measurements were performed.

Table 1

Analytical data, whole-rock samples, Et-Then Group basalts

| Sample No. This Work | Field: GFA- | Depth* in m | Rb ppm | Sr ppm | $^{87}Sr/^{86}Sr$ average | $^{87}Rb/^{86}Sr$ |
|---|---|---|---|---|---|---|
| 1 | 78-503 | 590.79 | 34.40 | 345.4 | 0.71257 ± 0.00010 | 0.2879 ± 0.0058 |
| 2 | 78-502 | 407.70 | 62.52 | 551.1 | 0.71501 ± 0.00010 | 0.3280 ± 0.0066 |
| 3 | 81-81 | 172.87 | 47.47 | 394.4 | 0.71457 ± 0.00010 | 0.3480 ± 0.0070 |
| 4 | 81-86 | 307.89 | 32.22 | 187.2 | 0.71877 ± 0.00010 | 0.4976 ± 0.0100 |
| 5 | 81-90 | 429.77 | 65.99 | 322.2 | 0.72184 ± 0.00010 | 0.5921 ± 0.0118 |
| 6 | 81-83 | 235.92 | 52.66 | 228.1 | 0.72338 ± 0.00010 | 0.6675 ± 0.0134 |
| 7 | 78-501 | 262.14 | 63.27 | 253.4 | 0.72513 ± 0.00010 | 0.7219 ± 0.0144 |
| 8 | 81-84 | 251.76 | 52.87 | 152.2 | 0.73233 ± 0.00010 | 1.0043 ± 0.0201 |

* Vertical drill hole, no. 1, Preble Island, Latitude 61° 37' N, Longitude 112° 29' W; NTS 85H/9W; Altitude: 190.5 m; Core size BQ, Wireline drilling, completed September 17, 1978, at 764.45 m.

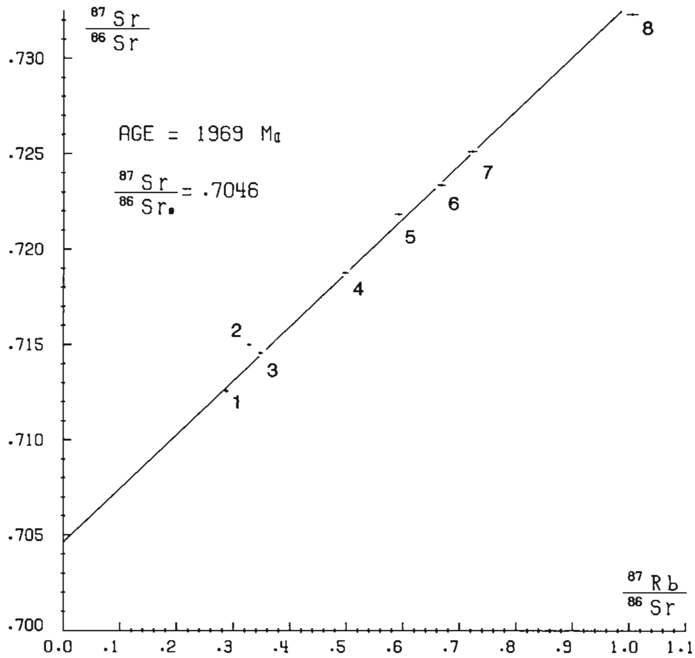


*Figure 4. Rb-Sr errorchron plot, Et-Then Group basaltic flows, Preble Island, Great Slave Lake.*

Eight samples were analyzed isotopically and the results are listed in Table 1 and plotted in Figure 4. Seven of the eight sample points are collinear and define an errorchron age of 1969 ± 82 Ma, initial $^{87}Sr/^{86}Sr$ ratio 0.7046 ± 0.0006, and MSWD 3.7. The initial ratio is somewhat higher than that obtained from oceanic basalts of this age, but falls within the range of those obtained for continental basalts.

## Discussion

This is the first radiometric age determination on the rocks of the Et-Then Group. The result of 1969 ± 82 Ma is middle to late Aphebian, in contrast to many suggestions in the literature of a Helikian age. It was expected that the age determination would be reliable on the basis of the good quality of samples, representing a little deformed and virtually unmetamorphosed sequence. There is little evidence for burial metamorphism, and although the aggregate thickness of Et-Then Group is approximately 4500 m, this full thickness is not exposed at any one locality, and, judging from the sedimentary facies represented, such a thickness of sediments may not have been deposited at any one place.

The age of Et-Then Group reported here is greater than published isotopic ages between 1860 and 1800 Ma for other Aphebian rocks of the area known to be older than the Et-Then Group. Figure 5 contains a summary of available, pertinent age results.

The discrepancies resulting from very similar Rb-Sr isochron ages of 1805 to 1846 Ma for the stratigraphically widely separated volcanic assemblages of the Wilson Island Group, Seton Formation and Pearson Formation have been discussed by Frith (1980) and Goff et al. (1982). These discrepancies have become more evident since then, with a new age measurement by W.R. Van Schmus and S.A. Bowring (personal communication, Van Schmus, 1982) of 1865 Ma on zircon from one of the diorite-monzonite laccoliths (Fig. 1, 5), which may be the most reliable of these ages. The laccoliths are younger than the three volcanic assemblages, as seen from their field relations (Stockwell, 1936a, b; Hoffman et al., 1977). The Rb-Sr dates on the assemblages are thus anomalously young in relation to the zircon date. Frith (1980) and Goff et al. (1982) proposed metamorphic resetting and 'tailing off' effects of metamorphism on the volcanic assemblages as the reasons for the discrepancies that they observed, which is a reasonable explanation also for the younger K-Ar ages on the laccoliths and the Geological Survey of Canada Rb-Sr isochron age of 1677 Ma on the Pearson Formation basalts. In the case of the Et-Then Group basalts however, the situation is different in that they appear to be unaffected by the metamorphic event or events, otherwise they too would have yielded a younger date. On the contrary, they give a date older than the zircon date on the laccolith, whereas the field relations show that the laccoliths are unconformably overlain by the Et-Then Group. The error limits of ±82 Ma associated with the 1969 Ma age of Et-Then Group basalts do not result in its overlap with the 1865 Ma laccolith zircon age. This suggests that the 1969 Ma date on the basalts is anomalously old. It is possible that an isochron age older than the time of extrusion of basalts could have resulted from crustal contamination. This possibility is supported by a weak inverse correlation between Sr content and $^{87}Sr/^{86}Sr$, under which circumstance a uniform addition of crustal radiogenic Sr to Et-Then Group basalts of differing Sr content might have resulted in an anomalously old apparent age. This would also lead to a slight increase in the initial $^{87}Sr/^{86}Sr$ ratio and indeed the observed initial ratio is in the upper range for continental tholeiitic basalts of this age.

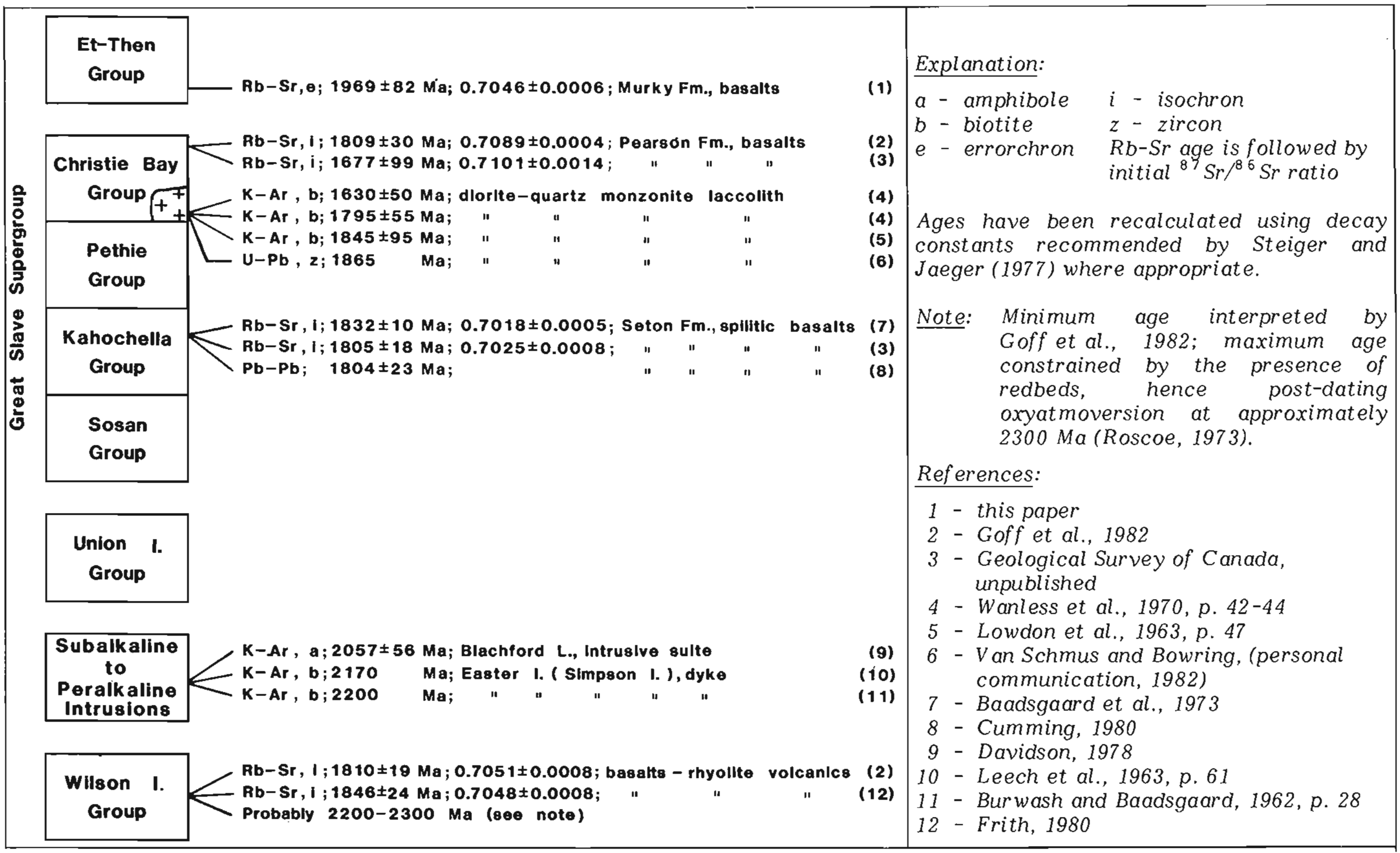


***Figure 5.*** *Summary of isotopic age determinations on the Aphebian rocks of the east arm of Great Slave Lake (modified after Goff et al., 1982, p. 346-347).*

However, the quantitative effects of such a phenomenon and its implictions to the magma genesis are, in this case, largely speculative.

It should be noted that the experimental points scatter slightly about the regression line, indicating an imperfectly closed system. This may be attributable to the crustal contamination as discussed above, or to alteration of the basalts as mentioned earlier.

In view of the above, the age of 1969 ± 82 Ma presented here should be regarded with caution until confirmed by independent means.

## Acknowledgments

Thanks are due to Ken Kwan, Project Geologist for S.E.R.U. Nucléaire (Canada) Limitée during 1978, for familiarizing one of the writers (SSG) with the geology and drill core of Preble Island in the field and to H. Knipping, Exploration Manager of the company, for reviewing this publication. S.E.R.U. Nucléaire (Canada) Limitée kindly provided permission to publish exploration data presented here. We would like to thank P.F. Hoffman and R.I. Thorpe of the Geological Survey of Canada for critically reading this manuscript.

## References

Baadsgaard, H., Morton, R.D., and Olade, M.A.D.
1973: Rb-Sr isotopic age for the Precambrian lavas of the Seton Formation, East Arm of Great Slave Lake, Northwest Territories; Canadian Journal of Earth Sciences, v. 10, no. 10, p. 1579-1582.

Burwash, R.A. and Baadsgaard, H.
1962: Yellowknife-Nonacho age and structural relations; Royal Society of Canada, Special Publication 4, p. 22-29.

Chandler, F.W.
1980: Proterozoic red-bed sequences of Canada; Geological Survey of Canada Bulletin 311, 53 p.

Cumming, G.L.
1980: Lead isochron dating of the Seton Formation, East Arm of Great Slave Lake, Northwest Territories; Canadian Journal of Earth Sciences, v. 17, no. 11, p. 1591-1593.

Davidson, A.
1978: The Blachford Lake intrusive suite: An Aphebian alkaline plutonic complex in the Slave Province, Northwest Territories; in Current Research, Part A, Geological Survey of Canada, Paper 78-1A, p. 119-127.

Fahrig, W.F. and Jones, D.L.
1969: Paleomagnetic evidence for the extent of Mackenzie igneous events; Canadian Journal of Earth Sciences, v. 6, no. 4, p. 679-688.

Fraser, J.A., Donaldson, J.A., Fahrig, W.F., and Tremblay, L.P.
1970: Helikian basins and geosynclines of the Northwestern Canadian Shield; in Symposium on Basins and Geosynclines of the Canadian Shield; Geological Survey of Canada, Paper 70-60, p. 213-238.

Frith, R.A.
1980: Rb-Sr studies of the Wilson Island Group, Great Slave Lake, District of Mackenzie; in Rubidium-strontium and uranium-lead isotopic age studies, Report 3; in Current Research, Part C, Geological Survey of Canada, Paper 80-1C, p. 229-233.

Goff, S.P., Baadsgaard, H., Muehlenbachs, K., and Scarfe, C.M.
1982: Rb-Sr isochron ages, magmatic $^{87}Sr/^{86}Sr$ initial ratios, and oxygen isotope geochemistry of the Proterozoic lava flows and intrusions of the East Arm of Great Slave Lake, Northwest Territories, Canada; Canadian Journal of Earth Sciences, v. 19, no. 2, p. 343-356.

Henderson, J.F.
1939: Taltson Lake map-area, Northwest Territories; Geological Survey of Canada, Map 525A (with marginal notes).

Hildebrand, R.S.
1981: Early Proterozoic LaBine Group of Wopmay Orogen: remnant of a continental volcanic arc developed during oblique convergence; in Proterozoic Basins of Canada, F.H.A. Campbell, ed.; Geological Survey of Canada, Paper 81-10, p. 133-156.

Hoffman, P.F.
1968: Stratigraphy of the lower Proterozoic (Aphebian) Great Slave Supergroup, East Arm of Great Slave Lake, District of Mackenzie; Geological Survey of Canada, Paper 68-42, 93 p.

1969: Proterozoic paleocurrents and depositional history of the East Arm fold belt, Great Slave Lake, Northwest Territories; Canadian Journal of Earth Sciences, v. 6, no. 3, p. 441-462.

1977: Preliminary geology of Proterozoic formations in the East Arm of Great Slave Lake, District of Mackenzie; Geological Survey of Canada, Open File 475 – Sheets A to L (NTS 75E, L, K; 85 H, I) scale 1:50 000.

Hoffman, P.F., Dewey, J.F., and Burke K.
1974: Aulacogens and their genetic relation to geosynclines, with a Proterozoic example from Great Slave Lake, Canada; in Modern and Ancient Geosynclinal Sedimentation, ed. R.H. Dott, Jr. and R.H. Shaver; Society of Economic Paleontologists and Mineralogists, Special Publication 19, p. 38-55.

Hoffman, P.F., Bell, I.R., Hildebrand, R.S., and Thorstad, L.
1977: Geology of the Athapuscow Aulacogen, East Arm of Great Slave Lake, District of Mackenzie; in Report of Activities, Part A, Geological Survey of Canada, Paper 77-1A, p. 117-129.

Irving, E., Park, J.K., and McGlynn, J.C.
1972: Paleomagnetism of the Et-Then Group and MacKenzie Diabase in the Great Slave Lake Area; Canadian Journal of Earth Sciences, v. 9, no. 6, p. 744-755.

Leech, G.B., Lowdon, J.A., Stockwell, C.H., and Wanless, R.K.
1963: Age determinations and geological studies (including isotopic ages – Report 4); Geological Survey of Canada, Paper 63-17, 140 p.

Lowdon, J.A., Stockwell, C.H., Tipper, H.W., and Wanless, R.K.
1963: Age determinations and geological studies, (including isotopic ages – Report 3); Geological Survey of Canada, Paper 62-17, 140 p.

McGlynn, J.C. and Irving, E.
1978: Multicomponent magnetization of the Pearson Formation (Great Slave Supergroup, N.W.T.) and the Coronation loop; Canadian Journal of Earth Sciences, v. 15, no. 4, p. 642-654.

Roscoe, S.M.
1973: The Huronian Supergroup, a Paleoaphebian succession showing evidence of atmospheric evolution; in Uranium Stratigraphy and Sedimentation, G.M. Young ed., Geological Association of Canada, Special Paper no. 12, p. 31-47.

Reinhardt, E.W.
1969a: Wilson Island – Petitot Islands area, East Arm of Great Slave Lake; in Report of Activities, Part A, April to October, 1968; Geological Survey of Canada, Paper 69-1, Part A, p. 177-181.

1969b: Geology of the Precambrian rocks of Thubun Lakes map-area in relationship to the McDonald Fault system, District of Mackenzie; Geological Survey of Canada, Paper 69-21, p. 29.

1972: Occurrence of exotic breccias in the Petitot Islands and Wilson Island map-areas, East Arm of Great Slave Lake, District of Mackenzie; Geological Survey of Canada, Paper 72-25, p. 43.

Steiger, R.H. and Jaeger, E., compilers
1977: Subcommission on Geochronology: convention on the use of decay constants in geo- and cosmochronology; Earth and Planetary Science Letters, v. 36, no. 3, p. 359-362.

Stockwell, C.H.
1936a: Eastern portion of Great Slave Lake (west half); Geological Survey of Canada, Map 377A (with marginal notes).

1936b: Eastern portion of Great Slave Lake (east half); Geological Survey of Canada, Map 378A (with marginal notes).

Tremblay, L.P.
1972: Geology of the Beaverlodge Mining area, Saskatchewan; Geological Survey of Canada, Memoir 367, 265 p.

1973: Volcanic rocks of Beaverlodge area; in Volcanism and volcanic rocks, Geological Survey of Canada, Open File 164, p. 15-27.

Wanless, R.K. and Loveridge, W.D.
1972: Rubidium-strontium isochron age studies, Report 1; Geological Survey of Canada, Paper 72-23.

Wanless, R.K., Stevens, R.D., Lachance, G.R., and Delabio, R.N.
1970: Age determinations and geological studies, K-Ar isotopic ages, Report 9, Geological Survey of Canada, Paper 69-2A, 78 p.

# 8. U-Pb AGES ON ZIRCON FROM THE M'CLINTOCK WEST MASSIF AND THE MARKHAM FIORD PLUTON, NORTHERNMOST ELLESMERE ISLAND

H.P. Trettin, W.D. Loveridge, and R.W. Sullivan

*Trettin, H.P., Loveridge, W.D., and Sullivan, R.W., U-Pb ages on zircon from the M'Clintock West massif and the Markham Fiord pluton, northernmost Ellesmere Island; in Rb-Sr and U-Pb Isotopic Age Studies, Report 5, in Current Research, Part C, Geological Survey of Canada, Paper 82-1C, p. 161-166, 1982.*

**Abstract**

*Zircon from a small granitic sheet within the M'Clintock West massif, a mafic-ultramafic complex of ophiolitic aspect, yields a U-Pb concordia intercept age of 481 +7/-6 Ma which suggests seafloor spreading in the late Early Ordovician (Arenig). Zircon from the granitic Markham Fiord pluton has a concordia intercept age of 462 ± 11 Ma. This intrusion probably crystallized during the subsequent collisional orogeny in the early Middle Ordovician, no later than in early Black River time (earliest Caradoc).*

## Geological Setting

### M'Clintock West massif

The M'Clintock West massif (Frisch, 1974; Trettin, 1969, 1981) is the largest of five igneous complexes in the M'Clintock Inlet area that are ophiolitic in aspect and probably coeval (Fig. 1). It is separated by steeply dipping faults from Proterozoic (?) schist and marble on the south and from Ordovician formations on the north and west. On the east, it is unconformably overlain by clastic sediments of middle Pennsylvanian age. It consists of two suites of rock, one ultramafic to mafic and the other granitic in composition. The first is composed mainly of serpentinite and metamorphosed gabbro and diabase with local occurrences of wehrlite and schist, rich in chlorite and actinolite. The second comprises clinopyroxene-hornblende diorite, hornblende diorite, tonalite (trondhjemite) and albite-bearing granodiorite, occurring as small sheets and plugs.

The mafic and ultramafic rocks are comparable to parts of the ophiolite suite but the igneous stratigraphy is obscured by glaciers, talus and faults.

The granitic rocks probably are consanguineous, and hence coeval with the mafic rocks, for several reasons. First, they are confined to the ophiolites and absent from the adjacent country rocks. Second, they form such a small proportion of the complex that they can be interpreted as differentiation products. And third, as a suite they are comparable to the "plagiogranites" of many ophiolites, in spite of the fact that some bodies contain K-feldspar in addition to the predominant plagioclase.

The host rock of the zircon analyzed is a small sheet of fine- to medium-grained quartz monzodiorite composed of quartz (16%), oligoclase (51%), K-feldspar (23%), hornblende (6%) and actinolite (3%) with trace amounts of

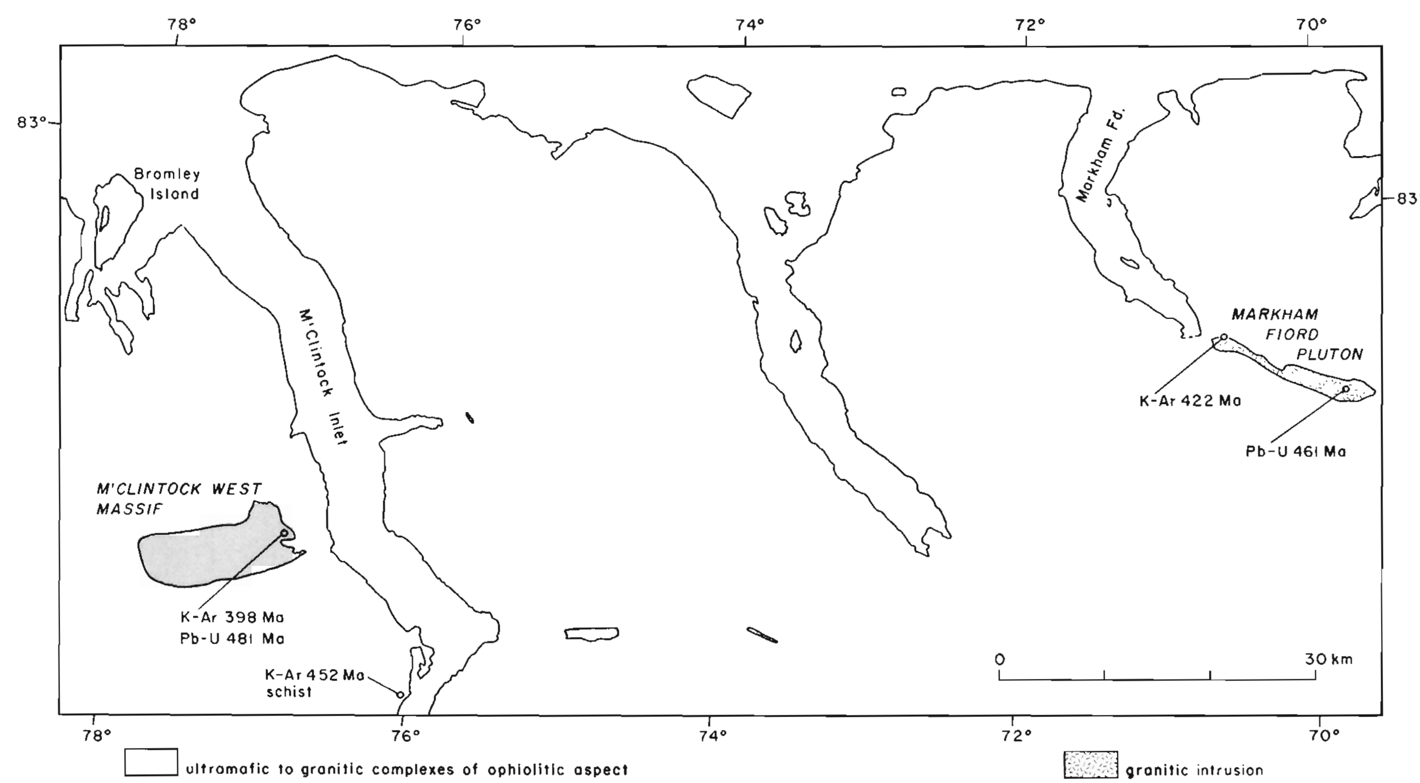


***Figure 1.*** *Sample locations, M'Clintock West massif and Markham Fiord pluton, northernmost Ellesmere Island.*

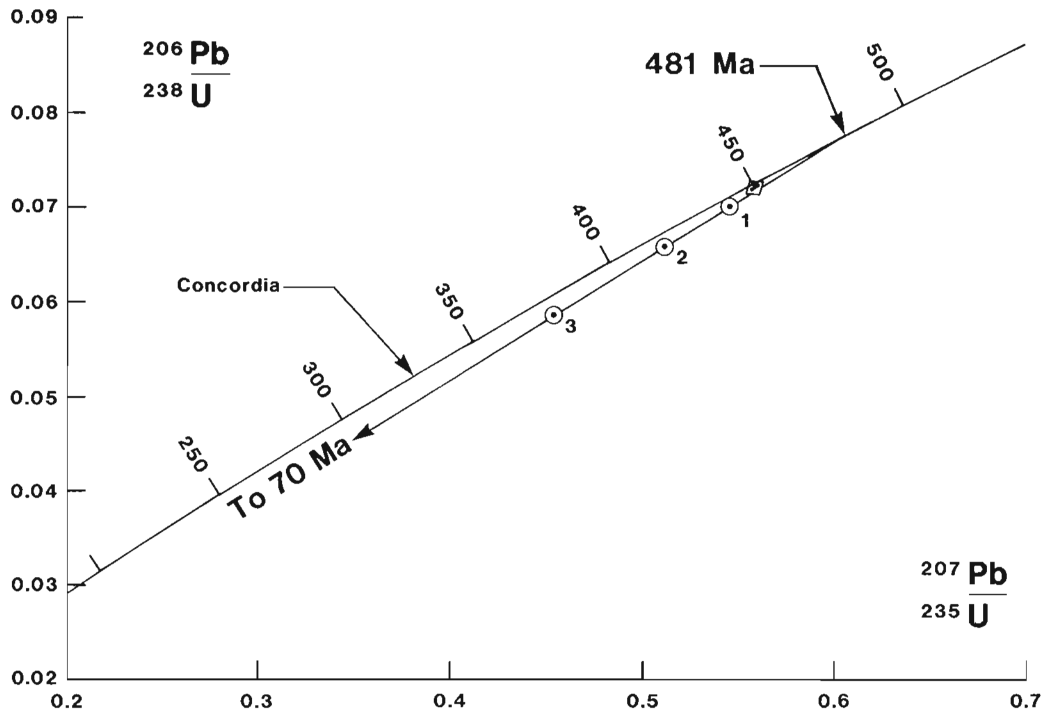


*Figure 2. Concordia diagram showing the results of U-Pb analyses of zircon concentrates from M'Clintock West massif (circles) and Markham Fiord pluton (diamond). See text for interpretation of Markham Fiord pluton results.*

Table 1

Analytical data, zircon fractions from M'Clintock West massif quartz monzonite and the Markham Fiord pluton, Ellesmere Island

| | | M'Clintock West massif | | | Markham Fiord pluton | | |
|---|---|---|---|---|---|---|---|
| Fraction number | | 1 | 2 | 3 | 1 | 2 | 3 |
| Fraction size, μm | | -105 + 74 | -74 + 62 | -105 + 74 | -149 + 105 | -105 + 74 | -149 + 105 |
| Magnetic or nonmagnetic | | nm | nm | mag | mag | nm | nm |
| Weight, mg | | 1.67 | 0.63 | 1.09 | 2.79 | 2.83 | 3.40 |
| Total Pb, ng | | 62.3 | 29.3 | 43.3 | 18.8 | 28.3 | 22.2 |
| Pb Blank, % | | 2.2 | 4.7 | 3.2 | 4.3 | 2.8 | 4.8 |
| Observed | $^{206}Pb/^{204}Pb$ | 1256 | 874.4 | 710.3 | 887.0 | 922.2 | 824.5 |
| *Abundances | $^{204}Pb$ | 0.04081 | 0.03044 | 0.08379 | 0.03357 | 0.05561 | 0.03308 |
| ($^{206}Pb$ = 100) | $^{207}Pb$ | 6.2520 | 6.0851 | 6.8450 | 6.1090 | 6.4317 | 6.0901 |
| | $^{208}Pb$ | 19.793 | 19.502 | 22.018 | 26.862 | 28.613 | 26.429 |
| Radiogenic Pb, ppm | | 104.1 | 111.8 | 109.0 | 22.97 | 25.24 | 23.20 |
| Radiogenic Pb, % | | 97.7 | 98.2 | 95.3 | 98.2 | 97.0 | 98.2 |
| Uranium, ppm | | 1393 | 1593 | 1732 | 280.8 | 307.0 | 285.9 |
| Atomic ratios: | $^{206}Pb/^{238}U$ | 0.070017 | 0.065755 | 0.058598 | 0.072327 | 0.072105 | 0.071995 |
| | $^{207}Pb/^{235}U$ | 0.54620 | 0.51151 | 0.45440 | 0.56046 | 0.55887 | 0.55671 |
| | $^{207}Pb/^{206}Pb$ | 0.056574 | 0.056415 | 0.056238 | 0.056197 | 0.056211 | 0.056078 |
| Ages, Ma: | $^{206}Pb/^{238}U$ | 436.3 | 410.5 | 367.1 | 450.2 | 448.8 | 448.2 |
| | $^{207}Pb/^{235}U$ | 442.5 | 419.5 | 380.4 | 451.8 | 450.8 | 449.4 |
| | $^{207}Pb/^{206}Pb$ | 475.0 | 468.8 | 461.8 | 460.2 | 460.7 | 455.5 |

*Corrected for Pb blank

apatite and opaque minerals. (Percentages are based on point count analysis of one thin section; plagioclase/plagioclase + K-feldspar ratio is inferred from peak heights on X-ray diffractogram, correction factor 0.95.)

A K-Ar determination on hornblende from the same body yielded an apparent age of 398 ± 20 Ma (recalculated from Wanless et al., 1968, using decay constants recommended by Steiger and Jaeger, 1977).

Markham Fiord pluton

About 90 km northeast of the M'Clintock West massif (Fig. 1), is a narrow, elongate granitic intrusion. It lies within a major fault zone and is in fault contact with rocks of late Paleozoic, Late Ordovician and uncertain early Paleozoic and/or Proterozoic age. The bounding faults probably were active during the Tertiary and perhaps also during Paleozoic orogenies.

The host rock of the zircon is composed mainly of plagioclase (calcic oligoclase), K-feldspar and quartz (total 90%) with lesser amounts of chlorite (7%), carbonate (2%) and opaque minerals (1%) and trace amounts of apatite (point count analysis). Peak heights of an X-ray diffractogram indicate that quartz/quartz + feldspar is about 25% (correction factor 0.48) and plagioclase/plagioclase + K-feldspar 79% (correction factor 0.95). Corresponding mineral percentages are quartz 22%, plagioclase 54% and K-feldspar 14%. (Point count was impractical because of the texture of the rock.)

The size distribution is bimodal. A population of medium-sized crystals (about 0.6-4.3 mm) is embedded in a matrix of fine crystals (0.1 mm). Graphic intergrowths of quartz and feldspar are common and some spherulites also are present. The plagioclase is intensely altered to white mica.

A K-Ar determination on hornblende from a different locality (Fig. 1) gave an apparent age of 422 ± 37 Ma (Stevens et al., 1982, p. 25).

**Analytical Procedures and Results**

Techniques for the concentration of zircon, its separation into fractions of differing physical characteristics, and the extraction and analysis of Pb and U are described by Sullivan and Loveridge (1980). U and Pb isotopic analyses were performed on three fractions from each of the two zircon concentrates. The analytical results are listed in Table 1 and displayed on a concordia diagram (Fig. 2). A description of the zircon morphologies is presented in the Appendix. Sample locations are shown in Figure 1 and listed in the Appendix.

M'Clintock West massif quartz monzodiorite: the three zircon fractions analyzed yielded data points, collinear within analytical uncertainty, defining a chord which cuts the concordia curve at 481 + 7/-6 Ma and 70 ± 23 Ma (Fig. 2).

Markham Fiord pluton: in this case the three zircon fractions yielded data points which form a very short, almost concordant, linear pattern (Fig. 2). The spread between these points is not sufficiently great to adequately define a chord on the concordia diagram, so we have interpreted the results using constraints on the associated lower concordia intercept ages. Since the U-Pb and $^{207}Pb/^{206}Pb$ age results for the three fractions all differ by less than two per cent from their mean of 453 Ma, it is apparent that a realistic upper concordia intercept age will probably be not much older than this. For mid Palaeozoic U-Pb zircon ages, lower concordia intercept ages commonly fall between 0 and 200 Ma. Using these extremes to define the lower concordia intercept ages, one can fit chords to the experimental points which give upper concordia intercept ages of 459 Ma (from 0 Ma) and 466 Ma (from 200 Ma). Analytical uncertainty introduces an additional uncertainty in age of ± 7 Ma. Thus we interpret these results as indicating a concordia upper intercept age of 462 ± 11 Ma.

**Interpretation**

Unconformities and related earth movements

The present ages cannot be evaluated without a brief review of the Ordovician to Carboniferous orogenic history of this area as inferred from unconformities. Two major orogenies are recognized. The first, here provisionally referred to as the M'Clintock orogeny, is apparent from a high angular unconformity, overlain by strata of late Middle Ordovician (Black River or early Caradoc) age[1] (Christie, 1957; Trettin, 1969, 1981). Regional relationships suggest that the underlying rocks may range in age from Proterozoic to Early or Middle Ordovician, but they have not yet been dated. Thus the stratigraphic-structural relationships indicate only that the M'Clintock orogeny is pre-late Middle Ordovician.

The late Middle Ordovician to Late Silurian stratigraphic record is nearly complete except for two unconformities within the Upper Ordovician series that indicate faulting but not folding.

The second major unconformity separates generally intensely deformed lower Paleozoic strata from markedly less deformed middle and upper Paleozoic beds. The youngest strata beneath the unconformity are Late Silurian (late Ludlovian or Pridolian) in age. In most areas the overlying units are Late Carboniferous (early or middle Pennsylvanian) in age. Two older units, however, are preserved locally in the Clements Markham Inlet map area. The first is the Sail Harbour "Group", tentatively assigned to the Early Devonian (Mayr et al., 1982). Its base is concealed but it conforms structurally with the upper Paleozoic rather than the lower Paleozoic succession. The second unit is the Lower Carboniferous (Viséan) Emma Fiord Formation. These relationships suggest that folding occurred in latest Silurian-early Devonian time with recurrent block faulting until Late Carboniferous time.

Stratigraphic age of M'Clintock West massif

The present zircon age determination clearly falls into the Early or Middle Ordovician but requires discussion because the absolute time scale for this interval has not yet been settled. The following data are relevant:

1. Longman et al. (in press) obtained a U-Pb zircon age of 475 ± 3 Ma for granitic clasts from a conglomerate dated as early Llandeilo on the basis of graptolites. Allowing a minimum of 3 Ma for uplift and erosion, the conglomerate can be no older than 475 Ma. The present zircon age has confidence limits of 488 to 475 Ma; therefore it can be no younger than early Llandeilo.
2. Bluck et al. (1980) report a K-Ar (amphibole) age of 478 ± 8 Ma for the middle Arenig, based on stratigraphic dating of the metamorphic aureole of the Ballantrae ophiolite in Scotland. According to this interpretation the M'Clintock West massif would be Arenig in age but the conclusions of Bluck et al. are based on interpretation of complex field relationships.
3. Ross et al. (1982) have recently published revised fission track ages on zircon and apatite from tuffs and bentonites of British stratotypes. They obtained ages of 493 ± 11 Ma from Arenig strata, of 487 ± 13 Ma from

[1] The terms Early, Middle and Late Ordovician are used, in the sense of Barnes et al. (1981), for the Canadian, Champlainian and Cincinnatian Epochs of North American stratigraphic nomenclature; the term Middle Ordovician is not used in Britain.

lower Llanvirn strata and of 476 ± 10 and 478 ± 12 Ma from lower Llandeilo strata. These data suggest that the M'Clintock West massif is about late Llanvirn in age with confidence limits in the Arenig and Llandeilo.

In conclusion, the massif probably is Arenig or Llanvirn in age. We have no direct information supporting one assignment or the other but prefer the Arenig age because the fission track ages appear to be too old when compared with results obtained by the U-Pb, Rb-Sr and K-Ar methods.

The inferred early Middle Ordovician or older age of the M'Clintock West massif permits (but does not prove) correlation with a small body of altered diabase and serpentinized peridotite on Bromley Island that is nonconformably overlain by upper Middle Ordovician limestone (cf. Trettin, 1969, Fig. 3, 4).

## Stratigraphic age of Markham Fiord pluton

This pluton is Middle Ordovician according to current time scales but its position within this Epoch is problematic. It is Llanvirn in age according to the time scale of Rundle (1981) based on an average K-Ar age of 468 ± 8 Ma for the Eycott Group volcanics, dated as early Llanvirn on the basis of graptolites, and on a Rb-Sr isochron of 438 ± 6 Ma for the Threlkeld microgranite, considered as early Llandeilo on the basis of indirect stratigraphic evidence.

Longman et al., in their study of the Benan and Tormichell conglomerates, Ayrshire, Scotland (op. cit.), suggest that uplift and erosion of the 475 ± 3 Ma old source terrane of the granite clasts took less than 10 Ma. If one assumes that it required 3 to 9 Ma, one arrives at an age between 463 and 475 Ma for the early Llandeilo conglomerate. Accordingly, the Markham Fiord pluton (confidence limits 451-473 Ma) probably is no older than early Llandeilo or, possibly, late Llanvirn.

Ross et al. (1982) obtained diverse and internally conflicting fission track ages, ranging from 450 ± 12 Ma to 469 ± 12 Ma on formations of middle and late Caradocian ages, placing the Markham Fiord pluton in this interval.

Combining all this information with the stratigraphic-structural record of the M'Clintock Inlet region, we arrive at the conclusion that the Markham Fiord pluton probably crystallized during the M'Clintock orogeny in the earlier part of the Middle Ordovician – no later than in early Black River time (earliest Caradoc), and more likely in the Llanvirn or Llandeilo.

## Tectonic implications of zircon ages and significance of related K-Ar ages

The present determinations have resulted in fundamental changes in the interpretation of the tectonic history of northernmost Ellesmere Island. The mafic-ultramafic belt (Fig. 1) appears to have been overlapped stratigraphically by formations of late Middle Ordovician to late Silurian age that show no evidence of having been separated by seafloor spreading and subsequently reassembled by collisional orogeny. The 481 Ma zircon age of the M'Clintock West massif finally permits interpretation of the mafic-ultramafic bodies in terms of seafloor spreading which was precluded in earlier interpretations (e.g. Trettin and Balkwill, 1979) by acceptance of the much younger (Early Devonian?) K-Ar age of 398 Ma.

The M'Clintock orogeny is now interpreted as a collision that followed the spreading. The two zircon ages suggest that it was mainly early Middle Ordovician in age but might have commenced in the latest Early Ordovician. The age for the Markham Fiord pluton demonstrates for the first time that it was accompanied by granitic intrusion. The end of the thermal event associated with this orogeny is probably defined by the K-Ar age of 452 ± 8 Ma obtained on a Proterozoic (?) schist at the head of M'Clintock Inlet (Fig. 1; Stevens et al., 1982, p. 24). The schist is unconformably overlain by clastic sediments of early Late Ordovician age, that are only slightly deformed. Evidently this particular area was stabilized during the M'Clintock orogeny to such an extent that subsequent orogenies resulted only in block-faulting and associated warping without folding and resetting of the argon clock.

By contrast, the K-Ar ages both of the M'Clintock West massif and Markham Fiord pluton were affected by later events. The former may be related to the inferred folding in latest Silurian-early Devonian time.

The present zircon determinations demonstrate surprising age relationships with rocks and events in parts of the Appalachian and Caledonian mobile belts. For example, trondhjemite of the Ballantrae ophiolite has a zircon age of 484 ± 4 Ma (Bluck et al., 1980) and trondhjemites of the Bay of Islands and Betts Cove ophiolites of Newfoundland have zircon ages of 508 ± 5 and 463 ± 6 Ma respectively (Mattinson, 1975). Ophiolite obduction in this area began in late Early Ordovician (Arenig) time and thrust faulting continued into the Middle Ordovician (Williams, 1979). This event, the Taconic Orogeny, is comparable in age, and to some extent also in character, to the M'Clintock orogeny.

**Acknowledgments**

We are indebted to O. van Breemen for critical reading and improvements of the manuscript.

**References**

Barnes, C.R., Norford, B.S., and Skevington, D.
1981: The Ordovician System in Canada: correlation chart and explanatory notes; International Union of Geological Sciences, Publication no. 8.

Bluck, B.J., Halliday, A.N., Aftalion, M., and Macintyre, R.M.
1980: Age and origin of Ballantrae ophiolite and its significance to the Caledonian Orogeny and Ordovician time scale; Geology, v. 8, p. 492-495.

Christie, R.L.
1957: Geological reconnaissance of the north coast of Ellesmere Island, District of Franklin, Northwest Territories; Geological Survey of Canada, Paper 56-9.

Frisch, T.
1974: Metamorphic and plutonic rocks of northernmost Ellesmere Island, Canadian Arctic Archipelago; Geological Survey of Canada, Bulletin 229.

Longman, C.D., Bluck, B.J., van Breemen, O., and Aftalion, M.
Ordovician conglomerates: constraints on the time scale; in Numerical Dating in Stratigraphy, ed. G.S. Odin, John Wiley and Sons, Chichester, England. (in press)

Mattinson, J.M.
1975: Early Paleozoic ophiolite complexes of Newfoundland: isotopic ages of zircons; Geology, v. 3, p. 181-183.

Mayr, U., Trettin, H.P., and Embry, A.F.
1982: Preliminary geological map and notes, Clements Markham Inlet and Robeson Channel map-areas, District of Franklin (NTS 120E,F,G); Geological Survey of Canada, Open File 833.

Ross, R.J. Jr., Naeser, C.W., Izett, G.A., Obradovich, J.D., Basset, M.G., Hughes, C.P., Cocks, L.R.M., Dean, W.T., Ingham, J.K., Jenkins, C.J., Rickards, R.B., Sheldon, P.R., Toghill, P., Whittington, H.B., and Zalasiewicz, J.
1982: Fission track dating of British Ordovician and Silurian stratotypes; Geological Magazine, v. 119, p. 135-153.

Rundle, C.C.
1981: The significance of isotopic dates from the English Lake District for the Ordovician-Silurian time scale; Geological Society of London, Journal, v. 138, p. 569-572.

Steiger, R.H. and Jaeger, E., compilers
1977: Subcommission on Geochronology: convention on the use of decay constants in geo- and cosmochronology; Earth and Planetary Science Letters, v. 36, no. 3, p. 359-362.

Stevens, R.D., Delabio, R.N., and Lachance, G.R.
1982: Age determinations and geological studies, K-Ar isotopic ages, Report 15; Geological Survey of Canada, Paper 81-2.

Sullivan, R.W. and Loveridge, W.D.
1980: Uranium-lead age determinations on zircon at the Geological Survey of Canada: current procedures in concentrate preparation and analysis; in Loveridge, W.D., Rubidium-strontium and uranium-lead isotopic age studies, Report 3; in Current Research, Part C, Geological Survey of Canada, Paper 80-1C, p. 161-246.

Trettin, H.P.
1969: Geology of Ordovician to Pennsylvanian rocks, M'Clintock Inlet, north coast of Ellesmere Island, Canadian Arctic Archipelago; Geological Survey of Canada, Bulletin 183.

1981: Geology of Precambrian to Devonian rocks, M'Clintock Inlet area, District of Franklin (NTS 340 E,H) – preliminary geological map and notes; Geological Survey of Canada, Open File 759.

Trettin, H.P. and Balkwill, H.R.
1979: Contributions to the tectonic history of the Innuitian Province, Arctic Canada; Canadian Journal of Earth Sciences, v. 16, no. 3, pt. 2, p. 748-769.

Wanless, R.K., Stevens, R.D., Lachance, G.R., and Edmonds, C.M.
1968: Age determinations and geological studies, K-Ar isotopic ages, report 8; Geological Survey of Canada, Paper 67-2, Part A, p. 60-61.

Williams, H.R.
1979: Appalachian Orogen in Canada; Canadian Journal of Earth Sciences, v. 16, p. 792-807.

## APPENDIX

Sample locations and descriptions of zircon concentrates, M'Clintock West massif quartz monzodiorite and Markham Fiord pluton, Ellesmere Island.

M'Clintock West massif quartz monzodiorite: Location: Lat. 82°41'00"; Long. 76°53'00"

Zircon concentrate: The zircon grains of this sample were mostly euhedral to slightly rounded, colourless through pale brown to dark translucent. In transmitted light the coloured crystals appeared light to dark (translucent) hyacinthe. Internal zoning was evident in many, but not all crystals, and rod, granular and bubble inclusions were common. The translucent crystals appeared to have suffered considerable surface alteration and tended to have more rounded terminations than the clear varieties. Crystal shape was generally short prismatic with an average elongation ratio of about 3:1. The relatively magnetic and nonmagnetic fractions differed primarily by the former containing more and larger inclusions and having more internal fractures.

Markham Fiord pluton: Location: Lat. 82°50'30"; Long. 69°48'30"

Zircon concentrate: The concentrate used for this determination consisted of essentially pure, clear, almost colourless euhedral zircon of very fresh appearance. About 10% of the crystals showed indications of coarse, incomplete zoning. Crystal shape was generally short prismatic with an average elongation ratio of about 3:1. The relatively nonmagnetic fraction consisted of very pale purple crystals with a few bubble and rod inclusions and rare black specks in about 40%, the remainder being quite clear and of "gem" quality. The relatively magnetic fraction was essentially similar but some crystals had reddish stains on their surfaces and some contained black speck inclusions.

# 9. A Rb-Sr STUDY OF THE NATKUSIAK BASALTS, VICTORIA ISLAND, DISTRICT OF FRANKLIN

W.R.A. Baragar and W.D. Loveridge

*Baragar, W.R.A. and Loveridge, W.D., A Rb-Sr study of the Natkusiak Basalts, Victoria Island, District of Franklin; in Rb-Sr and U-Pb Isotopic Age Studies, Report 5, in Current Research, Part C, Geological Survey of Canada, Paper 82-1C, p. 167-168, 1982.*

**Abstract**

*The age of the Natkusiak Formation of basaltic flows, Victoria Island, is of interest because of its paleomagnetic correlation with the Franklin Magnetic Interval. Rb-Sr results on six dolerites and eight flow basalt samples show linear trends suggesting ages of 2200 and 384 Ma, both of which are unacceptable in terms of a primary age for these rocks. The older age suggests that the dolerites are, contrary to previous belief, contaminated with crustal material, whereas the 384 Ma alignment is unexplained, but may also be due to contamination, or to late or post Devonian uplift.*

## Introduction

The Natkusiak plateau basalts and related sills are assumed to be late Hadrynian in age on the basis of K-Ar dating (640 Ma, Christie, 1964; 625 Ma, Palmer and Hayatsu, 1975) and paleomagnetic correlation (Palmer and Hayatsu, 1975) with the Franklin Magnetic Interval (Fahrig et al., 1971). More precise dating is desirable because of the extensive reach of the Franklin intrusions and in consequence their value as chronological bench marks. Moreover, a double paleomagnetic reversal found recently in a stratigraphic section of the Natkusiak basalts (Palmer et al., 1981) has the potential, with reliable dating, to be a global late Precambrian time horizon.

## Geological Setting

The Natkusiak Formation of basaltic flows rests with slight discordance on the Shaler Group of predominantly limestones, sandstones, and shales (Thorsteinsson and Tozer, 1962) and these in turn lie with marked unconformity on probable late Archean basement. The Shaler sediments are profusely intruded by sills of compositions similar to that of the flows and are probably their immediate precursors. Paleomagnetic pole directions for the sills, flows, and sediments are close to one another and indicate that all three could have formed within a short space of time (Palmer et al., in press). After emplacement they were warped into a gently folded northeasterly-trending syncline in which dips range from 0 to about 10 degrees. According to Thorsteinnson and Tozer (1962) folding took place before deposition of the overlying Paleozoic beds (Cambrian ?) and was followed later (Upper Devonian-pre-Cretaceous) by uplift and exposure of the Precambrian (Minto) arch.

The basalts and related dolerites are variably altered but the metamorphic grade is low, pumpellyite or less, and much of it can probably be attributed to the circulation of hydrothermal and groundwaters.

## Analytical Procedures and Results

Analytical procedures for Rb-Sr isotopic analyses of whole-rock samples were based on those described by Wanless and Loveridge (1972) with the exception that $^{87}Sr/^{86}Sr$ were obtained only from spiked Sr analyses in this study;

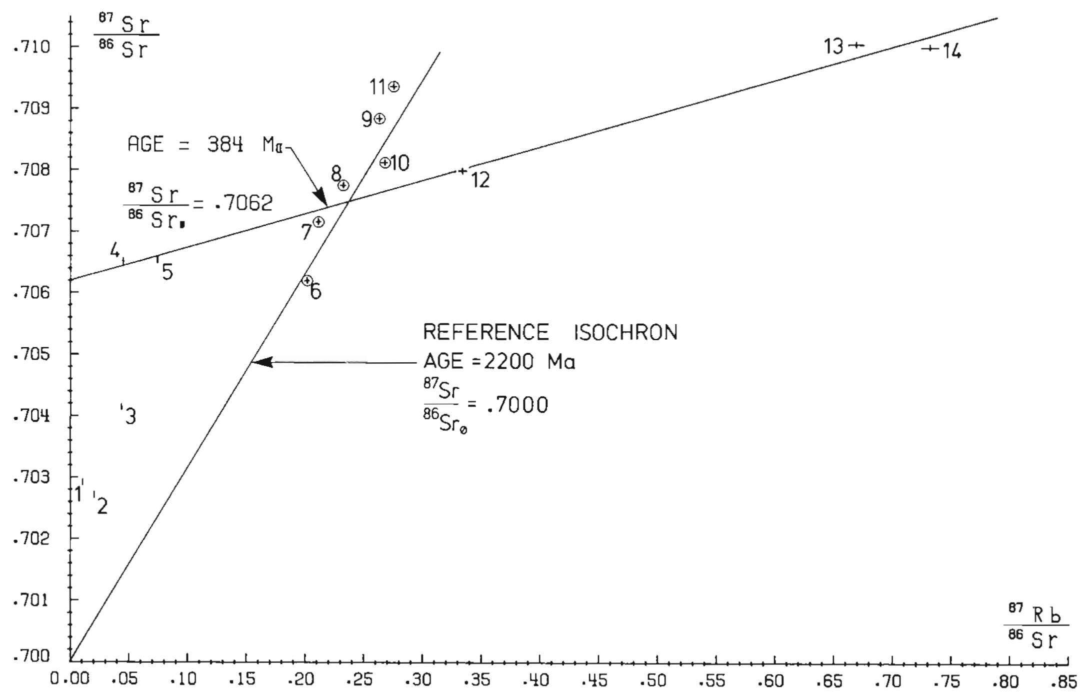


***Figure 1.*** *Results of Rb-Sr analyses of Natkusiak flow basalts (crosses) and dolerites (circles) compared with a reference isochron of age 2200 Ma, initial ratio 0.7000, and a regression line of age 384 Ma, initial ratio 0.7062, through five of the eight flow basalt data points.*

Table 1

Analytical data, whole-rock samples, Natkusiak Basalts, Victoria Island, District of Franklin

| Sample No. This Work | Field | Rb ppm | Sr ppm | $^{87}Sr/^{86}Sr$ ± 0.00010 | $^{87}Rb/^{86}Sr$ ± 2.0 % | Rock type | Location Latitude | Longitude |
|---|---|---|---|---|---|---|---|---|
| 1 | BLS-27-75 | 0.573 | 154.1 | 0.70292 | 0.0107 | Flow basalt | 71°51'30" | 112°25'40" |
| 2 | BLS-28-75 | 1.179 | 167.8 | 0.70271 | 0.0203 | " " | 71°51'40" | 112°25'40" |
| 3 | BLS-51A-75 | 2.748 | 182.4 | 0.70414 | 0.0436 | " " | 71°58'10" | 112°10'30" |
| 4 | BLS-67-75 | 3.034 | 194.2 | 0.70652 | 0.0452 | " " | 71°59'10" | 112°13'00" |
| 5 | BLS-64-75 | 3.017 | 117.5 | 0.70653 | 0.0742 | " " | 71°58'20" | 112°13'20" |
| 6 | BL-75-45 | 15.94 | 228.7 | 0.70620 | 0.2015 | Dolerite | 72°12'10" | 111°31'40" |
| 7 | BLS-3-75 | 21.44 | 293.7 | 0.70716 | 0.2111 | " " | 72°09'00" | 111°30'10" |
| 8 | BLS-16-75 | 22.84 | 284.5 | 0.70775 | 0.2321 | Doleritic granophyre | 72°12'10" | 111°28'10" |
| 9 | 75-HF-A | 19.80 | 217.7 | 0.70884 | 0.2629 | Dolerite | 72°51'50" | 110°04'30" |
| 10 | BLS-8-75 | 27.07 | 292.7 | 0.70812 | 0.2674 | " " | 72°12'40" | 111°33'30" |
| 11 | BLS-7-75 | 28.32 | 297.9 | 0.70936 | 0.2749 | " " | 72°12'50" | 111°32'20" |
| 12 | BLS-39-75 | 20.41 | 177.1 | 0.70799 | 0.3332 | Flow basalt | 71°50'10" | 112°11'40" |
| 13 | BL-75-132 | 10.75 | 46.53 | 0.71005 | 0.6679 | Amygdaloidal basalt | 71°47'50" | 112°12'00" |
| 14 | BL-75-51 | 8.762 | 34.67 | 0.71000 | 0.7307 | Amygdaloidal basalt | 71°51'50" | 112°21'40" |

no unspiked Sr measurements were performed. Measured $^{87}Sr/^{86}Sr$ were normalized to a value of 0.70800 for the $^{87}Sr/^{86}Sr$ of the MIT isotopic Sr standard (Eimer and Amend, $SrCo_3$, lot no. 492327).

The results of Rb-Sr analyses on fourteen samples, six dolerites and eight flow basalts are listed in Table 1 and plotted in Figure 1. Two linear trends are evident. The dolerite sample points cluster about a reference isochron of age 2200 Ma and initial $^{87}Sr/^{86}Sr$ of 0.7000, whereas five of the eight flow basalt results may be fitted by a regression line of age 384 ± 45 Ma, initial $^{87}Sr/^{86}Sr$, 0.7062 ± 0.0002 and MSWD, 12.82.

## Discussion

Neither of these results is satisfactory in terms of a primary age for the igneous rocks but they may have some significance. The dolerite samples were selected on the basis of their chemical analyses to give a suitably large range in Rb/Sr ratios. Accordingly, they included samples of what had been interpreted as late-stage differentiates of the doleritic magma, a granophyre and samples with minor granophyric segregations. In view of the age obtained from the dolerite samples it seems best to re-interpret these segregations as having been contaminated by the underlying Archean basement. Patchett et al. (1979) discuss contamination of late crystallizing interstitial alkali feldspars of Swedish dolerites by aqueous solutions derived from the older host rocks, which is probably the mechanism operative in this case as well. Restudy of the thin sections confirm that all the dolerite samples used for the age determination contain some interstitial granophyre, attesting that the sills must be regarded as widely contaminated.

If the 384 Ma alignment has any significance it could only be related to the late or post-Devonian uplift which may have renewed groundwater circulation and resulted in widespread variable alteration of the flows. More probably, samples 4, 5 and 12 have undergone the same type of contamination by radiogenic Sr as the dolerite samples, resulting in a fortuitous alignment with points 13 and 14.

The least altered samples of those analyzed are numbers 1 and 2. Both are close to the vertical axis of the diagram and would seem to indicate an initial ratio consistent with an uncontaminated magma. Other samples that could represent primary magmatic ratios are numbers 13 and 14. These are from flow tops containing coarse amygdaloidal fillings of K-rich feldspar and they probably formed shortly after emplacement from locally-derived constituents. It would be reasonable to expect, therefore, that they had the same isotopic ratios as the flow itself at the time of its formation. If this is the case ages of 776 and 705 Ma may be calculated for samples 13 and 14 respectively based on an initial $^{87}Sr/^{86}Sr$ of 0.70265 derived from the averaged results of samples 1 and 2. This is an age range that would be entirely compatible with the K-Ar dating and the paleomagnetic data.

## References


Christie, R.L.
1964: Diabase-gabbro sills and related rocks of Banks and Victoria Islands, Arctic Archipelago; Geological Survey of Canada, Bulletin 105.

Fahrig, W.F., Irving, E., and Jackson, G.D.
1971: Paleomagnetism of the Franklin diabases; Canadian Journal of Earth Sciences, v. 8, no. 4, p. 455-467.

Palmer, H.C. and Hayatsu, A.
1975: Paleomagnetism and K-Ar dating of some Franklin lavas and diabases, Victoria Island; Canadian Journal of Earth Sciences, v. 12, no. 8, p. 1439-1447.

Palmer, H.C., Baragar, W.R.A., Foster, J.H., and Fortier, M.C.
1981: Polarity sequence during the Franklin Magnetic Interval; (Abstract) International Association of Geomagnetism and Aeromony. Bulletin 45.

Paleomagnetism of the Nakusiak magmatic province and Shaler sediments; Canadian Journal of Earth Sciences. (in press)

Patchett, P.J., van Breemen, O., and Martin, R.F.
1979: Sr isotopes and the structural state of feldspars as indicators of post magmatic hydrothermal activity in continental dolerites; Contributions to Mineralogy and Petrology, v. 69, p. 65-73.

Thorsteinsson, R. and Tozer, E.T.
1962: Banks, Victoria, and Stefansson Islands, Arctic Archipelago; Geological Survey of Canada, Memoir 330.

Wanless, R.K. and Loveridge, W.D.
1972: Rubidium-strontium isochron age studies, Report 1; Geological Survey of Canada, Paper 72-23.

# 10. UPDATED Rb-Sr AGES FROM THE INGILIK POINT GNEISS COMPLEX, BAKER LAKE REGION, DISTRICT OF KEEWATIN

Mikkel Schau, W.D. Loveridge, and R.D. Stevens

*Schau, M., Loveridge, W.D., and Stevens, R.D., Updated Rb-Sr ages from the Ingilik Point Gneiss Complex, Baker Lake region, District of Keewatin; in Rb-Sr and U-Pb Isotopic Age Studies, Report 5, in Current Research, Part C, Geological Survey of Canada, Paper 82-1C, p. 169-171, 1982.*

**Abstract**

*Zircon from a leucocratic layer of gneiss from the Ingilik Point Gneiss Complex previously yielded an Archean U-Pb concordia intercept age of 2675 + 33/-11 Ma. Rb-Sr age determinations on subsamples from two gneissic blocks from the same locality yield an isochron age of 2069 ± 66 Ma with initial ratio 0.7044 ± 0.0002 and an errorchron of age 1908 ± 108 Ma and initial ratio 0.705. Hand samples collected nearby yielded a nonlinear set of data points. K-Ar mineral ages for gneiss and nearby gabbros range from 1982 to 1895 Ma. The Rb-Sr age results are interpreted as having been updated from the original 2675 Ma age of emplacement by a series of more recent events terminating at 1895 Ma.*

## Geological Setting

The Ingilik Point Gneiss Complex (Schau and Ashton, 1980; unit 6, Schau et al., 1982) consists of layered granitoid gneiss and amphibolite and occurs adjacent to and south of the main Chesterfield Fault zone in the Baker Lake region. It is the country rock onto which the more southerly late Archean Kramanituar Complex (unit 5, Schau et al., 1982) has been emplaced and upon which the unconformably overlying Proterozoic Dubawnt Group rests (unit 10, Schau et al., 1982). The complex is cut by late Archean (?) granitic batholiths and by small gabbroic stocks which generally cut across the gneissosity but which may have a portion which is locally sheared and conformable with the gneissosity.

A sample of a leucocratic layer in biotite-bearing hornblende-quartz-plagioclase gneiss from the Ingilik Point Gneiss Complex has yielded zircon with a U-Pb concordia intercept age of 2675 + 33/-11 Ma (Schau, 1980) and biotite with a K-Ar age of 1895 ± 44 Ma (Table 1). In an attempt to confirm the Archean age for this gneiss as indicated by the U-Pb result on zircon, a series of Rb-Sr analyses was undertaken on three suites of samples from the same immediate area. A block of gneiss (1/8 $m^3$) taken from the same locality as the zircon sample, was split into four along its gneissosity so that the leucocratic layer which previously yielded zircon for U-Pb analysis was one of the subsamples used for Rb-Sr measurement (slab WN-506-78). A similar block of gneiss taken a short distance away (slab 399) yielded a second suite of subsamples while random hand specimens taken a few metres from the latter site yielded the third suite.

## Analytical Procedures and Results

Analytical procedures for Rb-Sr isotopic analyses of whole-rock samples were based on those described by Wanless and Loveridge (1972) with the exception that $^{87}Sr/^{86}Sr$ were obtained only from spiked Sr analyses in this study: no unspiked Sr measurements were performed. $^{87}Sr/^{86}Sr$ were normalized to a value of 0.7080 for the MIT isotopic Sr standards (Eimer and Amend Sr $CO_3$, lot 492327).

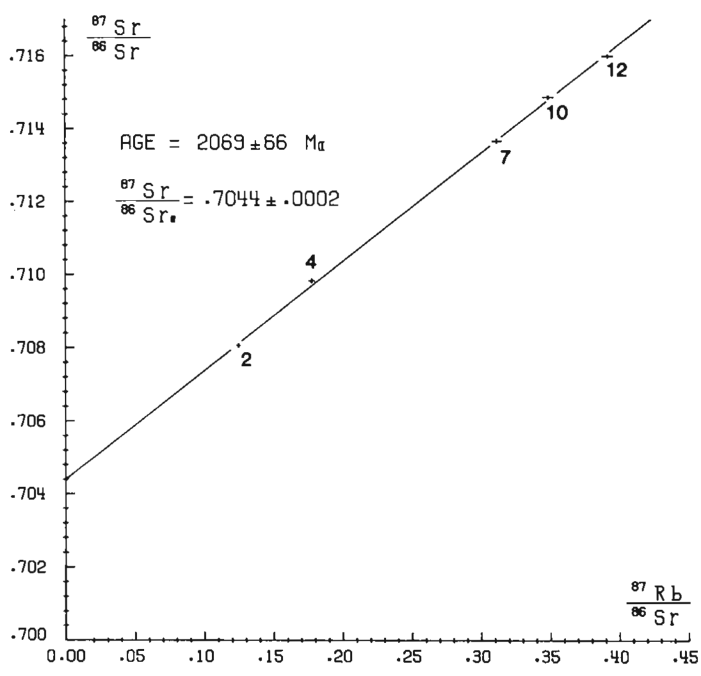


*Figure 1. Rb-Sr isochron diagram showing results of analyses of slabs from block WN-506-78, Ingilik Point Gneiss complex.*

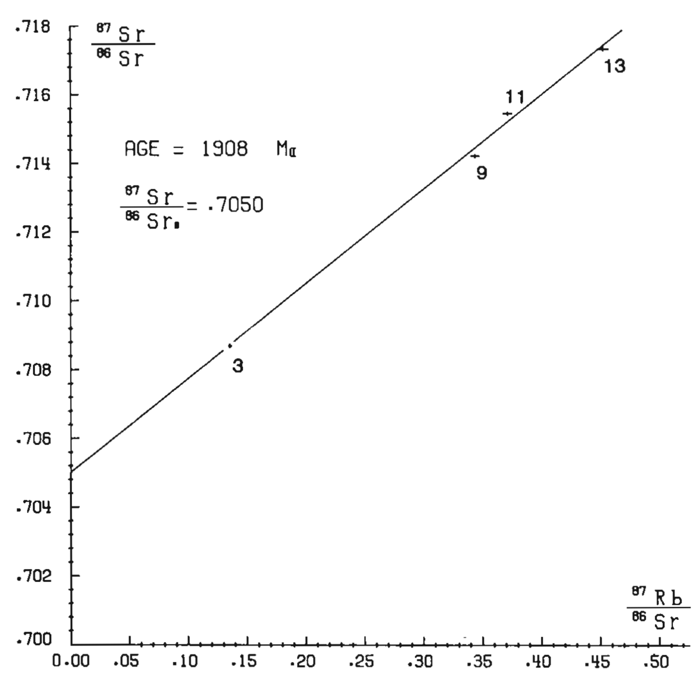


*Figure 2. Rb-Sr errorchron showing results of analyses of slabs from block 399, Ingilik Point Gneiss Complex.*

Table 1

K-Ar dates from mineral concentrates,
Ingilik Point Gneiss Complex and gabbro stocks

| Sample | Mineral | Rock | %K | % $^{40}$Ar rad. | $^{40}Ar/^{40}K$ | Age (Ma) | Location Latitude | Longitude |
|---|---|---|---|---|---|---|---|---|
| WN-506-78 | Biotite | Gneiss | 6.80 | 99.4 | 0.1948 | 1895 ± 44 | 64° 11' | 93° 59½' |
| H3 | Hornblende | Gabbro | 0.60 | 96.9 | 0.2049 | 1954 ± 105 | 64° 11' | 93° 56' |
| H2 | Hornblende | Gabbro | 0.93 | 99.2 | 0.2077 | 1971 ± 78 | 64° 12' | 93° 57' |
| 400 | Hornblende | Gabbro | 0.38 | 98.2 | 0.2096 | 1982 ± 164 | 64° 13' | 93° 58' |

Table 2

Analytical data, whole-rock samples from the
Ingilik Point Gneiss Complex

| Sample no. | Suite* | Rb ppm | Sr ppm | $^{87}Sr/^{86}Sr$ (± 0.00010) | $^{87}Rb/^{86}Sr$ |
|---|---|---|---|---|---|
| 1 | hand | 19.13 | 446.4 | 0.70773 | 0.1239 ± 0.0025 |
| 2 | 506 | 16.21 | 375.8 | 0.70807 | 0.1247 ± 0.0025 |
| 3 | 399 | 18.96 | 404.6 | 0.70869 | 0.1355 ± 0.0027 |
| 4 | 506 | 23.44 | 381.1 | 0.70983 | 0.1778 ± 0.0036 |
| 5 | hand | 26.83 | 308.9 | 0.71091 | 0.2511 ± 0.0050 |
| 6 | hand | 31.73 | 317.9 | 0.71214 | 0.2886 ± 0.0058 |
| 7 | 506 | 46.65 | 433.1 | 0.71366 | 0.3114 ± 0.0062 |
| 8 | hand | 47.32 | 413.7 | 0.71439 | 0.3307 ± 0.0066 |
| 9 | 399 | 51.71 | 434.8 | 0.71420 | 0.3438 ± 0.0069 |
| 10 | 506 | 47.12 | 390.8 | 0.71487 | 0.3486 ± 0.0070 |
| 11 | 399 | 50.98 | 396.7 | 0.71543 | 0.3715 ± 0.0074 |
| 12 | 506 | 55.57 | 410.3 | 0.71600 | 0.3916 ± 0.0078 |
| 13 | 399 | 62.93 | 402.3 | 0.71731 | 0.4522 ± 0.0090 |

*Suite: 506 = from block WN-506-78
399 = from block 399
hand = hand specimen

The results of Rb and Sr analyses on the gneiss samples are given in Table 2 and depicted on isochron diagrams (Fig. 1, 2, 3). Analyses of slabs from block WN-506-78 yielded an isochron: age 2069 ± 66 Ma, initial ratio 0.7044 ± 0.0002 and MSWD 1.44 (Fig. 1) whereas analyses of slabs from block 399 yielded an errorchron: age 1908 ± 108 Ma, initial ratio 0.7050 ± 0.0004 and MSWD 4.5 (Fig. 2). Data points from the adjacent hand specimens did not form a linear pattern, but are shown on Figure 3 which combines all results from this study.

The gabbro stocks (unit 8c, Schau et al., 1982) give K-Ar dates intermediate in age to the isochron and the errorchron (Table 1). Analytical techniques for K-Ar age determination are as described in Stevens et al. (1982).

## Discussion

A reference isochron of age 2675 Ma and initial $^{87}Sr/^{86}Sr$ ratio 0.7013 is shown in Figure 3 in addition to the 2069 Ma, 0.7044 initial ratio isochron determined on the slabs from block WN-506-78. The 2675 Ma age of the reference isochron is that of the zircon measurement; the initial ratio of 0.7013[1] was chosen to investigate the possibility that the precursors of the gneisses were derived from the mantle at about 2700 Ma. The reference isochron passes through the upper cluster of data points and provides a reasonable fit to two results, 5 and 6, which do not fall within the 2069 Ma trend. It provides a plausible model for the Rb-Sr systematics prior to re-equilibration at about 2069 Ma.

In addition the 2069 Ma isochron has an initial ratio of 0.7044 ± 0.0002 which is clearly greater than the mantle ratio of 0.7020[1] at 2069 Ma. Thus the Rb-Sr results are compatible with isotopic re-equilibration at about 2069 Ma of mantle derived rocks of original age 2675 Ma but incompatible with primary mantle derivation at 2069 Ma.

We present two models to explain these radiometric ages. Model A, the model favoured by the authors, is that the gneiss complex formed, in part by plutonic addition, during the late Archean (about 2675 Ma). Subsequent shearing, gabbro intrusion, and deformation affected the Ingilik Point Gneiss Complex in an irregular manner so that small volumes were isotopically and mechanically isolated during the interval about 2100 to 1850 Ma (determined jointly from the Rb-Sr and K-Ar results).

An alternative model (B) is that the zircon in the leucocratic layer under study (dated at 2675 Ma) could be a detrital relict of a sedimentary precursor and the age reported is that of the antecedent to the sedimentary rock. Lacking other constraints, the time of gneissification could be much younger, possibly even 2069 Ma as suggested by the isochron age on the slabs from block WN-506-78.

[1] Recently published mantle $^{87}Sr/^{86}Sr$ growth curves are strongly model dependant but, over the period of time 2000-2700 Ma, do not differ substantially from the curve which may be derived from the present day bulk earth Rb-Sr isotopic ratios of Jacobsen and Wasserburg (1979) which yield $^{87}Sr/^{86}Sr$ of 0.7013 at 2675 Ma and 0.7020 at 2069 Ma.

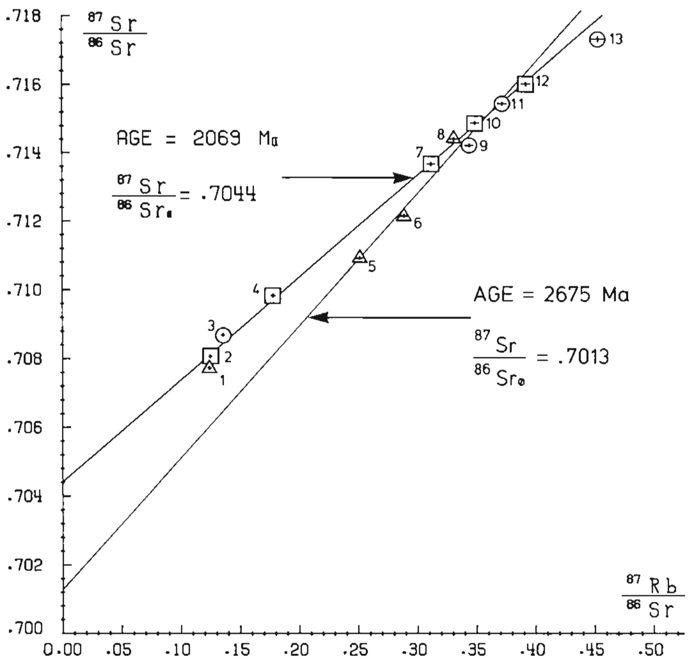


***Figure 3.*** *Rb-Sr isochron diagram showing results of analyses of slabs from block WN-506-78 (squares), slabs from block 399 (circles), and hand specimens (triangles), from the Ingilik Point Gneiss Complex compared with reference isochrons of age 2675 Ma (initial ratio 0.7013) and 2069 Ma (initial ratio 0.7044).*

In an effort to choose between the two models, we note:

1. the Ingilik Point Gneisses are country rock and basement to many units in the area and are thought to be among the older complexes in the region (Schau et al., 1982).
2. the zircon is from a leucocratic layer and hence is likely to have formed when the gneiss layers developed. (One might expect relict zircon to be associated with the relict, more mafic layers). The zircon morphology is such that neither model is clearly preferred; zircon grains are subhedral to rounded with elongations of up to 4:1 and are mostly clear but with a substantial red to orange fraction showing complex internal zoning (Schau, 1980). However, model A is supported by the relative concordance of the zircon U-Pb ages which suggests minimal secondary disruption to the U-Pb systems.
3. massive gabbros with K-Ar ages averaging 1966 ± 35 Ma intrude the dated gneisses indicating that the bulk of the gneissification was completed by about 1966 Ma. The gabbro stocks have chilled margins and contain angular fragments of the country rock (the gneiss) suggesting that they were emplaced at shallow depth.

On balance the authors favour model A but further work on granitic plutons cutting the Ingilik Point Gneisses is required to completely resolve the problem.

## References


Jacobsen, S.B. and Wasserburg, G.J.
1979: The mean age of mantle and crustal reservoirs; Journal of Geophysical Research, v. 84, no. B13, p. 7411-7427.

Schau, M.
1980: Zircon ages from a granulite-anorthosite complex and a layered gneiss complex northeast of Baker Lake, District of Keewatin; in Loveridge, W.D., Rubidium-strontium and uranium-lead isotopic age studies, Report 3, in Current Research, Part C, Geological Survey of Canada, Paper 80-1C, p. 237-238.

Schau, M. and Ashton, K.E.
1980: Geological Map of the granulite and anorthosite complex at the southeast end of Baker Lake, 56D1, 56C4, parts of 55N16 and 55N13; Geological Survey of Canada, Open File 712.

Schau, M., Tremblay, F., and Christopher, A.
1982: Geology of Baker Lake map area, District of Keewatin: a progress report; in Current Research, Part A, Geological Survey of Canada, Paper 82-1A, p. 143-150.

Stevens, R.D., Delabio, R.N., and Lachance, G.R.
1982: Age determinations and geological studies; K-Ar isotopic ages, Report 15, Geological Survey of Canada, Paper 81-2, p. 1.

Wanless, R.K. and Loveridge, W.D.
1972: Rubidium-strontium isochron age studies, Report 1; Geological Survey of Canada, Paper 72-23.

# 11. A U-Pb STUDY OF ZIRCON FROM GRANITIC BASEMENT BENEATH THE YELLOWKNIFE SUPERGROUP, POINT LAKE, DISTRICT OF MACKENZIE

J.B. Henderson, W.D. Loveridge and R.W. Sullivan

*Henderson, J.B., Loveridge, W.D., and Sullivan, R.W., A U-Pb study of zircon from granitic basement beneath the Yellowknife Supergroup, Point Lake, District of Mackenzie; in Rb-Sr and U-Pb Isotopic Age studies, Report 5, in Current Research, Part C, Geological Survey of Canada, Paper 82-1C, p. 173-178, 1982.*


### Abstract

*At Point Lake, District of Mackenzie, granitic basement at some distance from the unconformity with the overlying approximately 2670 Ma Yellowknife Supergroup has been dated by T.E. Krogh using the U-Pb method on zircon, at 3152 Ma. This report presents results of a U-Pb study on zircon from the same granite but collected at a locality only a few hundred metres from the unconformity. These results differ from those of Krogh in that a very large common lead component of Archean age was found in the zircon as well as an indication that the zircon had undergone an additional lead loss/uranium gain event. We interpret the combined results as indicating emplacement of the granite at 3152 Ma followed by zircon radiogenic lead loss/uranium gain together with gain of common lead near the unconformity at the time of erosional unroofing of the granite (prior to 2670 Ma). The last event affecting the U-Pb zircon systematics was lead loss at about 166 Ma. These results confirm that the granite is basement and not an unroofed synvolcanic pluton.*


## Introduction

Archean mafic volcanics and sediments of the Yellowknife Supergroup lie unconformably above granitic basement at Point Lake in the west-central Slave Province 280 km northeast of Yellowknife, District of Mackenzie. The basement-supracrustal relationship was first recognized by Stockwell (1933). The area has been mapped at 1:250 000 scale (Bostock, 1980) and at 1:50 000 scale (Henderson and Easton, 1977; Henderson, 1977). A more detailed description of the geology of the region can be found in these reports.

In 1974, prior to detailed mapping, material was collected by Henderson for U-Pb zircon dating from a locality (65°14'N, 113°04.5'W) a few hundred metres from the unconformity surface in order to determine whether the granite was a significantly older basement to the supracrustal rocks or whether it was an unroofed synvolcanic pluton subsequently covered by continuing volcanism and sedimentation. Due to the sparse content of zircon in the collected material and the scattered nature of the results obtained, a second collection at the same location was made by J.C. McGlynn in 1975.

## Geological Setting and Sample Description

The area sampled is at the fault controlled depositional margin of a basin containing Yellowknife supracrustal rocks (Fig. 1). The basin formed as a graben-like structure due to extension of the sialic crust (Henderson, 1981). Mafic volcanism took place along the basin boundary faults. The main basinal fill is greywacke-mudstone turbidites derived from sialic basement and felsic volcanic sources both within and, probably more importantly, outside the basin. In the marginal area are shallow water crossbedded sandstones and conglomerates containing both granitic and mafic volcanic clasts derived from the erosion of rising fault scarps.

At Point Lake both the mafic volcanics and basinal tubidites overlie the same granitic basement. At many localities where the unconformity is exposed there is a distinct Archean weathered horizon in the granite. The granitic material collected for this study was from well outside the weathered horizon. To the west, granitic to tonalitic gneisses locally containing amphibolite and pelitic schist zones may also represent basement to the Yellowknife Supergroup. These gneisses have recently been mapped by Easton et al. (1982) who present arguments in favour of the basement interpretation.

The basement granite is a grey to buff, massive, even grained, medium- to coarse-grained rock with distinctive opalescent quartz. Although there is no fabric, the rock is extensively fractured with the fracture surfaces coated with chlorite or biotite depending on metamorphic grade. The original mafic minerals are altered to chlorite but where more metamorphosed, decussate masses of fine biotite replace the chlorite. The quartz masses are polycrystalline due to crushing which accounts for their opalescent aspect. Plagioclase and microcline are present in varied proportions. The plagioclase is moderately altered with scattered flakes of white mica. The microcline is commonly perthitic. Zircon most commonly occurs with the mafic mineral aggregates.

## Related Age Measurements

Krogh and Gibbins (1978; Krogh, personal communication, 1981) has performed U-Pb analyses on zircon from the same granitic basement sampled at a greater distance from the unconformity. He obtained satisfactory results on three zircon concentrates yielding a chord cutting concordia at 3152 ± 2 and 166 Ma (reference chord, Fig. 2). Common lead constituted only a few per cent of the total lead in the zircon analyzed by Krogh in contrast with the remarkably high common lead content of the zircon of this study.

The Yellowknife supracrustal rocks in the Point Lake area have not as yet been dated, although elsewhere in the Slave Province U-Pb zircon ages include: at Yellowknife, 280 km southwest, 2650 Ma for volcanic rocks (Green and Baadsgaard, 1971) and 2680 Ma for greywackes (Geological Survey of Canada, unpublished); at Back River, 225 km to the southeast, 2667 Ma on rhyolite and 2672 Ma for greywacke (Lambert and Henderson, 1980); and at Hackett River, 225 km to the northeast, 2666 Ma on synvolcanic granodiorite (Frith and Loveridge, 1982). Thus, the age of supracrustal rocks at the Point Lake area is probably essentially the same as the approximate 2670 Ma age of deposition of Yellowknife Supergroup rocks elsewhere in the Slave Province.

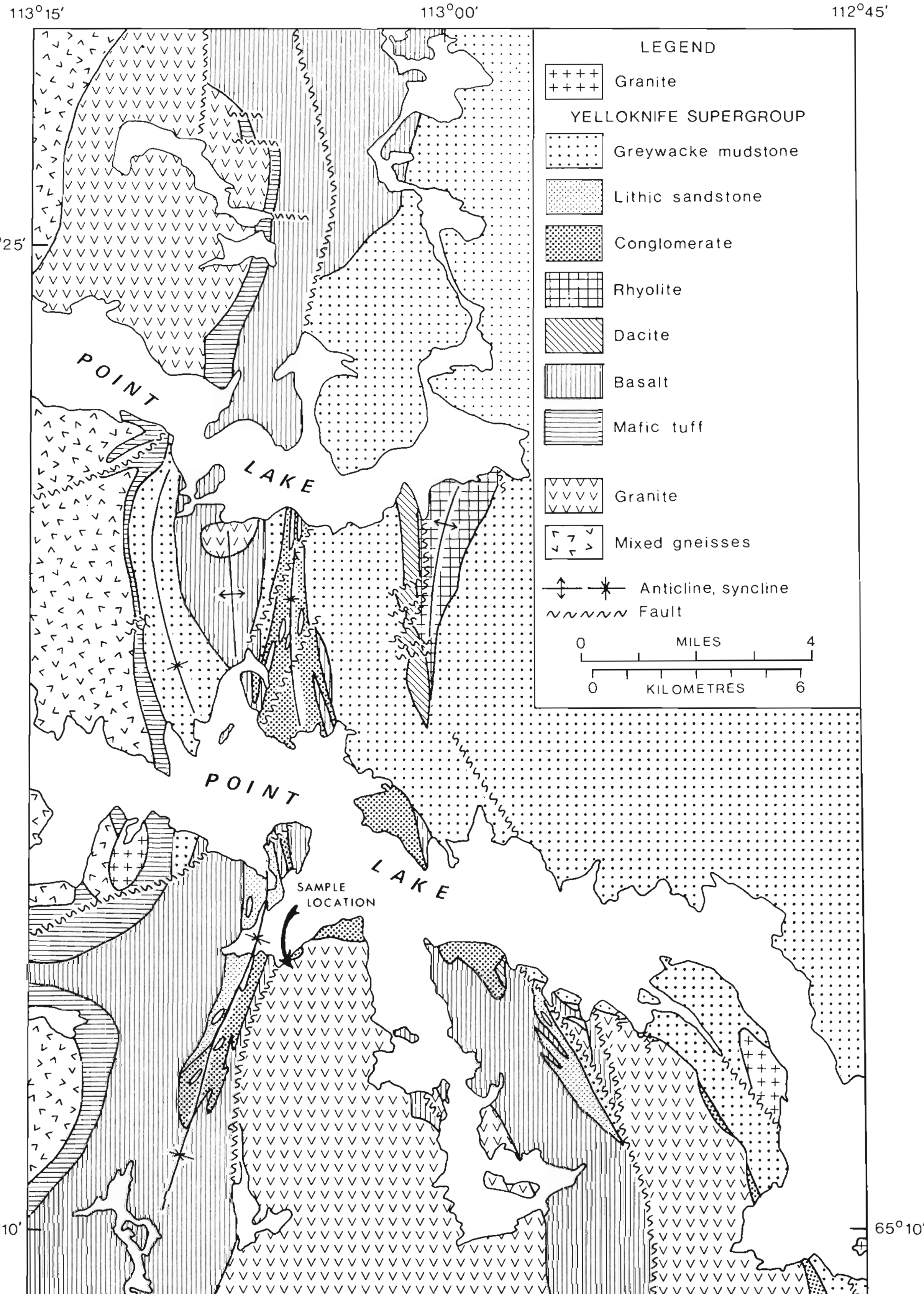


*Figure 1. Geological map and sample location, Point Lake area, District of Mackenzie.*

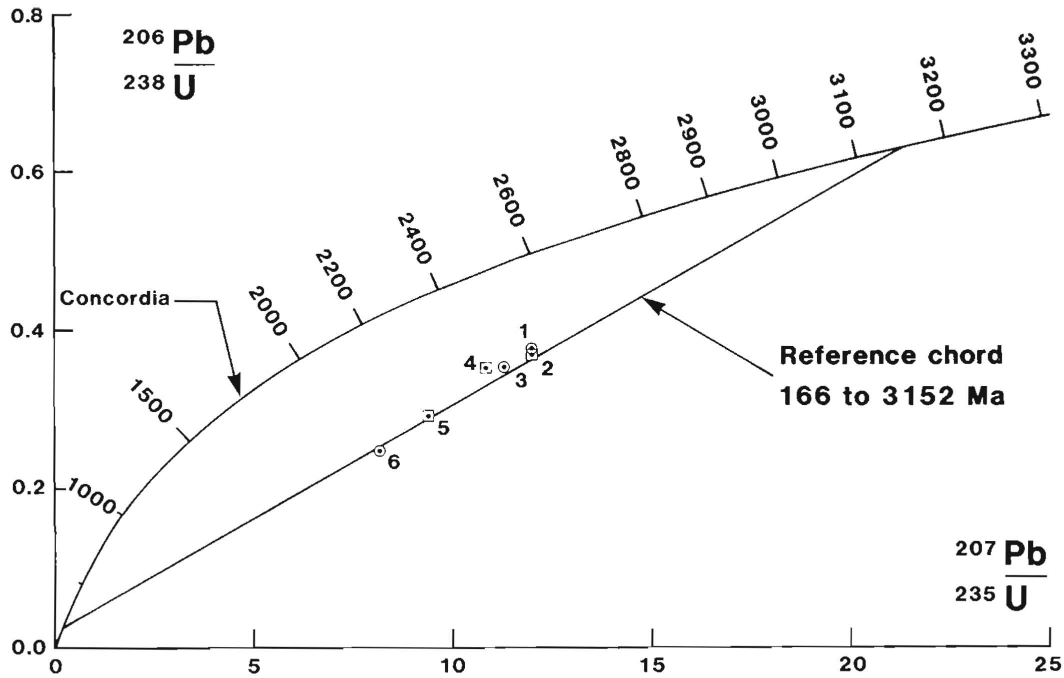


***Figure 2.*** *Concordia diagram showing the results of U-Pb analyses on zircon (this study) compared with a reference chord defined by the results of Krogh (personal communication, 1981). Circles: samples collected in 1974; squares: samples collected in 1975.*

## Analytical Procedures and Results

U-Pb analyses were performed on six zircon fractions in this study, three concentrated from the material collected by Henderson in 1974 (circles, concordia diagram, Fig. 2) and three from that collected by McGlynn in 1975 (squares, Fig. 2). Analytical results are presented in Table 1 and zircon morphology descriptions are in the Appendix. Techniques used in the concentration of zircon and the analyses of lead and uranium are variants of those described in Sullivan and Loveridge (1980). Fractions 3, 5 and 6 were not separated according to grain size but consisted of all remaining zircon material at that time, combined and hand picked for purity. The amounts of zircon used in fractions 5 and 6 were too small to be accurately weighed, so lead and uranium contents could not be determined although isotopic ratios of lead to uranium were obtained with the usual precision.

The six data points obtained are not collinear but cluster near the chord defined by the work of Krogh (ibid., reference chord, Fig. 1). These results differ from those of Krogh both in their scatter about the chord and in their exceptionally high common lead contents of 21 to 51 per cent. We interpret these high common lead contents as having been caused by diffusive incorporation of ambient common lead into the zircon at the time of erosional unroofing of the granite as indicated by proximity to the unconformity. The reasoning behind this interpretation is discussed later in this section.

The high common lead component provides an analytical problem in that knowledge of the common lead isotopic composition is prerequisite to precise determination of the radiogenic lead compositions. Since the analytical results do not yield concordant ages, an indirect method of estimating the common lead isotopic composition was employed. From the equation $\frac{^{207}Pb}{^{204}Pb}_p = \frac{^{207}Pb_c + ^{207}Pb_r}{^{204}Pb_c}$ (where p = present, c = common and r = radiogenic) and a comparable equation in $^{206}Pb/^{204}Pb$, one may derive:

$$\frac{^{207}Pb}{^{204}Pb}_p = \frac{^{206}Pb}{^{204}Pb}_p \times R + \frac{^{207}Pb}{^{204}Pb}_c - \frac{^{206}Pb}{^{204}Pb}_c \times R$$

(where R = $^{207}Pb_r/^{206}Pb_r$, i.e. the radiogenic $^{207}Pb/^{206}Pb$ ratio). This is the equation of a straight line with slope equal to R and y intercept $\frac{^{207}Pb}{^{204}Pb}_c - \frac{^{206}Pb}{^{204}Pb}_c \times R$.

The slope and y intercept value obtained from fitting a series of experimental data points to the above equation may be used to characterize a model lead which satisfies the y intercept equation.

Treated in this manner, the data from the six zircon fractions show a linear trend of slope 0.2353 ± 0.0080 and intercept 11.02 ± 0.68, suggesting an age for the radiogenic component of 3090 ± 60 Ma but yielding a poorly defined Archean common lead isotopic composition (equivalent to a Stacey and Kramers, 1975, model lead of age 3300+400/-900 Ma).

Since these results are generally consistent with the 3152 Ma upper intercept age determined by Krogh, a 3150 Ma (Stacey and Kramers, 1975) model lead composition was used when subtracting the common lead component from the measured results. The data listed in Table 1 and displayed in Figure 1 were obtained in this manner.

Table 1

Analytical data, zircon fractions from granitic basement, collected near the unconformity at Point Lake, District of Mackenzie

| | | | | | | | |
|---|---|---|---|---|---|---|---|
| Sample number | | 74 | 75 | 74 | 75 | 75 | 74 |
| Fraction number | | 1 | 2 | 3 | 4 | 5 | 6 |
| Fraction size, μm | | -74 | -62 | comb. | +62 | comb. | comb. |
| Weight, mg | | 1.80 | 0.42 | 1.18 | 0.92 | n.a. | n.a. |
| Total Pb, ng | | 560.2 | 162.7 | 371.4 | 148.7 | 14.03 | 17.56 |
| Pb blank, % | | 0.6 | 1.0 | 1.5 | 1.0 | 13.1 | 9.2 |
| Observed | $^{206}Pb/^{204}Pb$ | 82.94 | 51.28 | 45.69 | 55.72 | 119.07 | 78.70 |
| * Abundances | $^{204}Pb$ | 1.192 | 1.930 | 2.156 | 1.778 | 0.5580 | 1.067 |
| ($^{206}Pb$=100) | $^{207}Pb$ | 36.453 | 45.163 | 47.349 | 42.412 | 29.630 | 35.732 |
| | $^{208}Pb$ | 60.445 | 89.755 | 103.99 | 84.867 | 31.017 | 53.614 |
| Radiogenic Pb, | ppm | 530.8 | 478.6 | 459.8 | 347.1 | n.a. | n.a. |
| " " | % | 63.7 | 50.9 | 48.8 | 53.3 | 79.1 | 65.9 |
| Uranium, ppm | | 1100. | 945.4 | 888.4 | 726.5 | n.a | n.a |
| Atomic ratios | $^{206}Pb/^{238}U$ | 0.37669 | 0.36828 | 0.35330 | 0.35251 | 0.29134 | 0.24818 |
| | $^{207}Pb/^{235}U$ | 11.979 | 12.002 | 11.289 | 10.822 | 9.3950 | 8.1640 |
| | $^{207}Pb/^{206}Pb$ | 0.23062 | 0.23634 | 0.23174 | 0.22265 | 0.23387 | 0.23857 |
| Ages, Ma | $^{206}Pb/^{238}U$ | 2061 | 2021 | 1950 | 1947 | 1648 | 1429 |
| | $^{207}Pb/^{235}U$ | 2603 | 2605 | 2547 | 2508 | 2377 | 2249 |
| | $^{207}Pb/^{206}Pb$ | 3056 | 3095 | 3064 | 3000 | 3079 | 3110 |

* Corrected for Pb Blank

Sample number: 74 denotes 1974 collection (HBA-J-240-1-74); 75 denotes 1975 collection (WN-45-75).
Fraction size: comb. indicates that all grain sizes were combined. Fractions 5 and 6: weights, Pb contents and U contents are not available; see text.

These results suggest that the time of incorporation of common lead into the zircons is related to the unroofing to near surface level of the granite in this locality as indicated by its proximity to the unconformity, rather than more recently (i.e. subsequent to 166 Ma, the lower intercept age of the chord). The Archean isotopic composition obtained for the common lead component is consistent with its derivation from the basement terrane at the time of unroofing, but not with the "modern day" lead composition currently existent in most crustal rocks. Zircon uranium contents are sufficiently high (700 to 1100 ppm, Table 1) that only a few hundred Ma would have been required for radiation damage to the crystal structure to have been great enough to allow diffusive penetration of common lead; the minimum age of the unconformity (2670 Ma) allows up to 480 Ma for this to have occurred. Significantly, the high common lead component is seen only in the zircon samples collected near the unconformity and not in the more distant samples collected by Krogh.

The scatter of experimental points from this study, about the chord determined by Krogh, suggests a multistage history for the zircon from the granite near the unconformity. We interpret these results as indicating the occurrence of radiogenic lead loss or uranium gain in addition to common lead gain at the time of erosional unroofing. The model we propose is that of a three stage system with emplacement of the granite at 3152 Ma, radiogenic lead loss and/or uranium gain as well as comon lead gain by zircon in the granite near the unconformity probably two hundred to four hundred Ma later at the time of unroofing and, finally, lead loss at about 166 Ma (or perhaps slightly more recently as suggested by the position of data point 6 just below the chord determined by Krogh). The lack of lead loss at intermediate times between about 2670 and 166 Ma suggests that zircon was annealed by burial and/or metamorphic events in the late Archean.

## Discussion

The model we have presented, of emplacement of the granite at 3152 Ma with common lead gain and radiogenic lead loss and/or uranium gain by zircon in granite material near the unconformity at the time of unroofing prior to 2670 Ma, followed by more recent (about 166 Ma) lead loss is consistent with the known Archean geological history of the Point Lake area. The results obtained are in essential agreement with those of Krogh collected from the same granite at some distance from the unconformity. The 3152 Ma age of deposition of the granite, when compared with the approximate 2670 Ma age for Yellowknife Supergroup rocks elsewhere in the Slave Province confirms that it is basement and not an unroofed synvolcanic granitic pluton.

## References


Bostock, H.H.
1980: Geology of the Itchen Lake Area, District of Mackenzie; Geological Survey of Canada, Memoir 391, 101 p.

Easton, R.M., Boudle, R.L., and Zalusky, L.
1982: Evidence for gneissic basement to the Archean Yellowknife Supergroup in the Point Lake area, Slave Structural Province, District of Mackenzie; in Current Research, Part B, Geological Survey of Canada, Paper 82-1B, p. 33-41.

Frith, R.A. and Loveridge, W.D.
1982: Ages of Yellowknife Supergroup volcanic rocks, granitoid intrusive rocks, and regional metamorphism is the northeastern Slave Structural Province; in Current Research, Part A, Geological Survey of Canada, Paper 82-1A, p. 225-237.

Green, D.C. and Baadsgaard, H.
1971: Temporal evolution and petrogenesis of an Archean crustal segment at Yellowknife, N.W.T., Canada. Journal of Petrology, v. 12, p. 177-217.

Henderson, J.B.
1977: Keskarrah Bay, Northwest Territories; Geological Survey of Canada Open File 447.

1981: Archaean basin evolution in the Slave Province, Canada; in Precambrian Plate Tectonics, ed. A. Kröner, Elsevier, Amsterdam, p. 213-235.

Henderson, J.B. and Easton, R.M.
1977: Archean supracrustal-basement rock relationships on the Keskarah Bay map area, Slave Structural Province, District of Mackenzie; in Report of Activities, Part A, Geological Survey of Canada, Paper 77-1A, p. 217-221.

Krogh, T.E. and Gibbins, W.
1978: U-Pb isotopic ages of basement and Supracrustal rocks in the Point Lake area of the Slave Structural Province, Canada; in Abstracts with Programs, Geological Association of Canada, Mineralogical Association of Canada, Geological Society of America, v. 3, p. 438.

Lambert, M.B. and Henderson, J.B.
1980: A uranium-lead age of zircons from volcanics and sediments of the Back River volcanic complex, eastern Slave Province, District of Mackenzie; in Loveridge, W.D., Rubidium-strontium and uranium-lead isotopic age studies, Report 3; in Current Research, Part C, Geological Survey of Canada, Paper 80-1C, p. 239-242.

Stacey, J.S. and Kramers, J.D.
1975: Approximation of terrestrial lead isotope evolution by a two stage model; Earth and Planetary Science Letters, v. 26, p. 207-221.

Stockwell, C.H.
1933: Great Slave Lake – Coppermine River area, Northwest Territories; Geological Survey of Canada, Summary Report, 1932, Part C, p. 37-63.

Sullivan, R.W. and Loveridge, W.D.
1980: Uranium-lead age determinations on zircon at the Geological Survey of Canada: current procedures in concentrate preparation and analysis; in Loveridge, W.D. Rubidium-strontium and uranium-lead isotopic age studies, Report 3; in Current Research, Part C, Geological Survey of Canada, Paper 80-1C, p. 161-246.

## APPENDIX

Description of zircon concentrates from granitic basement, collected near the unconformity at Point Lake, District of Mackenzie.

Latitude 65°14'N; longitude 113°04.5'W.

Sample HBA-J-240-1-74 collected in 1974 by J.B. Henderson.

Fraction 1. The -74 μm size fraction was acid washed, yielding a sample which consisted of 95% zircon ranging from 2:1 to 4:1 elongation and of generally euhedral to subhedral shape. Some crystals had a frosty appearance while some were amber. Many grains had complex internal structures and some were clearly zoned. Rare parallel twins were observed.

Fraction 3. The total remaining material from all size fractions was hand picked to yield a concentrate consisting of 75% frosty, tan, translucent, euhedral zircon crystals and fragments with a wide size range plus 25% clear, transparent crystals and fragments.

Fraction 6. All residues were again hand picked to obtain a tiny, unweighed concentrate consisting of better than 99% euhedral zircon crystals and fragments of which 80% were translucent, tan-grey of larger sizes with obvious inner and outer domains (cores and rims?), plus smaller, clear, colourless to pink types. In transmitted light zonal structure was clearly visible in larger crystals. One end to end twin pair was observed.

Sample WN-45-74 collected in 1975 by J.C. McGlynn.

Fractions 2 and 4. The total zircon concentrate was hand picked to produce pure zircon consisting mainly of euhedral, semitransparent, tan crystals and fragments, plus minor transparent, clear light purple (hyacinth) grains of more rounded to tear-shaped form, plus totally clear, transparent, colourless, "gem quality" euhedral crystals, and a very small number of deep reddish yellow, translucent crystals. Bubble inclusions were visible in many of the larger crystals. This sample was then sieved to produce +62 and -62 μm fractions which were separately analyzed.

Fraction 5. The residues from the above operations were again hand picked to produce a very small, unweighed, concentrate of pure zircon of all size fractions. This sample consisted of 95%(+) zircon ranging from large to very fine, from tan to very clear and pink, and from euhedral to rounded. Some cored crystals were observed in which the cores were pinkish.

## ERRATA

Geological Survey of Canada Paper 80-19

Proposals for time classification and correlation of Precambrian rocks and events in Canada and adjacent areas of the Canadian Shield.

Part 1: A time classification of Precambrian rocks and events.

C.H. Stockwell

p. 14 Caption for Table 2 should read "Time units and estimated ages of boundaries." Delete "(formal units ... lower case letters)".

Heading for last column should be "Ma" not "ma".

p. 40 Left column, line 12 – "$^{40}$AR-$^{39}$AR age" should read "$^{40}$Ar-$^{39}$Ar age".

p. 67 Figure 13, and pocket Figure 17 – Under symbols, "ORGANIC" should read "OROGENIC".

p. 84 Figure 19. "SUBPROVINCIAL" should read "SUBPROVINCE".

p. 87 Right column, last paragraph, 2nd line "the greywacke" should read "and greywacke".

caption for pocket Figure 11 – "metamorphic notes" should read "metamorphic nodes", and in the last column, "CULTER" should read "CUTLER".

Geological Survey of Canada Paper 82-1B,

Current Research Part B, Report 23, p. 169

The photographs in Figure 23.1 and Figure 23.2 should be interchanged.

## Author Index

## NOTE TO CONTRIBUTORS

Submissions to the *Discussion* section of *Current Research* are welcome from both the staff of the Geological Survey and from the public. Discussions are limited to 6 double-spaced typewritten pages (about 1500 words) and are subject to review by the Chief Scientific Editor. Discussions are restricted to the scientific content of Geological Survey reports. General discussions concerning branch or government policy will not be accepted. Illustrations will be accepted only if, in the opinion of the editor, they are considered essential. In any case no redrafting will be undertaken and reproducible copy must accompany the original submissions. Discussion is limited to recent reports (not more than 2 years old) and may be in either English or French. Every effort is made to include both *Discussion* and *Reply* in the same issue. *Current Research* is published in January, June and November. Submissions for these issues should be received not later than November 1, April 1, and September 1 respectively. Submissions should be sent to the Chief Scientific Editor, Geological Survey of Canada, 601 Booth Street, Ottawa, Canada, K1A 0E8.

## *AVIS AUX AUTEURS D'ARTICLES*

*Nous encourageons tant le personnel de la Commission géologique que le grand public à nous faire parvenir des articles destinés à la section* discussion *de la publication* Recherches en cours. *Le texte doit comprendre au plus six pages dactylographiées à double interligne (environ 1500 mots), texte qui peut faire l'objet d'un réexamen par le rédacteur en chef scientifique. Les discussions doivent se limiter au contenu scientifique des rapports de la Commission géologique. Les discussions générales sur la Direction ou les politiques gouvernementales ne seront pas acceptées. Les illustrations ne seront acceptées que dans la mesure où, selon l'opinion du rédacteur, elles seront considérées comme essentielles. Aucune retouche ne sera faite aux textes et dans tous les cas, une copie qui puisse être reproduite doit accompagner les textes originaux. Les discussions en français ou en anglais doivent se limiter aux rapports récents (au plus de 2 ans). On s'efforcera de faire coincider les articles destinés aux rubriques* discussions et réponses *dans le même numéro. La publication* Recherches en cours *paraît en janvier, en juin et en novembre. Les articles pour ces numéros doivent être reçus au plus tard le 1er novembre, le 1er avril et le 1er septembre respectivement. Les articles doivent être renvoyés au rédacteur en chef scientifique: Commission géologique du Canada, 601, rue Booth, Ottawa, Canada, K1A 0E8.*

Energy, Mines and Resources Canada
Énergie, Mines et Ressources Canada